An organic geochemical approach to archaeological and environmental questions

Sean F. Jordan B.Sc.

Thesis submitted for the award of Ph.D.

Under the supervision of Dr. Brian P. Kelleher

School of Chemical Sciences
Dublin City University

Submitted July 2016

Declaration

I hereby certify that this material, which I now submit for assessment on the programme of study leading to the award of Ph.D is entirely my own work, and that I have exercised reasonable care to ensure that the work is original, and does not to the best of my knowledge breach any law of copyright, and has not been taken from work of others save and to the extent that such work has been cited and acknowledged within the text of my work.

Signed:.....ID.No.:.....Date:.....

For Amy.
For always being there for me.
I couldn't have done it without your love and
encouragement throughout good times and bad.
This is yours as much as it is mine.
Thanks for hanging in there.

Acknowledgements

I would like to thank the Irish Research Council for funding this work.

Dr. Brian Kelleher has been an excellent mentor. His passion for the field has been a source of constant inspiration for me. A special thank you to him for his support, guidance, friendship, and motivation throughout my entire academic life.

I am indebted to Dr. Shane O'Reilly and Dr. Brian Murphy for their mentorship, encouragement, patience, and friendship. Some great times were had in the OGRe Lab both on land and at sea.

I would like to thank all of my colleagues and friends from DCU especially Dr. Margaret McCaul, Dr. Michal Szpak, Dr. Kris Hart, Dr. Adam Porter, and Niall Durham. Their friendship and support has been invaluable throughout the course of this work.

I would also like to thank all of the staff in the School of Chemical Sciences, especially the technical staff for all of their help over the years.

Finally, thank you to my collaborators throughout the years including Prof. Bill Mahaney (York University, Toronto), Prof. Chris Allen (Queens University, Belfast), Prof. Andre Simpson (University of Toronto Scarborough), and Xavier Monteys (Geological Survey of Ireland) for their expertise and guidance and for providing numerous research opportunities.

Table of contents

Contributions 1
Publications and accomplishments 3
List of abbreviations 7
Abstract 9

Chapter 1. Biomarkers and stable isotopes: Geochemical tools with vast applicability 10
1.1 Introduction 11
1.2 The global carbon cycle 14
1.2.1. Organic matter composition 17
1.2.2. Primary production 18
1.2.3. Terrestrial organic matter 19
1.2.4. Marine organic matter 21
1.3. Lipid biomarkers 22
1.3.1. Extraction methods 22
1.3.2. Analytical techniques 27
1.3.3. Lipid biomarker compound classes 29
1.3.3.1. n-Alkanes 31
1.3.3.2. n-Alkanols 33
1.3.3.3. n-Alkan-2-ones 34
1.3.3.4. Alkenones 35
1.3.3.5. Fatty acids 36
1.3.3.6. Phospholipid fatty acids 37
1.3.3.7. Steroids 39
1.3.3.8. Hopanoids 40
1.3.3.9. Other terpenoids 42
1.4 $\delta^{13}C$ 42
1.4.1. Definition and measurement 42
1.4.2. Isotopic fractionation 45
1.4.3. Compound specific stable isotope analysis 49
1.5. Applications 51
1.6. Project overview 56
References 57

Chapter 2. Chasing Hannibal: Using geochemical techniques to aid in tracing the route taken by the Carthiginian general to invade Italia in 218 BC 89
Abstract 90
2.1. Introduction 91
2.1.1. Hannibal's crossing 91
2.1.2. Faecal biomarkers 93
2.1.3. 5ß-stanols 95
2.1.4. Bile acids 96
2.2. Study area 97
2.2.1. Sampling site 97
2.2.2. Sampling and ^{14}C dating 98
2.3. Materials and methods 100
2.3.1. Sample preparation 100
2.3.2. Elemental analysis 100

2.3.3. Total lipid extraction ... 102
2.3.4. Isolation and derivatisation of neutral fraction from 2011 TLEs ... 102
2.3.5. Isolation and derivatisation of faecal biomarkers from 2013 TLEs ... 103
2.3.6. Gas chromatography – mass spectrometry (GC-MS) ... 104
2.4. Results ... 106
2.4.1. Preliminary investigation of samples from 2011 sampling trip ... 106
2.4.2. Total organic carbon (TOC) ... 106
2.4.3. Steroidal compounds ... 106
2.4.4. Bile acids ... 108
2.5. Discussion ... 108
2.6. Conclusion ... 113
References ... 113

Chapter 3 Mid-Holocene climate change and landscape formation in Ireland: Evidence from a geochemical investigation of a coastal ombrotrophic peat bog ... 128
Abstract ... 129
3.1. Introduction ... 130
3.2. Materials and methods ... 133
3.2.1. Sampling and sample location ... 133
3.2.2. Sample preparation ... 134
3.2.3. Radiocarbon dating ... 135
3.2.4. X-ray fluorescence analysis (XRF) ... 135
3.2.5. TOC and TN analysis ... 135
3.2.6. Lipid biomarker extraction ... 136
3.2.7. Gas chromatography – mass spectrometry (GC-MS) ... 136
3.2.8. Gas chromatography – isotope ratio mass spectrometry (GC-IRMS) ... 138
3.2.9. Statistical analysis ... 138
3.3. Results ... 139
3.3.1. Chronology of peat profile ... 139
3.3.2. Elemental composition ... 140
3.3.2.1. Total organic carbon (TOC) and total nitrogen (TN) ... 140
3.3.2.2. Total sulphur (TS) ... 141
3.3.3. Neutral compounds ... 146
3.3.4. $\delta^{13}C$ values ... 150
3.4. Discussion ... 150
3.4.1. Origin of OM in the Spiddal ombrotrophic peat bog ... 150
3.4.2. Climate change in Ireland during the mid-Holocene ... 152
3.5. Conclusions ... 155
References ... 157

Chapter 4. Characterisation of a marine pockmark site in Bantry Bay, Co. Cork, Ireland ... 164
Abstract ... 165
4.1. Introduction ... 166
4.2. Geological setting ... 170
4.3. Materials and methods ... 173
4.3.1. Seabed surveying ... 173
4.3.2. Sediment sampling ... 173
4.3.3. Porewater and gas analysis ... 176

4.3.4. Bulk physical and chemical analysis 177
4.3.5. Lipid biomarker analysis 177
4.4. Results 180
4.4.1. Geophysical analyses 180
4.4.2. Gas and porewater geochemistry 181
4.4.3. PSA and elemental analysis 184
4.4.4. PLFAs 187
4.4.5. Carbon isotope values of individual lipids 190
4.5. Discussion 194
4.6. Conclusions 201
References 202

Chapter 5. Final conclusions and future work 214
Appendices 219

Contributions

Chapter 2.

Sampling was carried out by Prof. William C. Mahaney (York University, Toronto), Dr. Christopher C. R. Allen and Jonathan Young (Queens University, Belfast), and Dr. Shane S. O'Reilly, Dr. Brian P. Kelleher, and Coren Pulleyblank (Dublin City University). Geological investigation was performed by Prof. William C. Mahaney. Radiocarbon dating was performed by Allen West (GeoScience Consulting, Arizona). Lipid biomarker analysis and interpretation of 2011 samples was performed by Dr. Brian T. Murphy and Dr. Shane S. O'Reilly.

Chapter 3.

This site was discovered by Prof. Michael Williams (National University of Ireland, Galway) who initially described the 'drowned forest'. Dr. Brian P. Kelleher assisted with sampling.

Chapter 4.

Dr. Stephen S. McCarron (National University of Ireland, Maynooth) was the Chief Scientist for the RV *Celtic Explorer* CE14_003 research cruise. Cruise preparation and planning was carried out in conjunction with Xavier Monteys (Geological Survey of Ireland). The onboard scientific party consisted of Dr. Daniel Praeg, Dr. Roberto Romeo, and Lorenzo Facchin (Istituto Nazionale di Oceanografia e di Geofisica

Sperimentale, Trieste), Dayton Dove (British Geological Survey, Edinburgh), Dr. Gill Scott, Shaun Harrigan, Martha Coleman, and Edel O'Donnell (National University of Ireland, Maynooth), Dr. Benjamin Thebaudeau (Geological Survey of Ireland), Michael Arrigan (National University of Ireland, Galway), and Elena Grimoldi (Durham University). Preparation and planning for sampling in Bantry Bay was conducted by Dr. Shane S. O'Reilly and myself. Multibeam and sub-bottom data processing and clean-up as well as initial interpretation was performed by Dr. Daniel Praeg, Dayton Dove, Lorenzo Facchin, Dr. Roberto Romeo, Dr. Benjamin Thebaudeau, and Dr. Shane S. O'Reilly. Analysis of gas samples was performed by Dr. Shane S. O'Reilly.

Publications and accomplishments

Peer-reviewed publications

Murphy, B.T., O'Reilly, S.S., Monteys, X., Reid, B.F., Szpak, M.T., McCaul, M. V., **Jordan, S.F.**, Allen, C.C.R., Kelleher, B.P., 2016. The occurrence of PAHs and faecal sterols in Dublin Bay and their influence on sedimentary microbial communities. Mar. Pollut. Bull. doi:10.1016/j.marpolbul.2016.02.066

Mahaney, W.C., Allen, C.C.R., Pentlavalli, P., Kulakova, A., Young, J.M., Dirszowsky, R.W., West, A., Kelleher, B., **Jordan, S.**, Pulleyblank, C., O'Reilly, S., Murphy, B.T., Lasberg, K., Somelar, P., Garneau, M., Finkelstein, S.A., Sobol, M.K., Kalm, V., Costa, P.J.M., Hancock, R.G. V, Hart, K.M., Tricart, P., Barendregt, R.W., Bunch, T.E., Milner, M.W., 2016. Biostratigraphic Evidence Relating to the Age-Old Question of Hannibal's Invasion of Italy, I: History and Geological Reconstruction. Archaeometry. doi:10.1111/arcm.12231

Mahaney, W.C., Allen, C.C.R., Pentlavalli, P., Kulakova, A., Young, J.M., Dirszowsky, R.W., West, A., Kelleher, B., **Jordan, S.**, Pulleyblank, C., O'Reilly, S., Murphy, B.T., Lasberg, K., Somelar, P., Garneau, M., Finkelstein, S.A., Sobol, M.K., Kalm, V., Costa, P.J.M., Hancock, R.G. V, Hart, K.M., Tricart, P., Barendregt, R.W., Bunch, T.E., Milner, M.W., 2016. Biostratigraphic Evidence Relating to the Age-Old Question of Hannibal's Invasion of Italy, II: Chemical Biomarkers and Microbial Signatures. Archaeometry. doi:10.1111/arcm.12228

Mahaney, W.C., Somelar, P., Dirszowsky, R.W., Kelleher, B., Pentlavalli, P., McLaughlin, S., Kulakova, A.N., **Jordan, S.**, Pulleyblank, C., West, A., Allen, C.C.R., 2016. A Microbial Link to Weathering of Postglacial Rocks and Sediments, Mount Viso Area, Western Alps, Demonstrated through Analysis of

a Soil/Paleosol Bio/Chronosequence. J. Geol. 124, 149–169. doi:10.1086/684442

O'Reilly, S.S., Pentlavalli, P., Flanagan, P.V., Allen, C.C.R., Monteys, X., Szpak, M.T., Murphy, B.T., **Jordan, S.F.**, Kelleher, B.P., 2016. Abundance and diversity of sedimentary bacterial communities in a coastal productive setting in the Western Irish Sea. Cont. Shelf Res. 113, 1–9. doi:10.1016/j.csr.2015.12.002

O'Reilly, S.S., Hryniewicz, K., Little, C.T.S., Monteys, X., Szpak, M.T., Murphy, B.T., **Jordan, S.F.**, Allen, C.C.R., Kelleher, B.P., 2014. Shallow water methane-derived authigenic carbonate mounds at the Codling Fault Zone, western Irish Sea. Mar. Geol. 357, 139–150. doi:10.1016/j.margeo.2014.08.007

O'Reilly, S.S., Szpak, M.T., Flanagan, P. V., Monteys, X., Murphy, B.T., **Jordan, S.F.**, Allen, C.C.R., Simpson, A.J., Mulligan, S.M., Sandron, S., Kelleher, B.P., 2014. Biomarkers reveal the effects of hydrography on the sources and fate of marine and terrestrial organic matter in the western Irish Sea. Estuar. Coast. Shelf Sci. 136, 157–171. doi:10.1016/j.ecss.2013.11.002

Mahaney, W.C., Allen, C.C.R., Pentlavalli, P., Dirszowsky, R., Tricart, P., Keiser, L., Somelar, P., Kelleher, B., Murphy, B., Costa, P.J.M., **Jordan, S.**, O'Reilly, S., Juligj, P., 2014. Polybius' "previous landslide": Proof that Hannibal's invasion route crossed the col de la traversette. Mediterr. Archaeol. Archaeom. 14, 77–94.

Hart, K.M., Szpak, M.T., Mahaney, W.C., Dohm, J.M., **Jordan, S.F.**, Frazer, A.R., Allen, C.C.R., Kelleher, B.P., 2011. A bacterial enrichment study and overview of the extractable lipids from paleosols in the Dry Valleys, Antarctica: implications for future Mars reconnaissance. Astrobiology 11, 303–21. doi:10.1089/ast.2010.0583

Oral presentations

From Chapter 2.

Irish Mass Spectrometry Society Meeting 2014, Dublin, Ireland

British Organic Geochemical Society Meeting 2014, Liverpool, UK

Irish Mass Spectrometry Society Meeting 2015, Dublin, Ireland

From Chapter 3.

Conference on Analytical Sciences Ireland (CASi) 2016, Dublin, Ireland

Conference of Irish Geographers 2016, Dublin, Ireland

Poster presentations

From Chapter 2.

INFOMAR Seminar 2013, Galway, Ireland

Geoscience Seminar 2013, Dublin, Ireland

From Chapter 4.

Atlantic Ireland 2014, Dublin, Ireland

From Chapter 3.

Conference on Analytical Sciences Ireland (CASi) 2016, Dublin, Ireland

Research surveys

February 2014 – Shipboard scientist aboard RV *Celtic Explorer* cruise CE14_003 to Galways Bay, Bantry Bay, and the Celtic Shelf (Funded through the Marine Institute under the Marine Research Sub-Programme)

June 2010 - Shipboard scientist aboard RV *Celtic Voyager* cruise CV10_28 to the Irish Sea (Funded through the INFOMAR program).

Extracurricular modules and training

April 2015 – Strategic Marine Alliance for Research and Training (SMART) and the Marine Institute (MI), Science@Sea 2015 two-day practical course aboard the RV *Celtic Voyager,* Cork Harbour and Approaches

January 2014 - Dublin Regional Higher Education authority (DRHEA) Graduate Training Element CS551A Advanced Analytical Techniques, Dublin City University.

January 2014 - Dublin Regional Higher Education authority (DRHEA) Graduate Training Element CS507A Multivariate Statistics, Dublin City University.

List of abbreviations

AB	-	Acoustic Blanking
ACL	-	Average Chain Length
ANME	-	Anaerobic MEthanotrophic archaea
AOM	-	Anaerobic Oxidation of Methane
ASE	-	Accelerated Solvent Extraction
AT	-	Acoustic Turbidity
BC	-	Before Christ
BHP	-	Bacteriohopanepolyol
BHT	-	Bacteriohopanetetrol
BP	-	Before Present
brFA	-	branched Fatty Acid
CAM	-	Crassulacean Acid Mechanism
CI	-	Chemical Ionisation
CPI	-	Carbon Preference Index
CSIA	-	Compound Specific stable Isotope Analysis
cyFA	-	cyclic Fatty Acid
DCA	-	Deoxycholic Acid
DGGE	-	Denaturing Gel Gradient Electrophoresis
DIC	-	Dissolved Inorganic Carbon
DOC	-	Dissolved Organic Carbon
DOM	-	Dissolved Organic Matter
EA-IRMS	-	Elemental Analysis – Isotope Ratio Mass Spectrometry
EI	-	Electron-impact Ionisation
EOP	-	Even-over-Odd Predominance
FID	-	Flame Ionisation Detector
FISH	-	Fluorescence In Situ Hybridisation
GC	-	Gas Chromatography
GC-C-IRMS	-	Gas Chromatography – Combustion – Isotope Ratio Mass Spectrometry
GC-FID	-	Gas Chromatography – Flame Ionisation Detection
GC-IRMS	-	Gas Chromatography – Isotope Ratio Mass Spectrometry
GC-MS	-	Gas Chromatography – Mass Spectrometry
GDGT	-	Glycerol Dialkyl Glycerol Tetraether
HMW	-	High Molecular Weight
HPLC	-	High Performance Liquid Chromatography
IC	-	Inorganic Carbon
INFOMAR	-	Integrated mapping for the sustainable development of Ireland's marine resource
IPCC	-	Intergovernmental Panel on Climate Change
IRMS	-	Isotope Ratio Mass Spectrometry
LADS	-	Laser Airborne Depths Sounder
LC-MS	-	Liquid Chromatography – Mass Spectrometry
LCA	-	Lithocholic Acid
LIDAR	-	Light Detection and Ranging
LMW	-	Low Molecular Weight
MAE	-	Microwave Assisted Extraction
MS	-	Mass Spectrometry
MUFA	-	Monounsaturated Fatty Acid

MWP	-	Medieval Warm Period
OC	-	Organic Carbon
OEP	-	Odd-over-Even Predominance
OM	-	Organic Matter
PAH	-	Polycyclic Aromatic Hydrocarbon
PDB	-	PeeDee Belemnite
PEP	-	Phosphoenol Pyruvate
PgC	-	Petagrams Carbon
PLFA	-	Phospholipid Fatty Acid
POC	-	Particulate Organic Carbon
POM	-	Particulate Organic Matter
PUFA	-	Polyunsaturated Fatty Acid
RT	-	Retention Time
SATFA	-	Saturated Fatty Acid
SCM	-	Soil Continuum Model
SMTZ	-	Sulfate Methane Transition Zone
SOM	-	Soil Organic Matter
SPE	-	Solid Phase Extraction
SRB	-	Sulfate Reducing Bacteria
SST	-	Sea Surface Temperature
TLE	-	Total Lipid Extract
TN	-	Total Nitrogen
TOC	-	Total Organic Carbon
TS	-	Total Sulfur
UAE	-	Ultrasonically Assisted Extraction
VPDB	-	Vienna PeeDee Belemnite
XRF	-	X-Ray Fluorescence

Abstract

Organic geochemistry is the study of the sources, transport, and fate of carbon based molecules in the environment. In particular, lipid biomarkers are employed as a means of tracking this carbon and understanding the complex interactions involved in its global biogeochemical cycling. In this thesis, organic geochemical techniques were applied to several research areas to glean information from organic matter in an effort to answer several research questions. In Chapter 2, lipid biomarkers derived from faecal material were analysed from archaeological soils in the Italian Alps. This data provided potential evidence of the passage of Hannibal of Carthage's army as it crossed the Alps to invade Italia in 218 BC. Analysis of material from a peat bog in Spiddal, Co. Galway which featured the remnants of a 'drowned forest' provided a record of Ireland's palaeoclimate during the Mid-Holocene in Chapter 3. Evidence of significant climatic events were uncovered including a cool period in the Northern Hemisphere attributed to the '4.2 ka event'. A warming climate and rising sea levels ca. 2000 BP were suggested as possible factors in the drowning of the forest. In Chapter 4, a characterisation of gas seepage in Bantry Bay, Co. Cork was carried out. Sites included an area of seabed depressions known as a pockmark field. Geophysical and geochemical data suggested that these seafloor features were formed via the expulsion of biogenic methane from deep within the sediments of the bay. Porewater geochemistry and lipid biomarker analysis revealed distinct sulphate methane transition zones (SMTZ) beneath the seafloor and provided an insight into the microbial activity of the area including the occurrence of the anaerobic oxidation of methane (AOM).

Chapter 1

Biomarkers and stable isotopes: Geochemical tools with vast applicability

1.1. Introduction

Organic geochemistry can be defined as the study of the organic material present in terrestrial, marine, and extra-terrestrial environments to determine its source, composition, and fate. For decades, researchers have been employing geochemical techniques to investigate a variety of questions in a multitude of environments ranging from deep ocean hydrothermal vents (Blumenberg et al., 2007; Hawkes et al., 2015; Summit et al., 2000) to Antarctic ice (Spaulding et al., 2013), from Amazon rainforest soils (Taube et al., 2013) to the 67P/Churyumov-Gerasimenko comet (Goesmann et al., 2015). Any material containing organic matter (OM) holds potentially valuable information relating to its formation and/or the ongoing biological processes within it, which can be elucidated through organic geochemical analysis.

OM is comprised of carbon based molecules derived from living and dead organisms (Oades, 1988). In materials such as soils, sediments, and rocks it exists as a heterogeneous mixture which originates from past and present organisms (Kelleher and Simpson, 2006). Whilst much of the OM present in these materials is formed *in situ*, a significant proportion is transported from other locations through various environmental and biological processes (Baldock et al., 2004; Hedges and Oades, 1997; Hedges, 1992). Therefore, analysis of the composition of OM not only provides an insight into the biota at a specific site, but also into the cycling of OM on a global scale. Understanding OM cycling is essential for our understanding of global environmental processes, and in particular how these pertain to future climatic change (Falkowski et al., 2000).

Alfred Treibs (Treibs, 1936) discovered petraporphyrins in shales, bitumens, and crude oils and proposed that these compounds were actually the remnants of chlorophylls synthesised by ancient plants (Eganhouse, 1997). This discovery is seen as the beginning of the study of biological marker molecules. Biological markers or biomarkers are lipid-derived compounds that can be traced to particular biological precursor molecules (Eganhouse, 1997; Eglinton and Calvin, 1967; Killops and Killops, 2005). These compounds are a significant component of OM due to their presence in all living organisms. Their recalcitrant nature and their source specificity make them ideal molecules for use as biomarkers (Eglinton and Hamilton, 1967; Peters et al., 2005). These chemical fossils derive from living organisms and constitute a natural archive of environmental information. From the plant leaf waxes of ancient vegetation to the membrane phospholipids of active microbial communities, lipid biomarker investigations provide data on a plethora of past and present ecosystems and represent a key geochemical analytical tool.

Stable isotope analysis is another important approach in organic geochemistry which began with the development (Nier, 1947) and refinement (McKinney et al., 1950) of a mass spectrometer capable of determining variations in isotopic abundance ratios (Degens, 1969). Determination of the relative proportions of isotopes of individual elements (e.g. $D/^{1}H$, $^{18}O/^{16}O$, $^{13}C/^{12}C$, etc.) offers another perspective on the formation, preservation, and degradation of OM (Peters et al., 2005). This analysis is performed on bulk OM and individual compounds as well as isolated liquids and gasses. Measurements of δD and $\delta^{18}O$ are most commonly applied to water and trace gasses, and are particularly important for the analysis of ice cores (e.g. Gkinis et al., 2014; Seierstad et al., 2014). Analysis of these isotope ratios has enabled researchers to reconstruct global temperature changes over millions of years (Ghosh and Brand,

2003). $\delta^{13}C$ values are particularly valuable in the study of OM due to its carbon-based nature (Killops and Killops, 2005; Peters et al., 2005). Whilst often performed on bulk material, this analysis is particularly diagnostic when applied to individual analytes in the form of compound-specific isotope analysis (CSIA) (Pancost and Pagani, 2006).

Organic geochemical techniques originate from the investigation of hydrocarbons in the field of fossil fuel exploration. Throughout its existence the discipline has spread to a much more diverse range of topics both in academia and industry. Whilst still an essential facet of petroleum and natural gas inspection, organic geochemistry forms an important component of global carbon cycle research, the study of the evolution of life, palaeoclimatology, archaeology, agriculture, pollution investigations, and astrobiology amongst others (e.g. Gao et al., 2016; Gold et al., 2016; Lin and Simpson, 2016; Miller et al., 2016; Murphy et al., 2016; Pagès et al., 2016).

The aim of this review is to outline the role of organic geochemical techniques in a multitude of disciplines with a particular focus on the use of lipid biomarkers and stable isotope ratios. The following sections will discuss in detail; I. organic matter on Earth in a range of terrestrial and marine ecosystems including its structure and global cycling, II. the use of lipid compounds as biomarker molecules including extraction techniques and analytical methods, III. $\delta^{13}C$ values for both bulk OM and specific biomarkers as a diagnostic tool in geochemistry together with standard analytical methodology, and IV. the myriad applications of these approaches in modern scientific research.

1.2. The global carbon cycle

The intricate relationships between biological, geological, and chemical processes which recycle materials and energy on Earth are known as biogeochemical cycles (Hedges, 1992). These cycles involve complex interactions between the atmosphere and terrestrial and marine ecosystems that can range in time-scales from microseconds to eons (Hedges, 1992). It is this complexity and vast coverage of time and space that makes understanding biogeochemical cycles a difficult task.

The global carbon cycle involves interactions between three main carbon reservoirs, namely the atmosphere, the terrestrial biosphere, and the oceans (Fig. 1.1.). Estimates of the quantity of carbon in various global reservoirs vary between accounts, however they are generally in the region of the values mentioned here (values after Falkowski et al., 2000). The largest carbon stock on Earth is inorganic carbon stored in sedimentary rocks which comprises > 60,000,000 PgC. This is followed by the organic carbon in these rocks composed of kerogen, bitumen, and hydrocarbon gases which account for a further 15,000,000 PgC. In terms of the more active carbon reservoirs, the atmosphere represents 720 PgC, the majority of which is in the form of CO_2. 2,000 PgC is contained in the organic material in the terrestrial biosphere with 600 – 1,000 PgC attributed to living biomass, and a further 1,200 PgC attributed to non-living biomass. In contrast, the total organic carbon in the oceans accounts for 1,000 PgC with a further 37,400 PgC stored as dissolved inorganic carbon (DIC). The total carbon content of all fossil fuels on the planet is 4,130 PgC. As anthropogenic processes are returning previously stable carbon back into the active cycle both directly (i.e. through the burning of fossil fuels) and indirectly (e.g. increasing temperatures leading to the release of carbon from reservoirs such as arctic permafrost

and marine gas hydrates), knowledge of the sources, transport mechanisms, and eventual fate of this element is essential to our ability to mitigate the effects of a changing climate.

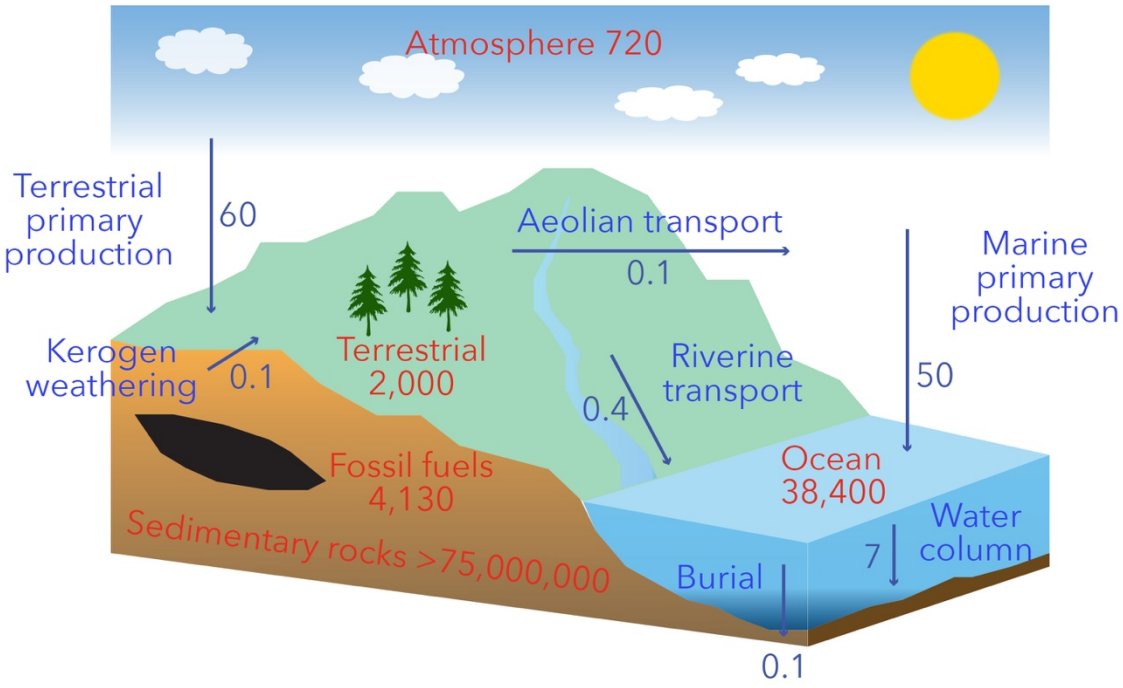

Figure 1.1. The organic carbon cycle as part of the global carbon cycle (values after Falkowski et al., 2000; Hedges and Oades, 1997; Hedges, 1992)

Organic carbon fluxes throughout the carbon cycle occur through a variety of means. Weathering of kerogen in sedimentary rocks results in the reintroduction of a relatively small amount (0.1 PgC yr^{-1}) of organic carbon to the global cycle (values after Hedges, (1992) and Hedges and Oades, (1997)). Terrestrial primary production, predominantly occurring via land plant photosynthesis accounts for 60 PgC yr^{-1}. Of this terrestrial carbon, 0.4 PgC yr^{-1} is transported to the oceans as dissolved organic carbon (DOC) via riverine discharge (0.4 PgC yr^{-1}) and aeolian input (0.1 PgC yr^{-1}).

This transport to the sea is the only significant route to preservation of terrestrially derived organic matter occurring at present (Hedges, 1992). Primary production by marine phytoplankton results in the fixation of particulate organic carbon (POC) (50 PgC yr $^{-1}$). Some of this (4 PgC yr $^{-1}$) is transported through the water column as 'particle rain' or 'marine snow' whilst another portion (3 PgC yr $^{-1}$) is metabolised to DOC by marine biota such as zooplankton. The amount of carbon buried in marine sediments each year is estimated to equal the amount of carbon that is sourced from the weathering of sedimentary rocks (0.1 PgC yr $^{-1}$).

Table 1.1. Reservoirs and fluxes of C within the global carbon cycle (Values after Falkowski et al., 2000; Hedges and Oades, 1997; Hedges, 1992)

Gobal Carbon Cycle

Carbon Reservoirs			**Carbon Fluxes**	
Sedimentary rocks	>75,000,000		Kerogen	0.1
IC		> 60,000,000	Terrestrial PP	60
OC		15,000,000	Riverine discharge	0.4
Atmosphere (CO2)	720		Aeolian transport	0.1
Terrestrial (OC)	2000		Marine PP	50
Living		600-1000	Water column (POC)	4
Non-living		1200	DOC	3
Marine	38,400		Sediment burial	0.1
IC		37,400		
OC		1,000		
Fossil fuels	4,130			

1.2.1. Organic matter composition

OM is the fraction of soils and sediments that is composed of material derived from living and dead organisms. It is a complex mixture of organic compounds of different chemical structures, multiple sources, and varied reactivities (Goni and Hedges, 1995). The major constituent of organic matter is carbon, occurring in a wide range of natural and synthetic polymers such as lignin and cellulose (Walther, 2009). Knowledge of carbon bio-sequestration in both oceanic and terrestrial systems is imperative if we are to understand carbon cycling as it pertains to climate change (Bloom et al., 2016; Otto et al., 2005). OM contains huge amounts of carbon and plays an important role in regulating anthropogenic changes to the global carbon cycle. It also plays essential roles in agriculture (Stocking, 2003), water quality (Lal et al., 2004), immobilization and transport of nutrients and anthropogenic chemicals (Linn et al., 1993), while also concealing exciting opportunities for the discovery of novel compounds for potential use in industry and medicine (Flaig, 1997; Ling et al., 2015). Carbon cycling in the environment is a complex topic, and new work is constantly adding to our understanding of these complexities (Bloom et al., 2016; Butman et al., 2016; Carolan and Fornara, 2016; Coppola and Druffel, 2016; Landry and Matthews, 2016; Simkus et al., 2016; Spohn et al., 2016). The source of carbon and also its eventual destination are questions that are highly important and relevant to the global climate change debate (Weiping et al., 2011). One of the ways in which these questions can be answered is by studying OM in the environment and tracing its sources, transportation, and eventual fate.

1.2.2. Primary production

Photosynthesis is the primary source of new OM on Earth (Peters et al., 2005). Even non-phototrophic communities rely on recycling sedimentary carbon that was originally fixed by photosynthetic organisms. Chemoautotrophy provides another means of organic matter production in non-photosynthetic communities, such as those present at hydrothermal vents and in soil (Hart et al., 2013; Nakagawa and Takai, 2008). This contribution is believed to constitute a minor percentage of total organic matter (Peters et al., 2005), however it is possible that its significance may be underestimated.

Vascular plants are the main photosynthetic organisms in terrestrial settings but, excluding some seagrasses, they are absent from the marine environment (Hedges and Oades, 1997). The dominant primary producers in marine systems are single-celled phytoplankton (Baldock et al., 2004; Hedges and Oades, 1997). Photosynthesis results in the fixation of organic carbon compounds from CO_2 in the presence of sunlight (Eq. 1):

$$CO_2 + H_2O \xrightarrow{light} CH_2O + O_2$$

As light is an essential requirement of photosynthesis, in marine settings this process is limited to the photic zone which extends to a depth of 100 m.

Prior to deposition and during the early stages of burial, these primary products are transformed by biological, chemical, and physical processes (Killops and Killops, 2005; Peters et al., 2005). These processes, termed diagenesis, are mainly biological and occur under relatively low temperature (< 50 °C) in the upper fraction of soils and sediments. Following diagenesis, at greater depths and higher temperatures (50 – 150

°C), catagenesis occurs thermally altering the organic matter in rocks resulting in the production of oil over millions of years. Metagenesis occurs at temperatures ranging from 150 – 200 °C, leading to the production of gas from the breakdown of organic molecules (Peters et al., 2005). It is diagenesis which results in the organic material of primary interest to organic geochemists.

1.2.3. Terrestrial organic matter

Soil OM (SOM) is a heterogeneous mixture of primarily plant and microbial origin (Lehmann and Kleber, 2015). The global soil carbon pool of 2500 Pg is 3.3 and 4.5 times the size of the atmospheric (760 Pg) and biotic (560 Pg) pools respectively (Lal, 2004). SOM is comprised of a complex variety of constituents across a range of sizes and chemical compositions. Therefore, it is often classified into multiple fractions for discussion, which traditionally involved the alkaline extraction of soils resulting in humic acids, fulvic acids, and humin fractions. Other material classes, such as macro-organic matter (> 250 μm) (Oades, 1988), have also been included in these descriptions. Exactly where biogeochemically important compounds fit into these classification systems is a source of confusion. Some descriptions suggest that they are a part of the humic substances (e.g. Killops and Killops, 2005), an umbrella term for humic acids, fulvic acids, and humin, whereas others differentiate between humic substances and non-humic substances defining them as non-biochemical and biochemical fractions respectively (Oades, 1988).

Recently it has been suggested that the most beneficial model to adopt going forward in terms of a more comprehensive description of SOM which would aid in multidisciplinary research is that of the soil continuum model (SCM) (Lehmann and Kleber, 2015) (Fig. 1.2.). The SCM model defines SOM as a continuum of organic

molecules that are constantly being degraded by the soil biota towards molecules of a smaller size (Lehmann and Kleber, 2015). This model also includes constant formation and destruction of soil aggregates with SOM as well as adsorption and desorption of SOM to mineral surfaces within the matrix. This suggested model adheres to and improves on the idea that SOM is a complex, heterogenous mixture of predominantly plant and microbial origin, and that humic material is a part of this mixture, and not a distinct chemical category (Kelleher and Simpson, 2006). Nevertheless, some key elements are still missing from this model. For instance, there appears to be no accounting for microbial contribution to and alteration of OM. Also CH_4 is not included, nor does it provide for interactions of CO_2 and CH_4 within the soil. However, from a geochemistry perspective, this description supports the basis that chemical analysis of SOM provides an insight into the sources of this heterogenous material and its eventual fate in the global carbon cycle.

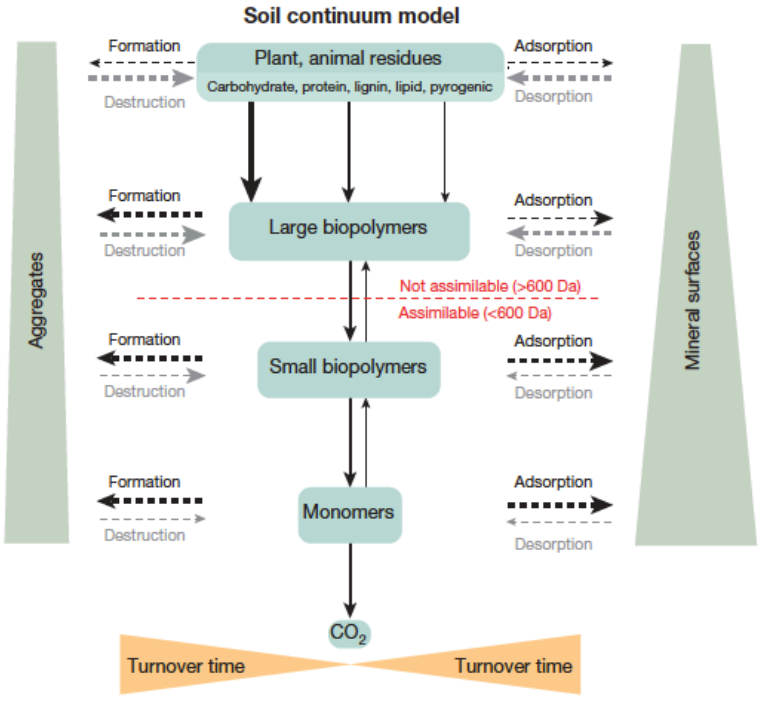

Figure 1.2. The soil continuum model for soil organic matter composition (from Lehmann and Kleber, 2015)

1.2.4. Marine organic matter

Marine OM is generally described in terms of two fractions; particulate organic matter (POM) resulting from the primary production of marine phytoplankton, and dissolved organic matter (DOM) biogeochemically produced throughout the water column. Significant amounts of POM and DOM are also derived from terrestrial inputs to the oceans (Hedges et al., 1997). Microscopic photosynthetic plants, phytoplankton, are the main primary producers in the oceans. Their concentrations are highest in areas where nutrient rich colder waters are pushed to the surface in a process known as upwelling. These conditions often result in phytoplankton blooms, where large conglomerations of phytoplankton occur due to the increase in available nutrients. However, only about 0.1% of the total ocean is comprised of persistent upwelling regions (Hedges and Oades, 1997). The remains of these phytoplankton along with those of other microorganisms such as zooplankton and other organic debris fall through the water column as POM. Some of this POM is converted to DOM through various biogeochemical processes such as phytoplankton exudation, metabolisation by grazers, viral-induced cell lysis, and decomposition of detritus (Hasumi and Nagata, 2014). Only a relatively small proportion (~5%) of marine OM from primary production reaches the sea floor (Galimov, 2006).

OM in some coastal regions has been shown to be dominated by terrestrial OM (van Dongen et al., 2000). This OM is transported to the marine environment via two main processes; aeolian transport and riverine transport. Rivers represent the major source of terrestrial OM to the marine environment, with the world's ten largest rivers accounting for approximately 40% of the fresh water and particulate matter entering the ocean (Bianchi et al., 2002). Thus the OM within marine sediments is comprised of a combination of terrestrial and marine OM. This OM is subject to

degradation over time by bacterial communities that are present within marine sediments.

1.3. Lipid biomarkers

In organic geochemistry, biomarkers is the term used for chemical compounds present in OM that act as indicators of their source organisms. These molecular markers were originally termed chemical fossils (Eglinton and Calvin, 1967) and have since proved to be a powerful forensic technique in organic geochemical studies. The term lipids represents a multitude of organic molecules of varying chemical composition and as such, it has obtained multiple definitions. Perhaps the definition most suitable from an organic geochemistry viewpoint is that lipids are all of the compounds produced by organisms that are insoluble in water but soluble in solvents that dissolve fats (Killops and Killops, 2005). Lipids are present in all living organisms and, depending on their chemical structure, are vital for membrane composition, energy storage, and regulation of metabolic processes (Laureillard et al., 1997). Their high level of recalcitrance coupled with the ability to trace their origins to specific source organisms makes lipids particularly useful as biomarkers. This section will focus on some of the important classes of lipid biomarker compounds that are routinely used in organic geochemical investigations and which are amenable to gas chromatography (GC).

1.3.1. Extraction methods

Organic extracts containing biomarker compound classes are generally separated from the sample matrix by extraction with organic solvents. The polarity of

these solvents depends on the chemistry of the analytes of interest and extraction techniques often utilise a solvent regime consisting of extraction with multiple solvents and solvent mixtures.

Lipids are ubiquitous in the environment and as such, pose a significant contamination risk for organic geochemists. Introduction of lipids derived from surfaces other than the sample matrix of interest such as work surfaces and even the researchers themselves, can lead to the analysis of compounds that are not present in the sample, thereby providing false results. Also, other chemical compounds that are soluble in organic solvents, such as phthalates from plastic materials, can appear in chromatograms potentially dwarfing and/or co-eluting with compounds of interest, making interpretation of data difficult. To avoid these contamination issues, organic geochemical methods involve the use of ultra-clean organic-free techniques, a chemist's version of the biologist's aseptic technique.

Samples are stored in organic-free materials, glass receptacles or aluminium foil that has been fired in a muffle furnace at temperatures > 450 °C for ~ 8 hrs, similar to the conditions used for analysis of total organic carbon via loss on ignition (Skjemstad and Baldock, 2007). All glassware and ceramics are thoroughly washed and fired. Stainless steel tools for sampling and preparation are washed and sonicated in solvent to remove organics. Plastic materials are avoided, with Teflon (thoroughly cleaned and solvent washed) taking its place where possible. Laboratory gloves are always worn to prevent contamination from contact with the skin and sample handling is avoided. All aqueous solutions should be pre-extracted with a non-polar solvent such as $CHCl_3$ or CH_2CL_2 three to five times to remove any organic compounds prior to use. Procedural blanks are run to monitor background interferences.

Prior to extraction samples must be homogenised and are often dried. Homogenization ensures that the sub-sample analysed is representative of the whole sample. Drying of the samples facilitates a more efficient physical breakdown of the matrix and also allows the polarity of the extraction solvents to be controlled without interference from water.

Air-drying and oven-drying can potentially allow microbial action to continue during the drying process, altering the OM composition and subsequently providing a sample that is less representative of the environment from which it was taken. Similarly, both heat and light can cause degradation of some chemical bonds with heating above 37.5 °C attributed to significant alteration of lipid compounds. Therefore, oven-drying at temperatures above this should be avoided. Freeze-drying is the drying of the frozen sample material under vacuum via sublimation. This process is likely less damaging than oven or air drying and therefore results in a more representative sample for analysis. With all of these drying procedures, highly volatile low molecular weight compounds are usually lost prior to extraction.

Homogenization of soils and sediments is usually carried out by crushing of the dry sample using a mortar and pestle, followed by sieving to remove large debris and to provide a fraction (commonly < 850 μm in diameter) which is suitable for solvent extraction. Samples which are more difficult to homogenise such as rocks are often crushed using ball mills or custom manual crushing devices (e.g. Sherman et al., 2007). Electric blenders are often employed to homogenise samples which are to be wet-extracted e.g. fish or animal tissues (Azzouz et al., 2011; Lacaze et al., 2007).

Soxhlet extraction is one of the most commonly used extraction techniques employed by organic geochemists (Aquilina et al., 2010; Elhmmali et al., 1997; Kiriakoulakis et al., 2004; Laureillard et al., 1997; Strong et al., 2013; Xie et al., 2004).

A round-bottom flask containing solvent is seated in a heater and attached to a Soxhlet extractor containing a glass-fibre thimble into which the soil or sediment sample is weighed. This is connected to a liebig condenser. The solvent, usually a mixture of solvents (e.g. 9:1 CH_2Cl_2:CH_3OH), is heated and the vapour travels into the condenser where it is transformed to a liquid which subsequently drips into the sample chamber. Once the chamber fills, the solvent is forced back into the round bottom flask to begin the sequence again. The organic compounds extracted from the sample matrix remain in the flask whilst the solvent vapour continues the procedure. One extraction cycle usually lasts for 10-15 mins and the process is repeated for a period, usually in the range of 24 - 72 hrs. The extract is concentrated by rotary evaporation. Soxhlet extraction provides excellent recovery of neutral lipid compound classes, however the extraction time is quite long. Also, certain compounds which may be sensitive to heat may not be well represented in soxhlet extracts.

Ultrasonically assisted extraction (UAE) involves the sonication of a sample in organic solvent to facilitate the extraction of lipid compounds as is another common technique for the analysis of lipid biomarkers (e.g. Feng et al., 2010; Hart et al., 2011; Otto et al., 2005). The sample is weighed into a Teflon centrifuge tube to which a solvent is added. The mixture is sonicated (10-15 mins) and centrifuged to separate the liquid from the solid material. The supernatant is decanted and concentrated by rotary evaporation. This process must be repeated, often 3 – 5 times, to ensure good recovery of the compounds of interest and usually involves the use of multiple solvents e.g. CH_2Cl_2, followed by 1:1 CH_2Cl_2:CH_3OH, followed by CH_3OH (Otto et al., 2005; O'Reilly et al., 2012), subsequently combining all extracts. This method is significantly less time consuming than Soxhlet extraction and provides similar recovery of neutral compounds. It has also been shown to provide recovery of

phospholipid fatty acids (PLFAs) close to that of the more specialised method of Bligh and Dyer (1959).

The Bligh and Dyer method used for the extraction of polar lipids from soils and sediments was originally developed for the analysis of phospholipids in animal tissues and as such is often applied to soils and sediments for this purpose. A modified form of this method (White and Ringelberg, 1998) is used for the extraction of lipids from soils and sediments (e.g. O'Reilly et al. (2014)). Briefly, the sample is weighed into a Teflon centrifuge tube to which a mixture of a phosphate buffer, $CHCl_3$, and CH_3OH in a ratio of 0.8:1:2 is added. This mixture is sonicated briefly (< 2 min) and shaken overnight. The mixture is centrifuged and the supernatant transferred to a separating funnel to which further volumes of $CHCl_3$ and CH_3OH are added providing a ratio of 0.9:1:1 buffer:$CHCl_3$:CH_3OH. This is shaken and left to separate for a period of four hours. The organic extract is removed and concentrated by rotary evaporation. This method provides excellent recovery of both neutral and polar compounds, particularly PLFAs.

Accelerated solvent extraction (ASE) employs high pressure to provide high recovery extraction of numerous samples in minimal time with minimal solvent volumes, and has been utilized in some more recent geochemical studies (Jansen et al., 2013; Kaiser et al., 2014; Seki et al., 2012; Zhang et al., 2014). Similarly, microwave assisted extraction (MAE) is a highly efficient extraction method which has been applied to geochemical investigations (Bendle and Rosell-Mele, 2007; Gregg and Slater, 2010; Schmidt et al., 2010). The use of these techniques however is not widespread due mainly to the high cost of purchasing and maintaining the extraction equipment. It should be noted that the reduction in solvent consumption associated

with these more modern methods may provide long term reduction in costs as well as being more environmentally sound.

1.3.2. Analytical techniques

High performance liquid chromatography (HPLC) coupled to a mass spectrometer (LC-MS) has become an increasingly popular technique in the field of organic geochemistry. This enables the analysis of high molecular weight, polar compounds which are unsuitable for gas chromatography. In recent years there has been increasing focus on the utility of these compounds as biomarkers. For example the analysis of glycerol dialkyl glycerol tetraethers (GDGTs), membrane lipids derived from archaea and bacteria, has enabled the determination of soil pH, mean air temperature, terrestrial OM input to marine environments, and also sea surface temperature (SST) (Schouten et al., 2013). However, LC-MS instrumentation will not be further discussed here as this review will focus on those lipid biomarkers that are amenable to gas chromatography (GC) analysis.

GC enables the separation of a mixture of volatile organic compounds. In basic GC analysis samples are injected via a heated inlet, thereby volatilizing the organic compounds which travel, suspended in an inert carrier gas (usually He), through a capillary column containing a stationary phase. Compounds are separated based on their size and affinity for the stationary phase and can be identified according to their retention times (RTs) once detected. Two of the most common detectors used with GC in organic geochemistry are flame ionisation detectors (FID) and mass spectrometers (MS) (Fig. 1.3.). A FID uses a flame fuelled by hydrogen and air to combust the organic compounds that have been separated by GC. The ions produced during combustion, proportional to the quantity of the organic compound, are attracted

to a collector plate. These signals are displayed as peaks in a chromatogram using chromatographic software on a computer attached to the system. Each compound has a specific RT which can be used for identification purposes. When analysing unknown samples these RTs are confirmed by comparison with the analysis of known standard compounds. Individual compounds can be quantified by comparison of their peak area with a calibration curve prepared using the peak areas of relevant standards which are of similar composition to the analytes of interest. In order to ensure accuracy, and to account for variations in instrument performance, an internal standard is used. This is a known compound which is similar to the analytes of interest, but which does not occur naturally in the samples. A known concentration of this standard is added to the sample prior to GC-MS analysis, as well as to the individual standards in the calibration curve. The areas of all sample peaks can be related to that of the internal standard thereby normalising the results and allowing for accurate quantification.

The MS detector produces a chromatogram similar to that of the FID. This allows for the quantification of organic compounds in the same fashion as that described above. However, as well as the identification via specific RTs, the MS produces specific mass spectra from the fragmentation patterns of individual compounds during ionization. The MS can provide the molecular weight, the empirical formula, and often the complete structure of an unknown compound (Christie and Han, 2010). Most MS systems utilize an electron-impact ionisation (EI) source, however a chemical ionisation (CI) source can also be employed (Peters et al., 2005). In EI, when individual compounds travel into the ionisation chamber of the MS they are bombarded with electrons. These electrons cause the molecules to form positively charged ions which can fragment into smaller ions known as daughter ions. These ions are repelled by a positively charged repeller plate, forcing them to travel

through a magnetic field which leads to their separation based on individual mass to charge (*m/z*) ratios. Each ion is recorded and displayed as a specific peak within the mass spectrum of the original compound, with the most abundant ion (base peak) given the arbitrary value of 100. The molecular ion (M^+) is the term given to the ion derived from the parent molecule. These mass spectra contain the structural information required to deduce the source compound. Spectra are compared to library databases containing spectra from a multitude of previously identified compounds in an effort to obtain a match. In practice, identification involves a combination of approaches including the use of libraries, comparison to published mass spectra in the literature, and interpretation of fragmentation patterns.

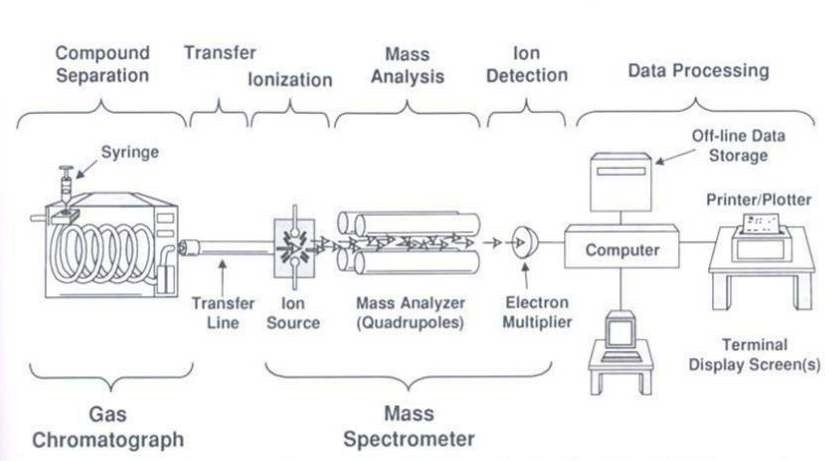

Figure 1.3. Schematic diagram of a typical gas chromatography - mass spectrometry system (from Peters et al., 2005)

1.3.3. Lipid biomarker compound classes

The range and diversity of lipid biomarkers is wide and ever expanding. The following section is an introduction to common classes of compounds employed in geochemical investigations. Table 1.2. lists some key biomarker compounds and their predominant sources.

Table 1.2. Predominant sources of some key lipid biomarkers and biomarker proxies

Biomarkers/Proxies	Source(s)	Reference(s)
n-Alkanes		
C15 - C19 OEP	Algae	(Blumer et al., 1971; Volkman, 2006)
C20 - C35 OEP	Higher plants	(Eglinton and Hamilton, 1967)
n-Alkanols		
C14 - C22 EOP	Algae	(Laureillard et al., 1997)
C16 - C36 EOP	Higher plants	(Pancost and Boot, 2004)
n-Alkan-2-ones		
C23 - C31 OEP	*Sphagnum Spp.*	(Baas et al., 2000)
C27	*Sphagnum Spp.*	(Nichols and Huang, 2007a)
Alkenones		
C37	*Prymnesiophyceae,* palaeoproductivity	(Prahl and Wakeham, 1987; Prahl et al., 1988)
C37:4	Sea-ice extent	(Rosell-Mele et al., 1998)
Uk'37	Palaeotemperature	(Prahl and Wakeham, 1987)
Fatty acids		
16:1ω7 and 18:1ω7	Bacteria	(Rajendran et al., 1992; Volkman, 2006; Zelles, 1999)
16:1ω5, 17:1ω6, and cy17:0ω5,6	*Desulfosarcina/ Desulfococcus*	(Elvert et al., 2003; Li et al., 2007)
10Me16:0	*Desulfobacter*	(Elvert et al., 2003; Li et al., 2007)
16:4ω1 and 16:3ω4	Diatoms	(Volkman, 2006)
*i*15:0 and *ai*15:0	*Desulfovibrio*	(Li et al., 2007)
MUFA(<C19):brFA	Aerobic/anaerobic bacteria	(Rajendran et al., 1992)

*cy*17:0/16:1ω7	Environmental stress	(Guckert et al., 1986; Mills et al., 2006)
Steroids		
ß-Sitosterol	Higher plants	(Volkman, 1986)
Dinosterol	Dinoflagellates, diatoms	(Volkman, 1986; Volkman et al., 1993)
Coprostanol	Human faeces	(Bethell et al., 1994; Bull et al., 2002, 1999a)
Ergosterol	Fungi	(Méjanelle et al., 2000)
Terpenoids		
ß-amyrin	Angiosperms	(Giri et al., 2015; Volkman, 2005)
Taraxer-4-one	*Ericacaea*	(Pancost et al., 2002)
Hopanoids		
2-methylhopanoids	Cyanobacteria	(Summons et al., 1999)

1.3.3.1. n-Alkanes

n-Alkanes are straight chain hydrocarbons that act as an important class of biomarkers in many environments (Pancost and Boot, 2004). Due to their lack of functional groups they are highly resistant to degradation. The distribution of *n*-alkanes in a particular environment is reflective of the source material of the OM. Short chain homologues with an odd-over-even predominance (C_{15} - C_{19}) are primarily derived from phytoplankton (Blumer et al., 1971; Volkman, 2006). An *n*-alkane distribution dominated by these homologues is therefore indicative of a marine influence in that environment. Long chain *n*-alkanes with an odd-over-even predominance (OEP) (C_{21} - C_{35+}) are indicative of an input from terrestrial plants as these compounds are commonly found in leaf epicuticular waxes (Eglinton and Hamilton, 1967). This distribution pattern is often employed to trace the input of terrestrial OM to marine sediments (e.g. Lin et al., 2014; Medeiros and Simoneit,

2008; Schmidt et al., 2010; Schubert and Stein, 1997). Even-over-odd (EOP) predominance of *n*-alkanes preserved in soils and sediments is considered unusual (Kuhn et al., 2010). This signature has been attributed to post-depositional reduction of fatty acids, input from specific bacteria, anthropogenic fossil fuel pollution or hydrocarbon seepage from underlying sources (Kuhn et al., 2010; Wang et al., 2010, and references therein). Mid-chain homologues, particularly C_{23} and C_{25}, play a key role in organic geochemical studies in peatland environments. These compounds are attributed to input from *Sphagnum* mosses, peat-forming plants which thrive in cold and wet conditions (Baas et al., 2000; Pancost et al., 2002). As such, the relative contributions from these homologues are compared to that from the long chain compounds to glean palaeoclimatic information from these settings (e.g. Ficken et al., 1998; Inglis et al., 2015; Nichols et al., 2006; Nott et al., 2000; Pancost et al., 2002; Xie et al., 2004; Zhang et al., 2014) (discussed in more detail in Chapter 3). The diagnostic utility of these mid-chain compounds is not constrained to peatland environments. *n*-Alkane distributions in sediments from estuaries in the Eurasian Arctic suggested a significant contribution from *Sphagnum* plants (van Dongen et al., 2008). Eastward decreases in these contributions were attributed to more arid conditions in the east. Interestingly, Kirkels et al., (2013) compiled a review of the consistency of *n*-alkane patterns in plaggen ecosystems and observed distinct patterns allowing the discrimination between inputs from shrubs, trees, and grasses to these soils. Geographic location was also observed in this study to affect the distribution of *n*-alkanes in tree species, suggesting the diagnostic potential of these biomarkers has not yet been fully realised.

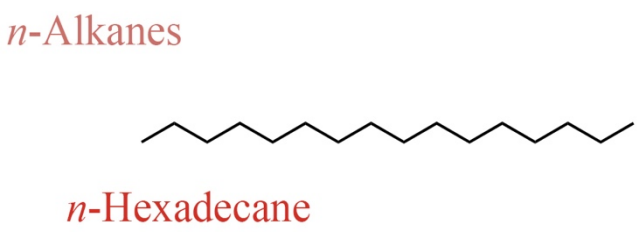

Figure 1.4. Example of an *n*-alkane structure

1.3.3.2. n-Alkanols

As they are found in significant quantities in the leaf waxes of vascular plants, *n*-alkanols are useful biomarkers for terrestrial OM in marine settings and are often employed as such (e.g. Carreira et al., 2011; Christodoulou et al., 2009; Fernandes et al., 1999). In higher plants, long chain *n*-alkanols are usually observed with an even-over-odd predominance (C_{16} – C_{36}) (Pancost and Boot, 2004). In marine derived OM, *n*-alkanols are generally found in low abundance in organisms, with homologues ranging from C_{14} to C_{22} generally attributed to phytoplankton and zooplankton sources (Laureillard et al., 1997; Volkman, 2006). *n*-Alkanols are a valuable biomarker class for distinguishing between marine and terrestrial OM sources due to this variation in homolog distribution. Furthermore, the level of degradation in a sample can be examined by determining the proportion of *n*-alkanols in the sum of the *n*-alkanes and *n*-alkanols (alc/alc+alk) (Poynter and Eglinton, 1990). This is suggested to be a result of the preferential degradation of *n*-alkanols due to the presence of the hydroxyl functional group.

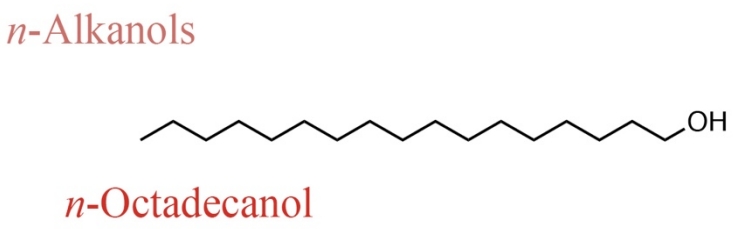

Figure 1.5. Example of an *n*-alkanol structure

1.3.3.3. n-Alkan-2-ones

Peat-forming plants of the genus *Sphagnum* were found to contain long chain odd carbon numbered (C_{23} – C_{31}) *n*-alkan-2-ones (Baas et al., 2000; Nichols and Huang, 2007b). Nichols and Huang (2007) suggested that this distinct distribution allows these compounds to be employed as relatively source specific biomarkers in peat, aiding in palaeoenvironmental reconstruction in these settings. However, more recent findings have isolated these compounds in a number of plant species in a bog setting including *Sphagnum*, *Ericaceae,* and some ferns (Ortiz et al., 2011). Furthermore, it has been suggested that the dominant contribution of these compounds to certain soils and peat bogs is not from plants, but is in fact derived from the microbial degradation of *n*-alkanes (Jansen and Nierop, 2009; Ortiz et al., 2011). This occurs via the oxidation of *n*-alkanes via the alkan-2-ol intermediate or by the oxidation and decarboxylation of fatty acids (Cranwell et al., 1987; Volkman, 2006; Wenchuan et al., 2009). Whilst this may limit the effective use of *n*-alkan-2-ones as a *Sphagnum* specific biomarker in peat settings, Jansen and Nierop (2009) employed this compound class to confirm the preservation of ancient *n*-alkane distributions in Ecuadorian andosols.

This microbial origin has been attributed to the presence of *n*-alkan-2-ones in lacustrine sediments (Cranwell et al., 1987), however Wenchuan et al. (2009)

suggested that these compounds were derived from blue-green algae and vascular plants in sediments from Taihu Lake in eastern China. In marine settings, the major source of *n*-alkan-2-ones is input from terrestrial OM, while microbial degradation is also noted as a contributor (Volkman, 2006). Hernandez et al. (2001) suggested that *n*-alkan-2-ones could be used as biomarkers for seagrass-derived organic matter in coastal environments.

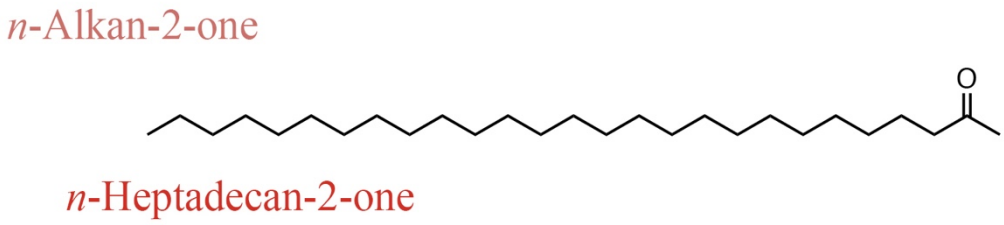

Figure 1.6. Example of an *n*-alkan-2-one structure

1.3.3.4. Alkenones

Alkenones are long-chain unsaturated ketones. They are highly important lipid biomarkers that are most notably used to determine sea surface temperatures (SSTs) in paleoenvironmental studies (Bendle and Rosell-Mele, 2007; Bentaleb et al., 1999; Brassell et al., 1986; Caniupán et al., 2011; Chapman et al., 1996; Conte et al., 1992; Prahl and Wakeham, 1987). Alkenones are ubiquitous in marine sediments throughout the world's oceans and extend back to the pre-pleistocene period (Marlowe et al., 1990; Seki et al., 2007). They are synthesised mainly by certain microalgae of the class *Prymnesiophyceae*, notably the marine coccolithophorids *Emiliania huxleyi* and *Gephyrocapsa oceanica* (Marlowe et al., 1984; Muller et al., 1998; Volkman, 2006). Brassell et al. (1986) introduced the ketone unsaturation index U^{k}_{37} which is calculated from the relative abundances of C_{37} methyl alkenones containing 2-4 double bonds. This was further calibrated by Prahl and Wakeham (1987), and this is the version

employed today (e.g. Muller et al., 1998). This index has been widely used as a paleo-proxy of sea surface temperature (SST) (Eglinton and Eglinton, 2008; Seki et al., 2007).

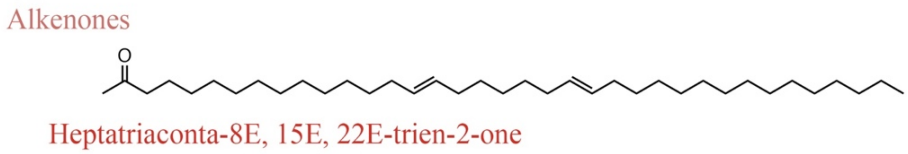

Figure 1.7. Example of an alkenone structure

1.3.3.5. Fatty acids

As fatty acids are found in all organisms they provide information about a multitude of OM sources (Volkman et al., 2008). Long chain *n*-alkanoic ($>C_{20:0}$) acids with an even over odd predominance are significant components of leaf epicuticular waxes (Cranwell et al., 1987; Eglinton and Hamilton, 1967; Shi et al., 2001; Volkman, 2006). Short chain *n*-alkanoic acids ($C_{12:0}$ - $C_{18:0}$) with an even over odd predominance are observed in all plants but are dominant in the lipids of algae and as such are attributed to an aquatic source (P.A. Cranwell et al., 1987; Peters et al., 2005; Shi et al., 2001). The $C_{16:0}$ and $C_{18:0}$ homologues are ubiquitous in the environment (Volkman, 2006). $C_{10:0}$ to $C_{22:0}$ *n*-alkanoic acids have been attributed to fungi, algae, and insects but only in trace amounts (Otto et al., 2005). Saturated and monounsaturated fatty acids (SATFAs and MUFAs respectively) in the range of C_{10} to C_{20} are attributed to bacteria in marine environments, whilst polyunsaturated (PUFAs) are rare (Bergé and Barnathan, 2005). Phytoplankton are the main producers of C_{18} – C_{22} PUFAs in aquatic environments, and as such are found in almost all marine organisms due to transfer through the food web (Burns et al., 2003; Volkman,

2006). PUFAs have also been used as indicators of viable algal cells in recent marine sediments (Shaw and Johns, 1986; Shi et al., 2001). Bacteria are also significant contributors of branched (*iso*- and *anteiso*-) fatty acids (Burns and Brinkman, 2011; Shi et al., 2001; Volkman, 2006). As well as interpretations of the distribution patterns of certain fatty acids, a number of proxies have been developed for source determination including; the sum of $C_{16:0}$ divided by the sum of $C_{18:0}$ as an indicator of zooplankton input, a low ratio of $C_{16:1}$ to $C_{16:0}$ also indicative of zooplankton, and a high ratio of $C_{18:1}\omega_7/C_{18:1}\omega_9 + C_{18:1}\omega_7$ attributed to bacteria (Burns and Brinkman, 2011).

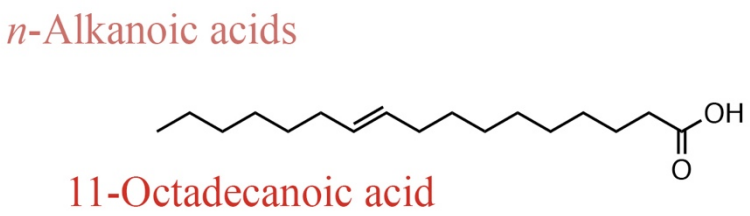

Figure 1.8. Example of an *n*-alkanoic acid structure

1.3.3.6. Phospholipid fatty acids (PLFAs)

Phospholipid fatty acids (PLFAs) are predominantly used as biomarkers in microbial ecology studies (Boschker and Middelburg, 2002; White, 1995; Zelles, 1999). Phospholipids are comprised of a hydrophobic fatty acid ester linked to a hydrophillic phosphate polar head group, and constitute a significant proportion of lipids in the cell membranes of bacteria and eukaryotes (Boschker and Middelburg, 2002; Peters et al., 2005). Phospholipids, present in the polar fractions of lipid extracts, can be cleaved to remove the polar group leaving the PLFA moiety remaining for analysis. In the environment, once a microorganism dies, the phospholipids are rapidly degraded in situ which makes PLFAs a biomarker class which are representative of

only viable microbial biomass (Boschker and Middelburg, 2002; Fang et al., 2006; Pinkart et al., 2002; Ringelberg, 1997; White, 1995; Zelles, 1999).

Certain groups of PLFAs as well as certain individual PLFAs are specific to their source organisms, hence their application in microbial ecology. In general, short to mid chain ($<C_{20}$) branched, cyclic, and odd-chain saturated and unsaturated PLFAs are of bacterial origin (O'Reilly et al., 2016). Unsaturated short-chain PLFAs are indicative of gram negative bacteria (Rajendran et al., 1992; Ringelberg et al., 1997). Saturated and monounsaturated PLFAs in marine environments are generally attributed to phytoplankton whilst polyunsaturated PLFAs are indicative of microeukaryotes (Rajendran et al., 1993, 1992; Zhukova, 2005). More specific interpretation of PLFAs can enable identification of certain microbial communities at genus level. For example, certain PLFAs (e.g. $C_{16:1}\omega_{5c}$, $10MeC_{16:0}$, $cyC_{17:0}\omega_{5,6}$) are specific to sulfate reducing bacteria which are involved in the anaerobic oxidation of methane (AOM). Niemann and Elvert (2008) showed that interpretation of combinations of certain bacterial fatty acids (*i*-$C_{15:0}$, *ai*-$C_{15:0}$, $C_{16:1}\omega_5$, and $cyC_{17:0}\omega_{5,6}$) could distinguish between specific groups of anaerobic methane oxidising microorganisms (ANMEs).

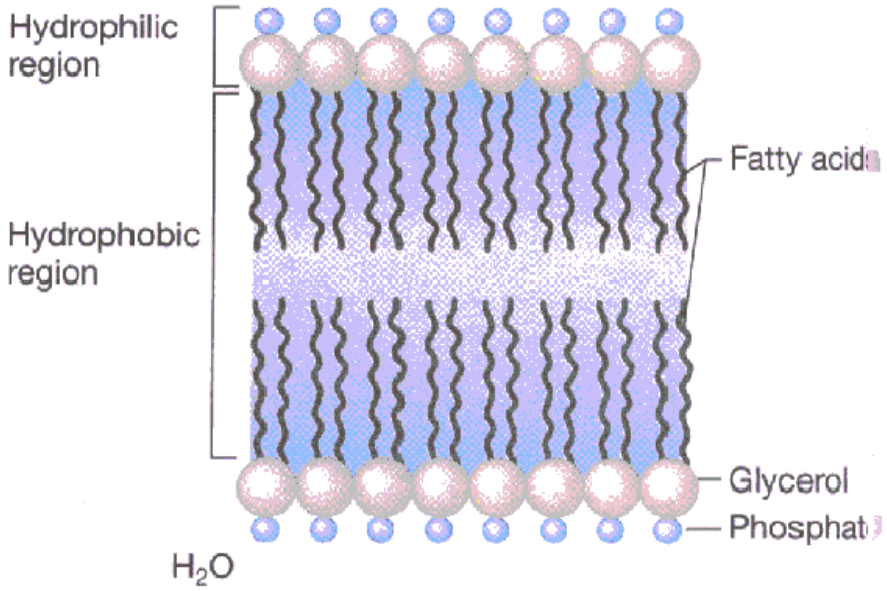

Figure 1.9. Diagram of a phospholipid bilayer in a bacterial membrane (reproduced from Kaur et al., 2005)

1.3.3.7. Sterols

Sterols are tetracyclic triterpenoids which occur in all eukaryotes where they primarily function to regulate membrane fluidity and permeability (Volkman, 2003). Some sterols are relatively ubiquitous such as the C_{27} sterol cholest-5-en-3ß-ol (cholesterol) and therefore have limited diagnostic utility, whilst other sterols can be indicative of large groups of organisms. For example vascular plants are the major source of the C_{29} sterol, 24-ethylcholest-5-en-3ß-ol (ß-sitosterol) (Volkman, 1986) whereas the C_{28} sterol, 24-methylcholesta-5,7,22-trien-3ß-ol (ergosterol) is dominant in fungi (Méjanelle et al., 2000; Otto et al., 2005). However, due to the variations in side chain alkylation, the presence of methyl groups, and double bond position in the ring system many sterols can be assigned to more specific sources (Volkman, 2006, 2005, 1986). Sterols are of limited diagnostic use in studies of terrestrial ecosystems, mainly distinguishing between inputs from plants and fungi. In marine environments sterol diversity is significantly greater allowing for organic matter source assignment

across a range of species of microalgae, fungi, bacteria, and sponges (Lee et al., 1979; Volkman, 2003). For example, 4-methyl sterols and the C_{30} sterol, 4α,23,24-trimethyl-5α-cholest-22E-en-3ß-ol (dinosterol) are biomarkers for dinoflagellates (Volkman, 2003, 2006). The presence of abundant sterols associated with vascular plants such as ß-sitosterol, 24-ethylcholest-5,22-dien-3ß-ol (stigmasterol), and 24-methylcholest-5-en-3ß-ol (campesterol), whilst also present in some marine microalgae, is often interpreted as indicative of the input of terrigenous OM to marine sediments (Hudson et al., 2001; Laureillard and Saliot, 1993; Wen-Yen and Meinschein, 1976).

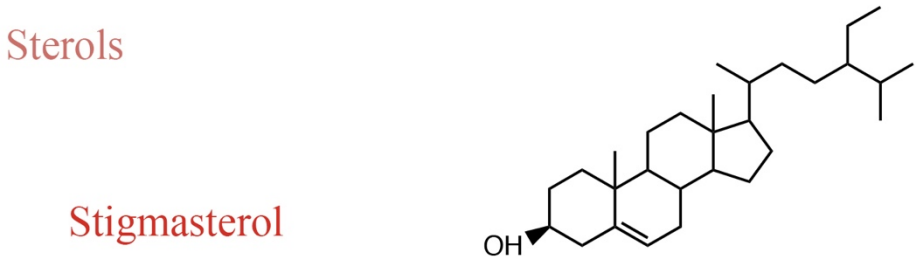

Figure 1.10. Example of a sterol structure

1.3.3.8. Hopanoids

Hopanoids, pentacyclic triterpenoids with a five-membered E-ring (Volkman, 2005), are largely confined to eubacteria although our knowledge of their phylogenetic distribution is incomplete. Bacterial hopanoids, or bacteriohopanepolyols (BHPs), have been found to occur in gram positive bacteria, gram negative bacteria, cyanobacteria, acetic acid bacteria, purple non-sulfur bacteria, nitrogen fixing bacteria, methylotrophs, and methanotrophs (Talbot et al., 2003 and references therein). Ubiquitous in both terrestrial soils and marine sediments, hopanoids are one of the most abundant natural products on Earth (Ourisson and Albrecht, 1992). They have not been detected in archaea or animals, but have been observed in some ferns, mosses, and fungi in small quantities (Mahato and Sen, 1997; Ourisson, 1987). Certain

hopanoids including bacteriohopanetetrol (BHT), appear to be sterol surrogates in bacteria (Ourisson and Rohmer, 1992). Their abundance may vary in response to osmotic stress in the marine sediment environment (e.g. high salinity, sugar, or ethanol concentrations) (Peters et al., 2005). Structural differences in hopanoid compounds can be diagnostic for specific source organisms. For example, methylation of the A-ring at C-2 has been found to occur in cyanobacteria and some alpha-proteobacteria whereas methylation at C-3 is found in some methanotrophs and acetic acid bacteria (Sáenz et al., 2011 and references therein). Summons et al. (1999) suggested that these 2-methylhopanoids indicated the presence of cyanobacteria in ancient sediments and could be used to date the beginning of oxygenic photosynthesis on Earth. Hopanoids are generally restricted to aerobic bacteria although some studies have implicated obligate anaerobes as a source for hopanoids in marine sediments (Pancost et al., 2005; Sinninghe Damsté et al., 2004; Thiel et al., 2003). Hopanoids can be used as indicators of maturity whereby 17ß,21ßH (ßß hopanoids) are linked to immature sediments whereas 17α,21ßH (αß hopanoids) and some 17ß,21αH (ßα hopanoids) are linked to older sediments (Ourisson and Albrecht, 1992). Certain hopanoid palaeoenvironmental proxies have also been developed such as; the total hopane ßß/(ßß + αß + ßα) ratio employed as a measure of maturity (e.g. Inglis et al., 2015), and the C_{35} homohopane index (C_{35} homohopanes/ΣC_{31} – C_{35} homohopanes) employed as an indicator of redox conditions (e.g. Tulipani et al., 2015).

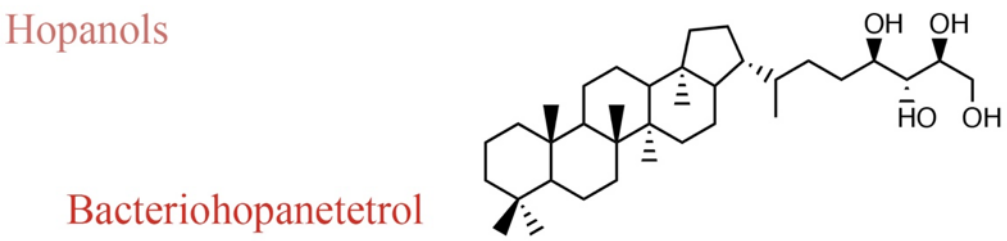

Figure 1.11. Example of a hopanol structure

1.3.3.9. Other terpenoids

Other terpenoids are often identified in extracts of soils and sediments due to their ubiquitous occurrence in higher plants. Distributions of diterpenoids and triterpenoids have been used to distinguish between inputs from conifers and angiosperms respectively in sediments (e.g. Schouten et al., 2007). However, terpenoids are subject to early degradation therefore they are restricted to indicators of modern vegetation inputs. Also, care must be taken to correct for differences in terpenoid production when interpreting these signatures (Diefendorf et al., 2014; Giri et al., 2015). It has been suggested that some terpenoids have more specific diagnostic utility. For example, Pancost et al. (2002) suggested that the pentacyclic triterpenoids taraxerol and taraxer-4-one may be specific biomarkers for *Ericaceae* input to peats. Some diterpenoids and triterpenoids can be employed to differentiate between conifers and angiosperms in palaeovegetation reconstructions (Giri et al., 2015; Otto and Simpson, 2005).

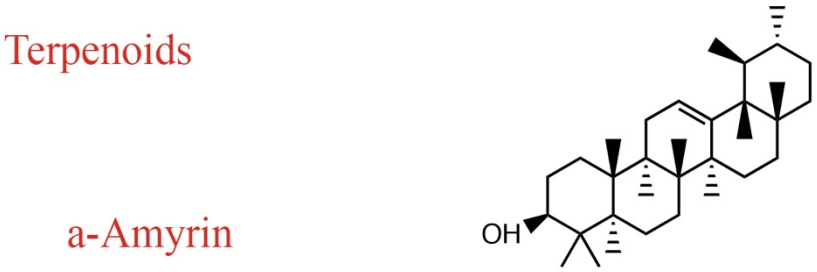

Figure 1.12. Example of a terpenoid structure

1.4. $\delta^{13}C$

1.4.1. Definition and measurement

OM can be further characterised by the interpretation of the isotopic abundances of the C within it. Approximately 98.89% of all C in environment is ^{12}C

whilst 1.11% is ^{13}C (Boutton, 1991a). The ratio of ^{13}C to ^{12}C is particularly useful in organic geochemistry due to the variations in isotopic fractionation pathways which provide unique values depending on the analyte. When reporting stable isotope measurements, data are reported as delta (δ) values (Peters et al., 2005). These δ values signify the deviation of the measured $^{13}C/^{12}C$ result from that of an international standard and are reported in parts per thousand or per mil (‰). The equation for calculating δ values is:

$$\delta^{13}C\ (‰) = [(R_{sample} - R_{standard})/R_{standard}] \times 10^3$$

where R is the isotope abundance ratio of ^{13}C to ^{12}C (Boutton, 1991b; Killops and Killops, 2005; Peters et al., 2005; West et al., 2006). The standard for $\delta^{13}C$ analysis is Vienna Pee Dee Belemnite (VPDB), which replaced the original standard of Peedee Belemnite (PDB) (Coplen, 1995, 1994). The value is that obtained for a carbonate material (NBS-19) whose composition is determined to be $\delta^{13}C = +1.95‰$ relative to the original PDB (Ghosh and Brand, 2003). A sample with a positive $\delta^{13}C$ value is said to be enriched whereas a sample with a negative value is said to be depleted in ^{13}C.

Analysis of the stable isotope ratio is performed using an isotope ratio mass spectrometer (IRMS) (Fig. 1.13.). For analysis of bulk OM the IRMS can be connected to an elemental analyser (EA-IRMS). Bulk soil and sediment samples (5-10 mg) are first acidified to remove inorganic C and combusted in metal capsules (Ag or Sn). During combustion in a furnace (~900 °C) in the presence of an O_2 donor (e.g. CuO) and a catalyst (e.g. Pt), the remaining organic carbon forms CO_2 which is separated

from other evolved gasses (e.g. H_2, NO_2 etc.) on a chromatographic column. This CO_2 reaches the IRMS where its specific $\delta^{13}C$ value is measured.

To investigate the $\delta^{13}C$ values of individual compounds within a sample, a technique known as compound specific isotope analysis (CSIA), a preliminary chromatographic separation is required as well as a combustion step to produce the gaseous analytes amenable to IRMS. To perform this analysis a GC can be coupled to an IRMS with the inclusion of a combustion furnace similar to that employed during EA, a hyphenated analytical technique known as GC combustion IRMS (GC-C-IRMS).

In GC-C-IRMS, as the individual volatile compounds elute from the column they are transported via carrier gas through a combustion furnace containing CuO and Pt. The C component of each compound forms CO_2 and continues through to the ion source of the IRMS, usually an EI source similar to that used in MS systems. The ions produced in the source travel along a flight tube in the presence of a magnetic field and are directed to a triple collector composed of three Faraday cups, each with a different resolving slit width, leading to the detection of varying ion beams from individual elements (i.e. ^{14}C, ^{13}C, and ^{12}C for C). The signals from each of these cups are processed via computer software to provide individual $\delta^{13}C$ values for each compound analysed. For both of these techniques, a standard reference gas (CO_2) is analysed prior to every measurement and assigned a delta value relative to VPDB. $\delta^{13}C$ values of the analytes are obtained via comparison with these reference values.

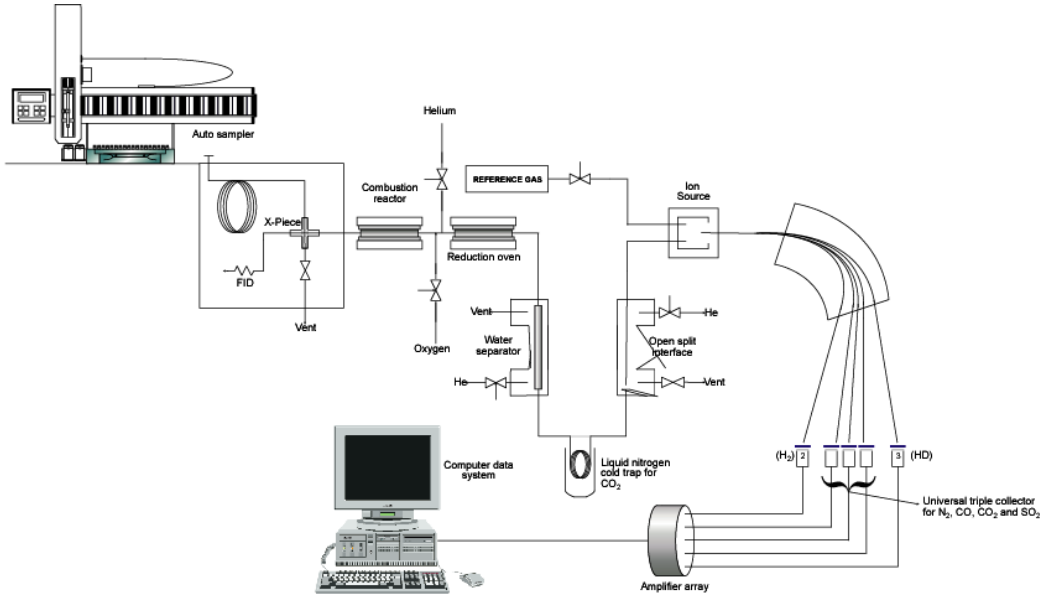

Figure 1.13. Schematic of a GC-C-IRMS system (from Pancost, 2003)

1.4.2. Isotopic fractionation

Atmospheric CO_2 $\delta^{13}C$ values range from -7.8 to -12‰ with variations between locations and seasons (Boutton, 1991b; Friedli et al., 1986; Galimov, 2006; Rieley et al., 1993). Other factors can also affect atmospheric CO_2 $\delta^{13}C$ values over longer time periods such as fossil fuel combustion. Coal, petroleum, and natural gas have mean $\delta^{13}C$ values of -25, -30, and -40‰ respectively resulting in an average value of -26‰ for anthropogenic CO_2 produced during the burning of fossil fuels (Boutton, 1991b). The constant input of this ^{13}C-depleted CO_2 to the atmosphere resulted in a decrease of atmospheric CO_2 $\delta^{13}C$ values by ~1.2‰ (relative to the PDB standard) from the end of the 17th century to 1980 (Friedli et al., 1986), a trend which is most likely continuing.

During the formation of OM certain biological processes favour a particular pathway which discriminates between ^{13}C and ^{12}C, usually favouring the lighter isotope providing a more efficient process (Fig. 1.14.). The $\delta^{13}C$ value of OM reflects

that of its biological origin, therefore isotopic fractionation allows organic geochemists to determine the source of OM in a sample according to its $\delta^{13}C$ value. The majority of plant species and the cyanobacteria utilize the C_3 pathway, the Calvin cycle, for photosynthesis (Galimov, 2006; Killops and Killops, 2005; Meyers, 1997). This pathway involves the fixation of CO_2 to the three-carbon compound phosphoglycerate via the enzyme ribulose-1,5-bisphosphate carboxylase (RuBisCO). This enzyme discriminates against $^{13}CO_2$ resulting in relatively depleted $\delta^{13}C$ values with plants following the C_3 pathway having $\delta^{13}C$ values ranging from -32 to -20‰ with a mean of -27‰ (Boutton, 1991b). High temperatures and low CO_2 levels can lead to loss of energy in C_3 plants due to photorespiration. Plants employing the C_4 and crassulacean acid metabolism (CAM) pathways overcome this issue through additional biochemical pathways which allow CO_2 fixation to occur at night (Collister et al., 1994). C_4 plants fix CO_2 through phosphoenol pyruvate (PEP) carboxylation, a pathway known as the Hatch-Slack cycle (Galimov, 2006). This pathway reduces CO_2 to either of two four-carbon compounds, malic or aspartic acid, and is less discriminatory towards $^{13}CO_2$ resulting in $\delta^{13}C$ values ranging from -17 to -9‰ with a mean of -13‰ (Boutton, 1991b). This lack of overlap in $\delta^{13}C$ values between the C_3 and C_4 pathways allows researchers to distinguish between contributions from these plant types to OM. CAM plants alternate their biochemical pathways, photosynthesizing via the Calvin cycle during the day and the Hatch-Slack cycle at night. As a result, CAM species have isotopic compositions intermediate between C_3 and C_4 plants ranging from -28 to -10‰, most commonly between -20 to -10‰ (Boutton, 1991b; Galimov, 2006).

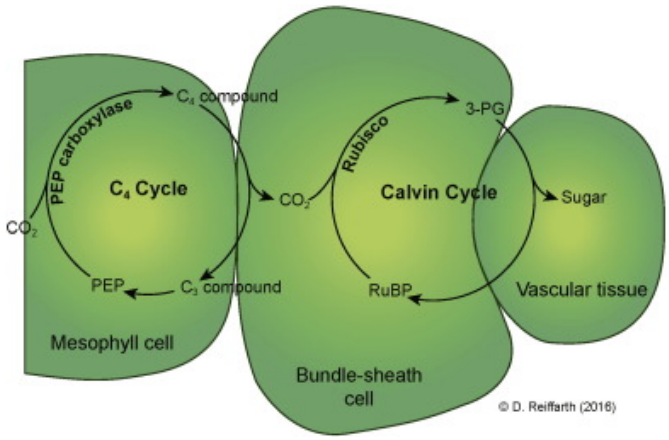

Figure 1.14. CO_2 fixation in C_4 plants proceeds via the C_4 or Hatch-Slack pathway in the mesophyll cells followed by the Calvin Cycle in the bundle-sheath cells. In C_3 plants, fixation occurs via the Calvin Cycle in the mesophyll cells only. (Reproduced from Reiffarth et al., 2016)

Most temperate regions, particularly forests, are dominated by C_3 plants whereas more C_4 and CAM plants are found in arid and semi-arid regions (Badewien et al., 2015; Eglinton and Eglinton, 2008; West et al., 2006). In general, the amount of flora comprised of C_4 species increases with a decrease in latitude and altitude (Boutton, 1991b). C_3 plants are generally trees and shrubs, C_4 plants consist of species like maize, tropical grasses and sedges, and species of desert or savannah vegetation whereas CAM plants consist of succulents such as cacti (Eglinton and Eglinton, 2008; Meyers, 1997; Peters et al., 2005). 119 x Pg of CO_2 carbon per year is fixed by C_3 plants whereas 31 x Pg per year is fixed by C_4 plants (Galimov, 2006; Lloyd and Farquhar, 1994). The annual contribution of CAM species to biomass production is insignificant. The differences in $\delta^{13}C$ values between these biochemical pathways are of particular importance for plaeoclimatic research, providing an insight into climate conditions derived from the identification of plant-type contributions to the OM.

In marine environments photosynthesis proceeds via the C_3 pathway in phytoplankton, however $\delta^{13}C$ values are not always identical to those of terrestrial plant species but are typically near -22‰ (Boutton, 1991b). This is possibly due to the use of dissolved HCO_3 as a carbon source but values can also be altered due to variations in temperature, salinity, and CO_2 availability. CO_2 solubility increases in colder waters leading to higher concentrations of CO_2 available to marine organisms, hence $\delta^{13}C$ values of oceanic plankton increase from high latitudes (-23 to -26‰) through temperate zones (-20 to -23‰) to equatorial waters (-18 to -20‰) (Galimov, 2006). Coastal marine environments prove more complex due to significant contributions from C_3 and C_4 plants as well as phytoplankton.

In freshwater ecosystems most carbon fixation also occurs through the C_3 pathway. Freshwater phytoplankton $\delta^{13}C$ values are however ^{13}C-depleted (-46 to -26‰ in lakes, -30 to -25‰ in rivers) due to the utilization of ^{13}C-depleted dissolved inorganic carbon (DIC) as a carbon source. Vegetation surrounding rivers and lakes consists of almost exclusively C_3 species except in some tropical low-land areas. Subsequently, freshwater wetlands are reflective of this input with OM $\delta^{13}C$ values ~-25‰ (Boutton, 1991b).

These variations in isotopic signatures enable researchers to distinguish between sources of OM in bulk materials. IRMS measurements carried out on CO_2 evolved during the combustion of the total organic carbon (TOC) within a soil or sediment can provide an overview of the predominant source of that material. This is particularly useful when tracing the input of terrigenous material to marine environments. From a palaeoenvironmental perspective, these values can also shed light on changes in vegetation type (e.g. from C_3 to C_4) throughout time which often correlate with climatic variations.

1.4.3. Compound specific stable isotope analysis (CSIA)

Measurement of isotopic fractionation combined with biomarker analysis is a common and effective approach in organic geochemistry (Galimov, 2006). $\delta^{13}C$ values of individual lipid compounds can provide valuable information on the source of organic C at a molecular level (Pancost and Pagani, 2006). This approach is often employed in palaeoenvironmental studies enabling researchers to discern variations in climate which are reflected in changes of vegetation type, with C_3 plants generally representative of cooler more temperate climates whilst C_4 plants commonly favour warmer conditions (Hoefs, 2009; Lamb et al., 2006; Pancost and Boot, 2004). For example, when analysing loess palaeosols in Hungary, CSIA enabled Schatz et al., (2011) to exclude the possibility of the expansion of C_4 grasses within the Carpathian Basin over the past 70 ka.

CSIA data is often obtained for the terrestrial OM in marine and lacustrine settings from which variations in continental climate can be determined. For example, Fornace et al. (2016) analysed stable carbon isotope ratios of *n*-alkanes from a shallow lake in the interior South American tropics in order to track climatic variation over the past 40 ka. They observed distinct changes in vegetation type from C_3 to C_4 that correlated with previous pollen data from the site. CSIA can also determine the influence of marine OM on typical terrestrial OM biomarker signatures. Volkman et al. (2008) adopted this approach to show that whilst seagrasses were a relatively small contributor to the OM in the sediments of a coastal inlet in Western Australia, they were a significant contributor of sitosterol which is commonly used as an indicator of higher plant input to marine settings.

CSIA is a powerful technique in the field of archaeological science as well. Studies employing this technique have led to several discoveries which have proved

to be pivotal in our understanding of early human civilisation (Copley et al., 2005a; Copley et al., 2005b, 2005c). Analysis of individual ($C_{16:0}$ and $C_{18:0}$) fatty acids from ancient potsherds excavated in Kazakhstan provided the earliest evidence of horse milking providing clear evidence of horse domestication ~ 3500 yrs BP (Outram et al., 2009) (Fig. 1.15.).

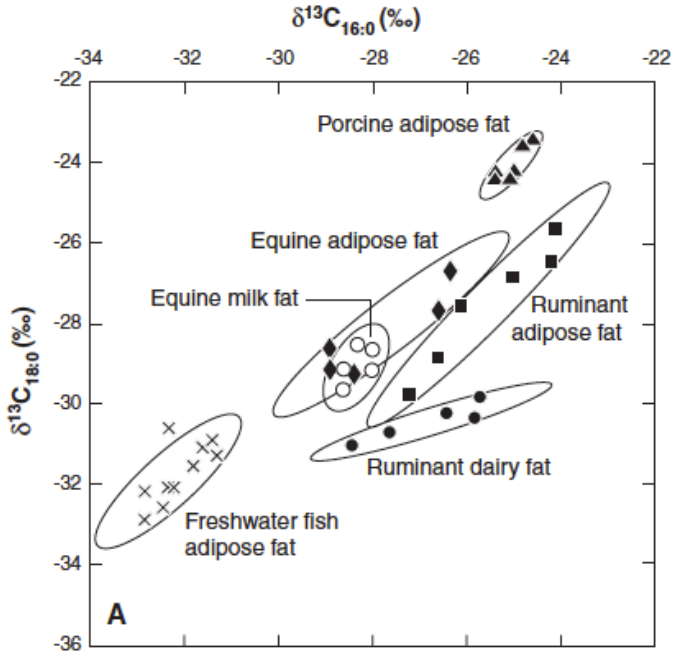

Figure 1.15. Scatterplot of $\delta^{13}C$ values obtained for fatty acids ($C_{16:0}$ and $C_{18:0}$) from archaeological potsherds with labels of identified sources (from Outram et al., 2009)

Carbon isotopic fractionation is particularly useful when carrying out studies in environments that are influenced by the presence of natural methane such as peatlands and marine cold seeps. Natural methane is characterised by significantly depleted $\delta^{13}C$ values ranging from -30 to -110‰ (Niemann and Elvert, 2008). Microbial communities which utilise this gas as a growth substrate via the anaerobic oxidation of methane (AOM) incorporate this depleted C into their biochemistry,

resulting in lipid compounds with relatively low $\delta^{13}C$ values. Identification of diagnostic lipid biomarkers with depleted $\delta^{13}C$ values (lower than -50‰) can therefore be used to analyse AOM communities in modern and ancient environments (Niemann and Elvert, 2008). Depleted $\delta^{13}C$ values have been observed for PLFA biomarkers extracted from marine seabed gas feature sediments (O'Reilly et al., 2014a; Pancost et al., 2007), and also from hopanoid compounds extracted from lignite (ancient wetland) settings (Inglis et al., 2015; Pancost et al., 2007) suggesting the occurrence of AOM in these environments.

It has become increasingly common to utilise CSIA of PLFA to investigate the affects of substrate on microbial populations. This represents a powerful new culture-independent method for environmental microbial ecology (Evershed et al., 2006). To accomplish this, an isotopically labelled substrate is added to a soil or sediment which is incubated for a period of time. This isotopic labelling can either be synthetic, such as ^{13}C sodium acetate (e.g. Arao, 1999) , or natural such as whole tissues or biochemical components derived from C_3 or C_4 vegetation (e.g. Waldrop and Firestone, 2003). Following the incubation, the material is solvent extracted and the polar lipid fraction is analysed by GC-C-IRMS. ^{13}C enriched PLFA identified using CSIA are thus indicative of the microbial species which favour the particular substrate used.

1.5. Applications

Since the publication of Treibs' original work, the field of organic geochemistry has expanded as a scientific discipline and is now an integral component of many research areas including but not limited to; natural resource exploration,

environmental forensics, palaeoclimatology, global carbon cycling, molecular ecology, archaeology, and criminal forensics.

In the modern day natural resource industry, organic geochemical techniques are used for a multitude of analytical purposes including determination of the quality of source rocks, screening of crude oils, and refinery assays amongst others. Hydrocarbon biomarker compounds in an oil sample can also be used as a form of chemical fingerprint to aid in tracing its origin in the case of an oil spill. In 2002, thousands of litres of oil were spilled into the Rouge River (Michigan, USA), and travelled through the Detroit River and on to Lake Eerie. Approximately 43 km of USA and Canadian shorelines were affected (Wang et al., 2004). Using a combination of biomarker compounds including *n*-alkanes and polycyclic aromatic hydrocarbons (PAH) analysed by GC-FID and GC-MS, Wang et al. (2004) identified the material as a mixture of lubrication oil and diesel. This sort of evidence aids law enforcement agencies in tracking polluters. CSIA enables researchers to identify the $\delta^{13}C$ values of hydrocarbons in oil spills which are also a unique fingerprint of the original source (Bayona et al., 2015; Li et al., 2009; Wang et al., 2013, 2007) and have been shown to be relatively resistant to influences of weathering in the environment (Wang et al., 2015, 2007).

PAH are commonly employed as pollution indicators in environmental forensics as they are predominantly of anthropogenic origin and can be toxic. Murphy et al. (2016) used a combination of PAH, faecal steroids, and PLFA to investigate the affect of pollution on microbial communities in Dublin Bay, Ireland. They observed significantly high concentrations of PAH, predominantly from the combustion of fossil fuels, as well as faecal sterols derived from sewage contamination (Fig. 1.16.). The PLFA results suggested that the microbial community structure in Dublin Bay

varied in response to anthropogenic pollution. Lipid biomarker techniques, including PLFA analysis, are increasingly important tools in microbial ecology. Geochemical analysis allows for culture independent studies of the identities and functioning of microorganisms in the environment (Boschker and Middelburg, 2002).

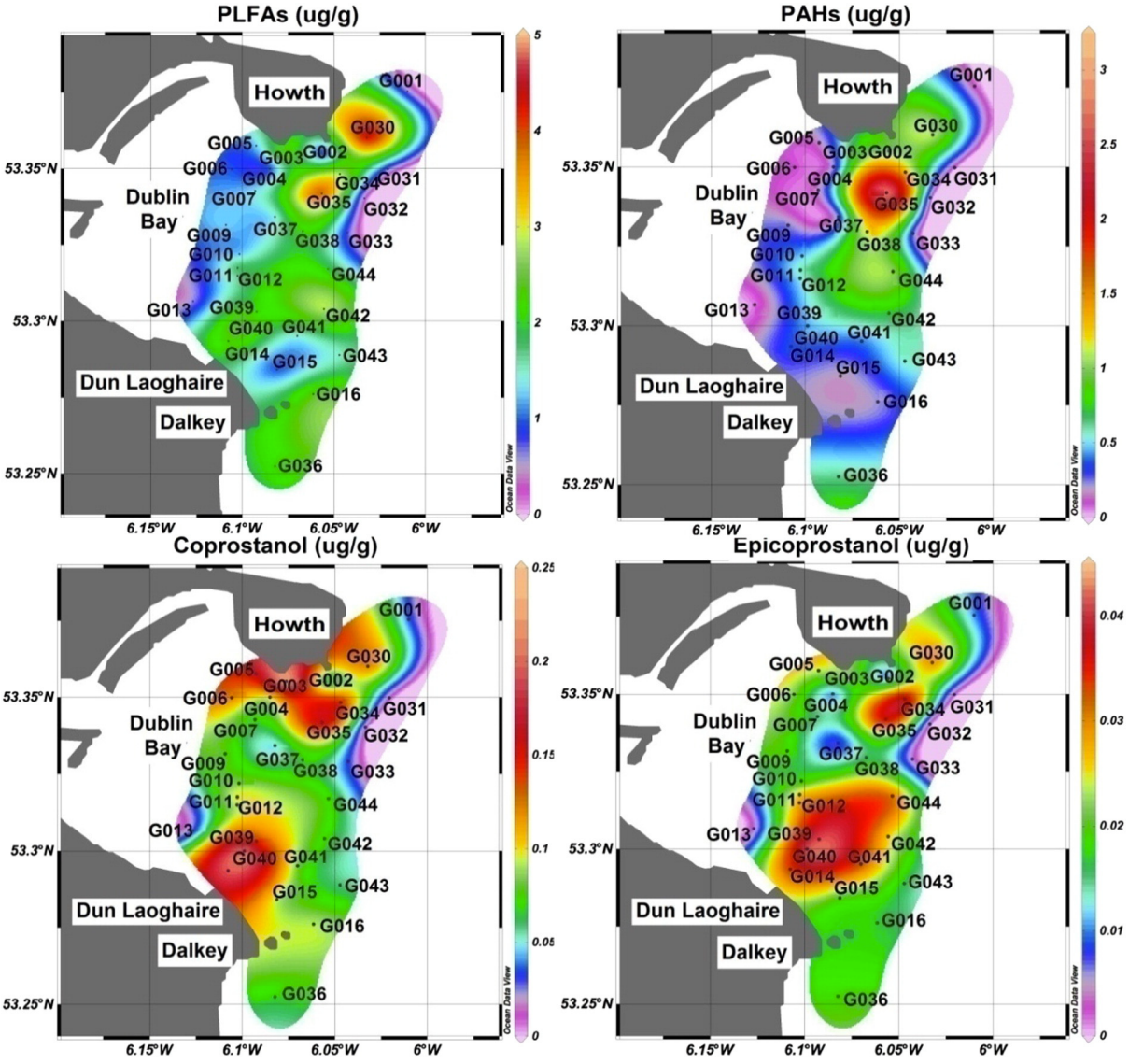

Figure 1.16. Spatial distributions of biomarker compounds (PAH, PLFA, Faecal Sterols) in Dublin Bay (from Murphy et al., 2016)

Organic geochemical techniques are important tools in the field of palaeoclimatology. Knowledge of past climatic variations is essential to our understanding of how the Earth will respond to pressures resulting from climate change in the future. Lipid biomarkers have been used to date the origin of O_2 in our atmosphere (Brocks et al., 1999; Summons et al., 1999), to detect changes in microorganism biochemistry related to temperature fluctuation (Prahl and Wakeham, 1987; Prahl et al., 1988; Rosell-Melé et al., 1995), to determine the extent of sea ice coverage during glacial periods (Belt et al., 2007; Rosell-Mele et al., 1998), and to determine changes in vegetation which are in turn related to atmospheric conditions (Jansen et al., 2013; Schatz et al., 2011; Xie et al., 2004; Zhang et al., 2014). Stable isotope ratios of air bubbles trapped in Arctic and Antarctic ice cores have provided detailed records of atmospheric CO_2 concentration over millennia (Leuenberger et al., 1992).

Knowledge of biogeochemical cycles is also essential in climate change research in order to aid in preventing further global temperature increases. Much of our prediction of future responses to climate change is based on modelling. It is the data collected through environmental analysis that allows these models to function. Carbon storage in the environment is still not fully understood and the potential for this carbon to be released under increasing environmental pressures is of global concern. Carbon has the potential to affect our future climate as increasing temperatures can lead to its release from sensitive reservoirs such as permafrost and marine clathrates (Köhler et al., 2014; Phrampus and Hornbach, 2012). In fact, the Intergovernmental Panel on Climate Change (IPCC) suggest that there is some agreement that a potential combined release totalling up to 350 PgC as CO_2 equivalent

could occur by 2100 (Ciais et al., 2013). Lipid biomarkers and stable isotopes enable researchers to gain insight into these environments at the molecular level.

The analysis of biogeochemical signatures in the environment not only provides information on the natural processes that occurred in the past but also on anthropogenic activity throughout time. In fact, geochemical techniques are being utilised increasingly in archaeological studies and are perhaps only beginning to be embraced by the archaeological community. Faecal steroid compounds in particular, originally employed as biomarkers in pollution investigations, have been used to investigate historical sites (Baeten et al., 2012; Bull et al., 2003, 1999b). Lipid biomarkers have also been used to investigate the dietary behaviour of ancient humans (Sistiaga et al., 2014) and animals (Gill et al., 2009; van Geel et al., 2008) through analysis of coprolite samples. Information on ancient human diet can also be gleaned from analysis of the organic residues found on cooking equipment at archaeological sites (Giorgi et al., 2010; Kherbouche et al., 2016; Mukherjee et al., 2008). Recently, microbially derived biomarker compounds provided evidence of tuberculosis cases in humans in ancient Hungary (Masson et al., 2013; Molnár et al., 2015) thereby adding to the ever expanding amount of geochemical applications in archaeology.

Law enforcement agencies can turn to organic geochemists to aid in forensic investigations. For example, Bull et al. (2009) used a combination of elemental, lipid biomarker, and stable isotope analysis to identify a gravesite that had previously contained the body of a murder victim. Stable isotope techniques have also been shown to be effective in determining the sources of explosive materials for the purpose of forensic investigations (Widory et al., 2009).

1.6. Project overview

The aim of this project was to apply the biomarker approach to a range of research topics and geological settings. As such, these techniques were employed to answer questions in the fields of archaeology, palaeoclimatology, geology, and microbial ecology.

In the year 218 BC, the Carthaginian military commander Hannibal Barca left Carthage with a large army of infantry, cavalry, and war elephants. He travelled through Iberia and crossed the Alps to defy the Roman Empire and invade Italia. Controversy over the exact route taken has continued for over two millennia. Locating this route is of great significance to archaeologists as it offers the prospect of identifying potential sites for excavation that may yield new information on the military culture of ancient Carthage. Using a combination of geoarchaelogical, microbiological, and geochemical techniques it has been possible to unearth indications that may be evidence of Hannibal's path of crossing (Chapter 2).

Following a period of unusually strong winds and high seas in the spring of 2014, a blanket peat bog formerly covered by a beach comprised of fine sand and large rocks was uncovered at a coastal site in Spiddal, Co. Galway, Ireland. The surface of the bog was littered with standing tree stumps, the remnants of a Holocene forest that had succumbed to a relatively sudden drowning. A combination of inorganic and organic geochemical techniques was applied to determine the cause of this rapid submersion and to glean palaeoclimatic information from the preserved record within the peat. The study represents the first use of a multiproxy lipid biomarker approach to investigate palaeoclimate conditions from a peat bog in Ireland (Chapter 3).

During the February 2014 RV Celtic Explorer research expedition as part of the Gateways 2 programme, it was necessary to shelter in Bantry Bay due to a period of rough weather. This was taken as an opportunity to investigate gas seepage sites previously identified by the INFOMAR mapping programme. Seismic signatures indicative of gas seepage within Bantry Bay prompted the geochemical analysis of gas and porewater samples obtained from vibracores taken at the areas of interest. Analysis of gas samples by gas chromatography – flame ionization detection (GC-FID) confirmed CH_4 as the source of the acoustic signatures. Analysis of SO_4^{2-} and H_2S from porewater samples indicates that anaerobic oxidation of methane (AOM) results in the consumption of this gas within the sediment leaving little or no release to the water column, which agrees with geophysical data. Lipid biomarkers were analysed to characterize the microbial communities involved in AOM at this site (Chapter 4).

References

Aquilina, a., Knab, N.J., Knittel, K., Kaur, G., Geissler, a., Kelly, S.P., Fossing, H., Boot, C.S., Parkes, R.J., Mills, R. a., Boetius, a., Lloyd, J.R., Pancost, R.D., 2010. Biomarker indicators for anaerobic oxidizers of methane in brackish-marine sediments with diffusive methane fluxes. Org. Geochem. 41, 414–426. doi:10.1016/j.orggeochem.2009.09.009

Arao, T., 1999. In situ detection of changes in soil bacterial and fungal activities by measuring 13C incorporation into soil phospholipid fatty acids from 13C acetate. Soil Biol. Biochem. 31, 1015–1020. doi:10.1016/S0038-0717(99)00015-2

Azzouz, A., Souhail, B., Ballesteros, E., 2011. Determination of residual pharmaceuticals in edible animal tissues by continuous solid-phase extraction and gas chromatography-mass spectrometry. Talanta 84, 820–8. doi:10.1016/j.talanta.2011.02.016

Baas, M., Pancost, R., Van Geel, B., Sinninghe Damsté, J.S., 2000. A comparative study of lipids in Sphagnum species. Org. Geochem. 31, 535–541. doi:10.1016/S0146-6380(00)00037-1

Badewien, T., Vogts, A., Rullkötter, J., 2015. n–Alkane distribution and carbon stable isotope composition in leaf waxes of C3 and C4 plants from Angola. Org. Geochem. doi:10.1016/j.orggeochem.2015.09.002

Baeten, J., Marinova, E., de Laet, V., Degryse, P., de Vos, D., Waelkens, M., 2012. Faecal biomarker and archaeobotanical analyses of sediments from a public latrine shed new light on ruralisation in Sagalassos, Turkey. J. Archaeol. Sci. 39, 1143–1159. doi:10.1016/j.jas.2011.12.019

Baldock, J.A., Masiello, C.A., Gélinas, Y., Hedges, J.I., 2004. Cycling and composition of organic matter in terrestrial and marine ecosystems. Mar. Chem. 92, 39–64.

Bayona, J.M., Domínguez, C., Albaigés, J., 2015. Analytical developments for oil spill fingerprinting. Trends Environ. Anal. Chem. 5, 26–34. doi:10.1016/j.teac.2015.01.004

Belt, S.T., Massé, G., Rowland, S.J., Poulin, M., Michel, C., LeBlanc, B., 2007. A novel chemical fossil of palaeo sea ice: IP25. Org. Geochem. 38, 16–27. doi:10.1016/j.orggeochem.2006.09.013

Bendle, J. a. P., Rosell-Mele, a., 2007. High-resolution alkenone sea surface temperature variability on the North Icelandic Shelf: implications for Nordic

Seas palaeoclimatic development during the Holocene. The Holocene 17, 9–24. doi:10.1177/0959683607073269

Bentaleb, I., Grimalt, J.O., Vidussi, F., Marty, J.C., Martin, V., Denis, M., Hatté, C., Fontugne, M., 1999. The C37 alkenone record of seawater temperature during seasonal thermocline stratification. Mar. Chem. 64, 301–313. doi:10.1016/S0304-4203(98)00079-6

Bergé, J., Barnathan, G., 2005. as biomarkers , biologically active compounds , and economical aspects Fatty acids from lipids of marine organisms : molecular biodiversity , roles as biomarkers , biologically active compounds , and economical aspects 49–125. doi:10.1007/b135782

Bethell, P.H., Bethell, P.H., Goad, L.J., Goad, L.J., Evershed, R.P., Evershed, R.P., 1994. The Study of Molecular Markers of Human Activity: The Use of Coprostanol in the Soil as an Indicator of Human Faecal Material. J. Archaeol. Sci. doi:10.1006/jasc.1994.1061

Bianchi, T.S., Mitra, S., McKee, B.A., 2002. Sources of terrestrially-derived organic carbon in lower Mississippi River and Louisiana shelf sediments: implications for differential sedimentation and transport at the coastal margin. Mar. Chem. 77, 211–223. doi:10.1016/S0304-4203(01)00088-3

Bligh, E.G., Dyer, W.J., 1959. A RAPID METHOD OF TOTAL LIPID EXTRACTION AND PURIFICATION. Can. J. Biochem. Physiol. 37, 911–917. doi:10.1139/o59-099

Bloom, A.A., Exbrayat, J.-F., van der Velde, I.R., Feng, L., Williams, M., 2016. The decadal state of the terrestrial carbon cycle: Global retrievals of terrestrial carbon allocation, pools, and residence times. Proc. Natl. Acad. Sci. U. S. A. 113, 1285–90. doi:10.1073/pnas.1515160113

Blumenberg, M., Seifert, R., Petersen, S., Michaelis, W., 2007. Biosignatures present in a hydrothermal massive sulfide from the Mid-Atlantic Ridge. Geobiology 5, 435–450. doi:10.1111/j.1472-4669.2007.00126.x

Blumer, M., Guillard, R.R.L., Chase, T., 1971. Hydrocarbons in marine phytoplankton. Mar. Biol. 8, 183–189.

Boschker, H.T.S., Middelburg, J.J., 2002. Stable isotopes and biomarkers in microbial ecology. FEMS Microbiol. Ecol. 40, 85–95. doi:10.1111/j.1574-6941.2002.tb00940.x

Boutton, T.W., 1991a. Stable carbon isotope ratios of natural materials: I. Sample preparation and mass spectrometric analysis. Carbon Isot. Tech. 1, 155.

Boutton, T.W., 1991b. Stable Carbon Isotope Ratios of Natural Materials: II. Atmospheric, Terrestrial, Marine, and Freshwater Environments, in: Coleman, D.C., Fry, B. (Eds.), Carbon Isotope Techniques. Academic Press Inc., London, pp. 173–185.

Brassell, S.C., Eglington, G., Marlowe, I.T., Pflaumann, U., Sarnthein, M., 1986. Molecular stratigraphy: a new tool for climatic assessment. Nature 320, 129–133.

Brocks, J.J., Logan, G.A., Buick, R., Summons, R.E., 1999. Archean Molecular Fossils and the Early Rise of Eukaryotes. Science (80-.). 285, 1033–1036.

Bull, I.D., Berstan, R., Vass, A., Evershed, R.P., 2009. Identification of a disinterred grave by molecular and stable isotope analysis. Sci. Justice 49, 142–9. doi:10.1016/j.scijus.2009.01.016

Bull, I.D., Elhmmali, M.M., Roberts, D.J., Evershed, R.P., 2003. The application of steroidal biomarkers to track the abandonment of a Roman wastewater course at the Agora (Athens, Greece). Archaeometry 45, 149–161. doi:10.1111/1475-

4754.00101

Bull, I.D., Lockheart, M.J., Elhmmali, M.M., Roberts, D.J., Evershed, R.P., 2002. The origin of faeces by means of biomarker detection. Environ. Int. 27, 647–654. doi:10.1016/S0160-4120(01)00124-6

Bull, I.D., Simpson, I. a., van Bergen, P.F., Evershed, R.P., 1999a. Muck'n'molecules: organic geochemical methods for detecting ancient manuring. Antiquity 3, 86–96. doi:10.1017/S0003598X0008786X

Bull, I.D., Simpson, I.A., Dockrill, S.J., Evershed, R.P., 1999b. Organic geochemical evidence for the origin of ancient anthropogenic soil deposits at Tofts Ness, Sanday, Orkney. Org. Geochem. 30, 535–556. doi:10.1016/S0146-6380(99)00020-0

Burns, K. a., Volkman, J.K., Cavanagh, J.-A., Brinkman, D., 2003. Lipids as biomarkers for carbon cycling on the Northwest Shelf of Australia: results from a sediment trap study. Mar. Chem. 80, 103–128. doi:10.1016/S0304-4203(02)00099-3

Burns, K., Brinkman, D., 2011. Organic biomarkers to describe the major carbon inputs and cycling of organic matter in the central Great Barrier Reef region. Estuar. Coast. Shelf Sci. 93, 132–141. doi:10.1016/j.ecss.2011.04.001

Butman, D., Stackpoole, S., Stets, E., McDonald, C.P., Clow, D.W., Striegl, R.G., 2016. Aquatic carbon cycling in the conterminous United States and implications for terrestrial carbon accounting. Proc. Natl. Acad. Sci. U. S. A. 113, 58–63. doi:10.1073/pnas.1512651112

Caniupán, M., Lamy, F., Lange, C.B., Kaiser, J., Arz, H., Kilian, R., Baeza Urrea, O., Aracena, C., Hebbeln, D., Kissel, C., Laj, C., Mollenhauer, G., Tiedemann, R., 2011. Millennial-scale sea surface temperature and Patagonian Ice Sheet

changes off southernmost Chile (53°S) over the past ~60 kyr. Paleoceanography 26, n/a–n/a. doi:10.1029/2010PA002049

Carolan, R., Fornara, D.A., 2016. Soil carbon cycling and storage along a chronosequence of re-seeded grasslands: Do soil carbon stocks increase with grassland age? Agric. Ecosyst. Environ. 218, 126–132. doi:10.1016/j.agee.2015.11.021

Carreira, R.S., Araújo, M.P., Costa, T.L.F., Spörl, G., Knoppers, B. a., 2011. Lipids in the sedimentary record as markers of the sources and deposition of organic matter in a tropical Brazilian estuarine–lagoon system. Mar. Chem. 127, 1–11. doi:10.1016/j.marchem.2011.07.002

Chapman, M.R., Shackleton, N.J., Zhao, M., Eglinton, G., 1996. Faunal and alkenone reconstructions of subtropical North Atlantic surface hydrography and paleotemperature over the last 28 kyr. Paleoceanography. doi:10.1029/96PA00041

Christie, W.W., Han, X., 2010. Lipid Analysis: Isolation, Separation, Identification and Lipidomic Analysis, 4th ed. Oily Press.

Christodoulou, S., Marty, J.-C., Miquel, J.-C., Volkman, J.K., Rontani, J.-F., 2009. Use of lipids and their degradation products as biomarkers for carbon cycling in the northwestern Mediterranean Sea. Mar. Chem. 113, 25–40. doi:10.1016/j.marchem.2008.11.003

Ciais, P., Sabine, C., Bala, G., Bopp, L., Brovkin, V., Canadell, J., Chhabra, A., DeFries, R., Galloway, J., Heimann, M., Jones, C., Le Quéré, C., Myneni, R.B., Piao, S., Thornton, P., 2013. Carbon and Other Biogeochemical Cycles, in: Stocker, T.F., Qin, D., Plattner, G.-K., Tignor, M., Allen, S.K., Boschung, J., Nauels, A., Xia, Y., Bex, V., Midgley, P.M. (Eds.), Climate Change 2013: The

Physical Science Basis. Contribution of Working Group I to the Fifth Assessment Report of the Intergovernmental Panel on Climate Change. Cambridge University Press, Cambridge, U.K and New York, USA, pp. 465–570. doi:10.1017/CBO9781107415324.015

Collister, J.W., Rieley, G., Stern, B., Eglinton, G., Fry, B., 1994. Compound-specific δ 13C analyses of leaf lipids from plants with differing carbon dioxide metabolisms. Org. Geochem. 21, 619–627. doi:10.1016/0146-6380(94)90008-6

Conte, M.H., Eglinton, G., Madureira, L. a S., 1992. Long-chain alkenones and alkyl alkenoates as palaeotemperature indicators: their production, flux and early sedimentary diagenesis in the Eastern North Atlantic. Org. Geochem. 19, 287–298. doi:http://dx.doi.org/10.1016/0146-6380(92)90044-X

Coplen, T.B., 1995. Discontinuance of SMOW and PDB. Nature 375, 285.

Coplen, T.B., 1994. Reporting of stable hydrogen, carbon, and oxygen isotopic abundances. Pure Appl. Chem. 66, 273–276.

Copley, M.S., Berstan, R., Dudd, S.N., Straker, V., Payne, S., Evershed, R.P., 2005. Dairying in antiquity. I. Evidence from absorbed lipid residues dating to the British Iron Age. J. Archaeol. Sci. 32, 485–503. doi:10.1016/j.jas.2004.07.004

Copley, M.S., Berstan, R., Mukherjee, A.J., Dudd, S.N., Straker, V., Payne, S., Evershed, R.P., 2005a. Dairying in antiquity. III. Evidence from absorbed lipid residues dating to the British Neolithic. J. Archaeol. Sci. 32, 523–546. doi:10.1016/j.jas.2004.08.006

Copley, M.S., Berstan, R., Straker, V., Payne, S., Evershed, R.P., 2005b. Dairying in antiquity. II. Evidence from absorbed lipid residues dating to the British Bronze Age. J. Archaeol. Sci. 32, 505–521. doi:10.1016/j.jas.2004.07.005

Coppola, A.I., Druffel, E.R.M., 2016. Cycling of Black Carbon in the Ocean.

Geophys. Res. Lett. 43, 4477–4482. doi:10.1002/2016GL068574

Cranwell, P.A., Eglington, G., Robinson, N., 1987. Lipids of aquatic organismns as potential contributors to lacustrine sediments - II. Org. Geochem. 11, 513–527.

Cranwell, P.A., Eglinton, G., Robinson, N., 1987. Lipids of aquatic organisms as potential contributors to lacustrine sediments—II. Org. Geochem. 11, 513–527. doi:10.1016/0146-6380(87)90007-6

Degens, E.T., 1969. Organic Geochemistry: Methods and Results, in: Eglinton, G., Murphy, M.T.J. (Eds.), . Springer Berlin Heidelberg, Berlin, Heidelberg, pp. 304–329. doi:10.1007/978-3-642-87734-6_14

Diefendorf, A.F., Freeman, K.H., Wing, S.L., 2014. A comparison of terpenoid and leaf fossil vegetation proxies in Paleocene and Eocene Bighorn Basin sediments. Org. Geochem. 71, 30–42. doi:10.1016/j.orggeochem.2014.04.004

Dongen, B.E. Van, Rijpstra, W.I.C., Philippart, C.J.M., Leeuw, J.W. De, Damste, J.S.S., 2000. Biomarkers in upper Holocene Eastern North Sea and Wadden Sea sediments 31, 1533–1543.

Eganhouse, R.P., 1997. Molecular Markers and Environmental Organic Geochemistry: An Overview, in: Eganhouse, R.P. (Ed.), Molecular Markers in Environmental Chemistry. American Chemical Society, p. 426.

Eglinton, G., Calvin, M., 1967. Chemical Fossils. Sci. Am. 216, 32–43.

Eglinton, G., Hamilton, R.J., 1967. Leaf Epicuticular Waxes. Sci. 156 , 1322–1335. doi:10.1126/science.156.3780.1322

Eglinton, T.I., Eglinton, G., 2008. Molecular proxies for paleoclimatology. Earth Planet. Sci. Lett. 275, 1–16. doi:10.1016/j.epsl.2008.07.012

Elhmmali, M.M., Roberts, D.J., Evershed, R.P., 1997. Bile acids as a new class of sewage pollution indicator. Environ. Sci. Technol. 31, 3663–3668.

doi:10.1021/es9704040

Elvert, M., Boetius, A., Knittel, K., Jørgensen, B.B., 2003. Characterization of Specific Membrane Fatty Acids as Chemotaxonomic Markers for Sulfate-Reducing Bacteria Involved in Anaerobic Oxidation of Methane. Geomicrobiol. J. 20, 403–419. doi:10.1080/01490450303894

Evershed, R.P., Crossman, Z.M., Bull, I.D., Mottram, H., Dungait, J.A., Maxfield, P.J., Brennand, E.L., 2006. 13C-Labelling of lipids to investigate microbial communities in the environment. Curr. Opin. Biotechnol. 17, 72–82. doi:10.1016/j.copbio.2006.01.003

Falkowski, P., Scholes, R.J., Boyle, E., Canadell, J., Canfield, D., Elser, J., Gruber, N., Hibbard, K., Högberg, P., Linder, S., Mackenzie, F.T., Moore III, B., Pedersen, T., Rosenthal, Y., Seitzinger, S., Smetacek, V., Steffen, W., 2000. The Global Carbon Cycle: A Test of Our Knowledge of Earth as a System. Science (80-.). 290, 291–296.

Fang, J., Chan, O., Joeckel, R.M., Huang, Y., Wang, Y., Bazylinski, D. a., Moorman, T.B., Ang Clement, B.J., 2006. Biomarker analysis of microbial diversity in sediments of a saline groundwater seep of Salt Basin, Nebraska. Org. Geochem. 37, 912–931. doi:10.1016/j.orggeochem.2006.04.007

Feng, X., Simpson, A.J., Gregorich, E.G., Elberling, B., Hopkins, D.W., Sparrow, A.D., Novis, P.M., Greenfield, L.G., Simpson, M.J., 2010. Chemical characterization of microbial-dominated soil organic matter in the Garwood Valley, Antarctica. Geochim. Cosmochim. Acta 74, 6485–6498. doi:10.1016/j.gca.2010.08.019

Fernandes, M.B., Elias, V.O., Cardoso, J.N., Carvalho, M.S., 1999. Sources and fate of n-alkanols and sterols in sediments of the Amazon shelf. Org. Geochem. 30,

1075–1087. doi:10.1016/S0146-6380(99)00085-6

Ficken, K.J., Barber, K.E., Eglinton, G., 1998. Lipid biomarker, ??13C and plant macrofossil stratigraphy of a Scottish montane peat bog over the last two millennia. Org. Geochem. 28, 217–237. doi:10.1016/S0146-6380(97)00126-5

Flaig, W., 1997. Humic Substances, Peats and Sludges, Humic Substances, Peats and Sludges. Elsevier. doi:10.1016/B978-1-85573-805-8.50038-0

Fornace, K.L., Whitney, B.S., Galy, V., Hughen, K.A., Mayle, F.E., 2016. Late Quaternary environmental change in the interior South American tropics: new insight from leaf wax stable isotopes. Earth Planet. Sci. Lett. 438, 75–85. doi:10.1016/j.epsl.2016.01.007

Friedli, H., Lotscher, H., Oeschger, H., Siegenthaler, U., Stauffer, B., 1986. Ice core record of the 13C/12C ratio of atmospheric CO2 in the past two centuries. Nature 324, 237–238.

Galimov, E.M., 2006. Isotope organic geochemistry. Org. Geochem. 37, 1200–1262. doi:10.1016/j.orggeochem.2006.04.009

Gao, X., Norwood, M., Frederick, C., McKee, A., Masiello, C.A., Louchouarn, P., 2016. Organic geochemical approaches to identifying formation processes for middens and charcoal-rich features. Org. Geochem. 94, 1–11. doi:10.1016/j.orggeochem.2016.01.007

Ghosh, P., Brand, W. a., 2003. Stable isotope ratio mass spectrometry in global climate change research. Int. J. Mass Spectrom. 228, 1–33. doi:10.1016/S1387-3806(03)00289-6

Gill, F.L., Crump, M.P., Schouten, R., Bull, I.D., 2009. Lipid analysis of a ground sloth coprolite. Quat. Res. 72, 284–288. doi:10.1016/j.yqres.2009.06.006

Giorgi, G., Salvini, L., Pecci, A., 2010. The meals in a Tuscan building yard during

the Middle Age. Characterization of organic residues in ceramic potsherds. J. Archaeol. Sci. 37, 1453–1457. doi:10.1016/j.jas.2010.01.005

Giri, S.J., Diefendorf, A.F., Lowell, T. V., 2015. Origin and sedimentary fate of plant-derived terpenoids in a small river catchment and implications for terpenoids as quantitative paleovegetation proxies. Org. Geochem. 82, 22–32. doi:10.1016/j.orggeochem.2015.02.002

Gkinis, V., Simonsen, S.B., Buchardt, S.L., White, J.W.C., Vinther, B.M., 2014. Water isotope diffusion rates from the NorthGRIP ice core for the last 16,000 years – Glaciological and paleoclimatic implications. Earth Planet. Sci. Lett. 405, 132–141. doi:10.1016/j.epsl.2014.08.022

Goesmann, F., Rosenbauer, H., Bredehoft, J.H., Cabane, M., Ehrenfreund, P., Gautier, T., Giri, C., Kruger, H., Le Roy, L., MacDermott, A.J., McKenna-Lawlor, S., Meierhenrich, U.J., Caro, G.M.M., Raulin, F., Roll, R., Steele, A., Steininger, H., Sternberg, R., Szopa, C., Thiemann, W., Ulamec, S., 2015. Organic compounds on comet 67P/Churyumov-Gerasimenko revealed by COSAC mass spectrometry. Science (80-.). 349, aab0689–aab0689. doi:10.1126/science.aab0689

Gold, D.A., Grabenstatter, J., de Mendoza, A., Riesgo, A., Ruiz-Trillo, I., Summons, R.E., 2016. Sterol and genomic analyses validate the sponge biomarker hypothesis. Proc. Natl. Acad. Sci. 113 , 2684–2689. doi:10.1073/pnas.1512614113

Goni, M.A., Hedges, J.I., 1995. Sources And Reactivities Of Marine-Derived Organic-Matter In Coastal Sediments As Determined By Alkaline Cuo Oxidation. Geochim. Cosmochim. Acta 59, 2965–2981.

GREGG, M.W., SLATER, G.F., 2010. A NEW METHOD FOR EXTRACTION,

ISOLATION AND TRANSESTERIFICATION OF FREE FATTY ACIDS FROM ARCHAEOLOGICAL POTTERY. Archaeometry 52, 833–854. doi:10.1111/j.1475-4754.2010.00518.x

Guckert, J.B., Hood, M. a, White, D.C., 1986. Phospholipid ester-linked fatty acid profile changes during nutrient deprivation of Vibrio cholerae: increases in the trans/cis ratio and proportions of cyclopropyl fatty acids. Appl. Environ. Microbiol. 52, 794–801.

Hart, K.M., Kulakova, A.N., Allen, C.C.R., Simpson, A.J., Oppenheimer, S.F., Masoom, H., Courtier-Murias, D., Soong, R., Kulakov, L.A., Flanagan, P. V, Murphy, B.T., Kelleher, B.P., 2013. Tracking the Fate of Microbially Sequestered Carbon Dioxide in Soil Organic Matter. Environ. Sci. Technol. 47, 5128–5137. doi:10.1021/es3050696

Hart, K.M., Szpak, M.T., Mahaney, W.C., Dohm, J.M., Jordan, S.F., Frazer, A.R., Allen, C.C.R., Kelleher, B.P., 2011. A bacterial enrichment study and overview of the extractable lipids from paleosols in the Dry Valleys, Antarctica: implications for future Mars reconnaissance. Astrobiology 11, 303–21. doi:10.1089/ast.2010.0583

Hasumi, H., Nagata, T., 2014. Modeling the global cycle of marine dissolved organic matter and its influence on marine productivity. Ecol. Modell. 288, 9–24. doi:10.1016/j.ecolmodel.2014.05.009

Hawkes, J.A., Rossel, P.E., Stubbins, A., Butterfield, D., Connelly, D.P., Achterberg, E.P., Koschinsky, A., Chavagnac, V., Hansen, C.T., Bach, W., Dittmar, T., 2015. Efficient removal of recalcitrant deep-ocean dissolved organic matter during hydrothermal circulation. Nat. Geosci. 8, 856–860. doi:10.1038/ngeo2543

Hedges, J.I., 1992. Global biogeochemical cycles: progress and problems. Mar. Chem. 39, 67–93. doi:10.1016/0304-4203(92)90096-S

Hedges, J.I., Keil, R.G., Benner, R., 1997. What happens to terrestrial organic matter in the ocean? Org. Geochem. 27, 195–212. doi:10.1016/S0146-6380(97)00066-1

Hedges, J.I., Oades, J.M., 1997. Comparative organic geochemistries of soils and marine sediments. Org. Geochem. 27, 319–361. doi:DOI: 10.1016/S0146-6380(97)00056-9

Hernandez, M.E., Mead, R., Peralba, M.C., Jaffé, R., 2001. Origin and transport of n-alkane-2-ones in a subtropical estuary: potential biomarkers for seagrass-derived organic matter. Org. Geochem. 32, 21–32. doi:10.1016/S0146-6380(00)00157-1

Hoefs, J., 2009. Stable Isotope Geochemistry, 6th ed. Springer-Verlag Berlin Heidelberg, Berlin, Heidelberg.

Hudson, E.D., Parrish, C.C., Helluer, R.J., 2001. Biogeochemistry of sterols in plankton, settling particles and recent sediments in a cold ocean ecosystem (Trinity Bay, Newfoundland). Mar. Chem. 76, 253–270.

Inglis, G.N., Collinson, M.E., Riegel, W., Wilde, V., Robson, B.E., Lenz, O.K., Pancost, R.D., 2015. Ecological and biogeochemical change in an early Paleogene peat-forming environment: Linking biomarkers and palynology. Palaeogeogr. Palaeoclimatol. Palaeoecol. 438, 245–255. doi:10.1016/j.palaeo.2015.08.001

Jansen, B., de Boer, E.J., Cleef, A.M., Hooghiemstra, H., Moscol-Olivera, M., Tonneijck, F.H., Verstraten, J.M., 2013. Reconstruction of late Holocene forest dynamics in northern Ecuador from biomarkers and pollen in soil cores.

Palaeogeogr. Palaeoclimatol. Palaeoecol. 386, 607–619. doi:10.1016/j.palaeo.2013.06.027

Jansen, B., Nierop, K.G.J., 2009. Methyl ketones in high altitude Ecuadorian Andosols confirm excellent conservation of plant-specific n-alkane patterns. Org. Geochem. 40, 61–69. doi:10.1016/j.orggeochem.2008.09.006

Kaiser, J., Ruggieri, N., Hefter, J., Siegel, H., Mollenhauer, G., Arz, H.W., Lamy, F., 2014. Lipid biomarkers in surface sediments from the Gulf of Genoa, Ligurian sea (NW Mediterranean sea) and their potential for the reconstruction of palaeo-environments. Deep Sea Res. Part I Oceanogr. Res. Pap. 89, 68–83. doi:10.1016/j.dsr.2014.04.009

Kaur, A., Chaudhary, A., Kaur, A., Choudhary, R., Kaushik, R., 2005. Phospholipid fatty acid – A bioindicator of environment monitoring and assessment in soil ecosystem. Curr. Sci. 89, 1103–1112.

Kelleher, B.P., Simpson, A.J., 2006. Humic Substances in Soils: Are They Really Chemically Distinct? Environ. Sci. Technol. 40, 4605–4611. doi:10.1021/es0608085

Kherbouche, F., Dunne, J., Merzoug, S., Hachi, S., Evershed, R.P., 2016. Middle Holocene hunting and herding at Gueldaman Cave, Algeria: An integrated study of the vertebrate fauna and pottery lipid residues. Quat. Int. doi:10.1016/j.quaint.2016.01.005

Killops, S., Killops, V., 2005. Introduction to Organic Geochemistry, 2nd ed. Blackwell Science Ltd., Oxford.

Kiriakoulakis, K., Bett, B.J., White, M., Wolff, G. a., 2004. Organic biogeochemistry of the Darwin Mounds, a deep-water coral ecosystem, of the NE Atlantic. Deep Sea Res. Part I Oceanogr. Res. Pap. 51, 1937–1954.

doi:10.1016/j.dsr.2004.07.010

Kirkels, F.M., Jansen, B., Kalbitz, K., 2013. Consistency of plant-specific n-alkane patterns in plaggen ecosystems: A review. The Holocene 23, 1355–1368. doi:10.1177/0959683613486943

Köhler, P., Knorr, G., Bard, E., 2014. Permafrost thawing as a possible source of abrupt carbon release at the onset of the Bølling/Allerød. Nat Commun 5.

Kuhn, T.K., Bowater, A., Grice, K., Gleixner, G., 2010. The occurrence of short chain n-alkanes with an even over odd predominance in higher plants and soils. Org. Geochem. 41, 88–95. doi:10.1016/j.orggeochem.2009.08.003

Lacaze, J.-P.C.L., Stobo, L.A., Turrell, E.A., Quilliam, M.A., 2007. Solid-phase extraction and liquid chromatography--mass spectrometry for the determination of free fatty acids in shellfish. J. Chromatogr. A 1145, 51–7. doi:10.1016/j.chroma.2007.01.053

Lal, R., 2004. Soil Carbon Sequestration Impacts on Global Climate Change and Food Security. Science (80-.). 304, 1623–1627.

Lal, R., Griffin, M., Apt, J., Lave, L., Morgan, M.G., 2004. Managing Soil Carbon. Sci. 304 , 393. doi:10.1126/science.1093079

Lamb, A.L., Wilson, G.P., Leng, M.J., 2006. A review of coastal palaeoclimate and relative sea-level reconstructions using δ13C and C/N ratios in organic material. Earth-Science Rev. 75, 29–57. doi:10.1016/j.earscirev.2005.10.003

Landry, J.-S., Matthews, H.D., 2016. Non-deforestation fire vs. fossil fuel combustion: the source of CO_2 emissions affects the global carbon cycle and climate responses. Biogeosciences 13, 2137–2149. doi:10.5194/bg-13-2137-2016

Laureillard, J., Pinturier, L., Fillaux, J., Saliot, A., 1997. Organic geochemistry of

marine sediments of the Subantarctic Indian Ocean sector : Lipid classes-sources and fate.

Laureillard, J., Saliot, A., 1993. Biomarkers in organic matter produced in estuaries: a case study of the Krka estuary (Adriatic Sea) using the sterol marker series. Mar. Chem. 43, 247–261. doi:10.1016/0304-4203(93)90230-L

Lee, C., Farrington, J.W., Gagosian, R.B., 1979. Sterol geochemistry of sediments from the western North Atlantic Ocean and adjacent coastal areas. Geochim. Cosmochim. Acta 43, 35–46. doi:10.1016/0016-7037(79)90044-9

Lehmann, J., Kleber, M., 2015. The contentious nature of soil organic matter. Nature 528, 60–68.

Leuenberger, M., Siegenthaler, U., Langway, C., 1992. Carbon isotope composition of atmospheric CO2 during the last ice age from an Antarctic ice core. Nature 357, 488–490.

Li, Y., Peacock, a, White, D., Geyer, R., Zhang, C., 2007. Spatial patterns of bacterial signature biomarkers in marine sediments of the Gulf of Mexico. Chem. Geol. 238, 168–179. doi:10.1016/j.chemgeo.2006.11.007

Li, Y., Xiong, Y., Yang, W., Xie, Y., Li, S., Sun, Y., 2009. Compound-specific stable carbon isotopic composition of petroleum hydrocarbons as a tool for tracing the source of oil spills. Mar. Pollut. Bull. 58, 114–7. doi:10.1016/j.marpolbul.2008.08.012

Lin, L.H., Simpson, M.J., 2016. Enhanced extractability of cutin- and suberin-derived organic matter with demineralization implies physical protection over chemical recalcitrance in soil. Org. Geochem. 97, 111–121. doi:10.1016/j.orggeochem.2016.04.012

Lin, T., Wang, L., Chen, Y., Tian, C., Pan, X., Tang, J., Li, J., 2014. Sources and

preservation of sedimentary organic matter in the Southern Bohai Sea and the Yellow Sea: evidence from lipid biomarkers. Mar. Pollut. Bull. 86, 210–8. doi:10.1016/j.marpolbul.2014.07.017

Ling, L.L., Schneider, T., Peoples, A.J., Spoering, A.L., Engels, I., Conlon, B.P., Mueller, A., Schaberle, T.F., Hughes, D.E., Epstein, S., Jones, M., Lazarides, L., Steadman, V.A., Cohen, D.R., Felix, C.R., Fetterman, K.A., Millett, W.P., Nitti, A.G., Zullo, A.M., Chen, C., Lewis, K., 2015. A new antibiotic kills pathogens without detectable resistance. Nature 517, 455–459.

Linn, D.M., Carski, T.H., Brusseau, M.L., 1993. Sorption and Degradation of Pesticides and Organic Chemicals in Soil, SSSA Special Publication. Soil Science Society of America and American Society of Agronomy, Madison, WI. doi:10.2136/sssaspecpub32

Lloyd, J., Farquhar, G., 1994. 13C discrimination during CO2 assimilation by the terrestrial biosphere. Oecologia 99, 201–215. doi:10.1007/BF00627732

Mahato, S.B., Sen, S., 1997. Advances in triterpenoid research, 1990–1994. Phytochemistry 44, 1185–1236. doi:10.1016/S0031-9422(96)00639-5

Marlowe, I.T., Brassell, S.C., Eglington, G., Green, J.C., 1984. Long-chain unsaturated ketones and esters in living algae and marine sediments. Org. Geochem. 6, 135–141.

Marlowe, I.T., Brassell, S.C., Eglinton, G., Green, J.C., 1990. Long-chain alkenones and alkyl alkenoates and the fossil coccolith record of marine sediments. Chem. Geol. 88, 349–375. doi:DOI: 10.1016/0009-2541(90)90098-R

Masson, M., Molnár, E., Donoghue, H.D., Besra, G.S., Minnikin, D.E., Wu, H.H.T., Lee, O.Y.-C., Bull, I.D., Pálfi, G., 2013. Osteological and biomolecular evidence of a 7000-year-old case of hypertrophic pulmonary osteopathy

secondary to tuberculosis from neolithic hungary. PLoS One 8, e78252. doi:10.1371/journal.pone.0078252

McKinney, C.R., McCrea, J.M., Epstein, S., Allen, H.A., Urey, H.C., 1950. Improvements in Mass Spectrometers for the Measurement of Small Differences in Isotope Abundance Ratios. Rev. Sci. Instrum. 21, 724. doi:10.1063/1.1745698

Medeiros, P.M., Simoneit, B.R.T., 2008. Multi-biomarker characterization of sedimentary organic carbon in small rivers draining the Northwestern United States. Org. Geochem. 39, 52–74. doi:10.1016/j.orggeochem.2007.10.001

Méjanelle, L., F. Lòpez, J., Gunde-Cimerman, N., Grimalt, J.O., 2000. Sterols of melanized fungi from hypersaline environments. Org. Geochem. 31, 1031–1040. doi:10.1016/S0146-6380(00)00094-2

Meyers, P.A., 1997. Organic geochemical proxies of paleoceanographic, plaeolimnologic, and plaeoclimatic processes. Org. Geochem. 27, 213–250.

Miller, K.E., Eigenbrode, J.L., Freissinet, C., Glavin, D.P., Kotrc, B., Francois, P., Summons, R.E., 2016. Potential Precursor Compounds for Chlorohydrocarbons Detected in Gale Crater, Mars, by the SAM instrument suite on the Curiosity Rover. J. Geophys. Res. Planets 121, n/a–n/a. doi:10.1002/2015JE004939

Mills, C.T., Dias, R.F., Graham, D., Mandernack, K.W., 2006. Determination of phospholipid fatty acid structures and stable carbon isotope compositions of deep-sea sediments of the Northwest Pacific, ODP site 1179. Mar. Chem. 98, 197–209. doi:10.1016/j.marchem.2005.10.001

Molnár, E., Donoghue, H.D., Lee, O.Y.-C., Wu, H.H.T., Besra, G.S., Minnikin, D.E., Bull, I.D., Llewellyn, G., Williams, C.M., Spekker, O., Pálfi, G., 2015. Morphological and biomolecular evidence for tuberculosis in 8th century AD

skeletons from Bélmegyer-Csömöki domb, Hungary. Tuberculosis (Edinb). 95 Suppl 1, S35–41. doi:10.1016/j.tube.2015.02.032

Mukherjee, A.J., Gibson, A.M., Evershed, R.P., 2008. Trends in pig product processing at British Neolithic Grooved Ware sites traced through organic residues in potsherds. J. Archaeol. Sci. 35, 2059–2073. doi:10.1016/j.jas.2008.01.010

Muller, P.J., Kirst, G., Ruhland, G., von Storch, I., Rosell-Mele, a, 1998. Calibration of the alkenone paleotemperature index U-37(K ') based on core-tops from the eastern South Atlantic and the global ocean (60 degrees N-60 degrees S). Geochim. Cosmochim. Acta 62, 1757–1772. doi:Doi 10.1016/S0016-7037(98)00097-0

Murphy, B.T., O'Reilly, S.S., Monteys, X., Reid, B.F., Szpak, M.T., McCaul, M. V., Jordan, S.F., Allen, C.C.R., Kelleher, B.P., 2016. The occurrence of PAHs and faecal sterols in Dublin Bay and their influence on sedimentary microbial communities. Mar. Pollut. Bull. doi:10.1016/j.marpolbul.2016.02.066

Nakagawa, S., Takai, K., 2008. Deep-sea vent chemoautotrophs: diversity, biochemistry and ecological significance. FEMS Microbiol. Ecol. 65, 1–14. doi:10.1111/j.1574-6941.2008.00502.x

Nichols, J.E., Booth, R.K., Jackson, S.T., Pendall, E.G., Huang, Y., 2006. Paleohydrologic reconstruction based on n-alkane distributions in ombrotrophic peat. Org. Geochem. 37, 1505–1513. doi:10.1016/j.orggeochem.2006.06.020

Nichols, J.E., Huang, Y., 2007a. C23–C31 n-alkan-2-ones are biomarkers for the genus Sphagnum in freshwater peatlands. Org. Geochem. 38, 1972–1976. doi:10.1016/j.orggeochem.2007.07.002

Nichols, J.E., Huang, Y., 2007b. C23-C31 n-alkan-2-ones are biomarkers for the

genus Sphagnum in freshwater peatlands. Org. Geochem. 38, 1972–1976. doi:10.1016/j.orggeochem.2007.07.002

Niemann, H., Elvert, M., 2008. Diagnostic lipid biomarker and stable carbon isotope signatures of microbial communities mediating the anaerobic oxidation of methane with sulphate. Org. Geochem. 39, 1668–1677. doi:10.1016/j.orggeochem.2007.11.003

Nier, A.O., 1947. A Mass Spectrometer for Isotope and Gas Analysis. Rev. Sci. Instrum. 18, 398. doi:10.1063/1.1740961

Nott, C.J., Xie, S., Avsejs, L. a., Maddy, D., Chambers, F.M., Evershed, R.P., 2000. n-Alkane distributions in ombrotrophic mires as indicators of vegetation change related to climatic variation. Org. Geochem. 31, 231–235. doi:10.1016/S0146-6380(99)00153-9

O'Reilly, S.S., Hryniewicz, K., Little, C.T.S., Monteys, X., Szpak, M.T., Murphy, B.T., Jordan, S.F., Allen, C.C.R., Kelleher, B.P., 2014a. Shallow water methane-derived authigenic carbonate mounds at the Codling Fault Zone, western Irish Sea. Mar. Geol. 357, 139–150. doi:10.1016/j.margeo.2014.08.007

O'Reilly, S.S., Pentlavalli, P., Flanagan, P.V., Allen, C.C.R., Monteys, X., Szpak, M.T., Murphy, B.T., Jordan, S.F., Kelleher, B.P., 2016. Abundance and diversity of sedimentary bacterial communities in a coastal productive setting in the Western Irish Sea. Cont. Shelf Res. 113, 1–9. doi:10.1016/j.csr.2015.12.002

O'Reilly, S.S., Szpak, M.T., Flanagan, P. V., Monteys, X., Murphy, B.T., Jordan, S.F., Allen, C.C.R., Simpson, A.J., Mulligan, S.M., Sandron, S., Kelleher, B.P., 2014b. Biomarkers reveal the effects of hydrography on the sources and fate of marine and terrestrial organic matter in the western Irish Sea. Estuar. Coast. Shelf Sci. 136, 157–171. doi:10.1016/j.ecss.2013.11.002

Oades, J.M., 1988. The retention of organic matter in soils. Biogeochemistry 5, 35–70. doi:10.1007/BF02180317

Ortiz, J.E., Díaz-Bautista, A., Aldasoro, J.J., Torres, T., Gallego, J.L.R., Moreno, L., Estébanez, B., 2011. N-Alkan-2-ones in peat-forming plants from the Roñanzas ombrotrophic bog (Asturias, northern Spain). Org. Geochem. 42, 586–592. doi:10.1016/j.orggeochem.2011.04.009

Otto, A., Shunthirasingham, C., Simpson, M.J., 2005. A comparison of plant and microbial biomarkers in grassland soils from the Prairie Ecozone of Canada. Org. Geochem. 36, 425–448. doi:10.1016/j.orggeochem.2004.09.008

Otto, A., Simpson, M.J., 2005. Degradation and Preservation of Vascular Plant-derived Biomarkers in Grassland and Forest Soils from Western Canada. Biogeochemistry 74, 377–409. doi:10.1007/s10533-004-5834-8

Ourisson, G., 1987. Bigger and better hopanoids. Nature 326, 126–127.

Ourisson, G., Albrecht, P., 1992. Hopanoids. 1. Geohopanoids: the most abundant natural products on Earth? Acc. Chem. Res. 25, 398–402. doi:10.1021/ar00021a003

Ourisson, G., Rohmer, M., 1992. Hopanoids. 2. Biohopanoids: a novel class of bacterial lipids. Acc. Chem. Res. 25, 403–408. doi:10.1021/ar00021a004

Outram, A.K., Stear, N.A., Bendrey, R., Olsen, S., Kasparov, A., Zaibert, V., Thorpe, N., Evershed, R.P., 2009. The Earliest Horse Harnessing and Milking. Science (80-.). 323, 1332–1335.

Pagès, A., Schmid, S., Edwards, D., Barnes, S., He, N., Grice, K., 2016. A molecular and isotopic study of palaeoenvironmental conditions through the middle Cambrian in the Georgina Basin, central Australia. Earth Planet. Sci. Lett. 447, 21–32. doi:10.1016/j.epsl.2016.04.032

Pancost, R.D., 2003. Gas chromatography - isotope ratio mass spectrometry (GC-IRMS) instrumentation, in: SIMSUG Short Course on Compound-Specific Isotope Analysis. School of Chemistry, University of Bristol.

Pancost, R.D., Baas, M., Van Geel, B., Sinninghe Damsté, J.S., 2002. Biomarkers as proxies for plant inputs to peats: An example from a sub-boreal ombrotrophic bog. Org. Geochem. doi:10.1016/S0146-6380(02)00048-7

Pancost, R.D., Boot, C.S., 2004. The palaeoclimatic utility of terrestrial biomarkers in marine sediments. New Approaches Mar. Org. Biogeochem. A Tribut. to Life Sci. John I. Hedges 92, 239–261. doi:DOI: 10.1016/j.marchem.2004.06.029

Pancost, R.D., Pagani, M., 2006. Marine Organic Matter: Biomarkers, Isotopes and DNA, in: Volkman, J.K. (Ed.), . Springer Berlin Heidelberg, Berlin, Heidelberg, pp. 209–249. doi:10.1007/698_2_007

Pancost, R.D., Steart, D.S., Handley, L., Collinson, M.E., Hooker, J.J., Scott, A.C., Grassineau, N. V, Glasspool, I.J., 2007. Increased terrestrial methane cycling at the Palaeocene-Eocene thermal maximum. Nature 449, 332–335.

Pancost, R.D., Zhang, C.L., Tavacoli, J., Talbot, H.M., Farrimond, P., Schouten, S., Sinninghe Damsté, J.S., Sassen, R., 2005. Lipid biomarkers preserved in hydrate-associated authigenic carbonate rocks of the Gulf of Mexico. Geobiol. Anc. Mod. Methane-Seeps - Geobiol. Anc. Mod. Methane-Seeps 227, 48–66. doi:DOI: 10.1016/j.palaeo.2005.04.035

Peters, K.E., Walters, C.C., Moldowan, J.M., 2005. The Biomarker Guide. Cambridge.

Phrampus, B.J., Hornbach, M.J., 2012. Recent changes to the Gulf Stream causing widespread gas hydrate destabilization. Nature 490, 527–530.

Pinkart, H.C., Ringelberg, D.B., Piceno, Y.M., MacNaughton, S.J., White, D.C., 2002. Biochemical approaches to biomass measurements and community structure analysis, in: Hurst, C.J., Crawford, R.L., Knudsen, R., MicInerney, M.J., Stetzenbach, L.D. (Eds.), Manual of Environmental Microbiology. ASM Press, Washington, pp. 101–113.

Poynter, J., Eglinton, G., 1990. MOLECULAR COMPOSITION OF THREE SEDIMENTS FROM HOLE 717C : 116, 155–161.

Prahl, F.G., Muehlhausen, L. a, Zahnle, D.L., 1988. Further evaluation of long-chain alkenones as indicators of paleoceanographic conditions. Geochim. Cosmochim. Acta 52, 2303–2310. doi:10.1016/0016-7037(88)90132-9

Prahl, F.G., Wakeham, S.G., 1987. Calibration of unsaturation patterns in long-chain ketone compositions for paleotemperature assessment . Nature 330, 367–369.

Rajendran, N., Matsuda, O., Imamura, N., Urushigawa, Y., 1992. Variation in Microbial Biomass and Community Structure in Sediments of Eutrophic Bays as Determined by Phospholipid Ester-Linked Fatty Acids. Appl. Envir. Microbiol. 58, 562–571.

Rajendran, N., Suwa, Y., Urushigawa, Y., 1993. Distribution of phospholipid ester-linked fatty acid biomarkers for bacteria in the sediment of Ise Bay, Japan. Mar. Chem. 42, 39–56. doi:10.1016/0304-4203(93)90248-M

Reiffarth, D.G., Petticrew, E.L., Owens, P.N., Lobb, D.A., 2016. Sources of variability in fatty acid (FA) biomarkers in the application of compound-specific stable isotopes (CSSIs) to soil and sediment fingerprinting and tracing: A review. Sci. Total Environ. 565, 8–27. doi:10.1016/j.scitotenv.2016.04.137

Rieley, G., Collister, J.W., Stern, B., Eglinton, G., 1993. Gas chromatography/isotope ratio mass spectrometry of leaf wax n-alkalines from

plants of differing carbon dioxide metabolisms. Rapid Commun. Mass Spectrom. 7, 488–491.

Ringelberg, D., 1997. Biomass, bioactivity and biodiversity: microbial ecology of the deep subsurface: analysis of ester-linked phospholipid fatty acids. FEMS Microbiol. Rev. 20, 371–377. doi:10.1016/S0168-6445(97)00019-3

Ringelberg, D.B., Sutton, S., White, D.C., 1997. Biomass, bioactivity and biodiversity: microbial ecology of the deep subsurface: analysis of ester-linked phospholipid fatty acids. FEMS Microbiol. Rev. 20, 371–377. doi:10.1111/j.1574-6976.1997.tb00322.x

Rosell-Mele, a, Jansen, E., Weinelt, M., Sarnthein, M., Koc, N., 1998. Variability of the Arctic front during the last climatic cycle: Application of a novel molecular proxy. Terra Nov. 10, 86–89. doi:10.1046/j.1365-3121.1998.00172.x

Rosell-Melé, A., Eglinton, G., Pflaumann, U., Sarnthein, M., 1995. Atlantic core-top calibration of the U37K index as a sea-surface palaeotemperature indicator. Geochim. Cosmochim. Acta 59, 3099–3107. doi:10.1016/0016-7037(95)00199-A

Sáenz, J.P., Wakeham, S.G., Eglinton, T.I., Summons, R.E., 2011. New constraints on the provenance of hopanoids in the marine geologic record: Bacteriohopanepolyols in marine suboxic and anoxic environments. Org. Geochem. 42, 1351–1362. doi:10.1016/j.orggeochem.2011.08.016

Schatz, A.-K., Zech, M., Buggle, B., Gulyás, S., Hambach, U., Marković, S.B., Sümegi, P., Scholten, T., 2011. The late Quaternary loess record of Tokaj, Hungary: Reconstructing palaeoenvironment, vegetation and climate using stable C and N isotopes and biomarkers. Quat. Int. 240, 52–61. doi:10.1016/j.quaint.2010.10.009

Schmidt, F., Hinrichs, K.-U., Elvert, M., 2010. Sources, transport, and partitioning of organic matter at a highly dynamic continental margin. Mar. Chem. 118, 37–55. doi:10.1016/j.marchem.2009.10.003

Schouten, S., Hopmans, E.C., Sinninghe Damsté, J.S., 2013. The organic geochemistry of glycerol dialkyl glycerol tetraether lipids: A review. Org. Geochem. 54, 19–61. doi:10.1016/j.orggeochem.2012.09.006

Schouten, S., Woltering, M., Rijpstra, W.I.C., Sluijs, A., Brinkhuis, H., Sinninghe Damsté, J.S., 2007. The Paleocene–Eocene carbon isotope excursion in higher plant organic matter: Differential fractionation of angiosperms and conifers in the Arctic. Earth Planet. Sci. Lett. 258, 581–592. doi:10.1016/j.epsl.2007.04.024

Schubert, C.J., Stein, R., 1997. Lipid distribution in surface sediments from the eastern central Arctic Ocean. Mar. Geol. 138, 11–25. doi:10.1016/S0025-3227(97)00017-0

Seierstad, I.K., Abbott, P.M., Bigler, M., Blunier, T., Bourne, A.J., Brook, E., Buchardt, S.L., Buizert, C., Clausen, H.B., Cook, E., Dahl-Jensen, D., Davies, S.M., Guillevic, M., Johnsen, S.J., Pedersen, D.S., Popp, T.J., Rasmussen, S.O., Severinghaus, J.P., Svensson, A., Vinther, B.M., 2014. Consistently dated records from the Greenland GRIP, GISP2 and NGRIP ice cores for the past 104 ka reveal regional millennial-scale δ18O gradients with possible Heinrich event imprint. Quat. Sci. Rev. 106, 29–46. doi:10.1016/j.quascirev.2014.10.032

Seki, O., Harada, N., Sato, M., Kawamura, K., Ijiri, A., Nakatsuka, T., 2012. Assessment for paleoclimatic utility of terrestrial biomarker records in the Okhotsk Sea sediments. Deep Sea Res. Part II Top. Stud. Oceanogr. 61-64, 85–92. doi:10.1016/j.dsr2.2011.03.008

Seki, O., Nakatsuka, T., Kawamura, K., Saitoh, S.-I., Wakatsuchi, M., 2007. Time-series sediment trap record of alkenones from the western Sea of Okhotsk. Mar. Chem. 104, 253–265. doi:DOI: 10.1016/j.marchem.2006.12.002

Shaw, P.M., Johns, R.B., 1986. Organic geochemical studies of a recent Inner Great Barrier Reef sediment—II. Factor analysis of sedimentary organic materials in input source determinations. Org. Geochem. 9, 237–244. doi:10.1016/0146-6380(86)90096-3

Sherman, L.S., Waldbauer, J.R., Summons, R.E., 2007. Improved methods for isolating and validating indigenous biomarkers in Precambrian rocks. Org. Geochem. 38, 1987–2000. doi:10.1016/j.orggeochem.2007.08.012

Shi, W., Sun, M.-Y., Molina, M., Hodson, R.E., 2001. Variability in the distribution of lipid biomarkers and their molecular isotopic composition in Altamaha estuarine sediments: implications for the relative contribution of organic matter from various sources. Org. Geochem. 32, 453–467. doi:10.1016/S0146-6380(00)00189-3

Simkus, D.N., Slater, G.F., Lollar, B.S., Wilkie, K., Kieft, T.L., Magnabosco, C., Lau, M.C.Y., Pullin, M.J., Hendrickson, S.B., Wommack, K.E., Sakowski, E.G., Heerden, E. van, Kuloyo, O., Linage, B., Borgonie, G., Onstott, T.C., 2016. Variations in microbial carbon sources and cycling in the deep continental subsurface. Geochim. Cosmochim. Acta 173, 264–283. doi:10.1016/j.gca.2015.10.003

Sinninghe Damsté, J.S., Rijpstra, W.I.C., Schouten, S., Fuerst, J.A., Jetten, M.S.M., Strous, M., 2004. The occurrence of hopanoids in planctomycetes: implications for the sedimentary biomarker record. Org. Geochem. 35, 561–566. doi:DOI: 10.1016/j.orggeochem.2004.01.013

Sistiaga, A., Berna, F., Laursen, R., Goldberg, P., 2014. Steroidal biomarker analysis of a 14,000 years old putative human coprolite from Paisley Cave, Oregon. J. Archaeol. Sci. 41, 813–817. doi:10.1016/j.jas.2013.10.016

Skjemstad, J.O., Baldock, J.A., 2007. Total and Organic Carbon, in: Carter, M.R., Gregorich, E.G. (Eds.), Soil Sampling and Methods of Analysis, Second Edition. CRC Press, Boca Raton, pp. 225 – 238. doi:doi:10.1201/9781420005271.ch21

Spaulding, N.E., Higgins, J.A., Kurbatov, A. V., Bender, M.L., Arcone, S.A., Campbell, S., Dunbar, N.W., Chimiak, L.M., Introne, D.S., Mayewski, P.A., 2013. Climate archives from 90 to 250ka in horizontal and vertical ice cores from the Allan Hills Blue Ice Area, Antarctica. Quat. Res. 80, 562–574. doi:10.1016/j.yqres.2013.07.004

Spohn, M., Klaus, K., Wanek, W., Richter, A., 2016. Microbial carbon use efficiency and biomass turnover times depending on soil depth – Implications for carbon cycling. Soil Biol. Biochem. 96, 74–81. doi:10.1016/j.soilbio.2016.01.016

SS, O., Hurley, S., Coleman, N., Monteys, X., Szpak, M., O’Dwyer, T., 2012. Chemical and physical features of living and non-living maerl rhodoliths . Aquat. Biol. 15, 215–224.

Stocking, M.A., 2003. Tropical Soils and Food Security: The Next 50 Years. Sci. 302 , 1356–1359. doi:10.1126/science.1088579

Strong, D., Flecker, R., Valdes, P.J., Wilkinson, I.P., Rees, J.G., Michaelides, K., Zong, Y.Q., Lloyd, J.M., Yu, F.L., Pancost, R.D., 2013. A new regional, mid-Holocene palaeoprecipitation signal of the Asian Summer Monsoon. Quat. Sci. Rev. 78, 65–76. doi:10.1016/j.quascirev.2013.07.034

Summit, M., Peacock, A., Ringelberg, D., White, D.C., Baross, J.A., 2000. Phospholipid fatty acid-derived microbial biomass and community dynamics in hot, hydrothermally influenced sediments from Middle Valley, Juan de Fuca Ridge, in: Zierenberg, R.A., Fouquet, Y., Miller, D.J., Normarck, W.R. (Eds.), Proceedings of the Ocean Drilling Program, Scientific Results. pp. 1–19.

Summons, R.E., Jahnke, L.L., Hope, J.M., Logan, G.A., 1999. 2-Methylhopanoids as biomarkers for cyanobacterial oxygenic photosynthesis. Nature 400, 554–557.

Talbot, H.M., Watson, D.F., Pearson, E.J., Farrimond, P., 2003. Diverse biohopanoid compositions of non-marine sediments. Org. Geochem. 34, 1353–1371. doi:10.1016/S0146-6380(03)00159-1

Taube, P.S., Hansel, F.A., Madureira, L.A. dos S., Teixeira, W.G., 2013. Organic geochemical evaluation of organic acids to assess anthropogenic soil deposits of Central Amazon, Brazil. Org. Geochem. 58, 96–106. doi:10.1016/j.orggeochem.2013.02.004

Thiel, V., Blumenberg, M., Pape, T., Seifert, R., Michaelis, W., 2003. Unexpected occurrence of hopanoids at gas seeps in the Black Sea. Org. Geochem. 34, 81–87. doi:DOI: 10.1016/S0146-6380(02)00191-2

Treibs, A., 1936. Chlorophyll- und Häminderivate in organischen Mineralstoffen. Angew. Chemie 49, 682–686. doi:10.1002/ange.19360493803

Tulipani, S., Grice, K., Greenwood, P.F., Haines, P.W., Sauer, P.E., Schimmelmann, A., Summons, R.E., Foster, C.B., Böttcher, M.E., Playton, T., Schwark, L., 2015. Changes of palaeoenvironmental conditions recorded in Late Devonian reef systems from the Canning Basin, Western Australia: A biomarker and stable isotope approach. Gondwana Res. 28, 1500–1515.

doi:10.1016/j.gr.2014.10.003

van Dongen, B.E., Semiletov, I., Weijers, J.W.H., Gustafsson, Ö., 2008. Contrasting lipid biomarker composition of terrestrial organic matter exported from across the Eurasian Arctic by the five great Russian Arctic rivers. Global Biogeochem. Cycles 22, n/a–n/a. doi:10.1029/2007GB002974

van Geel, B., Aptroot, A., Baittinger, C., Birks, H.H., Bull, I.D., Cross, H.B., Evershed, R.P., Gravendeel, B., Kompanje, E.J.O., Kuperus, P., Mol, D., Nierop, K.G.J., Pals, J.P., Tikhonov, A.N., van Reenen, G., van Tienderen, P.H., 2008. The ecological implications of a Yakutian mammoth's last meal. Quat. Res. 69, 361–376. doi:10.1016/j.yqres.2008.02.004

Volkman, J., 2003. Sterols in microorganisms. Appl. Microbiol. Biotechnol. 60, 495–506. doi:10.1007/s00253-002-1172-8

Volkman, J.K., 2006. Lipid Markers for Marine Organic Matter, in: Volkman, J.K. (Ed.), Marine Organic Matter: Biomarkers, Isotopes and DNA. Springer, p. 374.

Volkman, J.K., 2005. Sterols and other triterpenoids: source specificity and evolution of biosynthetic pathways. Org. Geochem. 36, 139–159. doi:10.1016/j.orggeochem.2004.06.013

Volkman, J.K., 1986. A review of sterol markers for marine and terrigenous organic matter. Org. Geochem. 9, 83–99. doi:DOI: 10.1016/0146-6380(86)90089-6

Volkman, J.K., Barrett, S.M., Dunstan, G.A., Jeffrey, S.W., 1993. Geochemical significance of the occurrence of dinosterol and other 4-methyl sterols in a marine diatom. Org. Geochem. 20, 7–15. doi:10.1016/0146-6380(93)90076-N

Volkman, J.K., Revill, A.T., Holdsworth, D.G., Fredericks, D., 2008. Organic matter sources in an enclosed coastal inlet assessed using lipid biomarkers and stable isotopes. Org. Geochem. 39, 689–710. doi:10.1016/j.orggeochem.2008.02.014

Waldrop, M.P., Firestone, M.K., 2003. Microbial community utilization of recalcitrant and simple carbon compounds: impact of oak-woodland plant communities. Oecologia 138, 275–284. doi:10.1007/s00442-003-1419-9

Walther, J.V., 2009. Essentials of Geochemistry, 2nd ed. Jones and Bartlett Publishers, LLC.

Wang, C., Chen, B., Zhang, B., He, S., Zhao, M., 2013. Fingerprint and weathering characteristics of crude oils after Dalian oil spill, China. Mar. Pollut. Bull. 71, 64–8. doi:10.1016/j.marpolbul.2013.03.034

Wang, M., Wang, C., He, S., 2015. Source Identification of Oil Spills Using Compound-Specific Carbon Isotope Analysis Based on "7–16" Oil Spill in Dalian, China. Aquat. Procedia 3, 197–202. doi:10.1016/j.aqpro.2015.02.211

Wang, Y., Fang, X., Zhang, T., Li, Y., Wu, Y., He, D., Wang, Y., 2010. Predominance of even carbon-numbered n-alkanes from lacustrine sediments in Linxia Basin, NE Tibetan Plateau: Implications for climate change. Appl. Geochemistry 25, 1478–1486. doi:10.1016/j.apgeochem.2010.07.002

Wang, Z., Fingas, M., Lambert, P., Zeng, G., Yang, C., Hollebone, B., 2004. Characterization and identification of the Detroit River mystery oil spill (2002). J. Chromatogr. A 1038, 201–214. doi:10.1016/j.chroma.2004.03.004

Wang, Z., Stout, S.A., W.A. Jeffrey, A., 2007. Oil Spill Environmental Forensics, Oil Spill Environmental Forensics. Elsevier. doi:10.1016/B978-012369523-9.50010-0

Weiping, H., Jørgensen, S.E., Fabing, Z., Yonggen, C., Zhixin, H., Longyuan, Y., 2011. A model on the carbon cycling in Lake Taihu, China. Ecol. Modell. 222, 2973–2991. doi:10.1016/j.ecolmodel.2011.04.018

Wen-Yen, H., Meinschein, W.., 1976. Sterols as source indicators of organic

materials in sediments. Geochim. Cosmochim. Acta 40, 323–330. doi:10.1016/0016-7037(76)90210-6

Wenchuan, Q., Dickman, M., Sumin, W., Ruijin, W., Pingzhong, Z., Jianfa, C., 2009. Evidence for an aquatic plant origin of ketones found in Taihu Lake sediments. Hydrobiologia 397, 149–154. doi:10.1023/A:1003624625076

West, J.B., Bowen, G.J., Cerling, T.E., Ehleringer, J.R., 2006. Stable isotopes as one of nature's ecological recorders. Trends Ecol. Evol. 21, 408–414. doi:10.1016/j.tree.2006.04.002

White, D.C., 1995. Chemical Ecology: Possible Linkage between Macro- and Microbial Ecology. Oikos 74, 177–184. doi:10.2307/3545646

White, D.C., Ringelberg, D.B., 1998. Signature Lipid Biomarker Analysis, in: Burlage, R.S., Atlas, R., Stahl, D., Geesey, G., Sayler, G. (Eds.), Techniques in Microbial Ecology. Oxford University Press, New York, pp. 255–272.

Widory, D., Minet, J.-J., Barbe-Leborgne, M., 2009. Sourcing explosives: a multi-isotope approach. Sci. Justice 49, 62–72. doi:10.1016/j.scijus.2008.11.001

Xie, S., Nott, C.J., Avsejs, L. a., Maddy, D., Chambers, F.M., Evershed, R.P., 2004. Molecular and isotopic stratigraphy in an ombrotrophic mire for paleoclimate reconstruction. Geochim. Cosmochim. Acta 68, 2849–2862. doi:10.1016/j.gca.2003.08.025

Zelles, L., 1999. Fatty acid patterns of phospholipids and lipopolysaccharides in the characterisation of microbial communities in soil: a review. Biol. Fertil. Soils 29, 111–129. doi:10.1007/s003740050533

Zhang, Y., Liu, X., Lin, Q., Gao, C., Wang, J., Wang, G., 2014. Vegetation and climate change over the past 800years in the monsoon margin of northeastern China reconstructed from n-alkanes from the Great Hinggan Mountain

ombrotrophic peat bog. Org. Geochem. 76, 128–135. doi:10.1016/j.orggeochem.2014.07.013

Zhukova, N. V, 2005. Variation in microbial biomass and community structure in sediments of peter the great bay (sea of japan/east sea), as estimated from fatty acid biomarkers. Ocean Sci. J. 40, 34–42. doi:10.1007/BF03022608

Chapter 2

Chasing Hannibal: Using geochemical techniques to aid in tracing the route taken by the Carthaginian general to invade Italia in 218 BC

Abstract

In 218 BC, the Carthaginian general Hannibal Barca led his army from New Carthage in Iberia across the Pyrenees and the Alps to invade Italia, the stronghold of the Roman Empire. The purpose of crossing the dangerous terrain of the Alps, a feat considered impossible at the time, was to catch the Romans by surprise. The exact route of this crossing has been the source of contention ever since. Analysis of faecal biomarker compounds was carried out in order to provide evidence that the army led by Hannibal had passed through the Guil Valley and Col de la Traversette in the Italian Alps as originally outlined by Sir Gavin de Beer (De Beer 1967). Samples taken from a grassy mire within the valley postulated to be a possible resting place for the army during their crossing were investigated. The presence of 5ß-stigmastanol and deoxycholic acid, common biomarkers for herbivorous mammalian faecal input, was observed in all samples within the mire. A significant spike in concentration which correlates with the ^{14}C date of Hannibal's crossing suggests that there was in fact a large amount of animal activity in this area at that time. This result forms part of a multidisciplinary body of evidence including historical, geological, and microbiological analyses which point to this route as the one taken by Hannibal Barca.

2.1. Introduction

2.1.1. Hannibal's crossing

In this study, geochemical techniques were employed to provide evidence on the actual route taken by the Carthaginian general, Hannibal Barca, as he led his army to invade Italia in 218 BC. There are three main paths proposed as the original route taken by Hannibal (Fig. 2.1.) (Mahaney et al. 2010a). These routes contain separate cols as the transit points into Italia and are referred to as the northern, southern, and intermediate routes (Mahaney et al. 2008b). The northern route (Lazenby 1998, Hart 1967) suggests passage by either the Col du Mont Cenis or the Col du Clapier, whilst the intermediate route (Connolly 1981) passes through the Col de Montgenevre. Both of these routes rely purely on analysis of topography and previous historical arguments, taken from the interpretation of texts written by classical historians Polybius (Scott-Kilvert 1980) and Livy (De Selincourt 1965) (Mahaney et al. 2008a). The third route was proposed by Sir Gavin De Beer and passes through the Guil Valley and the Col de la Traversette, exiting into the upper Po River catchment of Northern Italia (De Beer 1967). This southern route is the only route that is based on the ground truthing of specific environmental landmarks from the classical literature as well as original arguments and the topography of the area (Mahaney et al. 2008).

Investigations of the environmental parameters essential for identifying the route and specific locations for archaeological excavation (Mahaney 2004, Mahaney 2008, Mahaney 2013) appear to agree with De Beer's route. These investigations include the identification of a two-tiered rockfall reported by both Polybius and Livy as having blocked the path of Hannibal's army (Mahaney et al. 2010). Recently,

geomorphological investigations, including the identification of a 'previous landslide' described by Polybius, have provided further evidence that this was in fact the most likely course taken by the Carthaginian Army (Mahaney et al. 2014a, Mahaney et al. 2014b, Mahaney et al. 2008a, Mahaney et al. 2008b, Mahaney et al. 2010a, Mahaney et al. 2010b, Mahaney et al. 2008c). Identification of the exact route taken will aid full-scale archaeological excavations, potentially leading to discoveries of artifacts that could help us to better understand the military culture of Ancient Carthage (Mahaney et al. 2008b).

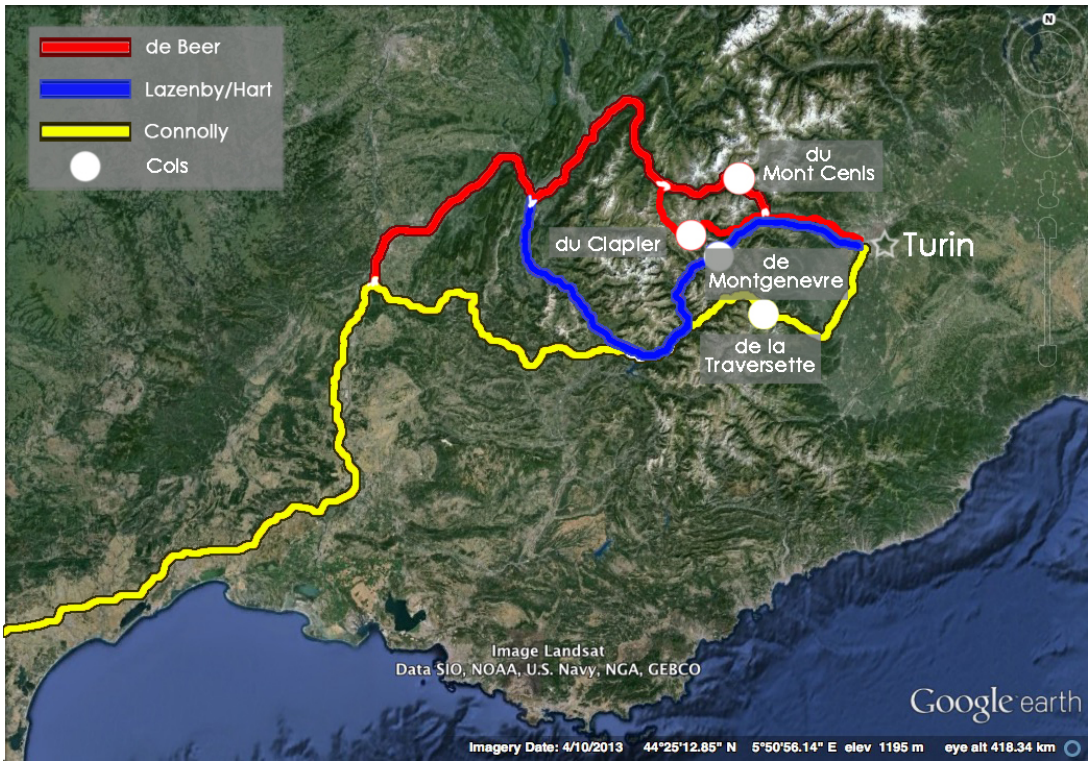

Figure 2.1. Satellite image (courtesy Google Earth) marked with the three main routes attributed to Hannibal's invasion.

Figure 2.2. Grassy mire site (Guil 5), excavations to right of centre. Reproduced from Mahaney et al. (2014b).

Whilst surveying the Guil Valley section of the route, a grassy mire (Fig. 2.2.) was located which could have potentially provided grazing and water for animals and soldiers (Mahaney et al. 2014). Cored soil samples were taken from this and surrounding areas and sub-sampled for multidisciplinary palaeo-environmental analysis. Here we present organic geochemical evidence that contributes to the debate and supports the view that the route taken by Hannibal was the southern route through the Guil Valley and the Col de la Traversette and not the northern or intermediate routes.

2.1.2. Faecal biomarkers

The identification of faecal biomarkers in soils and sediments can shed light on past anthropogenic activity (e.g. (Baeten et al. 2012, Bethell et al. 1994, Bull et

al. 2003, Bull et al. 1999, Evershed et al. 1997)). The methods used for detecting faecal input to environmental samples arise from research in the area of sewage pollution monitoring (Birk et al. 2012, Elhmmali et al. 1997, Elhmmali et al. 2000). There are two main groups of compounds used to monitor sewage pollution; 5ß-stanols and bile acids (Bull et al. 2002). Both of these classes of compounds are relatively resistant to degradation and have been used to detect faecal contamination in a variety of archaeological contexts (Baeten et al. 2012, Bethell et al. 1994, Birk et al. 2011, Bull et al. 2003, Bull et al. 1999, Evershed et al. 1997). These compounds are used not only as indicators of the presence of faecal material, but also to identify its origin (Bull et al. 2002). Knowledge of the source of faecal material in archaeological samples can shed light on ancient rural and urban land use in known human settlements (Baeten et al. 2012, Bethell et al. 1994, Bull et al. 2003, Shillito et al. 2011), but it can also allow for the detection of ancient activity in areas we know little about.

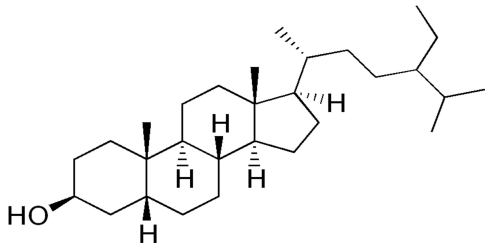

5ß-Stigmastanol

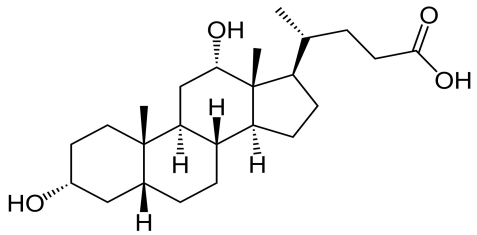

Deoxycholic acid

Figure 2.3. Structures of two faecal biomarker compounds.

2.1.3. 5ß-stanols

5ß-stanols are microbially mediated reduction products of higher molecular weight sterols (Δ^5-sterols) e.g. cholesterol, stigmasterol, campesterol etc. (Bull et al. 2002). This reduction process occurs in the intestinal tract of humans and most other higher mammals (Bethell et al. 1994). The major 5ß-stanol in human faeces is 5ß-cholestan-3ß-ol (coprostanol), which is the reduction product of the C_{27} sterol cholesterol and is therefore the main biomarker for human faecal pollution (Elhmmali et al. 2000, Bull et al. 1999, Bethell et al. 1994). 24-ethyl-5ß-cholestan-3ß-ol (5ß-stigmastanol) is a derivative of the C_{29} sterol sitosterol, a major sterol in higher plants (Fig. 2.3.) (Evershed et al. 1997). Thus 5ß-stigmastanol is one of the main biomarkers for herbivorous mammalian faecal material (Birk et al. 2011, Bull et al. 2002, Baeten et al. 2012, Leeming et al. 1996, Evershed et al. 1997). In the environment, Δ^5-sterols are mainly converted to 5α-stanols, however a minor proportion can also be converted to 5ß-stanols (Bull et al. 2002, Bull et al. 1999, Birk et al. 2011). When investigating faecal contamination the following ratio was proposed to evaluate the anthropogenic input to samples, with the values of 0.3 and 0.7 representative of the absence and presence of faecal contamination respectively (Grimalt 1990):

5ß-cholestan-3ß-ol:(5ß-cholestan-3ß-ol + 5α-cholestan-3ß-ol)

This ratio was later modified by (Bull 1997) for use in archaeological studies to account for the diagenetic transformation of coprostanol to the epimer 5ß-cholestan-3α-ol, without which the final ratio value in archaeological soils could be underestimated:

(5ß-cholestan-3ß-ol + 5ß-cholestan-3α-ol)/(5ß-cholestan-3ß-ol + 5ß-cholestan-3α-ol + 5α-cholestan-3ß-ol)

This ratio is also applicable to 5ß-stigmastanol in order to confirm the herbivorous origin of faecal material in soils and sediments with the epimer and 5α homologue replaced accordingly (24-ethyl-5ß-cholestan-3α-ol and 24-ethyl-5α-cholestan-3ß-ol respectively). Baeten et al. (2012) used both of the above ratios when studying a public latrine in Sagalassos, Turkey and observed a shift from human to animal faecal input over time, which they attributed to the ruralisation of the city.

2.1.4. Bile acids

Bile acids were first introduced as a molecular indicator of faecal pollution by Elhmmali et al. (1997). Primary bile acids are produced in the liver and subsequently enter the intestinal tract where they are transformed by microorganisms into secondary bile acids, a proportion of which are excreted from the body (Bull et al. 2002). It is these secondary bile acids such as deoxycholic acid (DCA) (Fig. 2.3.) and lithocholic acid (LCA) which are used to determine the presence and source of faecal material (Bull et al. 2002, Baeten et al. 2012, Bull et al. 1999, Bull et al. 2003, Elhmmali et al. 1997, Elhmmali et al. 2000, Goñi et al. 1998). DCA is the primary component in the faecal material of omnivores (e.g. humans) and some higher mammals (Elhmmali et al. 2000). Human faecal material also contains a significant amount of LCA whereas DCA is the dominant bile acid in the faeces of ruminant organisms (Bull et al. 1999, Bull et al. 2002, Tyagi et al. 2008). Therefore,

comparison of bile acid concentrations in soils and sediments can enable researchers to distinguish between sources of faecal contamination (Bull et al. 2002).

2.2. Study area

2.2.1. Sampling site

Soil samples were retrieved from a grassy mire situated 2581 m asl in the Italian Alps west of the Col de la Traversette, in the upper Guil Valley leading to the Po River catchment area (GPS - 44°42587N; 07°03274E) (Fig. 2.1.). The mire site lies adjacent to the headwaters of the Guil River and is subject to periodic overbank sedimentation as well as groundwater invasion in the lower beds. In a 2011 expedition two cores were taken from within the mire for mineralogical and microbiological analyses as well as ^{14}C dating. Eight samples were taken from different locations within the Guil Valley. A second expedition took place in 2013 wherein a ~ 65 cm deep section was excavated situated ~ 1 m from the original coring sites (Fig. 2.4.). A total of nine sub-samples were taken from this section.

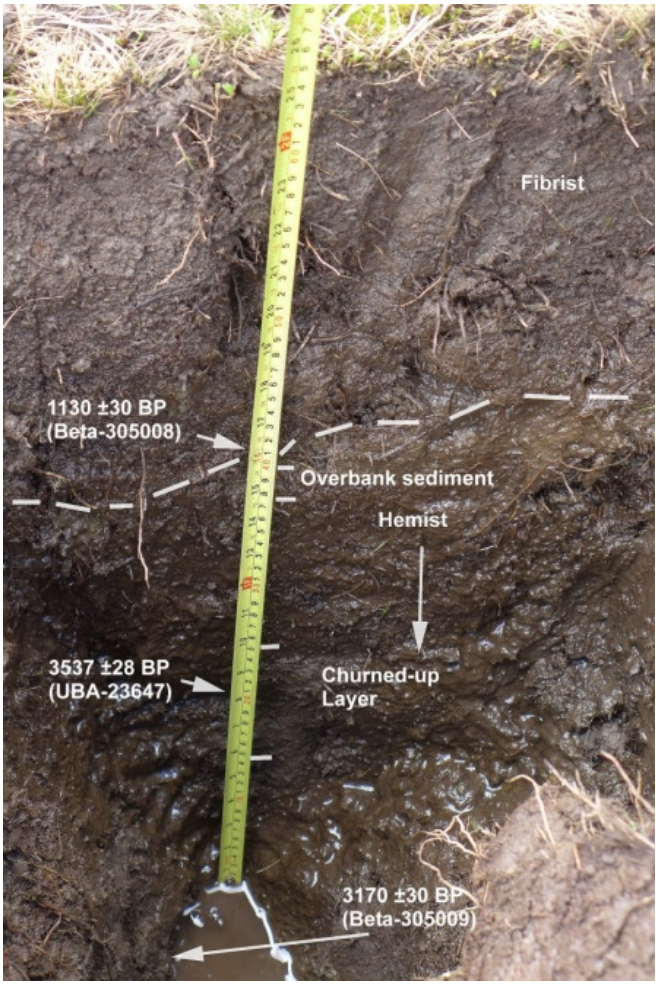

Figure 2.4. Excavated section from 2013 sampling site, labeled with sediment type and ^{14}C dates (sample numbers in parentheses). Reproduced from Mahaney et al. (2014b).

2.2.2. Sampling and ^{14}C dating

Nine sub-samples were obtained from the soil profile at varying depths as outlined in table 2.1. The top of the section is comprised of a Histic epipedon from 0 - ~ 25 cm depth containing root fibers from the grass above. The base of this Fibrist unit was dated to 1130 ± 30 yBP. Below the ~ 25 cm depth, the soil is classified as a Hemist with downward pronounced decomposition. This is followed by a ~ 15 cm churned-up bed in the presence of fluctuating groundwater. It consists of a finely disseminated peat lacking any fibrous character and few narrow roots. The base of

the section provided a ^{14}C date of 3170 ± 30 yBP whilst the midpoint of the churned-up layer yielded a ^{14}C age of 3537 ± 28 yBP reflecting a reworking of older samples either originating in the local landscape or influxed by human/animal traffic.

Bayesian probability statistics using OxCal conversions for raw dates were employed to account for fluctuations of radiocarbon content in the atmosphere over time. The results of the statistical analysis (Fig. 2.5.) place the Hannibal event (2168 cal yBP or 218 BC) within the churned-up layer (~ 40 – 45 cm) described previously. ^{14}C dating and associated statistical analyses were carried out by our collaborators at GeoScience Consulting.

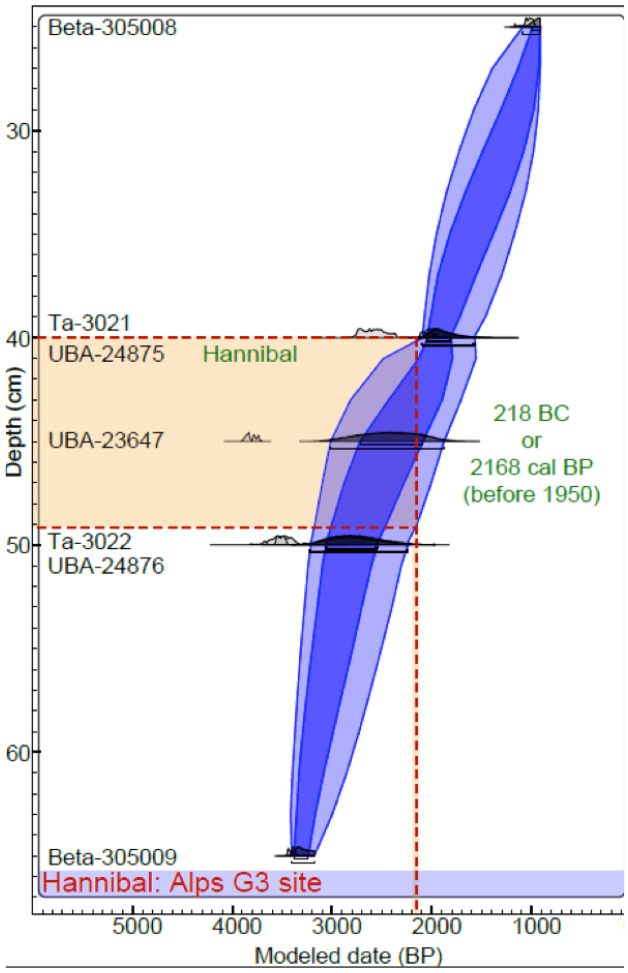

Figure 2.5. Bayesian statistical analyses of ^{14}C ages in the G5 core and G5A section. Reproduced from Mahaney et al. (2014b).

2.3. Materials and methods

2.3.1. Sample preparation

All samples were freeze-dried and homogenized using a mortar and pestle followed by passing through an 850 μm mesh sieve yielding a single < 850 μm particle size fraction prior to extraction.

All glassware was washed with hot soapy water, rinsed, and washed thoroughly with deionized water. After oven-drying the glassware was solvent washed with chloroform and subsequently furnaced for 8 hrs at 480 °C in a Lenton box furnace. All Teflon equipment was washed following the same procedure for glassware with the exception of replacing furnacing with a 30 minute sonication in chloroform prior to use. Stainless steel equipment was solvent washed with chloroform prior to use.

2.3.2. Elemental analysis

Elemental analysis was performed in triplicate using a Fisons NCS 1500 NA elemental analyser. Samples were treated with 1N HCl in Ag capsules following the procedure of Verardo et al. (1990) to remove carbonate. After drying overnight, the capsules were wrapped in Sn boats and combusted in the presence of O_2. The CO_2 evolved was measured and the total organic carbon (TOC) content (%) calculated by comparison with the certified reference standard acetanilide, which was analysed in conjunction with the samples.

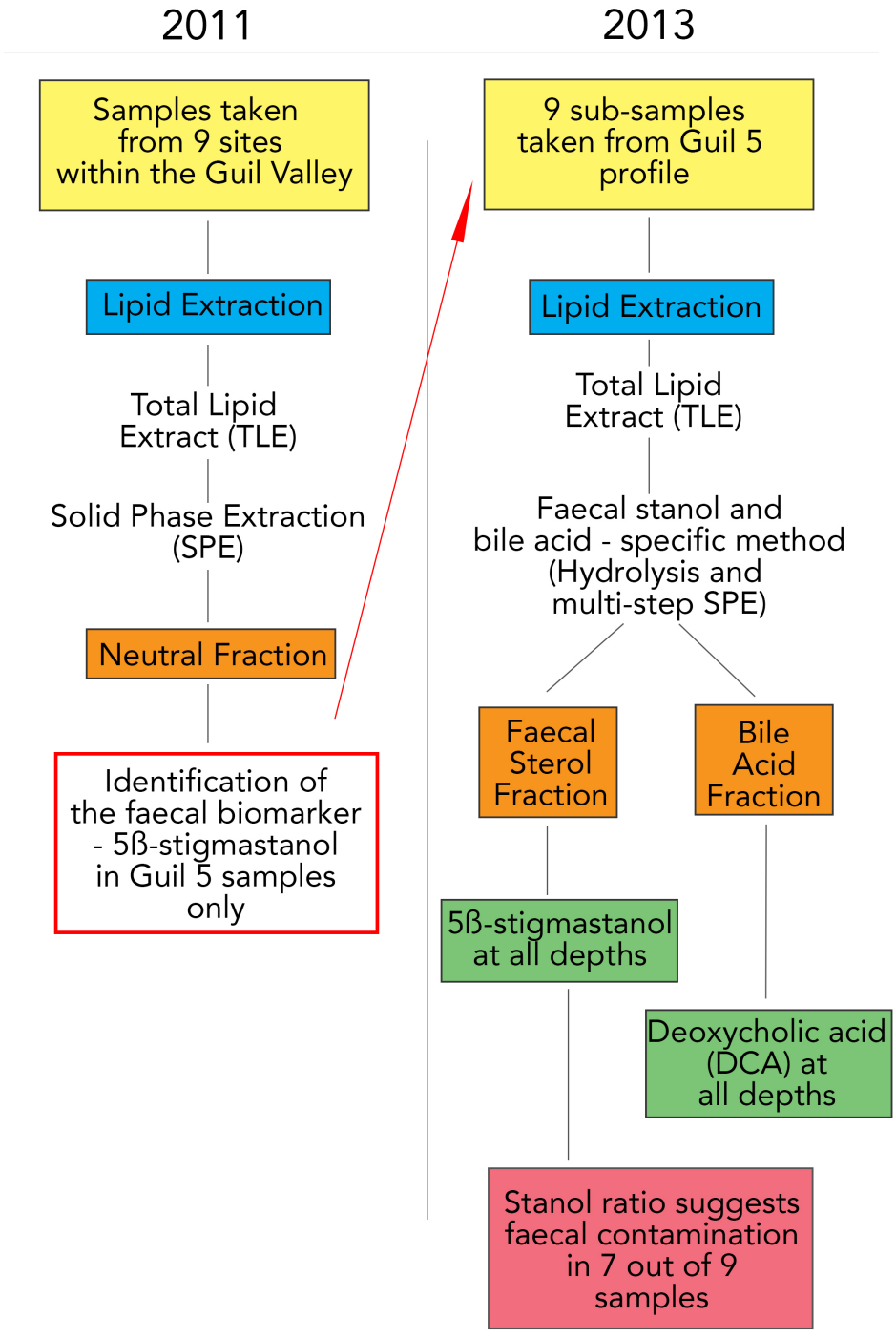

Figure 2.6. Flow chart highlighting the analyses carried out on samples taken during both the 2011 and the 2013 expeditions to the Guil Valley.

2.3.3. Total lipid extraction

Lipids were extracted from the 2011 and 2013 samples using ultrasonically assisted extraction following the method of Otto et al. (2005). Samples (1-3 g) were sonicated for 15 min with 10 mL methanol and centrifuged for 15 min at 6000 rpm. Supernatants were filtered through Whatman GF/A glass fibre filters. This procedure was repeated with solvents of decreasing polarity (10 mL 1:1 methanol:dichloromethane followed by 10 mL dichloromethane). Filtrates were combined, concentrated by rotary evaporation, and quantitatively transferred to a 2 mL glass vial. These total lipid extracts (TLEs) were dried under a stream of anhydrous N_2 prior to derivatisation.

2.3.4. Isolation and derivatisation of neutral fraction from 2011 TLEs

Neutral lipids from the 2011 samples were separated from the ultrasonically extracted TLEs following the method of Pinkart et al. (1998). Custom-made Bond-Elut solid phase extraction (SPE) columns packed with an aminopropylsilica solid phase (5mm diameter, PE, 500mg Ultra-Clean NH2, Agilent Technologies) were used for separation. These cartridges were washed with 5 mL hexane, 5 mL chloroform, 5 mL acetone, and 5 mL 6:1 methanol:chloroform prior to use. The dried TLE was suspended in 500 μL of chloroform, transferred to the cartridge, and subsequently pulled onto the stationary phase under vacuum. The neutral fraction was eluted with 5 mL chloroform. A glycolipid fraction was eluted next with 5 mL acetone followed by a polar lipid fraction eluted with 2.5 mL 6:1 methanol:chloroform and 2.5 mL 6:1 methanol:chloroform containing 0.2 M sodium acetate. All fractions were subsequently dried under anhydrous N_2 to a minimum

volume and transferred to a 2 mL glass vial. The glycolipid and polar lipid fractions were stored in -20 °C for future analysis.

Neutral lipid fractions were derivatised with N,O-bis-(trimethylsilyl)trifluoroacetamide (BSTFA) according to the method of Otto et al. (2005). Compounds were silylated using a mixture of 90 µL BSTFA and 10 µL pyridine at 70 °C for 2.5 hrs. After cooling, 100 µL 200 ppm 5α-cholestane (in hexane providing 100 ppm concentration) was added as an internal standard.

2.3.5. Isolation and derivatisation of faecal biomarkers from 2013 TLEs

Faecal stanols and bile acids were isolated and analysed following the method of Birk et al. (2012). The dried TLE was saponified with 0.7 M methanolic KOH overnight at room temperature. Following the addition of chloroform-extracted deionised H_2O the TLE was extracted three times with chloroform to provide a neutral fraction including stanols. The remaining aqueous fraction was acidified to pH < 2 with 6 N HCl and extracted three more times with chloroform to provide an acid fraction including bile acids.

SPE cartridges were prepared using silica gel (Machery-Nagel POLYGOPREP®, pore size 100 Å, mesh size 63 – 200 µm) which was furnaced at 480 ºC for 4 hrs to remove contaminants. This was activated (activated overnight at 120 ºC) and 5% deactivated (activated for 6 hrs at 200 ºC, deactivated by addition of 5% (w/w) deionised water) prior to packing (~ 1 g) into 5 mL glass SPE tubes with Teflon frits. The neutral fraction was suspended in 150 µL hexane and transferred to the 5% deactivated silica SPE cartridge, which was preconditioned with 5 mL hexane. Less polar substances were removed with 5 mL hexane. Steroidal compounds were eluted with 3 mL dichloromethane followed by 2 mL 2:1

dichloromethane:acetone, dried under anhydrous N_2, and transferred to a 2 mL glass vial.

The acid fraction was resuspended in 150 µL hexane and transferred to the activated silica SPE cartridge, which was preconditioned with 5 mL 2:1 dichloromethane:hexane. Less polar substances were removed with 5 mL 2:1 dichloromethane:hexane. Bile acids were eluted with 5 mL 2:1 dichloromethane:methanol, dried under anhydrous N_2 and transferred to a 2 mL glass vial.

Faecal biomarker compounds were derivatised according to the procedures outlined by Birk et al. (2012). Steroidal compounds were silylated with a 100 µL mixture of hexamethyldisilazane (HMDS), trimethylchlorosilane (TMCS), and pyridine (3:1:9) at 70 °C for 1 hr. Excess silylating agent was evaporated and the extract was resuspended in 100 µL 100 ppm 5α-cholestane (in dry toluene) as an internal standard.

Bile acids were silylated with 50 µL dry toluene, 98 µL BSTFA, and 2µL 1-(trimethylsilyl)imidazole (TSIM) at 80 °C for 1 hr. 50 µL 400 ppm 5α-cholestane (in dry toluene providing 100 ppm concentration) was added as an internal standard.

2.3.6. Gas chromatography - mass spectrometry (GC-MS)

Neutral lipids were immediately analyzed in triplicate on an Agilent model 7890N gas chromatograph equipped with a 7683 autosampler according to the conditions of Otto et al. (2006). The GC was coupled to an Agilent 5973N mass spectrometer operating in electron impact mode at 70 eV. The column used was a 30 m HP-5MS capillary column (0.25 mm i.d.,1 m film thickness). The sample (1 µL) was injected with a 2:1 split ratio. The GC inlet temperature was set at 280 °C

followed by the oven programme of; 65 °C held for 2 minutes, subsequently ramped at 6 °C/minute to 300 °C, and held there for 20 minutes.

Individual compounds were identified by the use of mass spectral library databases (NIST and Wiley) and comparison of mass spectrometric patterns with published mass spectra and authentic standards. Analytes were quantified from total ion peak area using multiple-point calibration curves of representative standards (nonadecane, methyl tetradecanoate, hexadecanol, stigmasterol, and α-amyrin).

Faecal stanol and bile acid fractions were immediately analyzed on the same Agilent instrument, following the method of Birk et al. (2012). The sample (1 μL) was injected with a 2:1 split ratio. The GC inlet temperature was set to 250 °C and the transfer line to 280 °C with a solvent delay of 14 minutes.

For the steroid fraction the oven programme was as follows; 80 °C held for 1.5 minutes, subsequently ramped at 12 °C/minute to 265 °C, then 0.8 °C/minute to 288 °C, followed by 10 °C/minute to 300 °C and held there for 12 minutes. For the bile acid fraction, the oven programme was; 80 °C held for 1.5 minutes, subsequently ramped at 20 °C/minute to 250°C, then 1.2 °C/minute to 287 °C, followed by 10 °C/minute to 300 °C and held there for 12 minutes.

Individual compounds were identified by the use of mass spectral library databases (NIST and Wiley) and comparison of mass spectrometric patterns with published mass spectra and authentic standards. Analytes were quantified from total ion peak area using multiple-point calibration curves of representative standards (stigmasterol). Percentage recovery was measured using an internal recovery standard added prior to extraction and was found to be > 95%. Procedural blanks were run to monitor background interferences.

2.4 Results

2.4.1. Preliminary investigation of samples from 2011 sampling trip

No faecal biomarker compounds were observed in the neutral lipid fractions of the samples taken during the 2011 sampling trip except at site Guil 5. 5ß-stigmastanol was identified in all depths at this site.

2.4.2. Total organic carbon (TOC)

TOC (%) values for each individual depth at the Guil 5 site are listed in table 2.1. The results show a minimum value of 6.24 % at 15-20 cm and a maximum value of 19.92 % at 30 – 35 cm. The value obtained for the churned-up layer at 40 – 45 cm was 16.6 %.

2.4.3. Steroidal compounds

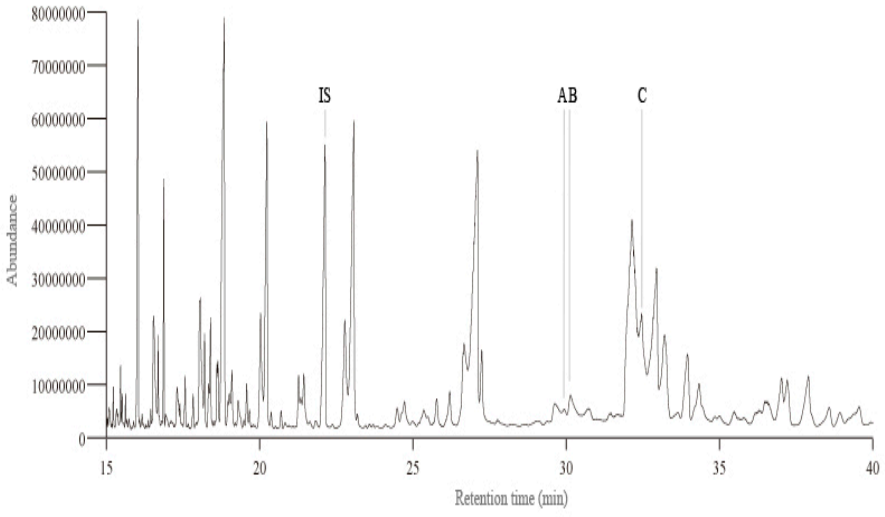

Figure 2.7. Chromatogram of steroid fraction from Guil 5, 50 – 55 cm depth. IS – internal standard (5α-cholestane), A – 5ß-stigmastanol, B – epi-5ß-stigmastanol, C - 5α-stigmastanol.

The 5ß-stanol, 24-ethyl-5ß-cholestan-3ß-ol (5ß-stigmastanol), was observed in varying concentrations in all depths in the Guil 5 section (Table 2.3.). The epimer (epi-5ß-stigmastanol) and the 5α homologue (5α-stigmastanol) of 5ß-stigmastanol were also identified in all depths. The minimum concentration was 4.3 µg/g OC and the maximum concentration detected was 30.6 µg/g. There is an overall decreasing trend from 0 – 60 cm however there is a peak from 35 – 45 cm with a maximum concentration of 22.7 µg/g OC in the 35 – 40 cm sample (Fig. 2.8.). Application of the stanol ratio confirmed the faecal origin of 5ß-stigmastanol with values > 0.7 in all sample depths except for 25 – 30 cm and 50 – 55 cm which provided values of 0.68 and 0.65 respectively (Grimalt 1990) (Table 2.1.).

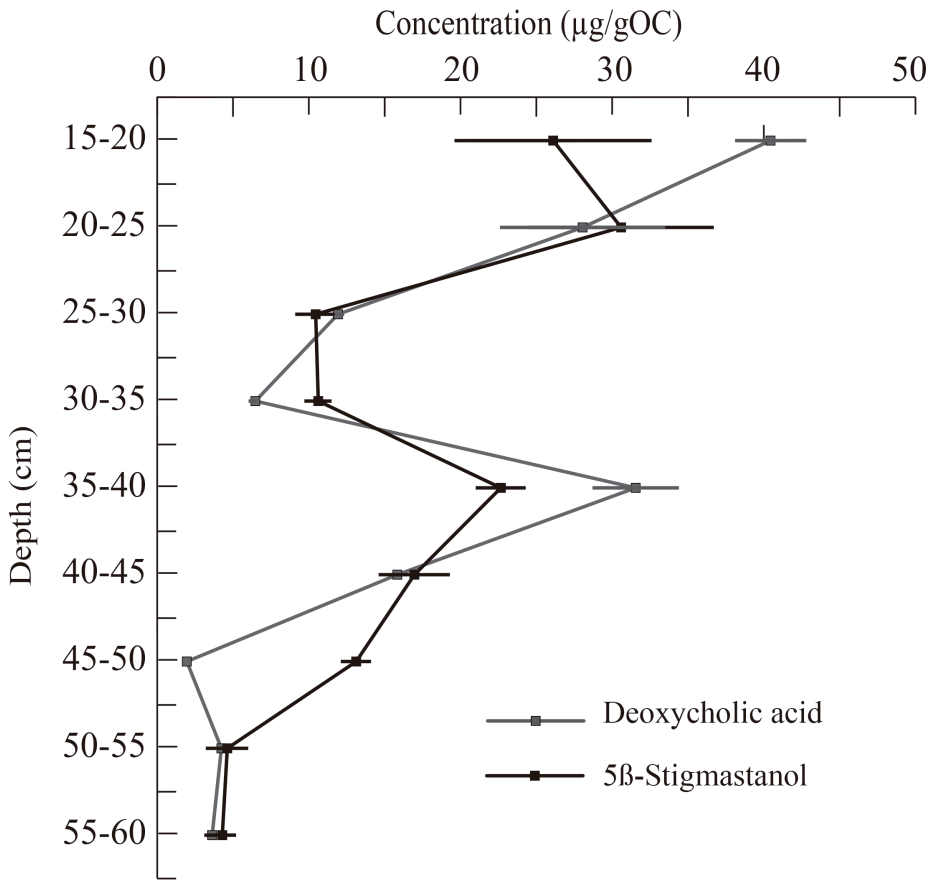

Figure 2.8. Levels of 5ß-stigmastanol and deoxycholic acid presented in µg/gOC for each sample within the G5 section.

2.4.4. Bile acids

Deoxycholic acid (DCA), a bile acid, was identified in the 2013 Guil 5 sample set. It was observed in varying concentrations at all depths with a minimum concentration of 2.0 µg/g OC and a maximum concentration of 40.4 µg/g OC (Table 2.2.). The DCA trend is very similar to that of 5ß-stigmastanol (Fig. 2.8.). There is a similar peak from 35 – 50 cm with a maximum concentration of 31.5 µg/g OC in the 35 – 40 cm sample.

Table 2.1. Results from 2013 samples. Organic carbon (OC%), concentrations of faecal biomarker compounds (µg/gOC), and stanol ratio values.

Depth (cm)	OC (%)	5ß-Stigmastanol (µg/g OC)	Deoxycholic acid (µg/g OC)	Stanol Ratio
15-20	6.2	26.1	40.4	0.78
20-25	19.0	30.6	28.0	0.78
25-30	18.7	10.4	11.9	0.68
30-35	19.9	10.6	6.5	0.73
35-40	10.9	22.7	31.5	0.84
40-45	16.6	17.0	15.8	0.83
45-50	18.4	13.1	2.0	0.76
50-55	16.0	4.6	4.2	0.65
55-60	14.2	4.3	3.6	0.89

2.5 Discussion

As expected in any soil or sediment profile the results from analysis of % TOC show a decreasing trend with depth overall. However, there is a sharp peak at ~ 20 – 35 cm suggesting a period of higher organic matter (OM) input. The Bayesian statistics indicate that the dates for this depth match that of the Medieval Warm Period (MWP) ~ 1000 - 1200 yBP (Cronin et al. 2010, Goosse et al. 2012, Mangini

et al. 2005, Mann et al. 2009) and therefore higher OM input would be expected during these warmer years. The level of TOC then decreases sharply followed by another peak from ~ 40 – 50 cm. This depth corresponds to the churned-up layer indicating a significant influx of organic matter during this period. It is possible that an army the size of Hannibal's could have caused this influx whilst travelling through the area. The decreasing OM trend continues after these depths.

Lipid biomarker analysis was carried out on samples taken from the 2011 Guil Valley sites (n = 9). This led to the identification of 5ß-cholestan-3ß-ol (5ß-stigmastanol) at site Guil 5 located within the mire. No faecal biomarkers were found at any of the other sampling sites in the region (e.g. Fig. 2.9.). Discovery of this biomarker compound prompted further organic geochemical investigations of this mire site.

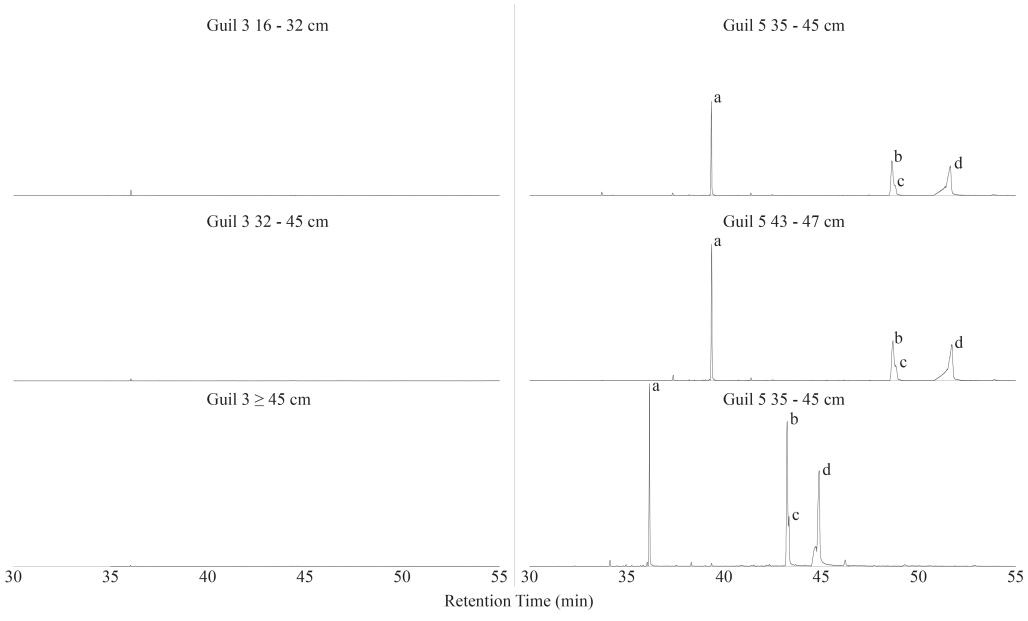

Figure 2.9. Comparison of extracted ion chromatograms (EIC m/z 398) for three similar layers from control sample Guil 3 and mire site sample Guil 5. Identified compounds in Guil 5 chromatograms are labelled; a – tricosanol, b – 5ß-stigmastanol, c - epi5ß-stigmastanol, d – 5a-stigmastanol. Guil 5 35-38 cm and 43-47

cm were run on a different instrument to the 50-53 cm sample, hence the difference in retention times.

Analysis of the 2013 Guil 5 samples confirmed the occurrence of 5ß-stigmastanol as well as the secondary bile acid, deoxycholic acid (DCA). Both of these compounds were present at all depths and displayed similar trends with increased input observed between depths of 20-25 cm and ~35-45 cm. Faecal contamination is supported by the use of the previously reported stanol ratio (Bull et al. 1999; Grimalt et al. 1990) (Fig. 2.10.).

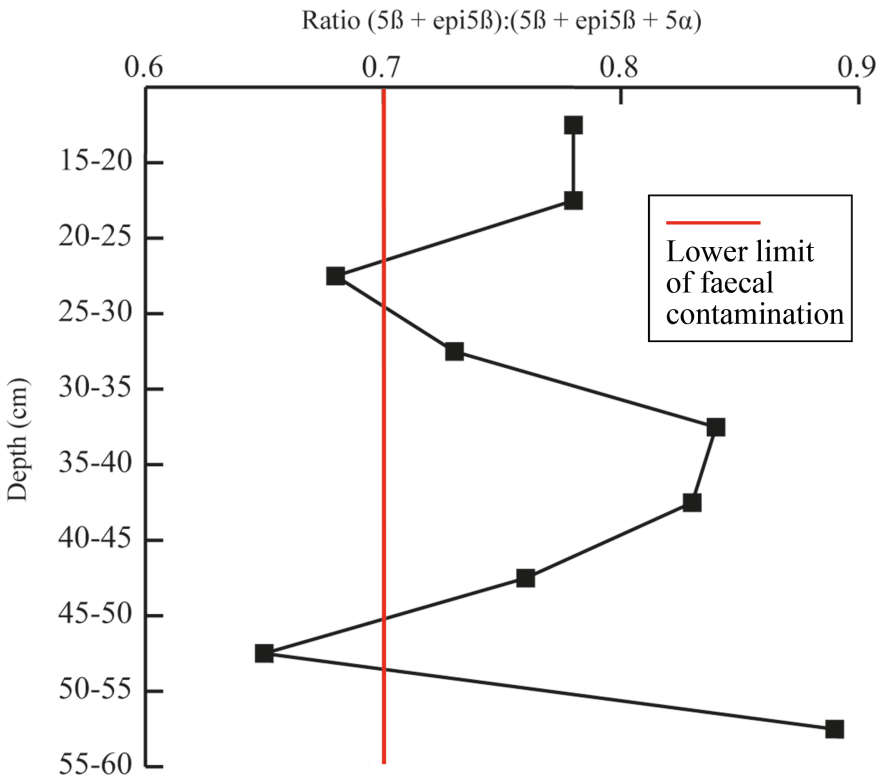

Figure 2.10. Plot of the stanol ratio (5ß+epi-5ß/5ß+epi-5ß+5α) (Grimalt 1990, Bull 1997) applied to peak areas integrated from *m/z* 398 ion extracted chromatograms.

5ß-stigmastanol is a 5ß-stanol commonly used as a biomarker for faecal material produced by ruminant mammals (Bull et al. 2002, Evershed et al. 1997). It was also the most abundant stanol observed in horse faeces by Leeming et al. (1996). DCA is a major secondary bile acid in the faeces of humans and some higher animals (Bull et al. 1999, Bull et al. 2002, Elhmmali et al. 2000). The presence of DCA in the absence of lithocholic acid (LCA) indicates a ruminant animal source for the faecal material (Bull et al. 2002).

Concentrations of faecal biomarkers 5ß-stigmastanol and DCA show almost identical profiles throughout the mire section. The maximum concentrations of both compounds across the 20-30 cm depths could be due to increased animal faecal matter input coinciding with the MWP. Increased temperatures could possibly have led to reduced snow cover at these altitudes making them more accessible and providing longer grazing periods as well as slightly drier conditions providing more space and plant cover for animals to graze. Where increased TOC values are observed at ~ 40-45 cm, the churned-up layer correlating to the Hannibal event, both of these faecal biomarkers observe a surge in concentration moving away from the decreasing values in higher depths.

The 35-45 cm depth lies within the churned up layer. As this is a water-logged mire site, there is potential for anaerobic microbial hydrogenation of higher plant sterols (i.e. ß-sitosterol) (e.g. Elhmmali et al. 2000) which could lead to the false assignment of a faecal source for the organic matter (Leeming et al. 1996). Microorganisms in the intestinal tract convert primary bile acids, formed in the liver, to secondary bile acids such as DCA (Bull et al. 2002, Elhmmali et al. 2000, Tyagi et al. 2007). To the authors' knowledge, bile acids are not known to be produced outside of the digestive system, which suggests a faecal input to this site. Also, the

high input of each individual compound coupled with the additional evidence of faecal contamination provided by the stanol ratio is further indicative of elevated mammalian faecal deposition in the churned up layer.

The presence of both 5ß-stigmastanol and DCA at all depths within the soil section could be due to one of two factors. Baeten et al. (2012) observed migration of both stanols and bile acids in archaeological soils. They suggested that due to the solubility of bile acids they are prone to leaching. Stanols are hydrophobic compounds making leaching less likely, however they have been associated with particulate matter in sewage and water columns and therefore may be subject to physical migration within the mire (Baeten et al. 2012, Isobe et al. 2002). However, as the elemental ratios show no evidence of leaching this scenario is unlikely.

It is possible that local fauna could be responsible for the low levels of faecal contamination that can be seen outside of the spikes in concentration at the 20-25 cm depth (attributed to the MWP) and the churned up layer. The *Capra ibex*, *Rupicapra rupicapra*, and *Marmota marmota* that are native to the region are ruminants, and therefore would contribute similar faecal signatures to those identified.

The most important factors in the argument proposed in this research are that no faecal biomarker compounds were observed in the control samples taken from the surrounding areas, and that the concentrations of the identified faecal compounds within the mire site show an increase at the depth associated with Hannibal's crossing. This suggests that at some point ~ 218 BC there must have been an increase in animal activity at this grassy mire site and not in the other surrounding locations investigated. It is likely that Hannibal's army would have taken the opportunity to rest at this site where both fresh water and ample grazing were available for the cavalry, valuable resources that can be scarce in this mountainous

landscape. It is interesting that the human faecal biomarker coprostanol was not observed in any of the sample sites. It is possible that another location nearby would have been used as a temporary latrine by the soldiers and further sampling in this area may lead to the discovery of such a site.

2.6 Conclusion

The aim of this research was to explore geochemical evidence that the Carthaginian Army led by Hannibal Barca had crossed the Alps via the route originally proposed by De Beer (1967). Extraction and analysis of faecal biomarker compounds has shown an increased input of faecal material to the churned-up layer, which dates to the same period as Hannibal's crossing, of the grassy mire within the Guil Valley along the route in question. This input is characteristic of herbivorous mammals and must have been due to a large number of these animals residing in this valley at the time of Hannibal's crossing. Whilst this evidence alone does not confirm that these animals were part of an ancient army, it does bolster the argument put forward by Mahaney et al. (2014) which includes historical, geological, and microbiological data.

References

Aboul-Kassim, T.A.T. and Simoneit, B.R.T., 1995. Petroleum hydrocarbon fingerprinting and sediment transport assessed by molecular biomarker and multivariate statistical analyses in the Eastern Harbour of Alexandria, Egypt. *Marine pollution bulletin,* 30(1), pp. 63-73.

Allen, M.A., Neilan, B.A., Burns, B.P., Jahnke, L.L. and Summons, R.E., 2010. Lipid biomarkers in Hamelin Pool microbial mats and stromatolites. *Organic Geochemistry,* 41(11), pp. 1207-1218.

Baeten, J., Marinova, E., De Laet, V., Degryse, P., De Vos, D. and Waelkens, M., 2012. Faecal biomarker and archaeobotanical analyses of sediments from a public latrine shed new light on ruralisation in Sagalassos, Turkey. *Journal of Archaeological Science,* 39(4), pp. 1143-1159.

Belicka, L.L. and Harvey, H.R., 2009. The sequestration of terrestrial organic carbon in Arctic Ocean sediments: A comparison of methods and implications for regional carbon budgets. *Geochimica et Cosmochimica Acta,* 73(20), pp. 6231-6248.

Belt, S.T., Massé, G., Rowland, S.J., Poulin, M., Michel, C. and Leblanc, B., 2007. A novel chemical fossil of palaeo sea ice: IP25. *Organic Geochemistry,* 38(1), pp. 16-27.

Bence, A.E., Kvenvolden, K.A. and Kennicutt II, M.C., 1996. Organic geochemistry applied to environmental assessments of Prince William Sound, Alaska, after the Exxon Valdez oil spill—a review. *Organic Geochemistry,* 24(1), pp. 7-42.

Bethell, P.H., Goad, L.J., Evershed, R.P. and Ottaway, J., 1994. The Study of Molecular Markers of Human Activity: The Use of Coprostanol in the Soil as an Indicator of Human Faecal Material. *Journal of Archaeological Science,* 21(5), pp. 619-632.

Birk, J.J., Dippold, M., Wiesenberg, G.L.B. and Glaser, B., 2012. Combined quantification of faecal sterols, stanols, stanones and bile acids in soils and terrestrial

sediments by gas chromatography–mass spectrometry. *Journal of Chromatography A,* 1242(0), pp. 1-10.

Birk, J.J., Teixeira, W.G., Neves, E.G. and Glaser, B., 2011. Faeces deposition on Amazonian Anthrosols as assessed from 5β-stanols. *Journal of Archaeological Science,* 38(6), pp. 1209-1220.

Blyth, A.J., Asrat, A., Baker, A., Gulliver, P., Leng, M.J. and Genty, D., 2007. A new approach to detecting vegetation and land-use change using high-resolution lipid biomarker records in stalagmites. *Quaternary Research,* 68(3), pp. 314-324.

Bull, I.D., 1997. New molecular methods for detecting natural and anthropogenic inputs to soils and sediments. *Ph.D Dissertation, University of Bristol*.

Bull, I.D., Elhmmali, M.M., Roberst, D.J. and Evershed, R.P., 2003. The Application of Steroidal Biomarkers to Track the Abandonment of a Roman Wastewater Course at the Agora (Athens, Greece)*. *Archaeometry,* 45(1), pp. 149-161.

Bull, I.D., Simpson, I.A., Van Bergen, P.F. and Evershed, R.P., 1999. Muck 'n' molecules: organic geochemical methods for detecting ancient manuring. *Antiquity,* 73(279), pp. 86-96.

Bull, I.D., Berstan, R., VASS, A. and Evershed, R.P., Identification of a disinterred grave by molecular and stable isotope analysis. *Science and Justice,* 49(2), pp. 142-149.

Bull, I.D., Lockheart, M.J., Elhmmali, M.M., Roberst, D.J. and Evershed, R.P., 2002. The origin of faeces by means of biomarker detection. *Environment international,* 27(8), pp. 647-654.

Bull, I.D., Lockheart, M.J., Elhmmali, M.M., Roberts, D.J. and Evershed, R.P., 2002. The origin of faeces by means of biomarker detection. *Environment international,* 27(8), pp. 647-654.

Bull, I.D., Simpson, I.A., Dockrill, S.J. and Evershed, R.P., 1999. Organic geochemical evidence for the origin of ancient anthropogenic soil deposits at Tofts Ness, Sanday, Orkney. *Organic Geochemistry,* 30(7), pp. 535-556.

Bull, I.D., Simpson, I.A., Dockrill, S.J. and Evershed, R.P., 1999. Organic geochemical evidence for the origin of ancient anthropogenic soil deposits at Tofts Ness, Sanday, Orkney. *Organic Geochemistry,* 30(7), pp. 535-556.

Caniupán, M., Lamy, F., Lange, C.B., Kaiser, J., Arz, H., Kilian, R., Baeza Urrea, O., Aracena, C., Hebbeln, D., Kissel, C., Laj, C., Mollenhauer, G. and Tiedmann, R., 2011. Millennial-scale sea surface temperature and Patagonian Ice Sheet changes off southernmost Chile (53°S) over the past ?60 kyr. *Paleoceanography,* 26(3), pp. -PA3221.

Charrié-Duhaut, A., Connan, J., Rouquette, N., Adam, P., Barbotin, C., De Rozières, M., Tchapla, A. and Albrecht, P., 2007. The canopic jars of Rameses II: real use revealed by molecular study of organic residues. *Journal of Archaeological Science,* 34(6), pp. 957-967.

Connolly, P., 1981. *Greece and Rome at War.* London, UK: MacDonald and Co.

Copley, M.S., Berstan, R., Mukherjee, A.J., Dudd, S.N., Straker, V., Payne, S. and Evershed, R.P., 2005. Dairying in antiquity. III. Evidence from absorbed lipid residues dating to the British Neolithic. *Journal of Archaeological Science,* 32(4), pp. 523-546.

Cronin, T.M., Hayo, K., Thunell, R.C., Dwyer, G.S., Saenger, C. and Willard, D.A., 2010. The Medieval Climate Anomaly and Little Ice Age in Chesapeake Bay and the North Atlantic Ocean. *Palaeogeography, Palaeoclimatology, Palaeoecology,* 297(2), pp. 299-310.

De Beer, G., 1967. *Hannibal's March.* London: Sidgwick and Jackson.

Eganhouse, R., P., 1997. Molecular markers and environmental organic geochemistry: an overview. In: R. Eganhouse P., ed, *Molecular Markers in Environmental Geochemistry.* Washington DC, USA: American Chemical Society, pp. 1-21.

Elhmmali, M.M., Roberts, D.J. and Evershed, R.P., 2000. Combined Analysis of Bile Acids and Sterols/Stanols from Riverine Particulates To Assess Sewage Discharges and Other Fecal Sources. *Environmental science & technology,* 34(1), pp. 39-46.

Elhmmali, M.M., Roberts, D.J. and Evershed, R.P., 1997. Bile Acids as a New Class of Sewage Pollution Indicator. *Environmental science & technology,* 31(12), pp. 3663-3668.

Evershed, R.P., Bethell, P.H., Reynolds, P.J. and Walsh, N.J., 1997. 5β-Stigmastanol and Related 5β-Stanols as Biomarkers of Manuring: Analysis of Modern

Experimental Material and Assessment of the Archaeological Potential. *Journal of Archaeological Science,* 24(6), pp. 485-495.

Evershed, R.P., Bethell, P.H., Reynolds, P.J. and Walsh, N.J., 1997. 5β-Stigmastanol and Related 5β-Stanols as Biomarkers of Manuring: Analysis of Modern Experimental Material and Assessment of the Archaeological Potential. *Journal of Archaeological Science,* 24(6), pp. 485-495.

Feng, X., Simpson, A.J., Gregorich, E.G., Elberling, B., Hopkins, D.W., Sparrow, A.D., Novis, P.M., Greenfield, L.G. and Simpson, M.J., 2010. Chemical characterization of microbial-dominated soil organic matter in the Garwood Valley, Antarctica. *Geochimica et Cosmochimica Acta,* 74(22), pp. 6485-6498.

Fietz, S., Huguet, C., Rueda, G., Hambach, B. and Rosell-Melé, A., 2013. Hydroxylated isoprenoidal GDGTs in the Nordic Seas. *Marine Chemistry,* 152(0), pp. 1-10.

Goñi, M.A., Ruttenberg, K.C. and Eglington, T.I., 1998. A reassessment of the sources and importance of land-derived organic matter in surface sediments from the Gulf of Mexico. *Geochimica et Cosmochimica Acta,* 62(18), pp. 3055-3075.

Goosse, H., Guiot, J., Mann, M.E., Dubinkina S. and Sallaz-Damaz, Y., 2012. The medieval climate anomaly in Europe: Comparison of the summer and annual mean signals in two reconstructions and in simulations with data assimilation. *Global and Planetary Change,* 84–85(0), pp. 35-47.

Grimalt, J.O., Fernández, P., Bayona, J.M., and Albaigés, J., 1990. Assessment of faecal sterols and ketones as indicators of urban sewage inputs to coastal waters, *Environmental Science and Technology,* 24 (3), pp. 357-363.

Hart, B.H.L., 1967. *Strategy.* London, UK: Faber and Faber.

Hart, K.M., Szpak, M.T., Mahaney, W.C., Dohm, J.M., Jordan, S.F., Frazer, A.R., Allen, C.C.R. and Kelleher, B.P., 2011. A bacterial enrichment study and overview of the extractable lipids from paleosols in the dry valleys, Antarctica: Implications for future Mars reconnaissance. *Astrobiology,* 11(4), pp. 303-321.

Hart, K.M., Oppenheimer, S.F., Moran, B.W., Allen, C.C.R., Kouloumbos, V., Simpson, A.J., Kulakov, L.A., Barron, L. and Kelleher, B.P., 2013. CO2 uptake by a soil microcosm. *Soil Biology and Biochemistry,* 57(0), pp. 615-624.

Heron, C., Nilsen, G., Stern, B., Craig, O. and Nordby, C., 2010. Application of lipid biomarker analysis to evaluate the function of 'slab-lined pits' in Arctic Norway. *Journal of Archaeological Science,* 37(9), pp. 2188-2197.

Hjulström, B. and Isaksson, S., 2009. Identification of activity area signatures in a reconstructed Iron Age house by combining element and lipid analyses of sediments. *Journal of Archaeological Science,* 36(1), pp. 174-183.

Hjulström, B., Isaksson, S. and Hennius, A., 2006. Organic Geochemical Evidence for Pine Tar Production in Middle Eastern Sweden During the Roman Iron Age. *Journal of Archaeological Science,* 33(2), pp. 283-294.

Huang, B., Tian, H., Wilkins, R.W.T., Xiao, X. and Li, L., 2013. Geochemical characteristics, palaeoenvironment and formation model of Eocene organic-rich

shales in the Beibuwan Basin, South China Sea. *Marine and Petroleum Geology,* 48(0), pp. 77-89.

Isaksson, S. and Hallgren, F., 2012. Lipid residue analyses of Early Neolithic funnel-beaker pottery from Skogsmossen, eastern Central Sweden, and the earliest evidence of dairying in Sweden. *Journal of Archaeological Science,* 39(12), pp. 3600-3609.

Isaksson, S., Karlsson, C. and Eriksson, T., 2010. Ergosterol (5, 7, 22-ergostatrien-3β-ol) as a potential biomarker for alcohol fermentation in lipid residues from prehistoric pottery. *Journal of Archaeological Science,* 37(12), pp. 3263-3268.

Isobe, K.O., Tarao, M., Zakaria, M.P., Chiem, N.H., Minh Le, Y. and Takada, H., 2002. Quantitative application of fecal sterols using gas chromatography-mass spectrometry to investigate fecal pollution in tropical waters: Western Malaysia and Mekong Delta, Vietnam. *Environmental Science and Technology,* 36(21), pp. 4497-4507.

Jansen, B., De Boer, E.J., Cleef, A.M., Hooghiemstra, H., Moscol-Olivera, M., Tonneijck, F.H. and Verstraten, J.M., 2013. Reconstruction of late Holocene forest dynamics in northern Ecuador from biomarkers and pollen in soil cores. *Palaeogeography, Palaeoclimatology, Palaeoecology,* 386(0), pp. 607-619.

Kagya, M.L.N., 1996. Geochemical characterization of Triassic petroleum source rock in the Mandawa basin, Tanzania. *Journal of African Earth Sciences,* 23(1), pp. 73-88.

Lazenby, J.F., 1998. *Hannibal's War.* Norman, Oklahoma: University of Oklahoma Press.

Leeming, R., Ball, A., Ashbolt, N. and Nichols, P., 1996. Using faecal sterols from humans and animals to distinguish faecal pollution in receiving waters. *Water research,* 30(12), pp. 2893-2900.

Li, S., Pang, X., Jin, Z., Yang, H., Xiao, Z., Gu, Q. and Zhang, B., 2010. Petroleum source in the Tazhong Uplift, Tarim Basin: New insights from geochemical and fluid inclusion data. *Organic Geochemistry,* 41(6), pp. 531-553.

Livy, T.L. and De Selincourt, A., 1965. *The War with Hannibal.* London, UK: Penguin Classics.

Lucquin, A., March, R.J. and Cassen, S., 2007. Analysis of adhering organic residues of two “coupes-à-socles” from the Neolithic funerary site “La Hougue Bie” in Jersey: evidences of birch bark tar utilisation. *Journal of Archaeological Science,* 34(5), pp. 704-710.

Mahaney, W.C., 2010. The Alpine invasion of Italia in 218 B.C.: Geological reconnaissance of the Alpine route. *American Journal of Ancient History,* 6.

Mahaney, W.C., Allen, C.C.R., Dirszowsky, R.W., Kelleher, B.P., Jordan, S.F., O'Reilly, S., West, A., Lasberg, K., Somelar, P., Kalm, V., Hart, K. and Julig, P., 2014b. *Geological, geochemical, and microbiological identification of sites of geoarchaeological interest in the Western Alps*

Mahaney, W.C., Allen, C.C.R., Pentlavalli, P., Dirszowsky, R.W., Tricart, P., Keiser, L., Somelar, P., Kelleher, B.P., Murphy, B., Costa, P.J.M. and Julig, P., 2014a. Polybius' 'previous landslide': Proof that Hannibal's invasion route crossed

the Col De La Traversette. *Journal Mediterranean Archaeology and Archaeometry,* 14(2).

Mahaney, W.C., Milner, M.W., Kapran, B., Tricart, P., Schwartz, S., Barendregt, R.W., Krinsley, D.H., Dorn, R.I., Trapido-Lurie, B., Boccia, S., Sodhi, R.N.S., Kalm, V. and Beukens, R., 2008a. Historical archaeology of the Hannibalic invasion of Italia:Technical applications. *Technical Briefs in Historical Archaeology,* 3, pp. 39-47.

Mahaney, W., 2013. *Hannibal's Odyssey: The Environmental Background to the Alpine Invasion of Italia.* New Jersey, USA: Gorgias Press.

Mahaney, W.C., Kapran, B., Kalm, V., Tricart, P., Carcaillet, C., Blarquez, O., Milner, M.W., Barendregt, R.W. and Somelar, P., 2010a. The Traversette (ITALIA) Rockfall: Geomorphological indicator of the Hannibalic invasion route. *Archaeometry,* 52(1), pp. 156-172.

Mahaney, W.C., Kapran, B. and Tricart, P., 2008b. Hannibal and The Alps: unravelling the invasion route. *Geology Today,* 24(6), pp. 223-230.

Mahaney, W.C., Tricart, P., Carcaillet C., Blarquez, O., Ali, A.A., Argant, J., Barendregt, R.W. and Kalm, V., 2010b. Hannibal's invasion route: An age-old question revisited within a geoarchaeological and palaeobotanical context. *Archaeometry,* 52(6), pp. 1096-1109.

Mahaney, W., Kalm, V., Dirszowsky, R., Milner, M., Sodhi, R., Beukens, R., Dorn, R., Tricart, P., Schwartz, S., Chamorro-Perez, E., Boccia, S., Barendregt, R., H. Krinsley, D., R. Seaquist, E., Merrick, D. and Kapran, B., 2008c. Hannibal's trek

across the alps: Geomorphological Analysis of sites of geoarchaeological interest. *Mediterranean Archaeology and Archaeometry,* 8(2), pp. 39-54.

Mahaney, W., 2004. A Geological/Topographical Reconnaissance of Hannibal's Invasion Route into Italia in 218 BC. In: D. Caldwell, J. Ehlen and R. Harmon, eds, Springer Netherlands, pp. 67-78.

Mangini, A., Spötl, C. and Verdes, P., 2005. Reconstruction of temperature in the Central Alps during the past 2000 yr from a δ18O stalagmite record. *Earth and Planetary Science Letters,* 235(3–4), pp. 741-751.

Mann, M.E., Zhang, Z., Rutherford, S., Bradley, R.S., Hughes, M.K., Shindell, D., Ammann, C., Faluvegi, G. and Ni, F., 2009. Global signatures and dynamical origins of the Little Ice Age and Medieval Climate Anomaly. *Science,* 326(5957), pp. 1256-1260.

McCreesh, N.C., Gize, A.P. and David, A.R., 2011. Ancient Egyptian hair gel: new insight into ancient Egyptian mummification procedures through chemical analysis. *Journal of Archaeological Science,* 38(12), pp. 3432-3434.

Nissenbaum, A., 1992. Molecular archaeology: Organic geochemistry of Egyptian mummies. *Journal of Archaeological Science,* 19(1), pp. 1-6.

Olsson, M. and Isaksson, S., 2008. Molecular and isotopic traces of cooking and consumption of fish at an Early Medieval manor site in eastern middle Sweden. *Journal of Archaeological Science,* 35(3), pp. 773-780.

O'Reilly, S., 2010. *Ground-truthing of gas-related seabed features in the Western Irish Sea: CV10_28 Cruise Report.* Dublin: Geological Survey of Ireland.

O'Reilly, S.S., Hryniewicz, K., Little, C.T.S., Monteys, X., Szpak, M.T., Murphy, B.T., Jordan, S.F., Allen, C.C.R. and Kelleher, B.P., 2014. Shallow water methane-derived authigenic carbonate mounds at the Codling Fault Zone, western Irish Sea. *Marine Geology,* 357(0), pp. 139-150.

O'Reilly, S.S., Szpak, M.T., Flanagan, P.V., Monteys, X., Murphy, B.T., Jordan, S.F., Allen, C.C.R., Simpson, A.J., Mulligan, S.M., Sandron, S. and Kelleher, B.P., 2014. Biomarkers reveal the effects of hydrography on the sources and fate of marine and terrestrial organic matter in the western Irish Sea. *Estuarine, Coastal and Shelf Science,* 136(0), pp. 157-171.

Otto, A., Gondokusomo, R. and Simpson, M.J., 2006. Characterization and quantification of biomarkers from biomass burning at a recent wildfire site in Northern Alberta, Canada. *Applied Geochemistry,* 21(1), pp. 166-183.

Otto, A., Shunthirasingham, C. and Simpson, M.J., 2005. A comparison of plant and microbial biomarkers in grassland soils from the Prairie Ecozone of Canada. *Organic Geochemistry,* 36(3), pp. 425-448.

Otto, A. and Simpson, M.J., 2007. Analysis of soil organic matter biomarkers by sequential chemical degradation and gas chromatography ? mass spectrometry. *Journal of Separation Science,* 30(2), pp. 272-282.

Otto, A. and Simpson, M.J., 2006. Sources and composition of hydrolysable aliphatic lipids and phenols in soils from western Canada. *Organic Geochemistry,* 37(4), pp. 385-407.

Outram, A.K., Kasparov, A., Stear, N.A., Varfolomeev, V., Usmanova, E. and Evershed, R.P., 2012. Patterns of pastoralism in later Bronze Age Kazakhstan: new evidence from faunal and lipid residue analyses. *Journal of Archaeological Science,* 39(7), pp. 2424-2435.

Pancost, R.D. and Boot, C.S., 2004. The palaeoclimatic utility of terrestrial biomarkers in marine sediments. *Marine Chemistry,* 92(1–4), pp. 239-261.

Peacock, E.E., Nelson, R.K., Solow, A.R., Warren, J.D., Baker, J.L. and Reddy, C.M., 2005. The West Falmouth oil spill: ~100 Kg of oil found to persist decades later. *Environmental Forensics,* 6, pp. 273-281.

Peters, K.E., Walters, C.C. and Moldowan, J.M., 2005. *The Biomarker Guide.* Second edn. Cambridge.

Pinkart, H.C., Devereux, R. and Chapman, P.J., 1998. Rapid separation of microbial lipids using solid phase extraction columns. *Journal of microbiological methods,* 34(1), pp. 9-15.

Polybius, Scott-Kilvert, I. and Walbank, F.W., 1980. *The Rise of the Roman Empire.* London, UK: Penguin Classics.

Salque, M., Bogucki, P.I., Pyzel, J., Sobkowiak-Tabaka, I., Grygiel, R., Szmyt, M. and Evershed, R.P., 2013. Earliest evidence for cheese making in the sixth millennium bc in northern Europe. *Nature,* 493(7433), pp. 522-525.

Shillito, L., Bull, I.D., Matthews, W., Almond, M.J., Williams, J.M. and Evershed, R.P., 2011. Biomolecular and micromorphological analysis of suspected faecal

deposits at Neolithic Çatalhöyük, Turkey. *Journal of Archaeological Science,* 38(8), pp. 1869-1877.

Simoneit, B.R.T., 2004. Biomarkers (molecular fossils) as geochemical indicators of life. *Advances in Space Research,* 33(8), pp. 1255-1261.

Stott, A.W., Evershed, R.P., Jim, S., Jones, V., Rogers, J.M., Tuross, N. and Ambrose, S., 1999. Cholesterol as a New Source of Palaeodietary Information: Experimental Approaches and Archaeological Applications. *Journal of Archaeological Science,* 26(6), pp. 705-716.

Teal, J.M., Farrington, J.W., Burns, K.A., Stegeman, J.J., Tripp, B.W., Woodin, B. and Phinney, C., 1992. The West Falmouth oil spill after 20 years: Fate of fuel oil compounds and effects on animals. *Marine pollution bulletin,* 24(12), pp. 607-614.

Tyagi, P., Edwards, D. and Coyne, M., 2008. Use of sterol and bile acid biomarkers to identify domesticated animal sources of fecal pollution. *Water, air, and soil pollution,* 187(1-4), pp. 263-274.

Versteegh, G.J.M., Bosch, H.-. and De Leeuw, J.W., 1997. Potential palaeoenvironmental information of C24 to C36 mid-chain diols, keto-ols and mid-chain hydroxy fatty acids; a critical review. *Organic Geochemistry,* 27(1–2), pp. 1-13.

Volkman, J.K., 2006. Lipid markers for marine organic matter. In: J.K. Volkman, ed, *Marine Organic Matter: Biomarkers, Isotopes and DNA.* Germany: Springer, pp. 27-70.

Volkman, J.K., Revill, A.T. a Murray, A.P., 1997. Applications of biomarkers for identifying sources of natural and pollutant hydrocarbons in aquatic environments. In: R. Eganhouse P., ed, *Molecular Markers in Environmental Geochemistry*. Washington DC, USA: American Chemical Society, pp. 110-132.

Chapter 3

Mid-Holocene climate change and landscape formation in Ireland: Evidence from a geochemical investigation of a coastal ombrotrophic peat bog

Abstract

Following a period of unusually strong winds and high seas in the spring of 2014, a blanket peat bog formerly covered by a beach comprised of fine sand and large rocks was uncovered at a coastal site in Spiddal, Co. Galway, Ireland. The surface of the bog was littered with standing tree stumps, the remnants of a Holocene forest that had succumbed to a relatively sudden drowning. A combination of inorganic and organic geochemical techniques was applied to determine the cause of this rapid submersion and to glean palaeoclimatic information from the preserved record within the peat. The study represents the first use of a multiproxy lipid biomarker approach to investigate palaeoclimate conditions from a peat bog in Ireland. The results provide evidence of climatic variation throughout a ca. 3500 yr timeframe during the mid-Holocene. Biomarker proxies displaying the relative contribution of *Shpagnum spp.* vs. higher plants were used to show changes in precipitation and temperature during peat formation. The data presented here correlate with described events, including the 4.2 ka event and the Subboreal-Subatlantic transition and show the benefit of a lipid biomarker method for investigating Ireland's peatland resources. In particular, the indication of colder/wetter conditions coinciding with the 4.2 ka event implies the possibility that its effects were felt in Ireland, contrary to some reports. The results suggest that a combination of warm and dry conditions followed by a rapid rise in sea level led to the growth and subsequent drowning of the ancient forest landscape.

3.1. Introduction

Peat bogs are important sites for palaeoclimate investigations. They contain a natural archive of past environmental change (Chambers et al., 2012) which, in ombrotrophic mires, have a direct relationship with precipitation. Ombrotrophic or 'cloud-fed' peat bogs are not influenced by ground and surface water, being affected solely by precipitation and evaporation (Nichols et al., 2006; Bingham et al., 2010; Zhang et al., 2014). This results in vegetation and organic matter (OM) which is well preserved in the anoxic environment and which is particularly sensitive to variation in local climate conditions (Blackford and Chambers, 1991; Pancost et al., 2002; McClymont et al., 2010).

Ireland has an abundance of ombrotrophic peat bogs representing an important resource of palaeoclimate information in Northwestern Europe. As such, the majority of Irish Holocene records derive from data from peat (Swindles et al., 2013). Researchers have applied several techniques, including testate amoebae, plant macrofossils, degree of humification and isotopic variation in cellulose to investigate fluctuation of Irish climate (e.g. Barber et al., 2000, 2003; Plunkett, 2006; Blundell et al., 2008; Swindles et al., 2010; Roland et al., 2014, 2015). Evidence for large climatic events has been reported using these approaches. For example, the Subboreal-Subatlantic transition is evidenced by widespread climatic deteriorations in both hemispheres. Using data from peat bogs, a shift to wetter/cooler conditions associated with this period in Ireland was attributed to a delayed response to solar forcing at 2800 cal. yr BP (Plunkett et al., 2004; Swindles et al., 2007).

Another such event is a period of global climatic change at ca. 4200 yr BP (4.2 ka event) which saw high temperatures in lower latitudes lead to severe drought, with

serious implications for human civilizations in these areas (Weiss et al., 1993). Higher latitudes are known to have experienced colder conditions during this time (Bond et al., 2001). Previous studies have obtained evidence of the impact of this event in Ireland from the peat record (Barber et al., 2003; Barber, 2007); however, more recent investigations using multiple proxies and multiple datasets have suggested that there is no compelling evidence (Swindles et al., 2013; Roland et al., 2014).

Due to the organic-rich nature of peat, lipid biomarkers offer a powerful approach for palaeoclimate investigation, particularly in settings where decomposition may hinder the use of these other techniques (Pancost et al., 2002). Analysis of lipid biomarkers provides an insight into the source of organic material on a molecular level (Eganhouse, 1997; Pancost and Boot, 2004; Simoneit, 2004; Peters et al., 2005). The development and refinement of multiple biomarker proxies play an important role in the investigation of past climatic change from the peat record (Nott et al., 2000; Pancost et al., 2002; Nichols et al., 2006; Nichols and Huang, 2007; Zheng et al., 2007; Bingham et al., 2010; Zhang et al., 2014; Schellekens et al., 2015). Many of these proxies involve comparison of compounds derived from peat-forming species of *Sphagnum* and vascular plants. *Sphagnum* plants favour colder and wetter conditions and thus thrive during periods of lower temperature and increased precipitation, which is reflected in the contribution of mid-chain *n*-alkanes (C_{23} and C_{25}), dominant in *Sphagnum* lipid profiles (Baas et al., 2000; Nott et al., 2000). Conversely, during times of increased temperature and drier conditions, long chain *n*-alkanes (C_{29} and C_{31}) dominant in vascular plants, provide increased water retention and protection from higher temperature, which is reflected in the peat record (McClymont et al., 2010; Zhang et al., 2014).

Other lipid compound classes and proxies can be used to study the input and relative changes in vegetation type on a broad taxonomic level. The *n*-alkanol average chain length (ACL) has been in an attempt to differentiate between relative inputs of *Ericaceae* and *Sphagnum* (Poynter and Eglinton, 1990; Pancost et al., 2002). This proxy may also provide insight into preservation state. C_{23} to C_{31} *n*-alkan-2-ones have been suggested as specific markers for *Sphagnum* (Nichols and Huang, 2007), whilst abundances of certain steroids and terpenoids have also been linked to change in vegetation (Pancost et al., 2002). The combination of these geochemical indicators has provided a toolkit for palaeoclimate studies in peat forming environments.

Pancost et al. (2011) investigated the use of the lipids derived from methanogenic archaea, archaeol and sn-2-hydroxyarchaeol, as potential biomarkers in ombrotrophic bogs, including Ballyduff Bog in Ireland. However, the work here represents the first comprehensive palaeoclimate study of an Irish peat bog utilizing lipid biomarker proxies.

This study aimed to investigate changes in local vegetation and climate over a 3500 yr period during the mid-Holocene by providing a new Irish palaeoclimate dataset within this period, and identifying the events that led to the flooding of this forested landscape.

3.2. Materials and methods

Figure 3.1. Map of Galway Bay area and sampling site location.

3.2.1. Sampling and sample location

Samples were taken from a recently exposed coastal ombrotrophic blanket peat bog in Spiddal, Co. Galway, Ireland (Fig. 3.1.). The bog is in a tidal zone and was previously submerged beneath a layer of sand. Due to a period of stormy weather and rough sea conditions (February 2014) the sand was removed, revealing the peat bog complete with protruding tree stumps of *Pinus* and *Quercus* origin (Williams and Doyle, 2014). The only living plant life growing on the peat surface was the marine alga *Cladophora rupestris*.

Sand and rock was cleared from the surface of the peat deposit. A ca. 1 m trench was dug into the bog and samples taken from the trench wall every ca. 5 cm. The entire profile was homogenous dark brown in colour, containing yellowish-brown

plant fragments throughout. There was no apparent fluctuation in colouration or mineralogy. Limestone bedrock was found at the base of the trench. Material was removed with a clean stainless steel spatula washed with MeOH and dichloromethane (DCM) and stored in furnaced Al foil. Samples were subsequently stored at -20 °C prior to analysis.

Figure 3.2. Study location, recently exposed peatland with protruding tree stump at Spiddal, Co. Galway, Ireland.

3.2.2. Sample preparation

All samples were freeze-dried, homogenized and passed through an 850 µm mesh sieve, yielding a single < 850 µm size fraction prior to extraction. All glassware was washed thoroughly, solvent washed with MeOH and $CHCl_3$ and furnaced for 8 h

at 480 °C in a Lenton box furnace. All Teflon equipment was sonicated in $CHCl_3$ prior to use. Stainless steel equipment was washed with $CHCl_3$.

3.2.3. Radiocarbon dating

Three samples of bulk material were dated at the Radiocarbon Dating Facility in Queens University, Belfast. Samples analysed were from 0-5, 55-60 and 105-110 cm, providing a top, middle and bottom sequence of ^{14}C age. The results were calibrated using OxCal 4.2 software in conjunction with the IntCal13 calibration curve. Age values for the non-dated layers were calculated from linear interpolation.

3.2.4. X-ray fluorescence analysis (XRF)

XRF measurements were taken using a handheld Thermo Scientific Niton XL3t device following the procedure of Radu and Diamond (2009). Samples were placed in 32 mm double open-ended sample cups, secured in place with polyester stuffing, and covered with polypropylene X-ray film (Premier Lab Supply, FL, USA). A sample cup assembly without sample was measured as a blank. All measurements were performed in triplicate using bulk mode for soil samples. An internal instrument calibration was performed prior to analysis.

3.2.5. TOC and TN analysis

Elemental analysis was performed in triplicate using a Fisons NCS 1500 NA elemental analyser following the procedure of Verardo et al. (1990) described previously in Chapter 2.

3.2.6. Lipid biomarker extraction

Samples (~2 g) were extracted using ultrasonically assisted extraction as described in Chapter 2 (Otto et al., 2005). Neutral lipids were separated from the total lipid extracs (TLE) following the method of Pinkart et al. (1998) as described in Chapter 2. The glycolipid and polar lipid fractions were stored at -20 °C for future analysis. Neutral lipid fractions were silylated prior to GC-MS analysis with N,O-bis-(trimethylsilyl)trifluoroacetamide (BSTFA) (Chapter 2.). 5α-Cholestane (100 µl, 100 ppm) was added to each sample as an internal standard.

3.2.7. Gas chromatography – mass spectrometry (GC-MS)

Aliquots (1 µl) of samples were immediately analysed in triplicate with an Agilent model 7890N gas chromatograph equipped with a 7683 autosampler according to the conditions of Otto et al. (2006) as described previously in Chapter 2 for the analysis of neutral lipid fractions. Individual compounds were assigned from comparison with mass spectral library databases (NIST and Wiley) and comparison of MS patterns with published spectra and authentic standards. Analytes were quantified from total ion peak area using multiple-point calibration curves of representative standards (nonadecane, hexadecanol, stigmasterol and α-amyrin). Percentage recovery was measured using an internal recovery standard added prior to extraction and was found to be > 95%. Procedural blanks were run to monitor background interferences.

The OEP was determined by calculating the carbon preference index (CPI) of the n-alkanes from C_{25} to C_{33} using the following equation (Bray and Evans, 1961):

$$CPI_{25\text{-}33} = 0.5 \times [(C_{25}+C_{27}+C_{29}+C_{31}+C_{33})/(C_{24}+C_{26}+C_{28}+C_{30}+C_{32})] + [(C_{25}+C_{27}+C_{29}+C_{31}+C_{33})/(C_{26}+C_{28}+C_{30}+C_{32}+C_{34})]$$

Values > 1 denote an OEP whereas values < 1 indicate an even/odd (EOP) predominance.

The P-aqueous (P_{aq}) ratio (Ficken et al., 2000), originally proposed to examine the input of algae to lake sediments, has been applied to measure the input of *Sphagnum* species to peat deposits (Nichols et al., 2006; Zhang et al., 2014; Inglis et al., 2015). This involves comparison of medium to long chain *n*-alkanes, as the former are predominant in both *Sphagnum* and aquatic macrophytes. The P-wax ratio (Zheng et al., 2007) was designed to evaluate the abundance of waxy *n*-alkanes vs. total *n*-alkanes.

$$P_{aq} = (C_{23}+C_{25})/C_{23}+C_{25}+C_{29}+C_{31})$$

$$P_{wax} = (C_{27}+C_{29}+C_{31})/(C_{23}+C_{25}+C_{27}+C_{29}+C_{31})$$

The average chain length (ACL) (Eglinton and Hamilton, 1967; Poynter and Eglinton, 1990) for the *n*-alkanes from C_{23} to C_{33} was calculated for each sample.

$$ACL_{23\text{-}33} = ((23(C_{23}) + 25(C_{25}) + 27(C_{27}) + 29(C_{29}) + 31(C_{31}) + 33(C_{33}))/(C_{23} + C_{25} + C_{27} + C_{29} + C_{31} + C_{33})$$

The ACL for *n*-alkanols was calculated based on the even homologues from C_{22} to C_{30}.

The *n*-alkanol to *n*-alkane ratio (Poynter and Eglinton, 1990) was employed as a measure of degradation due to the assumed higher degradation rate for *n*-alkanols due to the presence of the OH group.

$$(alc/alc+alk) = (C_{24} + C_{26} + C_{28}n\text{-alkanols})/(C_{24} + C_{26} + C_{28}n\text{-alkanols}) + (C_{27} + C_{29} + C_{31}n\text{-alkanes})$$

3.2.8. Gas chromatography – isotope ratio mass spectrometry (GC-IRMS)

All samples were analysed in triplicate using continuous flow IRMS and the same GC conditions as above. The GC instrument was coupled to an IsoPrime IRMS instrument (IsoPrime100) via a combustion furnace (GC5, CuO, Pt 650). The $\delta^{13}C$ values were measured against a CO_2 reference gas of known $\delta^{13}C$ value and are reported vs. a stable isotope reference standard (*n*-alkanes mixture B2, Indiana University, USA). Reproducibility was better than ± 0.5‰. The results were corrected for the addition of carbon during derivatization and only well resolved major analytes are reported here.

3.2.9. Statistical analysis

Elemental, biomarker proxy, $\delta^{13}C$ measurements, and individual sterol and terpenoid compound data were tested for any statistically significant correlation (Table A1) by calculating Pearson correlation coefficients (r) using PAST 3.10 software (Hammer et al., 2001). *P* values < 0.05 were considered to be statistically significant.

3.3. Results

3.3.1. Chronology of peat profile

^{14}C ages obtained for 0-5, 55-60 and 105-110 cm depths were 2095 ± 33 yr BP, 3376 ± 40 yr BP and 4769 ± 32 yr BP respectively. Calibrated age values obtained using OxCal 4.2 software employing the IntCal13 curve provided respective ages (Fig. 3.3.) of 2068 ± 51 cal yr BP (2σ 2150 - 1989 cal yr BP), 3621 ± 55 cal yr BP (2σ 3716 – 3483 cal yr BP) and 5512 ± 56 cal yr BP (2σ 5590 – 5333 cal yr BP). Calculated ages for the non-dated samples are listed in table 3.1. and the total timespan of the peat profile is ca. 3436 yr.

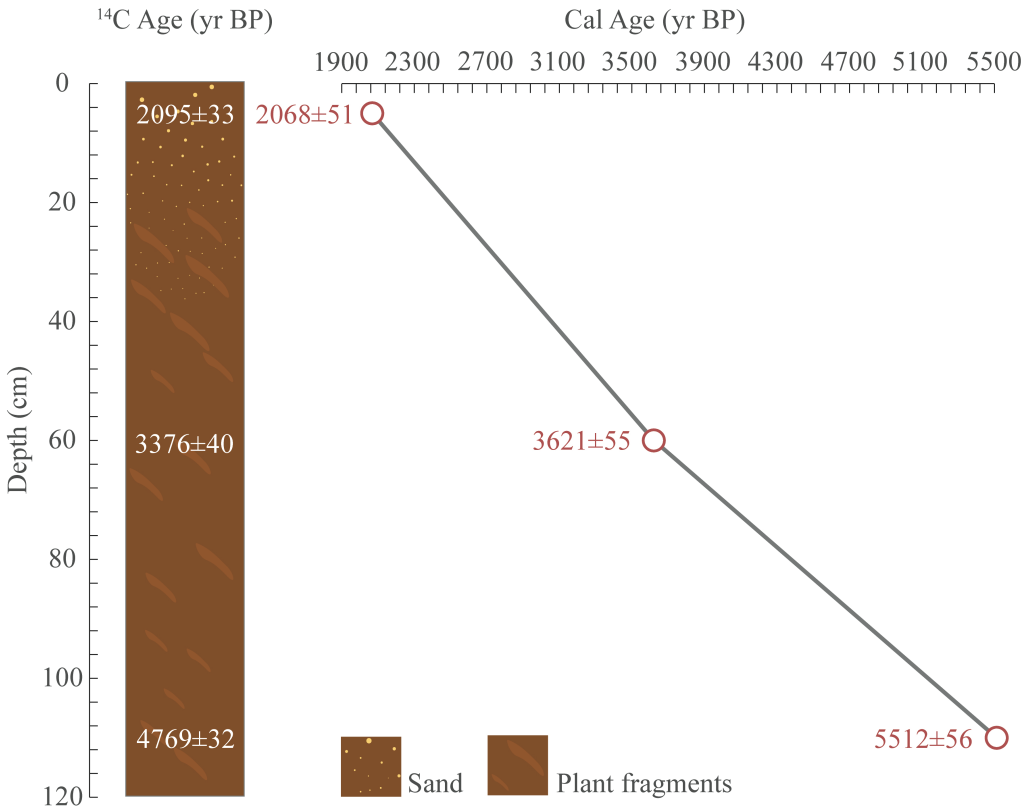

Figure 3.3. ^{14}C age values obtained from humic substances from three samples from the peat profile (left) as well as cal. age results calculated using OxCal 4.2 with IntCal13 calibration curve (right).

3.3.2. Elemental composition

3.3.2.1. Total organic carbon (TOC) and total nitrogen (TN)

TOC values ranged from 17.5% to 39.9% with an average value of 31.7%. The highest value was at ca. 3133 cal. yr BP whilst the lowest was at ca. 2152 cal. yr BP. The top two layers, spanning ca. 1988 cal. yr BP to 2152 cal. yr BP, contained the lowest amount of TOC, with a sharp increase occurring at 2479 cal. yr BP. From this sample to the bottom of the profile, values fluctuated relatively less and displayed a gentle decreasing trend.

The peat profile had an average TN value of 1.3%. The minimum of 0.7% was observed at ca. 5424 cal. yr. BP. Values increased over time to a maximum of 1.9% at ca. 3461 cal. yr. BP. This was followed by a steady decrease to 0.8% at ca. 2152 cal. yr. BP and a slight increase to 1.1% in the most recent material dated to ca. 1988 cal. yr. BP.

Average C/N values were 24.8, with a maximum of 40.7 and a minimum of 18.1. Overall, the results followed a similar trend to the TOC values (Fig. 3.4.). There was, however, a sharp increase to the maximum in the deepest layer, which was opposite to the decrease in TOC in this sample, indicating a lower N input.

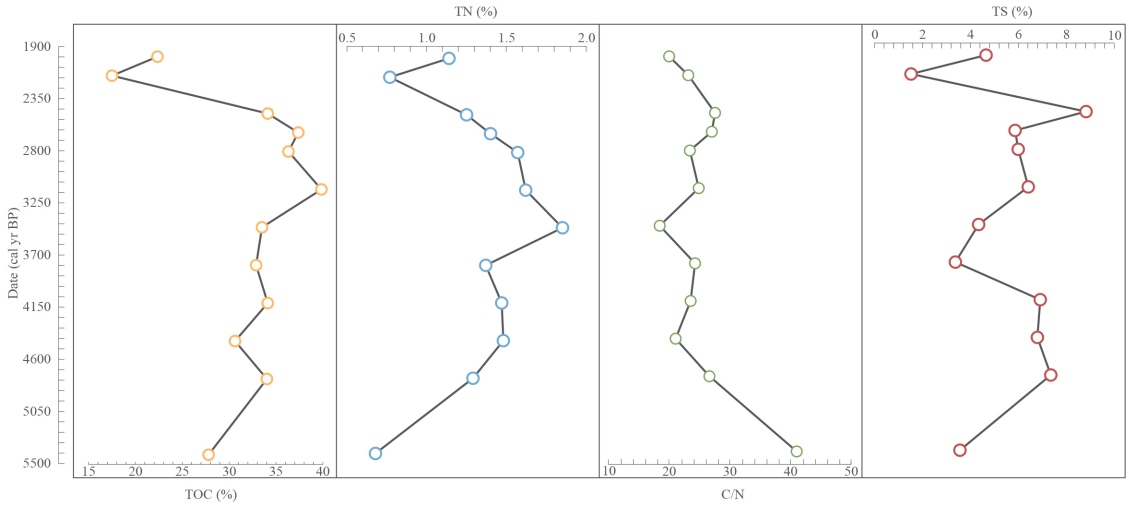

Figure 3.4. Total organic carbon (TOC %), total nitrogen (TN %), C/N ratio, and total sulfur (TS %) trends.

3.3.2.2. Total sulfur (TS)

TS displayed an overall average value of 5.5% (Fig. 3.4.). Values fluctuated throughout the profile. Similar values of 3.6 and 4.6% were observed for the bottom and top samples of the 1 m profile respectively. Levels remained around 6.5% between 4769 and 2642 cal. yr BP and were followed by a decrease to 4.3 and 3.4% at 3788 and 3460 cal. yr BP respectively. Values returned to ca. 6.5% for the next three samples dated from 3133 to 2642 cal. yr BP, and increased to a maximum value of 8.8% at 2479 cal. yr BP. A shift to the minimum value of 1.5% occurred at 2152 cal. yr BP.

Table 3.1.

Total organic carbon (TOC), total sulfur (TS), total nitrogen (TN) and C/N ratio as well as abundances of lipid compounds at each depth. Also shown are $\delta^{13}C$ values for specific biomarkers.

Depth (cm)	0-5	5-10	15-20	20-25	25-30	35-40	45-50	55-60	65-70	75-80	85-90	105-110
Age (cal yr BP) [a]	1988	2152	2479	2643	2807	3134	3461	3788	4115	4443	4770	5424
TOC (%)	22.4	17.5	34.2	37.4	36.3	39.9	33.5	32.9	34.1	30.6	34	27.8
TN (%)	1.1	0.8	1.3	1.4	1.6	1.6	1.9	1.4	1.5	1.5	1.3	0.7
C/N	19.7	22.8	27.2	26.7	23.1	24.6	18.1	23.9	23.2	20.7	26.3	40.7
TS (%)	4.6	1.5	8.8	5.9	6	6.4	4.3	3.4	6.9	6.8	7.3	3.6
n-Alkanes (µg/g OC)												
C_{23}	3.1	0.7	0.7	1.1	1.1	1.1	1.3	1.3	2.2	0.9	2.1	5.3
C_{25}	2.5	0.4	0.6	1.2	0.9	0.9	1.3	1.4	1.7	0.9	1.3	2.1
C_{27}	5.4	0.7	1.1	1.8	1.4	1.3	1.6	2.6	2.6	2.5	2.6	4.4
C_{29}	13.9	1.4	2.5	5.0	5.5	4.1	5.3	6.4	4.7	5.6	4.1	9.3
C_{31}	14.1	1.2	1.7	3.3	3.8	2.8	4.4	6.8	5.0	7.7	3.9	15.3

C_{33}	8.2	1.3	2.5	2.6	4.0	2.3	3.8	4.9	4.5	6.7	4.1	17.8
∑	47.1	5.8	9.0	14.8	16.6	12.5	17.6	23.4	20.6	24.2	18.1	54.1
n-Alkanols (µg/g OC)												
C_{22}	26.0	1.0	0.0	22.2	22.5	9.2	21.5	16.8	14.6	15.8	16.3	28.7
C_{24}	30.3	1.9	0.0	30.6	31.7	12.1	31.1	26.6	24.7	24.0	21.8	53.1
C_{26}	12.8	0.5	0.1	10.2	8.9	4.3	8.2	6.4	7.7	7.2	9.0	17.4
C_{28}	14.2	0.4	0.1	8.0	7.0	3.0	4.8	7.2	6.9	18.2	10.3	23.4
C_{30}	4.6	0.0	0.0	2.5	1.0	1.5	1.9	2.3	2.7	5.9	3.3	10.0
∑	88.0	3.9	0.2	73.5	71.1	30.0	67.4	59.3	56.5	71.2	60.8	132.6
n-Alkan-2-ones (µg/g OC)												
C_{23}	6.6	3.8	6.3	6.7	5.9	4.2	11.4	7.5	8.4	2.5	5.8	58.8
C_{25}	12.1	6.6	11.2	12.5	10.8	6.6	18.1	11.6	14.8	5.2	13.4	10.2
C_{27}	13.0	4.5	5.4	2.5	4.4	2.3	4.7	4.9	11.4	3.8	16.7	16.5
C_{29}	8.2	1.4	2.7	3.1	2.5	1.2	2.8	3.6	4.6	4.3	7.3	16.0
C_{31}	9.1	0.5	3.4	3.1	5.0	1.5	4.6	4.9	4.0	5.7	15.4	13.7
∑	48.9	16.8	29.1	27.8	28.5	15.8	41.6	32.5	43.1	21.4	58.6	115.3

Steroids (µg/g OC)												
Cholestanol	5.3	1.0	1.4	1.8	2.3	1.2	1.6	1.5	2.1	-	1.7	4.1
24-Ethycoprostanol	8.0	2.4	3.6	4.5	4.3	2.5	3.5	2.1	3.5	1.3	0.9	2.3
Campesterol	15.7	5.1	5.7	6.3	10.0	5.1	6.7	4.5	8.3	3.7	7.4	9.8
Campestanol	15.6	2.3	2.7	4.6	5.7	3.0	5.1	3.7	5.0	3.2	3.3	8.4
Stigmasterol	15.3	3.6	4.3	5.0	6.4	3.1	4.8	3.6	5.0	2.2	4.7	12.6
β-Sitosterol	86.4	23.3	25.3	30.3	41.0	23.0	36.1	23.8	40.9	18.4	56.4	41.7
Stigmastanol	70.0	15.9	20.2	24.8	28.4	15.7	26.2	20.1	31.2	13.8	26.3	39.4
∑	216.3	53.5	63.1	77.3	98.1	53.7	83.9	59.2	96.1	42.6	100.7	118.1
Terpenoids (µg/g OC)												
Taraxer-4-one	0.0	0.0	0.0	1.4	3.0	1.8	3.2	0.0	2.7	4.4	41.0	7.2
$\delta^{13}C$ (‰)												
n-Nonacosane	-32.9	-30.5	-31	-31.6	-31.2	-31.4	-32.5	-33.1	-33.2	-34.3	-33.8	-34.1

[a] Dates shown are values obtained from linear interpolation of calibrated ^{14}C ages.

3.3.3. Neutral compounds

Total *n*-alkane concentrations varied between 9.2 and 73.1 µg/g OC. All samples across the ca. 3436 yr period recorded similar *n*-alkane distributions dominated by long chain (C_{29}-C_{33}) compounds with an odd over even predominance (OEP) typical of a terrigenous plant input to (Table 3.1.). All the samples had CPI values > 1, with a minimum of 4.40 and a maximum of 31.48.

Throughout the profile there were periods of increased input from mid-chain *n*-alkanes (C_{23}-C_{25}), indicative of contribution from *Sphagnum* (Baas et al., 2000; Ficken et al., 2000; Nichols et al., 2006). The relative contribution from *Sphagnum* vs. other higher plants was assessed using the C_{23}/C_{31} ratio (Baas et al., 2000; Nott et al., 2000) (Fig. 3.5.). The values ranged from a minimum of 0.1 at ca. 4443 cal yr BP to a maximum of 0.6 at ca. 2152 cal yr BP. There appeared to be decreased C_{23} input from ca. 4600 to 4300 cal yr BP, ca. 3900 to 3700 cal yr BP, and in the surface sample at ca. 1988 cal yr BP. A predominance of C_{23} occurred at ca. 5000 to 4700 cal yr BP and ca. 4300 to 4000 cal yr BP, with the largest increase observed from ca. 2300 to 2100 cal yr BP. C_{31} is also in relatively high abundance in *Sphagnum,* whereas C_{29} homologue is relatively rare (Baas et al., 2000; Nott et al., 2000). As such, it has been suggested that the C_{23}/C_{29} ratio may be preferable for reconstructing *Sphagnum* vs. non-*Sphagnum* contribution to peat (Nichols et al., 2006). Our results showed minimal variation between the trends for both proxies (Fig. 3.5.).

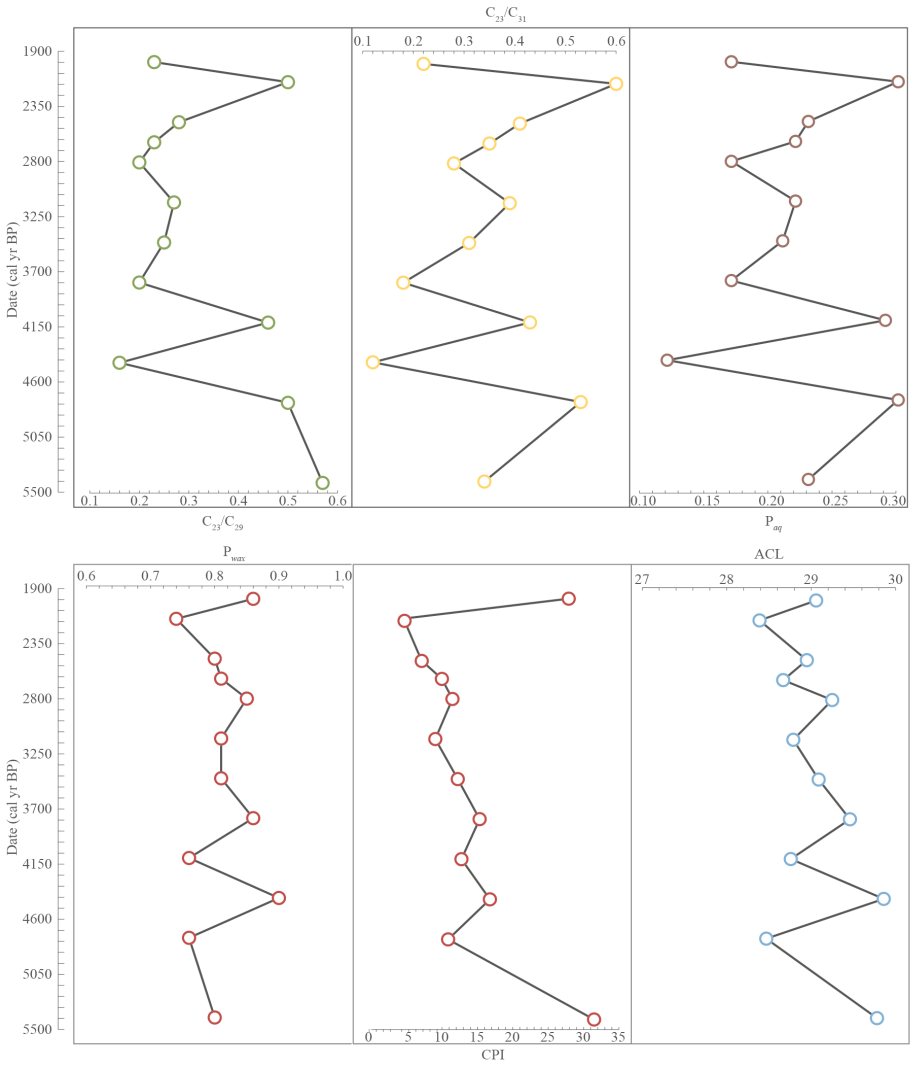

Figure 3.5. n-Alkane proxies assessing the relative amounts of *Sphagnum* present at each depth. From left to right: C_{23}/C_{29} ratio, C_{23}/C_{31} ratio, P-aqueous, P-wax, carbon preference index (CPI) from C_{25} – C_{33}, and average chain length (ACL) from C_{23} – C_{33}.

The maximum value for P_{aq} (0.3) was at ca. 2152 cal yr BP, and the minimum (0.1) at ca. 4443 cal yr BP. Overall, P_{aq} displayed a similar trend to that of the C_{23}/C_{29} and C_{23}/C_{31} proxies. P_{wax} values ranged between 0.7 and 0.9, following the same trend. The ACL ranged from 28.4 to 29.9. The same trend was observed for ACL as seen for P_{wax} (Fig. 3.5.).

n-Alkanol total concentrations ranged from 7.2 to 171.1 µg/g OC. The ACL for *n*-alkanols provided an overall average of 24.7, with little variation along the profile. However, marked increases in values were observed for ca. 4550 to 4350 cal yr BP and ca. 2550 to 2400 cal yr BP (Fig. 3.6.). *n*-Alkane to *n*-alkanol ratio values remained relatively constant from ca. 5424 to 2643 cal yr BP, with a minimum of 0.7 and a maximum of 0.8. At ca. 2479 cal yr BP there was a drop to 0, suggesting a period of reduced degradation. The rates increased to 0.5 at ca. 2152 cal yr BP and 0.6 at ca. 1988 cal yr BP at the surface (Fig. 3.6.).

Long chain *n*-alkan-2-ones have been proposed to be specific biomarkers for *Sphagnum* in ombrotrophic peat bogs (Nichols and Huang, 2007) and were present in all samples here. Total concentrations of these compounds varied between 22.1 and 144.5 µg/g OC.

Nichols and Huang (2007) proposed that heptacosan-2-one could be used as a *Sphagnum*-specific biomarker. We compared its concentration with that of the C_{31} *n*-alkane higher plant marker, to further investigate OM composition throughout the peat section ($C_{27\text{-one}}/C_{31\text{-ane}}$). A maximum value of 4.23 was observed at 4770 cal yr BP, whilst a minimum of 0.50 occurred at 4443 cal yr BP. The overall trend in the ratio was similar to that of the C_{23}/C_{31} *n*-alkane proxy (Fig. 3.6.).

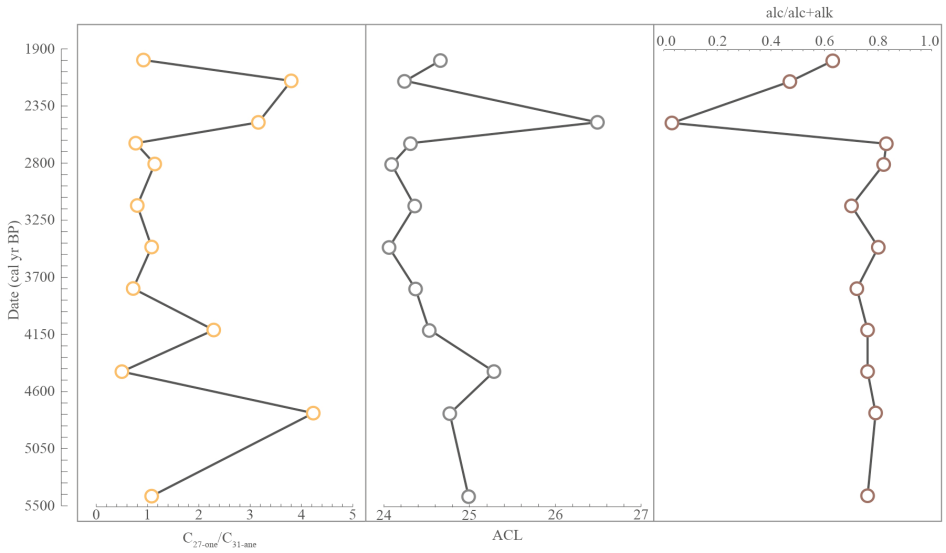

Figure 3.6. From left to right; ratio of C_{27} n-alkan-2-one/C_{31} n-alkane ($C_{27\text{-one}}/C_{31\text{-ane}}$), n-alkanol average chain length (ACL) from C_{22} – $C_{30,}$ and alc/alc+alk (measure of diagenesis) ratio.

Sterols, the most abundant lipid class in the profile, consisted predominantly of C_{29} homologues with a minor input of C_{27} and C_{28} compounds (Table 3.1.). This is a typical distribution in peatlands and indicative of a mainly higher plant contribution (Pancost et al., 2002). Overall, the distributions of sterols showed little variation throughout the profile.

Pancost et al. (2002) suggested that the triterpenoid taraxer-4-one may be of use as a biomarker for *Ericaceae* (heather) in ombrotrophic peat bogs. This is because it was only found in the extract *of Calluna vulgaris* roots and not in any of the *Sphagnum* tissue samples that were examined. Taraxer-4-one concentration ranged from 0 to 41 µg/g OC, with a general decreasing trend over time. The maximum value was observed at 4770 cal yr BP and was at least 5x greater than that for any other sample. Its input decreased continuously until 3788 cal yr BP, where taraxer-4-one was not detected.

3.3.4. $\delta^{13}C$ values

$\delta^{13}C$ measurements were analysed for representative compounds from each lipid class. namely C_{29} and C_{31} *n*-alkanes, C_{24} and C_{28} *n*-alkanols, C_{27} *n*-alkan-2-one and ß-sitosterol. No low molecular weight *n*-alkanes were within our detection range, nor were any terpenoids. The C_{29} *n*-alkane values displayed an increasing trend over time with a maximum value of -30.5‰ at 2152 cal yr BP and a minimum of -34.3‰ at 4443 cal yr BP. There was less variation in the C_{31} *n*-alkane values, with a maximum of -33.9‰ and a minimum of -35.8‰ at 4115 and 4770 cal yr BP respectively. Overall there was a gradual trend of depletion for this compound.

The C_{24} *n*-alkanol values ranged from -34.0 to -32.0‰, with an average of -32.9‰. C_{28} *n*-alkanol values were gradually depleted over time, with a maximum of -32.7‰ and a minimum of -34.8‰. The C_{28} *n*-alkanol values followed a similar trend to that of the C_{31} *n*-alkane.

C_{27} *n*-alkan-2-one values ranged from -33.3 to -31.4‰ at 4443 and 2152 cal yr BP respectively, becoming enriched over time. Values for ß-sitosterol show the greatest variation for all investigated compounds, with a minimum if -32.1‰ at 2479 cal yr BP and a maximum of -25.0‰ at 4770 cal yr BP.

3.4. Discussion

3.4.1. Origin of OM in the Spiddal ombrotrophic peat bog

The OM at the Spiddal peat bog site appears to be primarily of terrestrial origin. This is indicated by the predominance of lipid biomarkers of higher plant origin including the high molecular weight (HMW) *n*-alkanes with a strong OEP, the HMW

n-alkanols with an EOP, long chain *n*-alkan-2-ones, as well as the abundance of vascular plant steroids and terpenoids. A significant contribution from *Sphagnum* mosses is highlighted by the identification of low molecular weight (LMW) *n*-alkyl compounds throughout the peat profile. $\delta^{13}C$ values of individual biomarkers, with a minimum of ca. -35‰ and maximum of ca. -25‰ across the whole range, indicate a predominant contribution from C_3 plants (Ficken et al., 1998). López-Días et al. (2013) suggested a bacterial source for *n*-alkan-2-ones in a peat bog in Roñanzas, Northern Spain. However, $\delta^{13}C$ values for these compounds in the Spiddal peat are consistent with a terrestrial plant origin.

In contrast, the high TS values suggest an input of sulfate derived from seawater, with values > 3% in peat seen as indicative of a marine setting (Chou, 2012; Inglis et al., 2015). All but one of the samples (2152 cal yr BP) were above this limit. There was no correlation between TS and any other data here. Sulfur can be transported from the ocean to the atmosphere and the land through sea spray aerosols (Mahowald et al., 2011). It is possible that a proportion of the sulfur at this site was deposited by this mechanism due to the close proximity to the ocean. Although the peat bog was influenced by seawater at varying levels over time, the amount of marine OM input to the bog was negligible in comparison with the strong higher plant input during peat formation. Although some of the LMW *n*-alkyl compounds may originate from marine organisms, the lack of marine-specific sterols such as dinosterol or spongesterol (Lee et al., 1979; Volkman et al., 1993) could suggest that this influence is minor. Therefore, it would appear that the OM deposited during peat formation was predominantly of terrestrial origin allowing the peat record at this site to remain as a reliable indicator of palaeoenvironmental change, despite its coastal setting. Further analysis such as bulk $\delta^{13}C$ would provide more evidence to test this hypothesis.

3.4.2. Climate change in Ireland during the mid-Holocene

Using a combination of lipid classes analysed, it was possible to retrace variation in climatic conditions over time due to the response of the peat OM to change in precipitation. Pearson correlations show that there is good correlation between all of the biomarker proxies (Table A1); however, the C_{23}/C_{29} ratio shows the most variation. The $\delta^{13}C$ values for C_{31} *n*-alkane were 2.5‰ more positive on average than for the C_{29} *n*-alkane. Variation in carbon isotope values of up to 6‰ has been observed between *n*-alkanes within the same plant tissue (Rieley et al., 1993; Collister et al., 1994). There is a statistically significant correlation between the $\delta^{13}C$ values of the C_{27} *n*-alkan-2-one attributed to *Sphagnum* input, and that of the C_{29} *n*-alkane (r 0.70, $P < 0.02$). Neither of these show a correlation with the $\delta^{13}C$ value for the C_{31} *n*-alkane. This correlation over a ca. 3500 yr period could suggest that some of the C_{29} *n*-alkane input is derived from the species of *Sphagnum* contributing to peat formation at this site, implying that in this case the C_{23}/C_{31} and the $C_{27\text{-one}}/C_{31\text{-ane}}$ ratios are more reliable than the C_{23}/C_{29} ratio. Pancost et al. (2002) recommend that lipid biomarker data be used cautiously without the support of macrofossil analysis. Compound specific isotope analysis enables, however, more robust lipid biomarker data interpretation for peat samples where such additional data is not available.

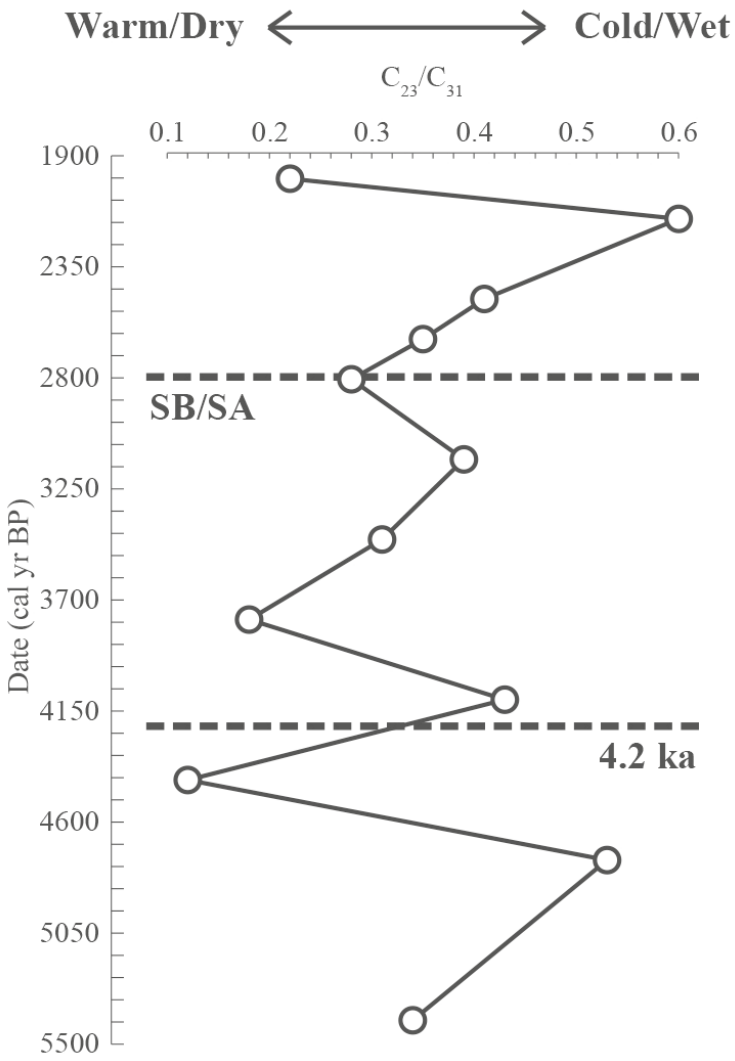

Figure 3.7. C_{23}/C_{31}n-alkane ratio trend displaying shifts between relatively warm and dry conditions and relatively cold and wet conditions indicated by the temperature gradient. Previously reported climatic events - the Subboreal-Subatlantic Transition (SB/SA) and 4.2 ka Event (4.2 ka) - are marked with dashed lines.

The high C_{23}/C_{29} *n*-alkane ratio at ca. 5424 cal yr BP is indicative of increased contribution from *Sphagnum* plants which suggests colder, wetter conditions occurred during this interval. However, all other proxies disagree with this, displaying values close to their respective averages. There is a conflict here between the C_{23}/C_{29} and C_{23}/C_{31} *n*-alkane proxies. At ca. 4770 cal. yr BP all the ratios point to an increase in

cold and wet conditions, with most indicating that this was one of the coldest and wettest periods throughout the investigated timeframe. These results agree somewhat with the idea of dry conditions becoming gradually wetter from ca. 5800 to 4800 cal. yr BP as outlined by Caseldine et al. (2005). However, no evidence of an extreme climatic event between 5200 and 5100 cal. yr BP as described by Caseldine et al. (2005) was observed at the Spiddal site.

Conditions shifted dramatically at ca. 4443 cal yr BP, providing the warmest and driest period in the record. All of the lipid biomarker proxies applied here are in agreement with this, showing an increased relative contribution from higher plants to the lipid record. Later, at ca. 4115 cal yr BP all indicators depict a return towards a colder, wetter climate. However, some proxies suggest that the shift is stronger than from other proxies. The C_{23}/C_{29} *n*-alkane, P_{aq}, and P_{wax} ratios suggest a distinct return to conditions similar to those at ca. 4770 cal yr BP, whilst the C_{23}/C_{31} *n*-alkane and the C_{27} *n*-alkan-2-one proxies suggest a less severe retraction. This date coincides with that of the 4.2 ka event. The identification of colder/wetter conditions at this time in our study would suggest that the effect of the event in Ireland is not yet clear. Also, the site in our study and that of Barber et al. (2003) were located in central Ireland, whereas Roland et al. (2014) investigated locations in the north of Ireland. Thus, regional differences in local conditions may explain discrepancies between studies. These contradictions show a need for further investigations of the palaeoclimate of Ireland around 4200 yr BP.

All the proxies provide evidence of a warmer and drier climate at ca. 3788 cal yr BP. The trends in the C_{23}/C_{29} *n*-alkane ratio and C_{27} *n*-alkan-2-one suggest that these conditions continue with little fluctuation for the next ca. 1300 yr, until ca. 2479 cal yr BP, where colder conditions return.The C_{23}/C_{31} *n*-alkane, P_{aq}, and P_{wax} ratios may

reflect change towards colder and wetter conditions at ca. 3134 cal yr BP, with a subsequent shift to relatively warmer conditions at ca. 2807 cal yr BP. The C_{27} *n*-alkan-2-one trend indicates the coldest/wettest conditions from all proxies at ca. 2479 cal yr BP.

At ca. 2152 cal yr BP all proxies indicate cold and wet conditions, one of the coldest and wettest periods of the entire profile. The shift towards colder/wetter conditions from ca. 2807 to 2152 cal. yr BP corresponds (Fig. 3.7.) with the Subboreal-Subatlantic transition. There is a sharp shift back to a warmer and drier climate in the shallowest sample representing ca. 1988 cal yr BP. This was one of the radiocarbon dated samples and was assigned an age of 2068 ± 51 cal yr BP, a similar date to that obtained by Williams and Doyle (2014) for a birch branch from the same site (2110 - 2084 cal yr BP).

The warmer and drier climate would have provided favourable conditions for the growth of a forest, which would ultimately become the 'drowned' forest that remains at the site today in the form of standing tree stumps. The cessation of peat formation coupled with the deposition of a sand layer covering the accrotelm and the embedded tree stumps, implies that there was a rapid rise in sea level at this time that engulfed the forest. Increasing TS also supports the influx of a marine influence. This was likely the only time in ca. 3500 yr that the site was submerged beneath the ocean, suggested by the lack of any sand layers throughout the 1 m peat profile.

3.5. Conclusions

A geochemical approach was used to investigate a peat bog profile from Spiddal, Co. Galway, Ireland. A suite of terrestrial plant derived lipid biomarkers and

published proxies revealed clear changes in vegetation type. This likely reflects high latitude changes in climate, and resulting changes in local environmental conditions during this mid-Holocene interval, some of which may have led to the rapid submersion of a forest at this location. Three distinct periods of cold and wet conditions were identified at 4770, 4115 and 2152 cal. yr BP, along with four periods of warmer and drier conditions at 4443, 3788, 2807 and 1988 cal. yr BP. These climatic extremes show some correlation with published records from Ireland attributed to climatic events, namely the 4.2 ka event and the Subboreal-Subatlantic transition. However, evidence of other climatic events such as the 5.2 ka event and the Roman Warm Period was not obtained. Our study found evidence of a 4.2 ka event with colder/wetter conditions in the dataset, similar to other peatland sites from central Ireland. This is contrary to the absence of evidence from peatland sites in the north of the island. This could suggest the possibility that this climatic event may not be absent from Ireland, but may not have affected all parts of the country. It would, however, be unusual for an event of this global magnitude to have such a localised impact, so further investigation of this incident is needed. Future work should involve a combination of multidisciplinary analytical techniques including geochemical methods in conjunction with analysis of testate amoebae, pollen and plant macrofossils. Work of this nature should also use multiple sampling locations to determine any spatial variability in the effect of this event. The results emphasise the importance of Ireland's peat resources as a record of palaeoenvironmental change. The organic geochemical approach has potential to provide a new dataset for Irish palaeoclimate research and should be utilised in future studies of ombrotrophic peat bogs, as well as the investigation of sites providing a greater spatial variability on the island. Here we show that a period of warm and dry conditions encouraged the growth

of the forest at this location around 2100 cal. yr BP and that a rapid rise in sea level in the following years is most likely responsible for its drowning.

References

Baas, M., Pancost, R., Van Geel, B., Sinninghe Damsté, J.S., 2000. A comparative study of lipids in Sphagnum species. Org. Geochem. 31, 535–541. doi:10.1016/S0146-6380(00)00037-1

Barber, K.E., 2007. Peatland records of Holocene climate change, in: Elias, S. (Ed.), Encyclopedia of Quarternary Science. Elsevier, Oxford, pp. 1884–1895.

Barber, K.E., Chambers, F.M., Maddy, D., 2003. Holocene palaeoclimates from peat stratigraphy: Macrofossil proxy climate records from three oceanic raised bogs in England and Ireland. Quat. Sci. Rev. 22, 521–539. doi:10.1016/S0277-3791(02)00185-3

Barber, K.E., Maddy, D., Rose, N., Stevenson, a. C., Stoneman, R., Thompson, R., 2000. Replicated proxy-climate signals over the last 2000 yr from two distant UK peat bogs: New evidence for regional palaeoclimate teleconnections. Quat. Sci. Rev. 19, 481–487. doi:10.1016/S0277-3791(99)00102-X

Bingham, E.M., McClymont, E.L., Väliranta, M., Mauquoy, D., Roberts, Z., Chambers, F.M., Pancost, R.D., Evershed, R.P., 2010. Conservative composition of n-alkane biomarkers in Sphagnum species: Implications for palaeoclimate reconstruction in ombrotrophic peat bogs. Org. Geochem. 41, 214–220. doi:10.1016/j.orggeochem.2009.06.010

Blackford, J.J., Chambers, F.M., 1991. Proxy records of climate from blanket mires: evidence for a Dark Age (1400 BP) climatic deterioration in the British Isles.

The Holocene 1, 63–67. doi:10.1177/095968369100100108

Blundell, A., Charman, D.J., Barber, K., 2008. Multiproxy late Holocene peat records from Ireland: towards a regional palaeoclimate curve. J. Quat. Sci. 23, 59–71.

Bond, G., Kromer, B., Beer, J., Muscheler, R., Evans, M.N., Showers, W., Hoffmann, S., Lotti-Bond, R., Hajdas, I., Bonani, G., 2001. Persistent Solar Influence on North Atlantic Climate During the Holocene. Sci. 294 , 2130–2136. doi:10.1126/science.1065680

Bray, E.E., Evans, E.D., 1961. Distribution of n-Paraffins as a clue to Recognition of Source Beds. Geochim. Cosmochim. Acta 22, 2–15. doi:10.1016/0016-7037(61)90069-2

Caseldine, C., Thompson, G., Langdon, C., Hendon, D., 2005. Evidence for an extreme climatic event on Achill Island, Co. Mayo, Ireland around 5200-5100 cal. yr BP. J. Quat. Sci. 20, 169–178. doi:10.1002/jqs.901

Chambers, F.M., Booth, R.K., De Vleeschouwer, F., Lamentowicz, M., Le Roux, G., Mauquoy, D., Nichols, J.E., van Geel, B., 2012. Development and refinement of proxy-climate indicators from peats. Quat. Int. 268, 21–33. doi:10.1016/j.quaint.2011.04.039

Chou, C.L., 2012. Sulfur in coals: A review of geochemistry and origins. Int. J. Coal Geol. 100, 1–13. doi:10.1016/j.coal.2012.05.009

Collister, J.W., Rieley, G., Stern, B., Eglinton, G., Fry, B., 1994. Compound-specific δ 13C analyses of leaf lipids from plants with differing carbon dioxide metabolisms. Org. Geochem. 21, 619–627. doi:10.1016/0146-6380(94)90008-6

Eganhouse, R.P., 1997. Molecular Markers and Environmental Organic Geochemistry: An Overview, in: Eganhouse, R.P. (Ed.), Molecular Markers in

Environmental Chemistry. American Chemical Society, p. 426.

Eglinton, G., Hamilton, R.J., 1967. Leaf Epicuticular Waxes. Sci. 156 , 1322–1335. doi:10.1126/science.156.3780.1322

Ficken, K.., Li, B., Swain, D.., Eglinton, G., 2000. An n-alkane proxy for the sedimentary input of submerged/floating freshwater aquatic macrophytes. Org. Geochem. 31, 745–749. doi:10.1016/S0146-6380(00)00081-4

Ficken, K.J., Barber, K.E., Eglinton, G., 1998. Lipid biomarker, ??13C and plant macrofossil stratigraphy of a Scottish montane peat bog over the last two millennia. Org. Geochem. 28, 217–237. doi:10.1016/S0146-6380(97)00126-5

Hammer, Ø., Harper, D.A.T., Ryan, P.D., 2001. PAST: Paleontological Statistics Software Package for education and data analysis. Palaeontolia Electronica 4.

Inglis, G.N., Collinson, M.E., Riegel, W., Wilde, V., Robson, B.E., Lenz, O.K., Pancost, R.D., 2015. Ecological and biogeochemical change in an early Paleogene peat-forming environment: Linking biomarkers and palynology. Palaeogeogr. Palaeoclimatol. Palaeoecol. 438, 245–255. doi:10.1016/j.palaeo.2015.08.001

Killops, S., Killops, V., 2005. Introduction to Organic Geochemistry, 2nd ed. Blackwell Science Ltd., Oxford.

Lee, C., Farrington, J.W., Gagosian, R.B., 1979. Sterol geochemistry of sediments from the western North Atlantic Ocean and adjacent coastal areas. Geochim. Cosmochim. Acta 43, 35–46. doi:10.1016/0016-7037(79)90044-9

López-Días, V., Blanco, C.G., Bechtel, A., Püttmann, W., Borrego, A.G., 2013. Different source of n-alkanes and n-alkan-2-ones in a 6000 cal. yr BP Sphagnum-rich temperate peat bog (Roñanzas, N Spain). Org. Geochem. 57, 7–10. doi:http://dx.doi.org/10.1016/j.orggeochem.2013.01.006

Mahowald, N., Ward, D.S., Kloster, S., Flanner, M.G., Heald, C.L., Heavens, N.G., Hess, P.G., Lamarque, J.-F., Chuang, P.Y., 2011. Aerosol Impacts on Climate and Biogeochemistry. Annu. Rev. Environ. Resour. 36, 45–74. doi:10.1146/annurev-environ-042009-094507

McClymont, E.L., Pendall, E., Nichols, J., 2010. Stable isotopes and organic geochemistry in peat : tools to investigate past hydrology, temperature and biogeochemistry. doi:10.1002/jqs.1295.Mitchell

Nichols, J.E., Booth, R.K., Jackson, S.T., Pendall, E.G., Huang, Y., 2006. Paleohydrologic reconstruction based on n-alkane distributions in ombrotrophic peat. Org. Geochem. 37, 1505–1513. doi:10.1016/j.orggeochem.2006.06.020

Nichols, J.E., Huang, Y., 2007a. C23-C31 n-alkan-2-ones are biomarkers for the genus Sphagnum in freshwater peatlands. Org. Geochem. 38, 1972–1976. doi:10.1016/j.orggeochem.2007.07.002

Nichols, J.E., Huang, Y., 2007b. C23–C31 n-alkan-2-ones are biomarkers for the genus Sphagnum in freshwater peatlands. Org. Geochem. 38, 1972–1976. doi:10.1016/j.orggeochem.2007.07.002

Nott, C.J., Xie, S., Avsejs, L. a., Maddy, D., Chambers, F.M., Evershed, R.P., 2000. n-Alkane distributions in ombrotrophic mires as indicators of vegetation change related to climatic variation. Org. Geochem. 31, 231–235. doi:10.1016/S0146-6380(99)00153-9

Otto, A., Shunthirasingham, C., Simpson, M.J., 2005. A comparison of plant and microbial biomarkers in grassland soils from the Prairie Ecozone of Canada. Org. Geochem. 36, 425–448. doi:10.1016/j.orggeochem.2004.09.008

Pancost, R.D., Baas, M., Van Geel, B., Sinninghe Damsté, J.S., 2002. Biomarkers as proxies for plant inputs to peats: An example from a sub-boreal ombrotrophic

bog. Org. Geochem. doi:10.1016/S0146-6380(02)00048-7

Pancost, R.D., Boot, C.S., 2004. The palaeoclimatic utility of terrestrial biomarkers in marine sediments. New Approaches Mar. Org. Biogeochem. A Tribut. to Life Sci. John I. Hedges 92, 239–261. doi:DOI: 10.1016/j.marchem.2004.06.029

Pancost, R.D., McClymont, E.L., Bingham, E.M., Roberts, Z., Charman, D.J., Hornibrook, E.R.C., Blundell, A., Chambers, F.M., Lim, K.L.H., Evershed, R.P., 2011. Archaeol as a methanogen biomarker in ombrotrophic bogs. Org. Geochem. 42, 1279–1287. doi:10.1016/j.orggeochem.2011.07.003

Peters, K.E., Walters, C.C., Moldowan, J.M., 2005. The Biomarker Guide. Cambridge.

Pinkart, H.C., Devereux, R., Chapman, P.J., 1998. Rapid separation of microbial lipids using solid phase extraction columns. J. Microbiol. Methods 34, 9–15. doi:10.1016/S0167-7012(98)00060-8

Plunkett, G.M., 2006. Tephra-linked peat humification records from Irish ombrotrophic bogs question nature of solar forcing at 850 cal. yr BC. J. Quat. Sci. 21, 9–16. doi:10.1002/jqs.951

Plunkett, G.M., Pilcher, J.R., McCormac, F.G., Hall, V.A., 2004. New dates for first millennium BC tephra isochrones in Ireland. The Holocene 14 , 780–786. doi:10.1191/0959683604hl757rr

Poynter, J., Eglinton, G., 1990. MOLECULAR COMPOSITION OF THREE SEDIMENTS FROM HOLE 717C : 116, 155–161.

Radu, T., Diamond, D., 2009. Comparison of soil pollution concentrations determined using AAS and portable XRF techniques. J. Hazard. Mater. 171, 1168–71. doi:10.1016/j.jhazmat.2009.06.062

Rieley, G., Collister, J.W., Stern, B., Eglinton, G., 1993. Gas chromatography/isotope ratio mass spectrometry of leaf wax n-alkalines from plants of differing carbon dioxide metabolisms. Rapid Commun. Mass Spectrom. 7, 488–491.

Roland, T.P., Caseldine, C.J., Charman, D.J., Turney, C.S.M., Amesbury, M.J., 2014. Was there a "4.2ka event" in Great Britain and Ireland? Evidence from the peatland record. Quat. Sci. Rev. 83, 11–27. doi:10.1016/j.quascirev.2013.10.024

Roland, T.P., Daley, T.J., Caseldine, C.J., Charman, D.J., Turney, C.S.M., Amesbury, M.J., Thompson, G.J., Woodley, E.J., 2015. The 5.2 ka climate event: Evidence from stable isotope and multi-proxy palaeoecological peatland records in Ireland. Quat. Sci. Rev. 124, 209–223. doi:10.1016/j.quascirev.2015.07.026

Schellekens, J., Bindler, R., Martínez-Cortizas, A., McClymont, E.L., Abbott, G.D., Biester, H., Pontevedra-Pombal, X., Buurman, P., 2015. Preferential degradation of polyphenols from Sphagnum – 4-Isopropenylphenol as a proxy for past hydrological conditions in Sphagnum-dominated peat. Geochim. Cosmochim. Acta 150, 74–89. doi:10.1016/j.gca.2014.12.003

Simoneit, B.R.T., 2004. Biomarkers (molecular fossils) as geochemical indicators of life. Adv. Sp. Res. 33, 1255–1261. doi:10.1016/j.asr.2003.04.045

Swindles, G.T., Blundell, a., Roe, H.M., Hall, V. a., 2010. A 4500-year proxy climate record from peatlands in the North of Ireland: the identification of widespread summer "drought phases"? Quat. Sci. Rev. 29, 1577–1589. doi:10.1016/j.quascirev.2009.01.003

Swindles, G.T., Lawson, I.T., Matthews, I.P., Blaauw, M., Daley, T.J., Charman,

D.J., Roland, T.P., Plunkett, G., Schettler, G., Gearey, B.R., Turner, T.E., Rea, H. a., Roe, H.M., Amesbury, M.J., Chambers, F.M., Holmes, J., Mitchell, F.J.G., Blackford, J., Blundell, A., Branch, N., Holmes, J., Langdon, P., McCarroll, J., McDermott, F., Oksanen, P.O., Pritchard, O., Stastney, P., Stefanini, B., Young, D., Wheeler, J., Becker, K., Armit, I., 2013. Centennial-scale climate change in Ireland during the Holocene. Earth-Science Rev. 126, 300–320. doi:10.1016/j.earscirev.2013.08.012

Swindles, G.T., Plunkett, G., Roe, H.M., 2007. A delayed climatic response to solar forcing at 2800 cal. BP: multiproxy evidence from three Irish peatlands. The Holocene 17, 177–182. doi:10.1177/0959683607075830

Verardo, D.J., Froelich, P.N., McIntyre, A., 1990. Determination of organic carbon and nitrogen in marine sediments using the Carlo Erba NA-1500 analyzer. Deep Sea Res. Part A. Oceanogr. Res. Pap. 37, 157–165. doi:10.1016/0198-0149(90)90034-S

Volkman, J.K., Barrett, S.M., Dunstan, G.A., Jeffrey, S.W., 1993. Geochemical significance of the occurrence of dinosterol and other 4-methyl sterols in a marine diatom. Org. Geochem. 20, 7–15. doi:10.1016/0146-6380(93)90076-N

Weiss, H., Courty, M.A., Wetterstrom, W., Guichard, F., Senior, L., Meadow, R., Curnow, A., 1993. The genesis and collapse of third millennium north mesopotamian civilization. Science (80-.). 261, 995–1004.

Williams, D.M., Doyle, E., 2014. Dates from drowned Mid-Holocene landscapes on the Central Western Irish Seaboard. Irish J. Earth Sci. 32, 23–27.

Zhang, Y., Liu, X., Lin, Q., Gao, C., Wang, J., Wang, G., 2014. Vegetation and climate change over the past 800years in the monsoon margin of northeastern China reconstructed from n-alkanes from the Great Hinggan Mountain

ombrotrophic peat bog. Org. Geochem. 76, 128–135. doi:10.1016/j.orggeochem.2014.07.013

Zheng, Y., Zhou, W., Meyers, P.A., Xie, S., 2007. Lipid biomarkers in the Zoigê-Hongyuan peat deposit: Indicators of Holocene climate changes in West China. Org. Geochem. 38, 1927–1940. doi:10.1016/j.orggeochem.2007.06.012

Chapter 4

Characterisation of a marine pockmark site in Bantry Bay, Co. Cork, Ireland

Abstract

A geophysical and geochemical investigation was carried out in Bantry Bay, a large marine inlet on the south coast of Ireland in Co. Cork. Multibeam and sub-bottom profile data obtained during the survey showed significant fluid migration in the shallow sediments of the bay. Concave depressions in the seabed, known as pockmarks and generally considered to be formed through the expulsion and resettling of sediment due to sub-seafloor fluid release, were observed in part of the bay. Three 6 m vibracores were taken inside the bay, two from within the pockmark field and one from an area without these seabed features. Further physical and chemical analyses were performed on the sediments. The fluid was identified as biogenic CH_4 and was quantified in all three vibracores. Clearly defined sulfate methane transition zones (SMTZ) were observed in two cores, one from inside the pockmark field and the other from outside. Analysis of phospholipid fatty acids (PLFAs) and archaeal isoprenoidal hydrocarbons was used to investigate the microbial ecology of these sediments. AOM seems to be the primary control of CH_4 release and is most likely mediated by symbiotic sulfate reducing bacteria (SRB) and anaerobic methanotrophic archaea (ANME).

4.1. Introduction

Pockmarks are marine geological features that were first described on the Scotian Shelf off Nova Scotia, Canada by King and MacLean (1970). They are concave depressions in the seabed sediment that are circular to ellipsoidal in shape. They can range from <1 to 200 m in diameter and up to 20 m deep (Hovland, 1987), however they are usually 30 to 40 m in diameter and 2 to 3 m deep (Acosta et al., 2001). Pockmarks can occur as single features, in a linear pattern known as a pockmark train, or in groups known as pockmark fields (Szpak et al., 2012). The formation and dynamics of these features is still not fully understood (Hovland et al., 2005) although they are predominantly thought to be the result of the expulsion of hydrocarbon gases and porewaters from the seafloor (O'Reilly, 2013). These are not isolated features but are distributed across the globe in a range of marine settings at varying depths from 30 to 300 m (Baraza and Ercilla, 1996; Hovland, 1987).

The importance of pockmarks is multifaceted. From a natural resource perspective pockmarks are important for two reasons. Firstly, petroleum systems analysts derive critical information from the interpretation of near-surface features relating to hydrocarbon migration (Abrams, 2005). Secondly, pockmarks have been shown to be associated with the presence of gas hydrates, however this is only at water depths greater than 500 m due to the pressure and temperature conditions required for hydrate formation (Judd and Hovland, 2009). Gas hydrates (also known as clathrates) consist of a gas, predominantly methane (CH_4), trapped within a cage-like lattice of hydrogen bonded water molecules (Judd and Hovland, 2009; Kvenvolden, 1995). There is potential for large scale extraction of marine gas

hydrates as an energy source, however there is still uncertainty surrounding its efficient exploitation (Beauchamp, 2004; Chatti et al., 2005; Lee and Holder, 2001).

The fact that pockmarks can act as indicators of active fluid flow raises their significance in terms of seabed construction (Hovland, 1987). This hydraulic activity represents the possibility of slope failure and seabed instability, therefore construction in pockmarked areas of marine infrastructure such as offshore pipelines may be hindered due to the necessary avoidance of these features (Hovland et al., 2002). Hovland et al. (2002) also advocated for wide scale multinational monitoring of pockmarks as in some instances they have been shown to become active several days prior to major earthquakes. Active venting of gas from pockmarks was observed at sites in California (Field and Jennings, 1987) and Greece (Hasiotis et al., 1996; Soter, 1999) before and during earthquake events. This activity suggests that they may be important precursor indicators that have been overlooked (Hovland et al., 2002).

The intrinsic relationship between pockmarks and CH_4 also warrants detailed monitoring due to the potential climate change implications. Geologic Emissions of Methane (GEM) including marine seeps have recently been recognized as second only to wetlands as a natural source of atmospheric methane (Etiope et al., 2008). As a greenhouse gas, CH_4 outweighs carbon dioxide (CO_2) by a factor of 25 times in terms of its global warming potential, and since pre-industrial times is estimated to have been responsible for approximately 20% of the Earth's warming (Yvon-Durocher et al., 2014). Active gas seepage from seabed sites such as pockmark features may be underestimated and it has been argued that there is a need for CH_4 flux revisions in terms of the global carbon cycle (Judd and Hovland, 2009). CH_4 hydrates also constitute a huge risk as some researchers warn that increasing global

temperatures may have caused the frozen cage of these structures to melt during the late Quaternary leading to the release of the bound CH_4 to the atmosphere, a theory known as the clathrate gun hypothesis (Kennett et al., 2003). This type of event has been linked to past periods of warming through the analysis of carbon isotopic variations in benthic foraminifera (Kennett et al., 2000). Kennett et al. (2000) identified at least 4 episodes of large-scale CH_4 release from sediments during the late Quaternary and suggested that these were caused by the dissociation of gas hydrates as a result of millennial-scale changes in bottom-water temperature.

Although high amounts of CH_4 are transported from deep reservoirs to shallow sediments, it is estimated that <3% reaches the atmosphere due to the anaerobic oxidation of methane (AOM) performed by microbial communities (Niemann and Elvert, 2008). The predominant mechanism of AOM is thought to be a symbiotic process whereby anaerobic methanotrophic archaea (ANME) and sulfate reducing bacteria (SRB) oxidise CH_4 to CO_2 whilst reducing sulfate (SO_4^{2-}) to hydrogen sulfide (H_2S) providing energy for both microbial consortia (Boetius et al., 2000; Elvert et al., 2003; Reeburgh, 2007; Valentine and Reeburgh, 2000). These communities are predominantly found in sediments, however they have also been found in anoxic marine and saline lacustrine water bodies, and in terrestrial mud volcanoes (Alain et al., 2006; Joye et al., 1999; Wakeham et al., 2003).

$$SO_4^{2-} + CH_4 \rightarrow HCO_3^- + H_2S + H_2O$$

This process occurs in a specific area of the seabed known as the sulfate-methane transition zone (SMTZ), where CH_4 seepage and SO_4^{2-} penetration from

seawater provide optimal conditions for AOM communities (Knittel and Boetius, 2009).

Lipid biomarkers are often used to classify AOM communities, and along with fluorescence in situ hybridization (FISH), have provided the primary evidence for AOM at cold seep environments such as pockmarks (Caldwell et al., 2008). PLFAs, non-polar fatty acids cleaved from their polar head groups for GC-MS analysis, provide quantitative measures of viable biomass and microbial community composition (Ringelberg et al., 1997; Zelles, 1997). Phospholipids are rapidly degraded after cell death making them excellent biomarkers for viable microbial cells (Navarrete et al., 2000; White et al., 1997). Certain PLFAs have been used as chemotaxonomic markers for SRB, such as $C_{16:1\omega5c}$ and $cyC_{17:0\omega5,6}$ as indicators of *Desulfosarcina/Desulfococcus* species (Elvert et al., 2003). Archaeal cell membranes are comprised of isoprenoid rather than straight chain carbon skeletons, analysis of which allows them to be differentiated from bacteria (Schouten et al., 2013). For example, King et al. (1998) used a combination of phytane, acyclic and cyclic C_{40} isoprenoids ($C_{40:0cy}$, $C_{40:1cy}$, $C_{40:2cy}$, $C_{40:3cy}$) to show that archaeal communities were widespread throughout the Black Sea.

As CH_4 is carbon-isotopically light, the analysis of $^{13}C/^{12}C$ ratios of individual biomarkers using compound specific isotope ratio mass spectrometry (IRMS) increases the applicability of lipid biomarker analysis to studies of AOM environments. $\delta^{13}C$ values of AOM derived lipids are typically significantly depleted with values <-50‰ (Elvert et al., 2003; Niemann and Elvert, 2008; van Dongen et al., 2007). Isolation of bacteria and archaea derived lipids combined with determination of their individual $\delta^{13}C$ signatures can help provide an overview of the

microbial consortia and their involvement in AOM within cold seep environments (e.g. Ge et al., 2015; Pancost et al., 2000).

The aims of this study were to (I) characterize a small pockmark field in Bantry Bay, Co. Cork, Ireland, (II) to determine possible causes of pockmark formation in this area, and (III) to determine the microbial ecology of these interesting seabed features. It is essential that we understand these features which occur frequently in Irish waters as they have the potential to be economically and environmentally important in the near future.

4.2. Geological setting

Figure 4.1. Map of Bantry Bay area and location of Bantry Bay in Ireland (inset).

Bantry Bay is the largest marine inlet situated in the South Munster Basin in the southwest of Ireland, leading in to the Atlantic Ocean (Fig. 4.1.). It is approximately 40 km long, 5 km wide at the head, 10 km wide at the mouth, spanning an area of 300 km^2. The bay contains two large islands; Bere Island in the outer bay and Whiddy Island in the inner bay. The Melagh, Owvane, Coomhola, Glengarriff, and Adrigole rivers all drain into Bantry Bay. The bedrock geology consists of Devonian strata dominated by Old Red Sandstone beneath Uppermost Devonian and Carboniferous marine sandstones and mudstones (Plets et al., 2015; Vermeulen et al., 2000). Several fault lines run through the bay (Fig. 4.2.). The Bantry Fault runs from the south east of Whiddy Island, continuing along the centre of the bay. The Owenberg River Fault lies north east of Whiddy Island before meeting the Bantry Fault. Also north east of Whiddy Island are the Glengarriff Harbour and Coolieragh Faults. The area has undergone extensive acoustic surveying as part of the Integrated Mapping for the Sustainable Development of Ireland's Marine Resources (INFOMAR) programme providing bathymetry, backscatter, and seabed classification for the bay. LIDAR has provided data on the nearshore and shallow areas of the bay. The water depth within Bantry Bay ranges from 0 to 60 m. The sediment type is predominantly mud to fine sand with increasing medium to coarse sand towards the mouth of the bay. There are areas of medium to coarse sand, coarse sand to gravel, and rock throughout the bay primarily along the perimeter. A pockmark field, covering an area of approximately 5 km^2, lies to the north of Whiddy Island in about 20 m water depth. The sediment type within the pockmark field is mud to fine sand.

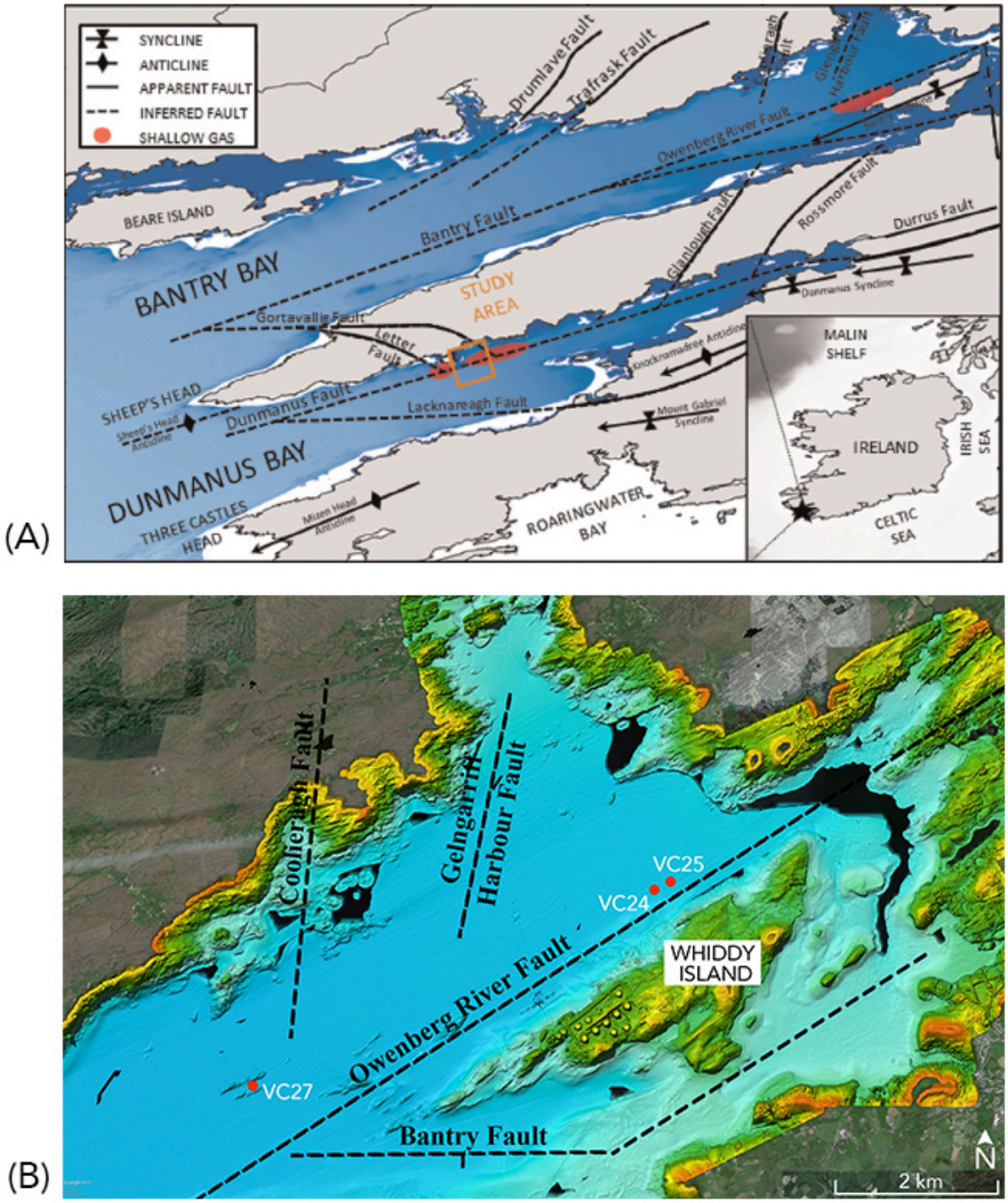

Figure 4.2. (A) Map of Bantry and Dunmanus Bays with fault lines and shallow gas accumulations marked (reproduced from Szpak et al., (2015)). (B) Bathymetric map of inner Bantry Bay showing locations of vibrocores.

4.3. Materials and methods

4.3.1. Seabed surveying

Surveying was carried out as part of the INFOMAR programme. Data was acquired onboard the research vessels; R.V. Celtic Explorer (2006 and 2014), R.V. Celtic Voyager (2007), and Irish Mist (2006) (Fig. 4.2.). Bathymetry and backscatter data were collected using Kongsberg Simrad EM1002 (95 kHz) and EM3002D (200 kHz) multibeam echo sounders. Multibeam data was processed using QTC Multiview software. Resulting bathymetric terrain models were gridded at 5 x 5 m.

Sub-bottom profiling was carried out during the CE14003 research cruise (2014) on board the R.V Celtic Explorer using a heave-corrected SES Probe 5000 3.5 kHz transceiver with a 4x4 transducer array (hull-mounted) and a CODA DA2000 acquisition system. Acquisition parameters, data logging, and interpretation were performed using the CODA Geokit suite.

LiDAR data was acquired by laser airborne depth sounder (LADS) on aircraft operated by Tenix LADS Corporation (2006)

4.3.2. Sediment sampling

Sediment vibracores were obtained during the CE14003 research cruise using a 6 m pneumatic vibracorer. Cores were sectioned at 1 m intervals and capped on deck. Core sections were split and archived halves were photographed and logged (Fig. 4.3.). Porewater samples were obtained by placing a Rhizon (Rhizoshere Research Products) connected to a 10 mL plastic syringe into the sediment. The syringe plunger was drawn back fully, held in place using a wooden spacer, the vacuum created a pressure gradient which drew porewater from the

sediment directly into the syringe. 1 mL of the porewater was transferred to a plastic vial along with 400 µL of 50 mM zinc acetate to quantitatively preserve sulfide as ZnS for analysis. The remainder (ca. 9 mL) was placed in a plastic vial along with 10 µL of chloroform to preserve for sulfate analysis. All porewater samples were refrigerated at 4ºC onboard for the duration of the cruise, for later analysis back in the laboratory (within 4 weeks).

Gas samples were immediately taken from the vibrocore sections. 10 mL plastic syringes with tops removed were plunged into the sediment to obtain two 10 cm^3 sediment plugs. These were injected into a 50 mL glass headspace vial containing 20 mL 2 M sodium hydroxide. The sample was capped and sealed using a butyl rubber septum and aluminium ring. Gas samples were homogenized, and stored upside-down in the dark at 4 ℃ for the duration of the cruise.

Sediment sub-samples were taken immediately after porewater and gas sub-samples. Particle size analysis (PSA) samples were placed in ziplock bags and stored at room temperature. Samples for lipid biomarker analysis were wrapped in fired Al foil and stored in ziplock bags at -20 ℃.

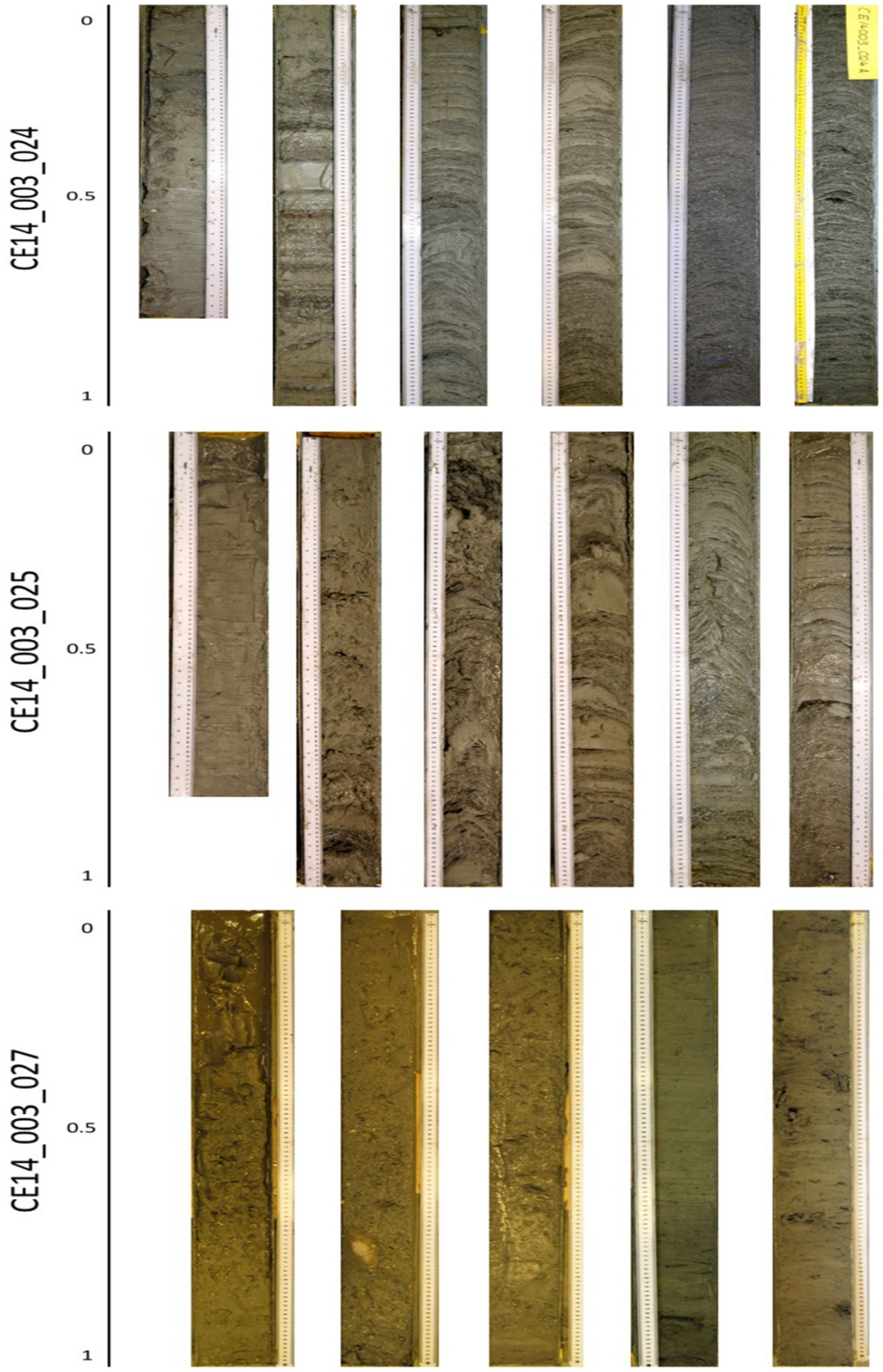

Figure 4.3. Complete sections of each vibrocore taken immediately after splitting. Depth in mbsf from left of image.

4.3.3. Porewater and gas analysis

Porewater H_2S concentrations were determined spectrophotometrically following the leucomethylene blue method of Fonselius et al. (1999). Samples were diluted (100 µL in 2400 µL) with O_2-free deionized H_2O prior to reagent addition. 20 µL 50 mM ZnAc solution, 30 µL N,N-Dimethyl-1,4-phenylenediammonium dichloride solution, and 30 µL $FeCl_3$ solution were added to each sample. These were mixed thoroughly and allowed to react for 1 hr. Absorbance was measured at 660 nm on a Shimadzu UV Mini 1240 and concentrations were determined by extrapolation from a calibration curve prepared with a range of Na_2S (0 – 1.5 ppm) standards. Standards were dissolved in artificial seawater prepared with commercially available sea salts (Sigma Aldrich, Dorset, UK).

SO_4^{2-} concentration in porewater was determined by the turbidimetric method. 10 mL of sample was stirred constantly and 2-3 drops of glycerol were added. Crushed $BaCl_2$, approximately 50 mg, was added to the mixture and stirring was continued for 1 minute after which an aliquot was taken and the absorbance measured at 420 nm on a Shimadzu UV Mini 1240. Further aliquots were taken after 2, 2.5, and 3 minutes and an average reading was calculated and used to determine concentration by extrapolation from a calibration curve. The calibration curve was prepared with Na_2SO_4 standards in a range of 10 to 100 ppm.

CH_4 analysis was performed on an Agilent 7820A GC-FID with a 30 m HP-PLOTQ column (Agilent, Santa Clara, USA). Column conditions were isothermal (50 ℃). CH_4 was quantified using calibration standards prepared from a 99.995% CH_4 standard (Sigma Aldrich, Dorset, UK).

4.3.4. Bulk physical and chemical analysis

PSA data was obtained by laser granulometry using a Mastersizer 2000 particle size analyser (Malvern, Worcestershire, UK) for fractions <1 mm and a dry sieving method for fractions >1 mm. Resulting data are reported as percentages of the total sample.

Elemental analysis was performed in triplicate using a Fisons NCS 1500 NA elemental analyser following the procedure of Verardo et al. (1990) described previously in Chapter 2.

4.3.5. Lipid biomarker analysis

Sediment samples were freeze-dried, ground, and sieved through an 850 μm mesh prior to extraction. Lipid compounds were extracted using a modified version of the Bligh-Dyer extraction (White et al., 1997). Approximately 30 g of sediment was extracted per sample in three separate procedures using 10 g each. Phosphate buffer (pH 7.2), $CHCl_3$, and CH_3OH were added to the sediment (0.8:1:2 v/v) in Teflon centrifuge tubes followed by sonication for 2 min. Extraction was performed in the dark for 18 hrs on a horizontal shaker. After centrifugation (15 min at 5000 rpm) supernatants were transferred to a separating funnel followed by additional phosphate buffer, $CHCl_3$, and CH_3OH to provide a ratio of 1:1:0.9 v/v. Organic and aqueous phases were allowed to separate for 4 hrs and the three total lipid extracts (TLEs) were combined and concentrated by rotary evaporation.

Elemental sulfur was removed with HCl activated copper overnight and TLEs were separated into relevant classes following the method described by Pinkart et al. (1998). The TLE was added to custom-made Bond-Elut SPE columns packed with an aminopropylsilica solid phase (5mm diameter, PE, 500mg Ultra-Clean NH2,

Agilent Technologies) and neutral lipids were eluted with 5 mL $CHCl_3$, glycolipids with 5 mL acetone, and polar lipids with 2.5 mL 6:1 (v/v) CH_3OH:$CHCl_3$ followed by 2.5 mL 0.05 M sodium acetate in 6:1 (v/v) CH_3OH: $CHCl_3$. Neutral and glycolipid fractions were stored at -20 ℃ for future analysis.

100 µL 1:1 (v/v) toluene:methanol was added to an aliquot of the polar fraction which was reacted with 100 µL sodium methoxide (50 ℃,30 mins) to derivatise phospholipids. Once cooled, 200 µL DI H_2O was added and the sample was neutralised with 70 µL 0.5 M HCl. Samples were extracted three times with 400 µL hexane:chloroform and combined organic layers were dried under anhydrous N_2 and re-suspended in hexane.

Double-bond positions of monounsaturated PLFAs were determined by the formation of dimethyl disulfide (DMDS) adducts as described by Nichols et al. (1986). Briefly, samples in 50 µL hexane were treated with 100 µL DMDS and 1-2 drops of iodine solution (6% (w/v) in diethyl ether at 50 ℃ for 48 hrs. 500µL hexane was added and samples were shaken after addition of 500 µL 5% (w/v) sodium thiosulfate to remove iodine. The organic layer was removed and combined with further organic layers following triplicate extraction of the aqueous layer with 4:1 hexane:chloroform. Extracts were dried under anhydrous N_2 and res-uspended in hexane prior to analysis.

Archaeal ether lipids were prepared under anhydrous N_2 by the addition of 200 µL boron tribromide to a dried aliquout of the polar lipid fraction. These were heated at 60 ℃ for 2 hrs. 200 µL superhydride solution was added after cooling and these were reheated at 60 ℃ for 2 hrs. After cooling, the reaction was quenched with 1 drop of DI H_2O. 400 µL DI H_2O was added and these were extracted 5 times with 400 µL hexane. Combined organic layers were dried under anhydrous N_2 and re-

suspended in hexane. 100 ppm 5α cholestane was added to all derivatised fractions as an internal standard prior to analysis.

Aliquots (1 μl) of samples were immediately analysed in triplicate with an Agilent model 7890N gas chromatograph equipped with a 7683 autosampler according to the conditions of Otto et al. (2006) as described previously in Chapter 2 for the analysis of neutral lipid fractions.

Individual compounds were assigned from comparison with mass spectral library databases (NIST and Wiley) and comparison of MS patterns with published spectra and authentic standards. Analytes were quantified from total ion peak area using multiple-point calibration curves of representative standards (methyl tetradecanoate and squalane). Percentage recovery was measured using an internal recovery standard added prior to extraction and was found to be > 95%. Procedural blanks were run to monitor background interferences.

All samples were analysed in triplicate using continuous flow IRMS as described in Chapter 3.

Lipid nomenclature is according to xCyωz, where x refers to the number of carbon atoms present, y refers to the number of double bonds on the carbon chain and z refers to the position of the first double bond from the methyl end. Iso and anteiso branching is denoted by '*i*' and '*ai*' respectively whilst the presence of the cyclopropane ring in a compound is denoted by '*cy*'.

4.4. Results

4.4.1. Geophysical analyses

Multibeam data suggest that the pockmarks north of Whiddy Island average ca. 10 m in diameter and ca. 0.03 m in depth. The positioning error between the recorded GPS position onboard the vessel and the actual sample location ranges from 20 – 30 m. Therefore, although both VC024 and VC025 were taken within the pockmark field, it is unsure whether either core penetrated directly into a single pockmark feature.

Sub-bottom profiles for all sampling locations show acoustic signatures indicative of gas migration within the sediment (Fig. 4.4.). A band of acoustic turbidity, dark reflections caused by gas bubbles which obscure reflections from deeper sediments (Judd and Hovland, 2009), runs concurrently at ca. 2 – 3 m below the sea floor (mbsf). This may suggest an accumulation of shallow gas within the sediment at this depth. Areas of acoustic blanking, due to a decrease in the backscatter of the acoustic signal below this band of turbidity may be indicative of vertical gas migration from deeper within the sediment (Szpak et al., 2012). There are no gas-related acoustic signatures above the band of turbidity or within the water column suggesting that there is little or no gas escape from the sediment.

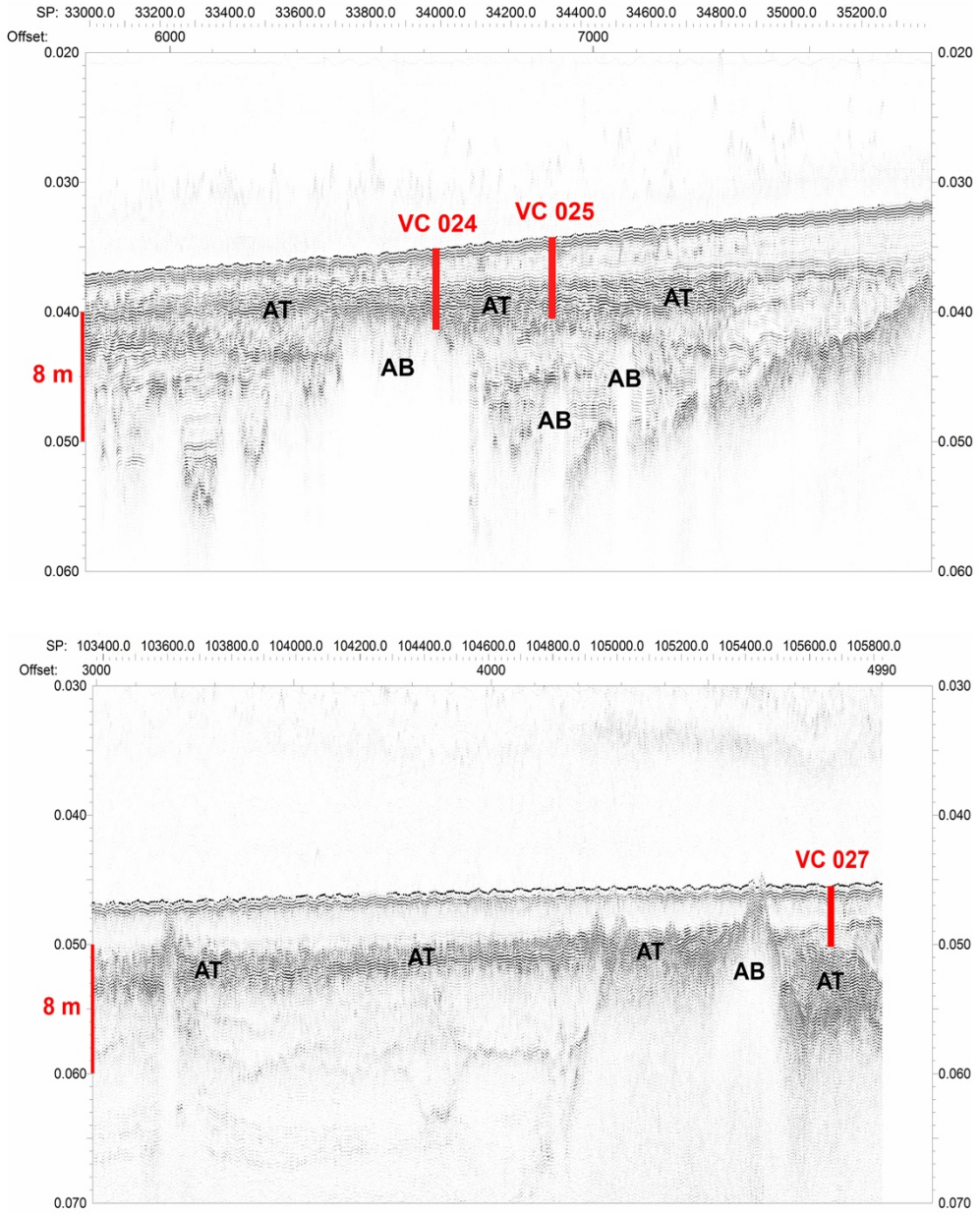

Figure 4.4. Sub-bottom profiles taken at the site of each vibrocore showing sampling locations (red line), acoustic turbidity (AT), and acoustic blanking (AB).

4.4.2. Gas and porewater geochemistry

The highest concentrations of CH_4 were observed in VC024, taken from the pockmark field (Fig. 4.5.). The maximum concentration of 3650 µM was observed in the core catcher sample corresponding with a depth of 5.77 mbsf. Values fluctuated

between 2620 and 3570 µM rising through the core before steadily decreasing from 3.28 mbsf (3680 µM) to the surface sample at 0.01 mbsf (2 µM), the minimum overall value for VC024. SO_4^{2-} concentrations for VC024 ranged from 0.1 to 0.5 mM displaying an overall decreasing trend from the surface, opposite to that of CH_4 (Fig. 4.5.). A minimum value was observed at 2.12 mbsf from which concentrations remain relatively constant through to the bottom of the core. The trend of H_2S concentrations was similar to that of CH_4, depleting towards the seafloor (Fig. 4.6.). H_2S was not present above 1.13 mbsf and below 4.88 mbsf. Concentrations fluctuated between these depths with a maximum concentration of 91 µM and a minimum concentration of 0 µM.

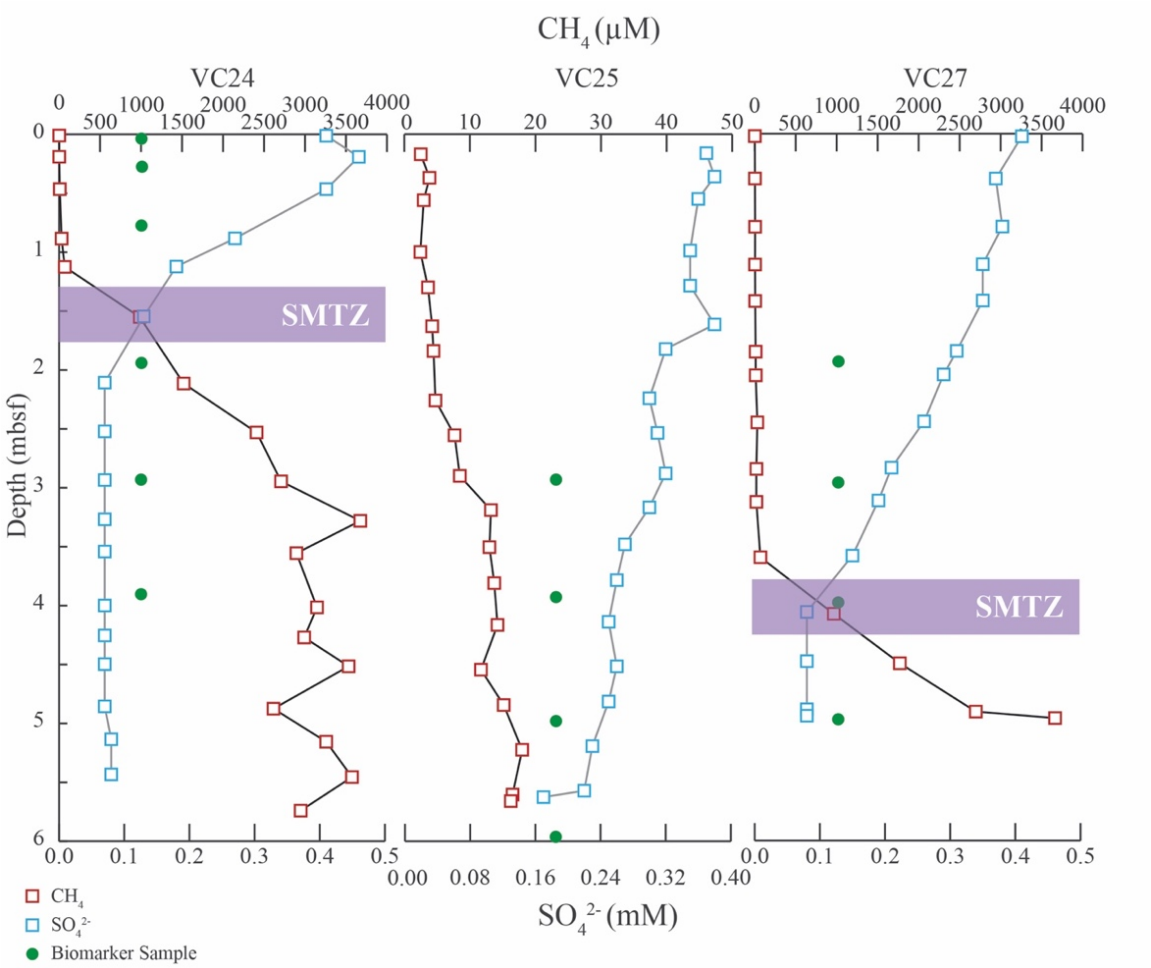

Figure 4.5. CH_4 and SO_4^{2-} profiles for each core. CH_4 values in µM, SO_4^{2-} values in mM. Green dots represent sub-sampling locations for lipid biomarker analysis.

CH_4 concentrations detected within VC025 were the lowest of the three vibracores analysed with a maximum observed at 5.23 mbsf (18 μM) and a minimum observed at 1 mbsf (Fig. 4.5.). Concentrations decrease gradually from the base of the core to the sediment surface from 16 μM to 3 μM. Concentrations of porewater SO_4^{2-} were relatively high throughout VC025 compared to VC024 and VC027 (Fig. 4.5.). Values were gradually depleted from the seafloor (0.17 mbsf) with a concentration of 0.4 mM to the deepest sample from the core (5.66 mbsf) with a concentration of 0.2 mM. H_2S concentrations fluctuated throughout the core with a maximum concentration of 30 μM, a minimum concentration of 0 μM, and an average of 15 μM (Fig. 4.6.). No H_2S was evident at 2.26 mbsf.

In VC027, outside the pockmark field, CH_4 concentrations decreased from 3660 μM at the base of the core (4.96 mbsf) to 965 μM at 4.08 mbsf before falling sharply to 70 μM at 3.6 mbsf (Fig. 4.5.). Depletion gradually continued from this depth to 1 μM at the surface of the core (0.02 mbsf). SO_4^{2-} concentrations followed an opposing trend with a maximum of 0.4 mM at 0.02 mbsf decreasing to a minimum of 0.1 mM at 4.08 mbsf and remained at this concentration to the base (4.96 mbsf) (Fig. 4.5.). H_2S was highest between 1.11 mbsf and 3.13 mbsf with a range of 53 to 111 μM, the maximum observed concentration (Fig. 4.6.). The H_2S trend followed a concave shape with the maximum value observed at 1.85 mbsf. From this point, concentrations decreased to a minimum concentration of 1 μM at 4.91 and 4.96 mbsf.

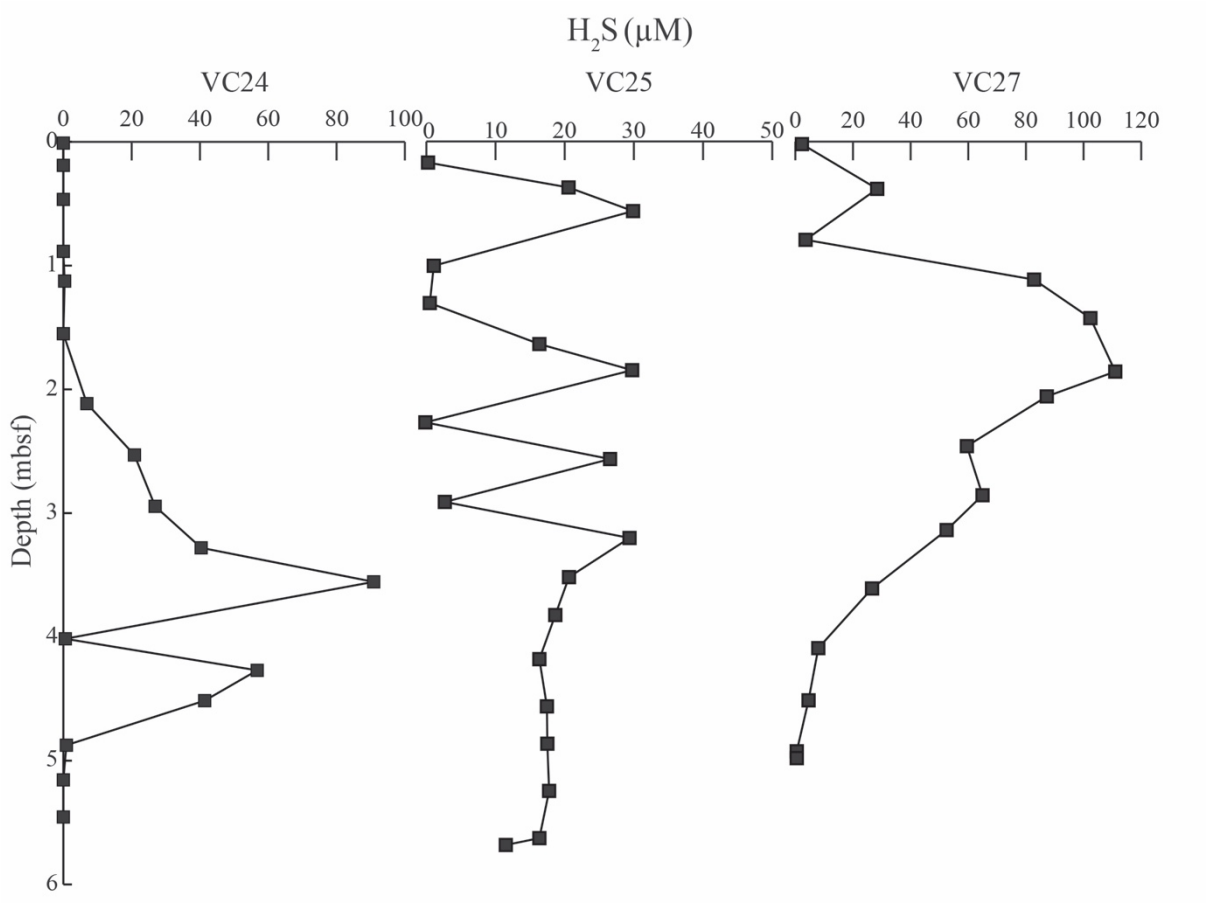

Figure 4.6. H_2S profiles for each core. Values in µM.

4.4.3. PSA and elemental analysis

The overall sediment type for the three cores taken from Bantry Bay was poorly to very poorly sorted sandy mud. Trends for mean pore size, percentage clay, silt, and sand are displayed in figures 4.8., 4.9., and 4.10. Mud percentages (clay + silt) ranged from 69.4 to 92.3% in VC24, from 42.2 to 81.2% in VC25, and from 29.3 to 84.0% in VC27 (Fig. 4.7.). The 42.2% value from VC25 was obtained at 4.99 mbsf, a sample comprised of poorly sorted muddy sand due to its high sand content (57.8%). The 29.3% value in VC27 was obtained at 1.93 mbsf where sediment type can be described as very poorly sorted, slightly gravelly, muddy sand due to its gravel (4.9%) and sand (65.8%) content. This gravel-containing layer had the largest mean particle size of 576.4 µm whereas the lowest value of 25.1 µm was

observed in VC24 at 0.77 mbsf, the layer with the highest overall mud content (92.3%). The mean particle size for the remaining samples ranged between 45.4 and 102.6 μm.

Total organic carbon (TOC) content was low throughout all cores with an average overall value of 0.6% (Fig. 4.7.). The highest observed values were 2 and 1.2% for VC24 0.025 and 0.27 mbsf respectively (Fig. 4.7.). No other sample had a value greater than 0.7%. In VC24, TOC decreased from 0.25 to 1.93 mbsf (2 to 0.3%) before increasing slightly to 0.5% at 2.92 mbsf and decreasing again to 0.3% at 3.9 mbsf. VC25 values were relatively constant (Fig. 4.7.). The TOC content of VC27 at 1.93 and 2.96 mbsf was 0.5% (Fig. 4.7.). This decreased to 0.4% at 3.98 mbsf and 0.3% at 4.97 mbsf.

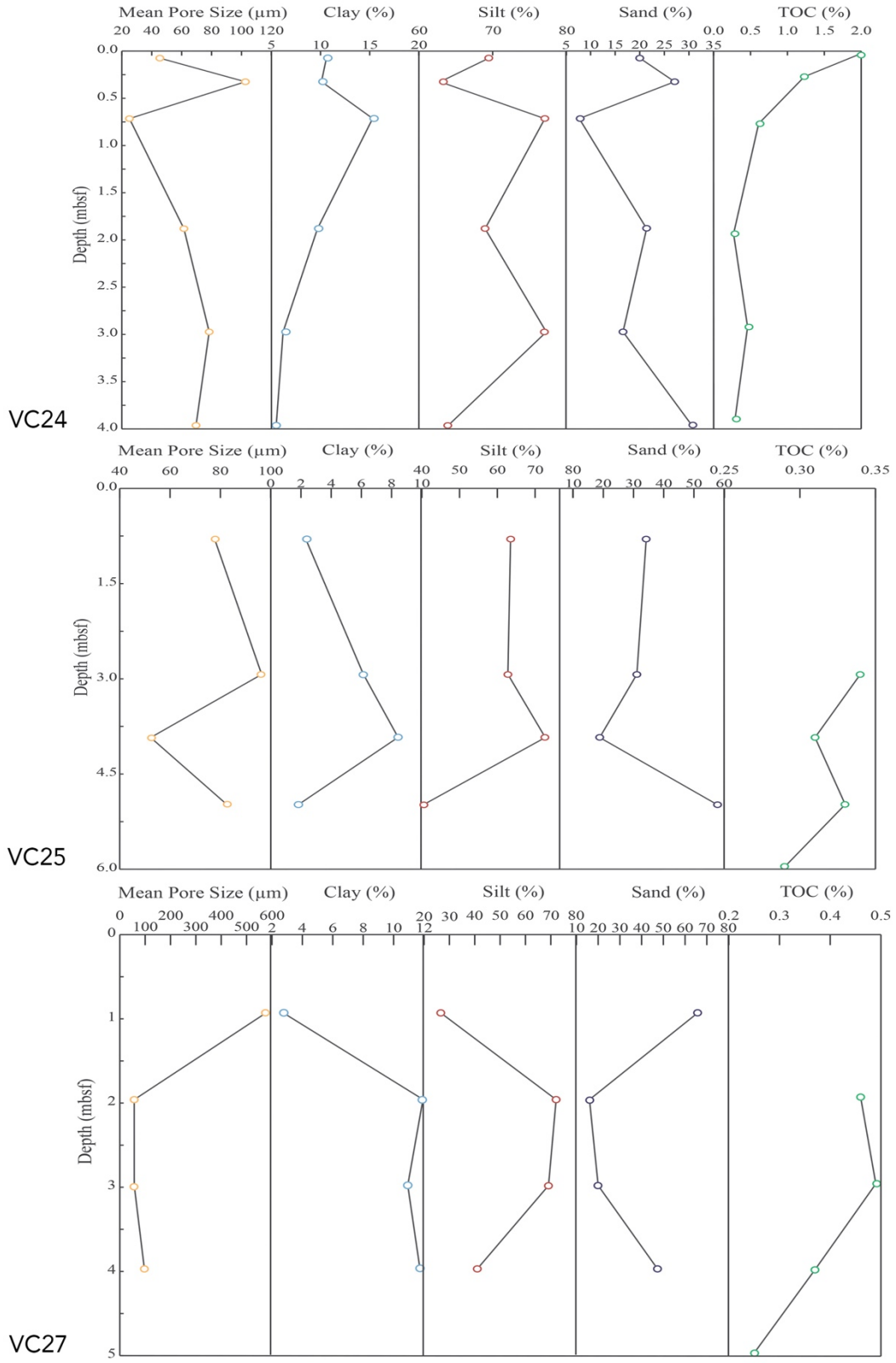

Figure 4.7. Mean particle size (µm), percentage clay, silt, and sand, as well as percentage TOC for VC24 (Top), VC25 (Middle), and VC27 (Bottom).

4.4.4. PLFAs

A summary of key PLFA concentrations is provided in table 4.1. The highest overall concentrations of PLFAs in all three vibrocores were observed in VC24. 310.1 and 235.2 μg gOC^{-1} were detected at 0.03 and 0.27 mbsf respectively, the largest quantities of PLFAs in all analysed samples. The remaining depths of VC24 contained between 31.1 (0.77 mbsf) and 90.1 μg gOC^{-1} (1.93 mbsf). Saturated fatty acids (SATFAs) and monounsaturated fatty acids (MUFAs) were the dominant PLFAs at 0.03 and 0.27 mbsf whilst SATFAs and branched fatty acids (brFAs) were dominant from 0.77 to 3.9 mbsf. Polyunsaturated fatty acids (PUFAs) were not found at 1.93 or 2.92 mbsf and were the smallest class of PLFAs at all other depths. SATFAs from 14:0 to 30:0 were identified throughout VC24. Shorter chain homologues were identified at 0.08 (10:0, 11:0, 12:0, 13:0), 0.270 (10:0, 11:0, 12:0, 13:0), and 0.77 (12:0, 13:0) mbsf. Longer chain homologues were observed at 0.27 (31:0, 32:0) and 1.93 (32:0) mbsf. C_{16} and C_{18} MUFAs were present at all depths throughout the core. A single C_{19} homologue was observed at all depths except 3.9 mbsf. C_{12}, C_{17}, and C_{20} MUFAs were identified at 0.03 and 0.27 mbsf whilst C_{13} and C_{14} were found only at 0.03 mbsf. The C_{17} homologue was also observed at 3.9 mbsf. C_{19} and C_{20} PUFAs were identified at 0.03 mbsf whilst C_{17}, C_{18}, and C_{20} were identified at 0.27 mbsf. A single diunsaturated C_{18} PUFA was observed at 0.77 mbsf and one diunsaturated C_{20} homologue was found at 3.9 mbsf. The diversity of brFAs varied substantially between depths throughout VC24. A range of homologues from C_{15} to C_{22} were observed at all depths. i15:0 and ai15:0 were identified at all depths as were i17:0 and ai17:0. It was not possible to identify the methyl branch location in a significant proportion of the brFAs.

Total PLFA concentrations ranged from 49.7 to 73.9 μg gOC^{-1} (5.96 and 2.93 mbsf respectively) in VC25. SATFAs were the dominant compounds throughout the core with concentrations approximately 10 times greater than MUFAs and brFAs. There were no PUFAs observed in any VC25 samples. C_{14} to C_{30} SATFAs were identified at all depths with an even over odd predominance. C_{12} and C_{13} homologues were observed at 2.93 and 4.98 mbsf, whilst C_{32} was identified at 2.93 mbsf only, the longest chain SATFA in VC25. From 2.93 to 4.98 mbsf C_{16}, C_{18}, and C_{19} MUFAs were observed. The C_{16} and C_{18} homologues were identified at 5.96 mbsf also but the C_{19} MUFA was not present. i15:0 and ai15:0 brFAs were observed at all depths throughout VC25. i13:0 and ai13:0 were identified at 3.93 and 5.96 mbsf whilst i14:0, i17:0, and ai17:0 were isolated at all depths. 3Me15:0 and 3Me17:0 were isolated from the sample taken at 2.93 mbsf but not from any other samples. Several other brFAs with unidentified methyl branch positions were observed at varying depths throughout VC25.

The highest concentration of PLFAs in VC27 was 77.4 μg gOC^{-1} observed at 3.98 mbsf. The lowest concentration was 51.2 μg gOC^{-1} which was observed at 1.93 mbsf. Similar to VC25, total SATFA concentrations were significantly greater than other PLFA classes. There was little variation in total concentrations of other PLFA classes throughout the core. MUFAs ranged from 4.2 to 6 μg gOC^{-1}, PUFAs from 1.2 to 1.7 μg gOC^{-1} (absent at 4.97 mbsf), and brFAs from 4.5 to 4.9 μg gOC^{-1}. C_{12} to C_{32} SATFAs were identified from 1.93 to 3.98 mbsf. The longest chain homologue in VC27, C_{33}, was isolated at 3.98 mbsf whilst a range of only C_{13} to C_{30} SATFAs was observed at 4.97 mbsf. C_{16}, C_{18}, and C_{19} MUFAs were observed at all depths. Two PUFAs were identified from 1.93 to 3.98 mbsf, one diunsaturated C_{17} and one diunsaturated C_{18}. brFA profiles were similar for all depths throughout

VC27. 3Me15:0, iso homologues of C_{14}, C_{15}, C_{16}, and C_{17}, and anteiso homologues of C_{15} and C_{17} were isolated at all depths. i13:0 and ai13:0 were identified at all depths except 4.97 mbsf. VC27 also contained various other brFAs whose methyl branch positions could not be identified.

The same five archaeal ether lipids were isolated from each sample taken from VC24, VC25, and VC27. These were; phytane, acyclic biphytane (cy40:0), and three cyclic biphytanes (cy40:1, cy40:2, and cy40:3). The cy40:0 was the major isoprenoid in all samples whilst the cy40:1 was the minor isoprenoid. Overall concentrations of archaeal lipids in VC24 increase from 4.6 μg gOC^{-1} at 0.03 mbsf to the maximum concentration of 13.9 μg gOC^{-1} at 2.92 mbsf. This maximum was also the highest concentration observed in all of the analysed samples. The concentration fell to 8.5 μg gOC^{-1} at 3.9 mbsf. The maximum concentration of VC25, 8.2 μg gOC^{-1}, was observed at 2.93 mbsf, followed by the VC25 minimum of 3.1 μg gOC^{-1} at 3.93 mbsf. The concentration increased to 6.6 μg gOC^{-1} at 4.98 mbsf and decreased slightly to 5 μg gOC^{-1} at 5.96 mbsf. Concentrations decreased continuously from 8.1 to 4.3 μg gOC^{-1} from 1.93 to 4.97 mbsf in VC27. All individual isoprenoids followed the same trend as the overall abundance (Fig. 4.8.).

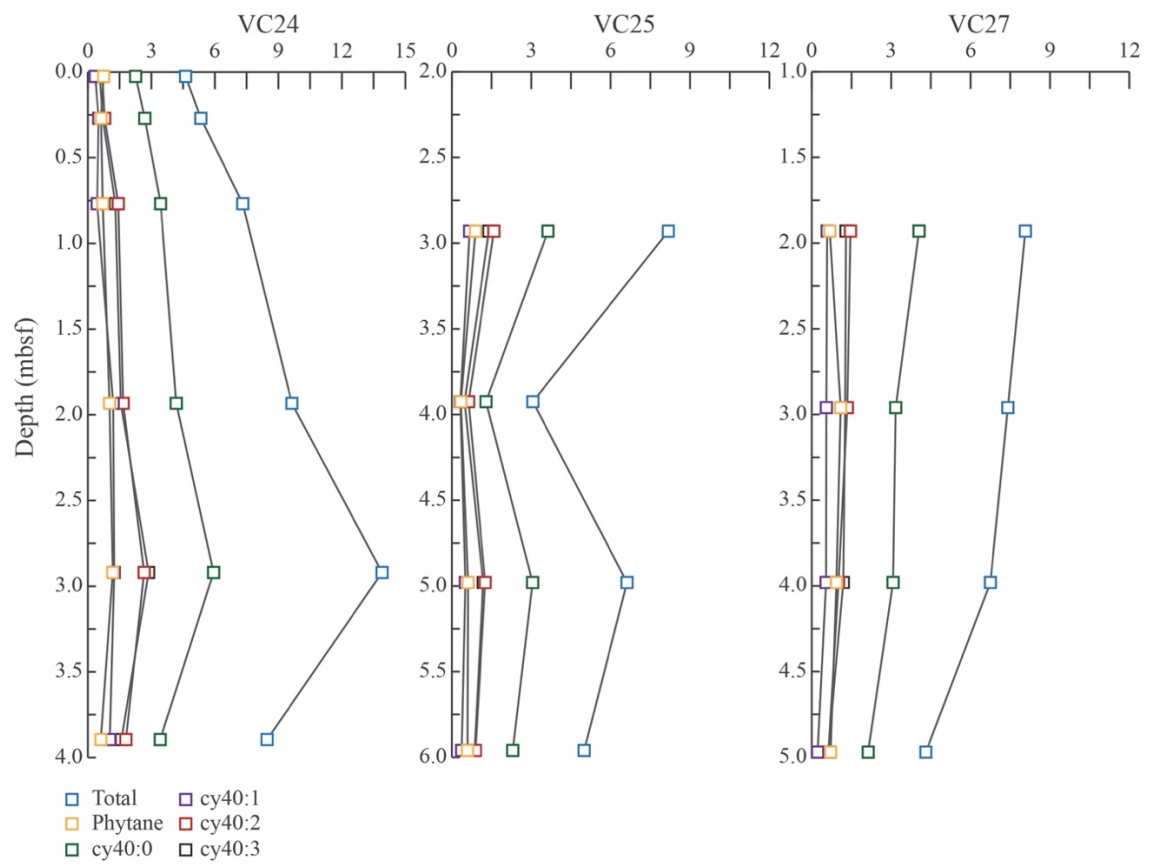

Figure 4.8. Concentrations (µg gOC^{-1}) of total and individyal archaeal ether-derived isoprenoid lipids for each sediment core.

4.4.5. Carbon isotope values of individual lipids

$\delta^{13}C$ values could not be obtained for most lipid compounds identified in the three Bantry Bay vibrocores. This was due to a combination of low abundance in polar lipid extracts and low sensitivity of the GC-IRMS instrument. $\delta^{13}C$ values for three PLFAs were measured in the VC24 0.27 sample which contribute to the study of these sediments. The MUFAs 16:1ω7 and 16:1ω5 provided $\delta^{13}C$ values of -31.0‰ and -46.1‰ respectively, and the SATFA 16:0 $\delta^{13}C$ value was -27.7‰.

Table 4.1. PLFA concentrations (µg gOC^{-1}) for each vibrocore taken in Bantry Bay. Total overall concentrations and total concentrations for certain groups of PLFAs are included (indicated by the prefix Σ). Individual concentrations of selected biomarker compounds from within each group are also shown. Depth in mbsf.

	VC24						VC25				VC27			
Depth	0.03	0.27	0.77	1.93	2.92	3.9	2.93	3.93	4.98	5.96	1.93	2.96	3.98	4.97
ΣPLFAs	310.1	235.2	31.1	90.1	51.2	44.0	73.9	57.2	56.9	49.7	51.2	68.9	77.4	63.0
ΣSATFAs	133.3	118.7	20.4	64.9	33.1	31.0	52.1	41.7	42.7	43.2	36.2	42.5	50.4	46.8
ΣMUFAs	91.1	52.0	2.6	2.3	3.4	1.9	5.2	3.9	1.4	8.5	4.2	5.9	6.0	5.8
ΣPUFAs	12.9	17.7	0.0	0.0	0.0	1.2	0.0	0.0	0.0	0.0	1.2	1.7	1.7	0.0
ΣbrFAs	64.6	32.6	4.3	4.4	12.2	7.6	7.2	5.1	5.2	4.4	4.9	4.9	4.5	5.3
SATFAs														
12:0	0.8	0.7	0.1	-	-	-	0.3	-	0.2	-	0.2	0.1	0.2	-
13:0	0.4	0.3	0.1	-	-	-	0.1	-	0.1	-	0.1	0.1	0.1	0.1
14:0	7.3	6.9	1.4	1.0	1.4	0.9	2.0	1.1	1.6	1.1	1.8	1.8	1.6	1.8
15:0	2.7	2.3	0.6	0.5	0.8	0.5	0.8	0.6	0.7	0.6	0.9	0.8	0.6	0.7

16:0	28.1	20.9	6.4	5.8	8.2	5.7	8.7	7.0	6.1	7.3	8.3	6.5	8.0	8.8
17:0	2.5	1.2	0.3	0.5	1.6	0.4	0.5	0.5	0.5	0.5	0.5	0.6	0.6	0.7
18:0	10.4	2.5	1.8	2.6	3.7	2.3	3.3	2.9	3.5	3.1	2.7	3.5	4.0	4.3
19:0	2.7	5.5	0.3	0.5	0.6	0.9	0.7	0.9	0.5	-	0.6	0.6	0.7	0.8
MUFAs														
16:1ω?	16.3	4.3	0.3	0.4	0.5	0.4	0.4	0.4	0.4	0.3	0.4	0.4	0.5	0.5
16:1ω7	2.7	0.9	-	-	-	-	-	-	-	-	-	-	-	-
16:1ω5	5.7	2.4	0.2	-	-	-	-	-	-	-	0.2	0.2	-	-
18:1ω9	12.1	0.8	0.5	1.3	0.7	1.0	0.9	1.0	1.0	1.3	0.9	1.0	0.7	0.8
18:1ω7	24.8	10.0	0.4	0.6	0.4	-	-	-	-	-	0.5	-	0.8	0.9
19:1ω?	10.6	3.1	1.2	4.5	1.8	1.1	3.9	2.5	2.9	-	2.3	4.3	4.0	3.6
PUFAs														
18:2ω?	-	-	-	-	-	-	-	-	-	-	0.4	0.6	0.7	-
20:4ω6	3.8	3.1	-	-	-	-	-	-	-	-	-	-	-	-
20:5ω3	3.7	5.5	-	-	-	-	-	-	-	-	-	-	-	-

brFAs														
*i*13:0	0.4	0.2	0.1	-	-	-	0.1	-	0.1	-	0.1	0.1	0.1	-
*ai*13:0	0.6	0.4	0.1	-	-	-	0.1	-	0.1	-	0.2	0.2	0.1	-
*i*15:0	7.7	3.4	0.5	0.6	0.8	0.8	0.8	0.6	0.5	0.5	0.6	0.7	0.6	0.6
*ai*15:0	14.4	7.6	0.9	1.2	0.5	0.5	1.7	1.1	1.2	1.2	1.6	1.4	1.1	1.2
3Me15:0	-	-	-	-	-	-	0.3	-	-	-	0.3	0.5	0.4	0.4
*i*16:0	3.2	2.4	-	-	-	0.5	0.7	0.8	-	-	0.6	0.7	0.5	0.5
*i*17:0	2.1	1.4	0.2	0.4	0.3	0.4	0.3	0.3	0.4	0.9	0.3	0.3	0.3	0.3
*ai*17:0	1.7	2.5	0.3	0.6	0.3	0.4	0.5	0.4	0.5	0.5	0.5	0.5	0.4	0.4
cyFAs														
*cy*17:0	-	4.4	-	-	-	-	-	-	-	-	-	-	-	-

4.5. Discussion

Gas seepage is widespread within Bantry Bay. CH_4 was detected in all three vibracores taken during this study, both inside and outside the pockmark field. Similarly, indications of fluid migration were observed in all sub-bottom scans taken in the bay. AB is observed below all AT signatures in the acoustic data (Fig. 4.4.) suggesting that upward migration is predominant in this setting (e.g. Szpak et al., 2012). It is possible to determine whether CH_4 is of a thermogenic or biogenic origin through the interpretation of GC-FID chromatograms. Thermogenic CH_4 also contains significant levels of C_2 to C_4 hydrocarbons whereas biogenic CH_4 does not (Faber and Stahl, 1984; Floodgate and Judd, 1992). All of the gas samples analysed from Bantry Bay were either free from these hydrocarbons or contained only trace levels, confirming a biogenic source for the CH_4 in these sediments. Organic carbon in marine sediments can be microbially oxidized via various electron acceptors, used in order of decreasing chemical potential. OM that is not oxidized aerobically or anaerobically can be reduced to CH_4 through the process of methanogenisis (Antler et al., 2014; Froelich et al., 1979). Previous work in Bantry Bay encountered black lacustrine sediments dated to 13-14 ka cal. BP (dates obtained from pollen isolated from the deposit), ca. 57 mbsf within a borehole off Whiddy Island (Plets et al., 2015; Stillman, 1968). Methanogenic microorganisms active within these organic-rich deposits could potentially be a source of biogenic CH_4 within the bay.

The depletion of SO_4^{2-} and CH_4 profiles within the sediment occurs at the SMTZ. The SMTZ corresponds with the zone of AOM as this is where CH_4 diffusing upwards from depth first encounters SO_4^{2-} diffusing downwards from the ocean (Antler et al., 2014; Lin et al., 2016; Valentine, 2002). This zone was clearly

observed in both VC24 and VC27. Although not visible in VC25, both CH_4 and SO_4^{2-} profiles appeared to follow the trend expected to result in a SMTZ. The gradient suggests depletion at ca. 9.7 mbsf should the SO_4^{2-} depletion rate remain constant. VC27 was intended as a control site as it was taken outside the pockmark field, however due to the seemingly ubiquitous presence of gas seepage within Bantry Bay, its geochemical portrait was similar to those expected from sediment with seepage (e.g. Blinova et al., 2011; Brodecka et al., 2013; Choi et al., 2013). Although AOM is affected by myriad conditions, in the majority of sediments higher organic content and CH_4 supply lead to shallower zones (Valentine, 2002). This holds true for the sediments investigated in this study in terms of CH_4 concentration, but higher average TOC content is expected for VC24 as the sample from this core included surface sediments. VC24, with an average CH_4 concentration of 2106.22 μM had the shallowest SMTZ at ca. 1.25 mbsf. The SMTZ occurred at ca. 3.75 mbsf in VC27, a core with an average CH_4 concentration of 618.64 μM and was most likely deeper again in VC25 with a CH_4 concentration of 9.3 μM.

In CH_4 seeps and vents advection is the dominant mixing process, and porewaters travelling upwards due to pressure gradients often contain high concentrations of CH_4 resulting from the decomposition of organic material in deeper sediments (Judd, 2004; Valentine, 2002). Due to the lack of a GPS beacon attached to the vibracorer onboard the *RV Celtic Explorer* it is impossible to be certain that either VC24 or VC25 penetrated directly into one of the pockmark features observed in the multibeam data. However, the high CH_4 concentrations observed in VC24 coupled with the shallow SMTZ were characteristic of sediments from within seepage sites. Pockmarks are generally considered to form as a result of seabed fluid expulsion with groundwater springs, hydrocarbon gas, and

hydrothermal gas thought to be the primary fluids responsible (Judd and Hovland, 2009; Szpak et al., 2012). Since Bantry Bay is in close proximity to land it is possible that groundwater discharge could have an effect on the seabed. Analysis of salinity in sediment porewater and the overlying water column is necessary to determine if freshening of the water occurs, indicating a groundwater influence. Conductivity measurement could not be obtained from Bantry Bay however, due to the substantial gas activity it is likely that biogenic CH_4 resulting from the decomposition of organic material, possibly from ancient lacustrine deposits, buried deep beneath the seafloor was the primary cause of pockmark formation.

Szpak et al. (2015) described a pockmark field in a similar setting in Dunmanus Bay, south of Bantry Bay. They concluded that these pockmarks were CH_4 generated and that the source of the gas was a venting mechanism occurring due to seal failure-renewal cycles of the Dunmanus Fault. They also argued against a groundwater influence. The CH_4 from Dunmanus also contained only trace levels of C_2 – C_4 hydrocarbons and Szpak et al. (2015) suggested that methanogenesis contributed somewhat to the gas in this location. The Bantry Bay pockmark field overlies the Owenberg River Fault which runs along the north west of Whiddy Island. It is possible that a similar venting mechanism occurs in Bantry as in Dunmanus. Both bays lie in the South Munster Basin and are similar in their geology (Vermeulen et al., 2000). It is also plausible that this venting mechanism does not occur in either setting and that methanogenesis is the primary source of CH_4 in both pockmark fields.

The number of individual PLFAs identified in a marine sediment is representative of the microbial diversity (Ogawa et al., 2003; Rajendran et al., 1994). VC24 surface sediments (0.03 – 0.27 mbsf) showed the most diversity of all samples

analysed. These sediments also contained the highest biomass of all those analysed determined by total PLFA concentrations of 310.1 and 235.2 μg gOC^{-1} at 0.03 and 0.27 mbsf respectively, compared to an average of 42.1 μg gOC^{-1} across all other samples. It is likely that surface sediments from cores VC25 and VC27 would contain similar biomass and diversity and as such little information can be drawn from the apparent uniqueness of these VC24 surface sediments compared to this sample set.

High levels of MUFAs and low levels of PUFAs is seen as indicative of the dominant contribution of bacterial communities to sediment biomass (Rajendran et al., 1995, 1992; Taylor and Parkes, 1983; Volkman et al., 1980). Bacteria appear to dominate the microbial ecology in all three vibrocores. Abundances of PUFAs are increased in the surface sediments of VC24, however MUFA abundances are still higher. Interestingly, at 0.8 and 3.9 mbsf in VC24, contributions of MUFAs and PUFAs are similar although MUFAs remain dominant. Comparison of MUFAs ($<C_{19}$) with total brFAs provides an insight to the aerobic/anaerobic conditions in the sediment. Values less than 1 indicate an anaerobic environment whereas values greater than 1 are representative of aerobic conditions (Rajendran et al., 1992). Only the shallower sediments of VC24 (1.12 and 1.08 for 0.03 and 0.27 mbsf respectively) are classified as aerobic using this approach.

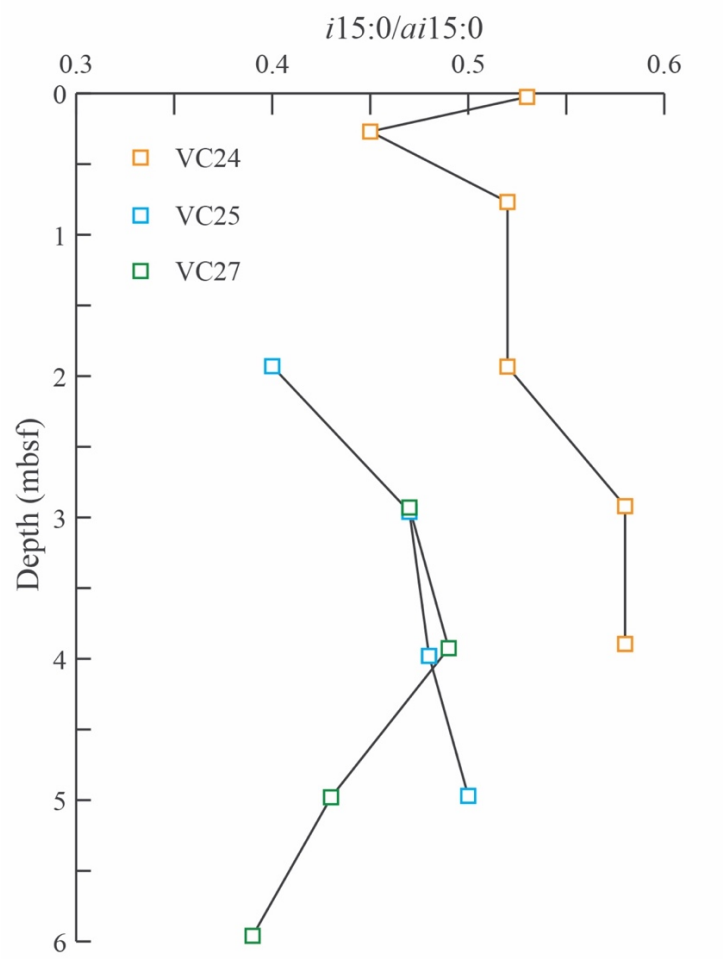

Figure 4.9. Combined plots of the i15:0/ai15:0 PLFA ratio for each core.

Mid-chain brFAs in marine sediments are often produced by SRB and are used as chemotaxonomic markers for these microorganisms (Dowling et al., 1986; Li et al., 2007). *i*15:0, *ai*15:0, *i*16:0, *i*17:0, and *ai*17:0 are all reported biomarkers for the *Desulfovibrio* species of SRB (Dowling et al., 1986; Findlay et al., 1990; Li et al., 2007; Rajendran et al., 1995; Taylor and Parkes, 1983). These compounds were present throughout all three vibracores taken in Bantry Bay, suggesting a significant contribution of SRB to the microbial ecosystem here. SRB tend to display a higher ratio of *i*15:0 to *ai*15:0 in their PLFA profiles (Dowling et al., 1986; O'Reilly, 2013). Applying this ratio to the Bantry Bay sediments resulted in substantially higher values observed in VC24 than VC25 or VC27, both of which had similar values

(Fig. 4.9.). This suggests that SRB are substantially higher contributors to the microbial community of VC24. *cy*17:0 is seen as a biomarker for *Desulfobacter* (Findlay et al., 1990; Rajendran et al., 1992) but is also used as a marker of environmental stress (Li et al., 2007; Navarrete et al., 2000). 16:1ω7 is converted to *cy*17:0 in conditions which slow growth rate (Navarrete et al., 2000). This compound was observed in only one sample in this study at 0.27 mbsf in VC24. Due to the high SO_4^{2-} concentration in this sample it is likely that it is produced by SRB, however its presence may suggest that there is some level of environmental stress at this depth. SO_4^{2-} is used as an electron acceptor and reduced to H_2S by these SRB (Peck, 1993). In AOM settings this leads to porewater profiles such as that observed in VC24 where H_2S trends were similar to that of CH_4 (Hensen et al., 2003). Interestingly, this trend was not observed in VC27. H_2S concentrations in this core were highest above the SMTZ and depleted gradually towards the base. In VC25 H_2S was observed at all depths, also above the SMTZ if present in deeper sediments. SO_4^{2-} was more abundant in both VC25 and VC27, therefore it is likely that conditions are favourable for SRB in these sediments compared to VC24 where SRB involved in AOM may be the primary SO_4^{2-} reducers.

Elvert et al. (2003) investigated marine sediments from above marine gas hydrates at Hydrate Ridge, in the North East Pacific Ocean. They determined that 16:1ω5, 17:1ω6, and *cy*17:0ω5,6 were specific membrane fatty acids for SRB of the *Desulfosarcinia/Desulfococcus* group which were involved in AOM at this site. 16:1ω5 was identified in four samples from the Bantry Bay vibracores; VC24 0.03 mbsf, VC24 0.27 mbsf, VC27 1.93 mbsf, and VC27 2.96 mbsf. Isotope ratio analysis provided significantly depleted $\delta^{13}C$ values for this compound at 0.27 mbsf in VC24 compared with those obtained from more ubiquitous bacterial PLFAs, 16:1ω7 and

16:0. These depleted values are representative of the incorporation of CH_4 derived C into the membranes of these SRB providing evidence of their involvement in AOM at this site. Unfortunately, $\delta^{13}C$ values from other samples or for other AOM-related biomarker compounds derived from bacteria or archaea could not be obtained.

Archaeal biomarkers are present at all depths in all three vibrocores taken in Bantry Bay. Once thought to be extremophilic, it is now known that these microorganisms inhabit a wide range of environments and as such their ubiquity in Bantry Bay sediments is not surprising (Oba et al., 2015; Pancost et al., 2001; Zhu et al., 2014). Archaea involved in AOM typically belong to three major anaerobic methanotroph (ANME) consortia; ANME-1 (related to *Methanosarcinales* and *Methanomicrobiales*), ANME-2 (members of the *Methanosarcinales*), and ANME-3 (related to *Methanococcoides*) (Caldwell et al., 2008). It is generally assumed that ANMEs oxidize and assimilate CH_4, following which CH_4-derived C is consumed by the SRB as CO_2 or a partially oxidized intermediate completing the symbiotic reaction (Alperin and Hoehler, 2009). Oba et al. (2006) observed that biphytanes released from polar archaeal membrane lipids in near-surface sediments from the Nankai Trough were derived from both methanotrophic and non-methanotrophic communities, indicated by their $\delta^{13}C$ values. It is likely that a proportion of the isoprenoid lipids identified in this study are produced by archaea involved in AOM, however this cannot be confirmed without further data such as carbon isotope values.

4.6. Conclusions

The migration of gas appears to be a widespread characteristic of the sediments of Bantry Bay as observed in multiple sub-bottom acoustic profiles. The expulsion of this gas into the water column has led to the formation of a pockmark field off the coast of Whiddy Island. This fluid flow affects not only the physical nature of the sea-floor in the bay but also the microbial ecosystem. The gas is CH_4 of a biogenic origin potentially derived from anaerobic degradation of ancient organic matter buried deep below the sea floor or from venting of geological faults. As CH_4 flows upwards from its origin it provides a substrate for certain microorganisms to thrive in the shallower sediments above. Archaea, possibly ANMEs, are present in these shallower sediments as are SRB. The CH_4 is steadily depleted before it escapes to the water column and SO_4^{2-} concentrations also become depleted in the opposite direction providing a well defined SMTZ. This is likely due to AOM carried out by these two groups of microorganisms in a symbiotic relationship, however further work is needed to confirm this pathway. This study suggests that AOM in Bantry Bay limits CH_4 emissions from the seafloor preventing the potential climatic implications of a release of this powerful greenhouse gas to the atmosphere. Szpak et al. (2015) and Szpak et al. (2012) observed similar conditions in pockmarked sites in Dunmanus Bay located to the east of Bantry Bay, and on the Malin Shelf off the north coast of Ireland. This indicates that marine CH_4 production may be common around the island of Ireland. Global estimates of the contribution of CH_4 from marine seepage sites are highly uncertain (Römer et al., 2014). Recently, release of CH_4 to the atmosphere has been observed in Arctic regions, areas particularly vulnerable to climate change, and these releases have been attributed to rising

temperatures (Shakhova et al., 2010; Westbrook et al., 2009). As CH_4 is a potent greenhouse gas, these releases serve only to increase rates of global climate change. AOM and the microbial consortia involved are important factors in the global methane cycle (Gauthier et al., 2015). For these reasons further study of these sites and their microbial ecology should be prioritised.

References

Abrams, M. a., 2005. Significance of hydrocarbon seepage relative to petroleum generation and entrapment. Mar. Pet. Geol. 22, 457–477. doi:10.1016/j.marpetgeo.2004.08.003

Acosta, J., Munoz, A., Herranz, P., Palomo, C., Ballesteros, M., Vaquero, M., Uchupi, E., 2001. Pockmarks in the Ibiza Channel and western end of the Balearic Promontory (western Mediterranean) revealed by multibeam mapping. Geo-Marine Lett. 21, 123–130. doi:10.1007/s003670100074

Alain, K., Holler, T., Musat, F., Elvert, M., Treude, T., Krüger, M., 2006. Microbiological investigation of methane- and hydrocarbon-discharging mud volcanoes in the Carpathian Mountains, Romania. Environ. Microbiol. 8, 574–90. doi:10.1111/j.1462-2920.2005.00922.x

Alperin, M.J., Hoehler, T.M., 2009. Anaerobic methane oxidation by archaea/sulfate-reducing bacteria aggregates: 2. Isotopic constraints. Am. J. Sci. 309, 958–984. doi:10.2475/10.2009.02

Antler, G., Turchyn, A. V., Herut, B., Davies, A., Rennie, V.C.F., Sivan, O., 2014. Sulfur and oxygen isotope tracing of sulfate driven anaerobic methane

oxidation in estuarine sediments. Estuar. Coast. Shelf Sci. 142, 4–11. doi:10.1016/j.ecss.2014.03.001

Baraza, J., Ercilla, G., 1996. Gas-charged sediments and large pockmark-like features on the Gulf of Cadiz slope (SW Spain). Mar. Pet. Geol. 13, 253–261. doi:10.1016/0264-8172(95)00058-5

Beauchamp, B., 2004. Natural gas hydrates: myths, facts and issues. Comptes Rendus Geosci. 336, 751–765. doi:10.1016/j.crte.2004.04.003

Blinova, V.N., Comas, M.C., Ivanov, M.K., Poludetkina, E.N., Matveeva, T.V., 2011. Active mud volcanism in the West Alboran Basin: Geochemical evidence of hydrocarbon seepage. Mar. Pet. Geol. 28, 1483–1504. doi:10.1016/j.marpetgeo.2011.06.001

Boetius, A., Ravenschlag, K., Schubert, C.J., Rickert, D., Widdel, F., Gieseke, A., Amann, R., Jørgensen, B.B., Witte, U., Pfannkuche, O., 2000. A marine microbial consortium apparently mediating anaerobic oxidation of methane. Nature 407, 623–6. doi:10.1038/35036572

Brodecka, A., Majewski, P., Bolałek, J., Klusek, Z., 2013. Geochemical and acoustic evidence for the occurrence of methane in sediments of the Polish sector of the southern Baltic Sea**The research was supported by the Polish Ministry of Science and Higher Education grant No. N306 441638 entitled ‘Occurrence and . Oceanologia 55, 951–978. doi:10.5697/oc.55-4.951

Caldwell, S.L., Laidler, J.R., Brewer, E.A., Eberly, J.O., Sandborgh, S.C., Colwell, F.S., 2008. Anaerobic Oxidation of Methane: Mechanisms, Bioenergetics, and the Ecology of Associated Microorganisms. Environ. Sci. Technol. 42, 6791–6799. doi:10.1021/es800120b

Chatti, I., Delahaye, A., Fournaison, L., Petitet, J.-P., 2005. Benefits and drawbacks

of clathrate hydrates: a review of their areas of interest. Energy Convers. Manag. 46, 1333–1343. doi:10.1016/j.enconman.2004.06.032

Choi, J., Kim, J.-H., Torres, M.E., Hong, W.-L., Lee, J.-W., Yi, B.Y., Bahk, J.-J., Lee, K.E., 2013. Gas origin and migration in the Ulleung Basin, East Sea: Results from the Second Ulleung Basin Gas Hydrate Drilling Expedition (UBGH2). Mar. Pet. Geol. 47, 113–124. doi:10.1016/j.marpetgeo.2013.05.022

Dowling, N.J.E., Widdel, F., White, D.C., 1986. Phospholipid Ester-linked Fatty Acid Biomarkers of Acetate-oxidizing Sulphate-reducers and Other Sulphide-forming Bacteria. Microbiology 132, 1815–1825. doi:10.1099/00221287-132-7-1815

Elvert, M., Boetius, A., Knittel, K., Jørgensen, B.B., 2003. Characterization of Specific Membrane Fatty Acids as Chemotaxonomic Markers for Sulfate-Reducing Bacteria Involved in Anaerobic Oxidation of Methane. Geomicrobiol. J. 20, 403–419. doi:10.1080/01490450303894

Etiope, G., Milkov, A., Derbyshire, E., 2008. Did geologic emissions of methane play any role in Quaternary climate change? Glob. Planet. Change 61, 79–88. doi:10.1016/j.gloplacha.2007.08.008

Faber, E., Stahl, W., 1984. Geochemical surface exploration for hydrocarbons in North Sea. Am. Assoc. Pet. Geol. Bull. 68, 363–386.

Field, M.E., Jennings, A.E., 1987. Seafloor gas seeps triggered by a northern California earthquake. Mar. Geol. 77, 39–51. doi:10.1016/0025-3227(87)90082-X

Findlay, R.H., Trexler, M.B., Guckert, J.B., White, D.C., 1990. Laboratory study of disturbance in marine sediments: response of a microbial community. Mar. Ecol. Prog. Ser. Oldend. 62, 121–133.

Floodgate, G.D., Judd, a. G., 1992. The origins of shallow gas. Cont. Shelf Res. 12, 1145–1156. doi:10.1016/0278-4343(92)90075-U

Fonselius, S., Dyrssen, D., Yhlen, B., 1999. Determination of hydrogen sulphide, in: Methods of Seawater Analysis. Wiley-VCH Verlag GmbH, pp. 91–100. doi:10.1002/9783527613984.ch5

Froelich, P.N., Klinkhammer, G.P., Bender, M.L., Luedtke, N.A., Heath, G.R., Cullen, D., Dauphin, P., Hammond, D., Hartman, B., Maynard, V., 1979. Early oxidation of organic matter in pelagic sediments of the eastern equatorial Atlantic: suboxic diagenesis. Geochim. Cosmochim. Acta 43, 1075–1090. doi:10.1016/0016-7037(79)90095-4

Gauthier, M., Bradley, R.L., Šimek, M., 2015. More evidence that anaerobic oxidation of methane is prevalent in soils: Is it time to upgrade our biogeochemical models? Soil Biol. Biochem. 80, 167–174. doi:http://dx.doi.org/10.1016/j.soilbio.2014.10.009

Ge, L., Jiang, S.-Y., Blumenberg, M., Reitner, J., 2015. Lipid biomarkers and their specific carbon isotopic compositions of cold seep carbonates from the South China Sea. Mar. Pet. Geol. 66, 501–510. doi:10.1016/j.marpetgeo.2015.02.005

Hasiotis, T., Papatheodorou, G., Kastanos, N., Ferentinos, G., 1996. A pockmark field in the Patras Gulf (Greece) and its activation during the 14/7/93 seismic event. Mar. Geol. 130, 333–344. doi:10.1016/0025-3227(95)00131-X

Hensen, C., Zabel, M., Pfeifer, K., Schwenk, T., Kasten, S., Riedinger, N., Schulz, H.D., Boetius, A., 2003. Control of sulfate pore-water profiles by sedimentary events and the significance of anaerobic oxidation of methane for the burial of sulfur in marine sediments. Geochim. Cosmochim. Acta 67, 2631–2647. doi:http://dx.doi.org/10.1016/S0016-7037(03)00199-6

Hovland, M., 1987. The Formation of Pockmarks and Their Potential Influence on Offshore Construction. Proc. Japan Soc. Civ. Eng. 388.

Hovland, M., Gardner, J. V., Judd, a. G., 2002. The significance of pockmarks to understanding fluid flow processes and geohazards. Geofluids 2, 127–136. doi:10.1046/j.1468-8123.2002.00028.x

Hovland, M., Svensen, H., Forsberg, C.F., Johansen, H., Fichler, C., Fosså, J.H., Jonsson, R., Rueslåtten, H., 2005. Complex pockmarks with carbonate-ridges off mid-Norway: Products of sediment degassing. Mar. Geol. 218, 191–206. doi:10.1016/j.margeo.2005.04.005

Joye, S.B., Connell, T.L., Miller, L.G., Oremland, R.S., Jellison, R.S., 1999. Oxidation of ammonia and methane in an alkaline, saline lake. Limnol. Oceanogr. 44, 178–188. doi:10.4319/lo.1999.44.1.0178

Judd, A., Hovland, M., 2009. Seabed Fluid Flow - The Impact on Geology, Biology and the Marine Environment. Cambridge University Press, Cambridge.

Judd, A.G., 2004. Natural seabed gas seeps as sources of atmospheric methane. Environ. Geol. 46, 988–996. doi:10.1007/s00254-004-1083-3

Kennett, J.P., Cannariato, K.G., Hendy, I.L., Behl, R.J., 2003. The Clathrate Gun Hypothesi, in: Methane Hydrates in Quaternary Climate Change: The Clathrate Gun Hypothesis. American Geophysical Union, pp. 105–107. doi:10.1002/9781118665138.ch6

Kennett, J.P., Cannariato, K.G., Hendy, I.L., Behl, R.J., 2000. Carbon Isotopic Evidence for Methane Hydrate Instability During Quaternary Interstadials. Science (80-.). 288, 128–133.

King, L.H., MacLean, B., 1970. Pockmarks on the Scotian Shelf. Geol. Soc. Am. Bull. 81, 3141–3148.

King, L.L., Pease, T.K., Wakeham, S.G., 1998. Archaea in Black Sea water column particulate matter and sediments—evidence from ether lipid derivatives. Org. Geochem. 28, 677–688. doi:10.1016/S0146-6380(98)00037-0

Knittel, K., Boetius, A., 2009. Anaerobic Oxidation of Methane: Progress with an Unknown Process. Annu. Rev. Microbiol. 63, 311–334. doi:10.1146/annurev.micro.61.080706.093130

Kvenvolden, K.A., 1995. A review of the geochemistry of methane in natural gas hydrate. Org. Geochem. 23, 997–1008. doi:10.1016/0146-6380(96)00002-2

Lee, S.-Y., Holder, G.D., 2001. Methane hydrates potential as a future energy source. Fuel Process. Technol. 71, 181–186. doi:10.1016/S0378-3820(01)00145-X

Li, Y., Peacock, a, White, D., Geyer, R., Zhang, C., 2007. Spatial patterns of bacterial signature biomarkers in marine sediments of the Gulf of Mexico. Chem. Geol. 238, 168–179. doi:10.1016/j.chemgeo.2006.11.007

Lin, Q., Wang, J., Algeo, T.J., Sun, F., Lin, R., 2016. Enhanced framboidal pyrite formation related to anaerobic oxidation of methane in the sulfate-methane transition zone of the northern South China Sea. Mar. Geol. 379, 100–108. doi:10.1016/j.margeo.2016.05.016

Navarrete, A., Peacock, A., Macnaughton, S., Urmeneta, J., Mas-Castellà, J., White, D., Guerrero, R., 2000. Physiological Status and Community Composition of Microbial Mats of the Ebro Delta, Spain, by Signature Lipid Biomarkers. Microb. Ecol. 39, 92–99.

Nichols, P.D., Guckert, J.B., White, D.C., 1986. Determination of monosaturated fatty acid double-bond position and geometry for microbial monocultures and complex consortia by capillary GC-MS of their dimethyl disulphide adducts. J.

Microbiol. Methods 5, 49–55. doi:10.1016/0167-7012(86)90023-0

Niemann, H., Elvert, M., 2008. Diagnostic lipid biomarker and stable carbon isotope signatures of microbial communities mediating the anaerobic oxidation of methane with sulphate. Org. Geochem. 39, 1668–1677. doi:10.1016/j.orggeochem.2007.11.003

O'Reilly, S.S., 2013. Organic Carbon Cycling in Marine Sediments and Seabed Seepage Features in Irish Waters. Dublin City University.

Oba, M., Sakata, S., Fujii, T., 2015. Archaeal polar lipids in subseafloor sediments from the Nankai Trough: Implications for the distribution of methanogens in the deep marine subsurface. Org. Geochem. 78, 153–160. doi:10.1016/j.orggeochem.2014.11.006

Oba, M., Sakata, S., Tsunogai, U., 2006. Polar and neutral isopranyl glycerol ether lipids as biomarkers of archaea in near-surface sediments from the Nankai Trough. Org. Geochem. 37, 1643–1654. doi:10.1016/j.orggeochem.2006.09.002

Ogawa, M., Tanimoto, D., Okamoto, T., Saito, Y., Jing, Z., Takeuchi, A., Naganuma, T., 2003. Ester-Linked Phospholipid Fatty Acids in Marine Sediments: Testing the Possibility of Methane Seepage in the Japan Sea. Aquat. Ecosyst. Health Manag. 6, 397–408. doi:10.1080/714044169

Pancost, R.., Hopmans, E.., Sinninghe Damsté, J.., 2001. Archaeal lipids in Mediterranean cold seeps: molecular proxies for anaerobic methane oxidation. Geochim. Cosmochim. Acta 65, 1611–1627. doi:10.1016/S0016-7037(00)00562-7

Pancost, R.D., Sinninghe Damste, J.S., de Lint, S., van der Maarel, M.J.E.C., Gottschal, J.C., 2000. Biomarker Evidence for Widespread Anaerobic Methane

Oxidation in Mediterranean Sediments by a Consortium of Methanogenic Archaea and Bacteria. Appl. Environ. Microbiol. 66, 1126–1132. doi:10.1128/AEM.66.3.1126-1132.2000

Peck, H.D., 1993. Bioenergetic Strategies of the Sulfate-Reducing Bacteria, in: Odom, J.M., Singleton, R. (Eds.), The Sulfate-Reducing Bacteria: Contemporary Perspectives. Springer New York, New York, NY, pp. 41–76. doi:10.1007/978-1-4613-9263-7_3

Pinkart, H.C., Devereux, R., Chapman, P.J., 1998. Rapid separation of microbial lipids using solid phase extraction columns. J. Microbiol. Methods 34, 9–15. doi:10.1016/S0167-7012(98)00060-8

Plets, R.M.K., Callard, S.L., Cooper, J.A.G., Long, A.J., Quinn, R.J., Belknap, D.F., Edwards, R.J., Jackson, D.W.T., Kelley, J.T., Long, D., Milne, G.A., Monteys, X., 2015. Late Quaternary evolution and sea-level history of a glaciated marine embayment, Bantry Bay, SW Ireland. Mar. Geol. 369, 251–272. doi:10.1016/j.margeo.2015.08.021

Rajendran, N., Matsuda, O., Imamura, N., Urushigawa, Y., 1995. Microbial community structure analysis of euxinic sediments using phospholipid fatty acid biomarkers. J. Oceanogr. 51, 21–38. doi:10.1007/BF02235934

Rajendran, N., Matsuda, O., Imamura, N., Urushigawa, Y., 1992. Variation in Microbial Biomass and Community Structure in Sediments of Eutrophic Bays as Determined by Phospholipid Ester-Linked Fatty Acids. Appl. Envir. Microbiol. 58, 562–571.

Rajendran, N., Matsuda, O., Urushigawa, Y., Simidu, U., 1994. Characterization of microbial community structure in the surface sediment of osaka bay, Japan, by phospholipid Fatty Acid analysis. Appl. Environ. Microbiol. 60, 248–57.

Reeburgh, W.S., 2007. Oceanic Methane Biogeochemistry. Chem. Rev. 107, 486–513. doi:10.1021/cr050362v

Ringelberg, D.B., Sutton, S., White, D.C., 1997. Biomass, bioactivity and biodiversity: microbial ecology of the deep subsurface: analysis of ester-linked phospholipid fatty acids. FEMS Microbiol. Rev. 20, 371–377. doi:10.1111/j.1574-6976.1997.tb00322.x

Römer, M., Torres, M., Kasten, S., Kuhn, G., Graham, A.G.C., Mau, S., Little, C.T.S., Linse, K., Pape, T., Geprägs, P., Fischer, D., Wintersteller, P., Marcon, Y., Rethemeyer, J., Bohrmann, G., 2014. First evidence of widespread active methane seepage in the Southern Ocean, off the sub-Antarctic island of South Georgia. Earth Planet. Sci. Lett. 403, 166–177. doi:http://dx.doi.org/10.1016/j.epsl.2014.06.036

Schouten, S., Hopmans, E.C., Sinninghe Damsté, J.S., 2013. The organic geochemistry of glycerol dialkyl glycerol tetraether lipids: A review. Org. Geochem. 54, 19–61. doi:10.1016/j.orggeochem.2012.09.006

Shakhova, N., Semiletov, I., Salyuk, A., Yusupov, V., Kosmach, D., Gustafsson, O., 2010. Extensive methane venting to the atmosphere from sediments of the East Siberian Arctic Shelf. Science 327, 1246–50. doi:10.1126/science.1182221

Soter, S., 1999. Macroscopic seismic anomalies and submarine pockmarks in the Corinth–Patras rift, Greece. Tectonophysics 308, 275–290. doi:10.1016/S0040-1951(99)00090-6

Stillman, C.J., 1968. The Post Glacial Change in Sea Level in Southwestern Ireland: New Evidence from Fresh-water Deposits on the Floor of Bantry Bay, The scientific proceedings of the Royal Dublin Society. Royal Dublin Society.

Szpak, M.T., Monteys, X., O'Reilly, S., Simpson, A.J., Garcia, X., Evans, R.L.,

Allen, C.C.R., McNally, D.J., Courtier-Murias, D., Kelleher, B.P., 2012. Geophysical and geochemical survey of a large marine pockmark on the Malin Shelf, Ireland. Geochemistry, Geophys. Geosystems 13, n/a–n/a. doi:10.1029/2011GC003787

Szpak, M.T., Monteys, X., O'Reilly, S.S., Lilley, M.K.S., Scott, G.A., Hart, K.M., McCarron, S.G., Kelleher, B.P., 2015. Occurrence, characteristics and formation mechanisms of methane generated micro-pockmarks in Dunmanus Bay, Ireland. Cont. Shelf Res. 103, 45–59. doi:http://dx.doi.org/10.1016/j.csr.2015.04.023

Taylor, J., Parkes, R.J., 1983. The Cellular Fatty Acids of the Sulphate-reducing Bacteria, Desulfobacter sp., Desulfobulbus sp. and Desulfovibrio desulfuricans. Microbiology 129, 3303–3309. doi:10.1099/00221287-129-11-3303

Valentine, D.L., 2002. Biogeochemistry and microbial ecology of methane oxidation in anoxic environments: a review. Antonie Van Leeuwenhoek 81, 271–282. doi:10.1023/A:1020587206351

Valentine, D.L., Reeburgh, W.S., 2000. New perspectives on anaerobic methane oxidation. Environ. Microbiol. 2, 477–484.

van Dongen, B.E., Roberts, A.P., Schouten, S., Jiang, W.-T., Florindo, F., Pancost, R.D., 2007. Formation of iron sulfide nodules during anaerobic oxidation of methane. Geochim. Cosmochim. Acta 71, 5155–5167. doi:10.1016/j.gca.2007.08.019

Verardo, D.J., Froelich, P.N., McIntyre, A., 1990. Determination of organic carbon and nitrogen in marine sediments using the Carlo Erba NA-1500 analyzer. Deep Sea Res. Part A. Oceanogr. Res. Pap. 37, 157–165. doi:10.1016/0198-0149(90)90034-S

Vermeulen, N.J., Shannon, P.M., Masson, F., Landes, M., 2000. Wide-angle seismic control on the development of the Munster Basin, SW Ireland. Geol. Soc. London, Spec. Publ. 180 , 223–237. doi:10.1144/GSL.SP.2000.180.01.11

Volkman, J.K., Johns, R.B., Gillan, F.T., Perry, G.J., Bavor, H.J., 1980. Microbial lipids of an intertidal sediment—I. Fatty acids and hydrocarbons. Geochim. Cosmochim. Acta 44, 1133–1143. doi:10.1016/0016-7037(80)90067-8

Wakeham, S.G., Lewis, C.M., Hopmans, E.C., Schouten, S., Sinninghe Damsté, J.S., 2003. Archaea mediate anaerobic oxidation of methane in deep euxinic waters of the Black Sea. Geochim. Cosmochim. Acta 67, 1359–1374. doi:10.1016/S0016-7037(02)01220-6

Westbrook, G.K., Thatcher, K.E., Rohling, E.J., Piotrowski, A.M., Pälike, H., Osborne, A.H., Nisbet, E.G., Minshull, T.A., Lanoisellé, M., James, R.H., Hühnerbach, V., Green, D., Fisher, R.E., Crocker, A.J., Chabert, A., Bolton, C., Beszczynska-Möller, A., Berndt, C., Aquilina, A., 2009. Escape of methane gas from the seabed along the West Spitsbergen continental margin. Geophys. Res. Lett. 36, n/a–n/a. doi:10.1029/2009GL039191

White, D.C., Ringelberg, D.B., MacNaughton, S.J., Srinivas, A., Schram, D., 1997. Signature Lipid Biomarker Analysis for Quantitative Assessment In Situ of Environmental Microbial Ecology, in: Eganhouse, R.P. (Ed.), Molecular Markers in Environmental Chemistry. American Chemical Society, Washington D.C., pp. 22–34.

Yvon-Durocher, G., Allen, A.P., Bastviken, D., Conrad, R., Gudasz, C., St-Pierre, A., Thanh-Duc, N., del Giorgio, P.A., 2014. Methane fluxes show consistent temperature dependence across microbial to ecosystem scales. Nature 507, 488–491.

Zelles, L., 1997. Phospholipid fatty acid profiles in selected members of soil microbial communities. Chemosphere 35, 275–294. doi:10.1016/S0045-6535(97)00155-0

Zhu, C., Yoshinaga, M.Y., Peters, C.A., Liu, X.-L., Elvert, M., Hinrichs, K.-U., 2014. Identification and significance of unsaturated archaeal tetraether lipids in marine sediments. Rapid Commun. Mass Spectrom. 28, 1144–52. doi:10.1002/rcm.6887

Chapter 5

Final conclusions and future work

In this work we applied organic geochemical techniques to a variety of settings and research topics. Lipid biomarker investigations in soil, peat, and marine sediments provided new information in the fields of archaeology, palaeoclimatology, and geology. It is hoped that the power of the organic geochemical approach in using lipid biomarker analyses to answer myriad research questions has been demonstrated. Each chapter has opened the door to multiple possibilities for future research work.

In Chapter 2, analysis of 5ß-stanols and bile acids, so-called faecal biomarkers, provided evidence of the deposition of faecal material in a remote Alpine location. Combined with interpretation of historical texts as well as geological and microbiological analyses, these results have been attributed to the crossing of the Alps by Hannibal of Carthage and his army in 218 BC to invade Rome. As there are other feasible sources for the chemical and biological signatures presented here, further analyses is required before this hypothesis can be confirmed. There is potential for further organic geochemical analysis of these soils to contribute more to this research. Food stuffs for humans and animals would have been carried by this army and may also have been deposited as waste. Identification of plant-derived lipids in these soils and their individual isotopic signatures may enable certain compounds from feed grains etc. to be distinguished from local vegetation. If a geophysical survey of the area were to be carried out, and artefacts discovered such as cooking equipment, these too could be analysed for their lipid content and isotopic abundances.

Analysis of ancient peat material in Chapter 3 represents the first time lipid biomarkers have been employed in a peat palaeoclimate study in Ireland. Several climatic shifts were identified in the peat record and a potential cause of the

submersion of the *in situ* 'drowned forest' was observed. These results correlate with those of previous studies using more traditional peat palaeoclimate approaches such as the analysis of plant macrofossils and testate amoebae. They also provide evidence of climatic events not observed in all other Irish peat studies suggesting a need for a more thorough investigation of these time periods. Higher resolution sampling and ^{14}C dating of this material would help to better constrain these results in what is clearly an interesting time in the palaeoclimate of Ireland. The vast abundance of peat bogs in Ireland represents a well preserved, detailed, and extensive palaeoclimate record. Further use of the organic geochemical approach, in combination with other analyses, would provide invaluable information on Ireland's past climate. This information is essential for our understanding of how the country will respond to climate changes in the future.

Active CH_4 seepage features in Bantry Bay provide another example of this process occurring in a coastal setting in Ireland. Chapter 4 provides a characterisation of these features from a geophysical and geochemical perspective. The presence of gas migration throughout the bay, in areas with and without characteristic seabed features, is interesting and suggests that this activity may be more prevalent along the Irish coast than previously thought. The identification of a clear SMTZ together with no observed gas signatures in the water column emphasizes the importance of AOM in its role in preventing CH_4 escape to the atmosphere. Further analysis of sediments from Bantry Bay would be beneficial. Further characterisation of archaeal communities within this setting could be carried out such as through the analysis of glycerol dialkyl glycerol tetraethers (GDGTs), the intact membrane lipids of archaea. This would provide more information on the types of archaea involved in AOM. $\delta^{13}C$ values for more individual lipid compounds

would also provide a better insight into all of the microbial species involved. A combination of these organic geochemical techniques with advanced microbiological analysis of the sediments using techniques such as denaturing gradient gel electrophoresis (DGGE), phylogenetic analysis of 16S RNA, and pyrosequencing would yield a comprehensive view of the microbial ecology of this setting. The hypothesis that deep organic-rich sediments are the source of the CH_4 in Bantry Bay is one that could be investigated by obtaining deep cores. These cores could also be used for characterisation of the geology beneath the surface sediments as well as an in-depth palaeoclimate study on a millennial scale. Further examination of INFOMAR bathymetry data for Ireland's coast may lead to the discovery of other locations experiencing ongoing active gas seepage. Detailed study of these sites should be encouraged in an effort to fully understand the quantities of CH_4 being produced in the seabed either thermogenically or biogenically and to determine the extent to which its release is being prevented by AOM. How these microbial communities will be affected by future climate change and how this will affect CH_4 release to the atmosphere are important questions that require answers.

The learning outcomes from this work have been significant and include lipid biomarker analysis, trace element analysis, compound specific stable isotope analysis, instrumentation techniques, statistical analysis, planning and implementation of field work in both marine and terrestrial settings, collaboration in multidisciplinary projects, independent research, time management, and science communication. So far, the scientific output has included publication in peer-reviewed journals, scientific reports, and poster and oral presentations at national and international conferences. There is also significant potential for further publications derived from the work in this thesis.

This work has exposed two particularly important settings for organic geochemical research in Ireland which are inextricably linked. Global climate change appears to be inevitable with rising temperatures predicted across the planet. As well as the requirement of a unified approach in dealing with the outcomes and preventing further change, each nation must have a complete understanding of the potential effects unique to their territory. CH_4 is present in coastal marine settings in Ireland, perhaps to a much greater extent than is currently known. Similarly, significant quantities of this potent greenhouse gas are likely trapped within the peat bogs on the island of Ireland, much of which has already been released to the atmosphere through intensive harvesting of this natural resource. A comprehensive study of CH_4 as it pertains to climate change is something that should be encouraged in this country. This study could include extensive geophysical surveying across land and sea, much of which has already been carried out by the INFOMAR and Tellus programmes. Chemical analysis of gas signatures in the atmosphere, water column, and sediments could also be carried out. Further to this, detailed study of the chemistry and microbiology of the sediments experiencing gas seepage could be implemented. A widespread survey of the sources and sinks of this gas across the terrestrial and marine territories of Ireland would represent not only an important resource of information for future planning but also a significant contribution to global scientific research.

Appendices

Appendix A. GC-MS standard calibration curves

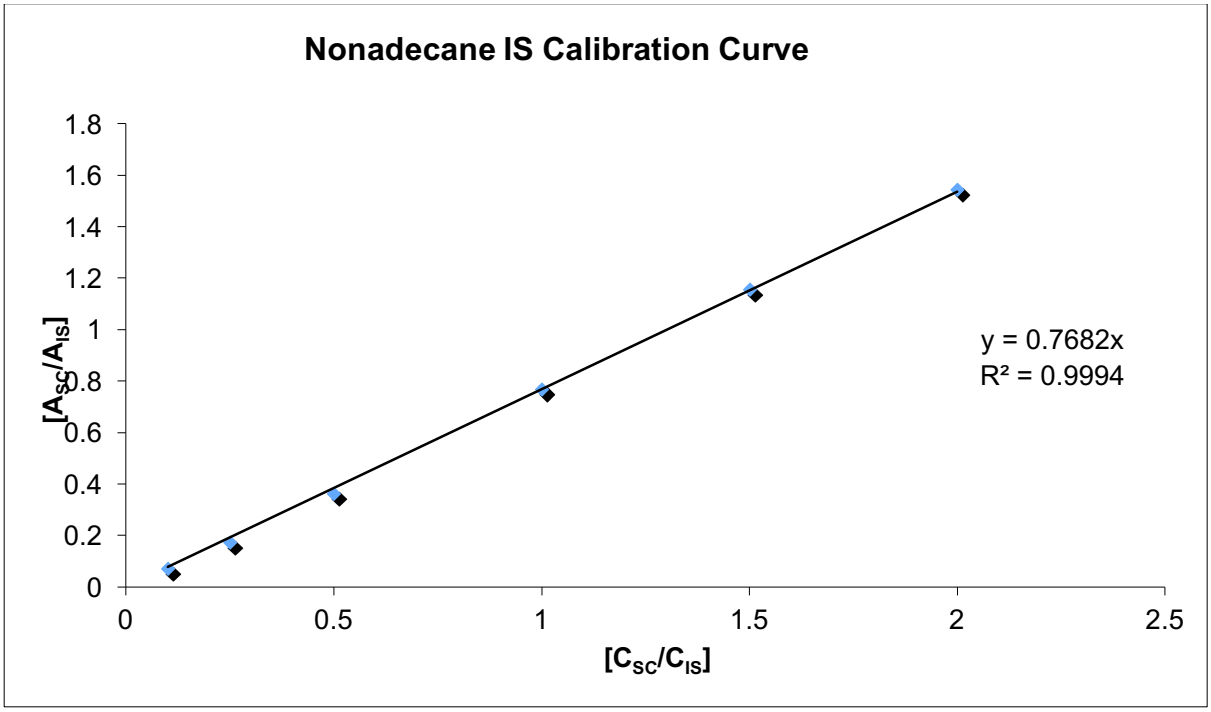

Figure A1. Nonadecane calibration curve.

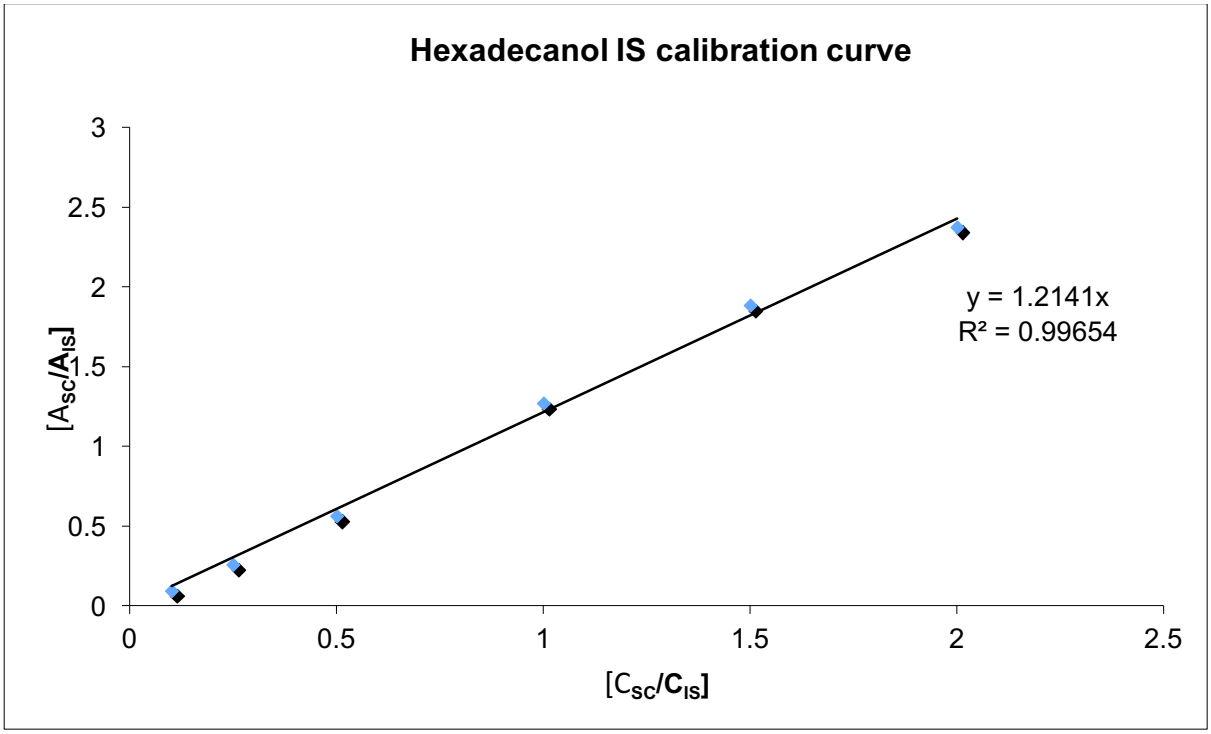

Figure A2. Hexadecanol calibration curve.

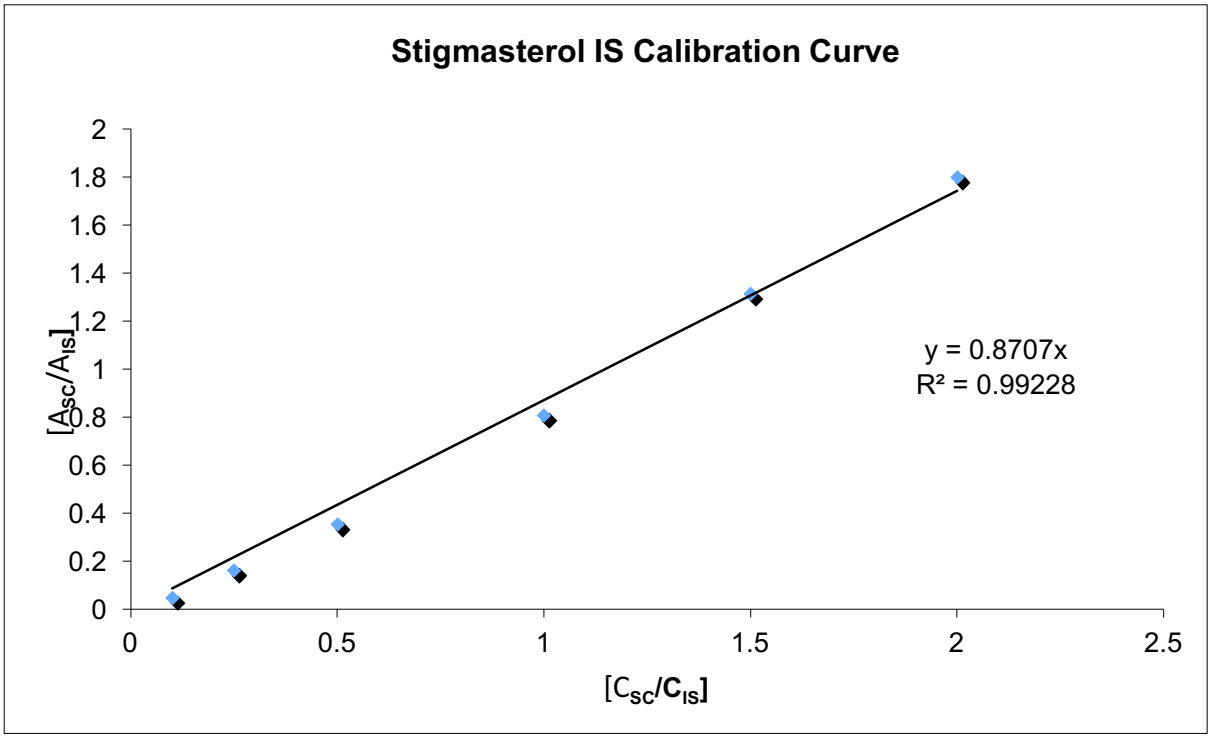

Figure A3. Stigmasterol calibration curve.

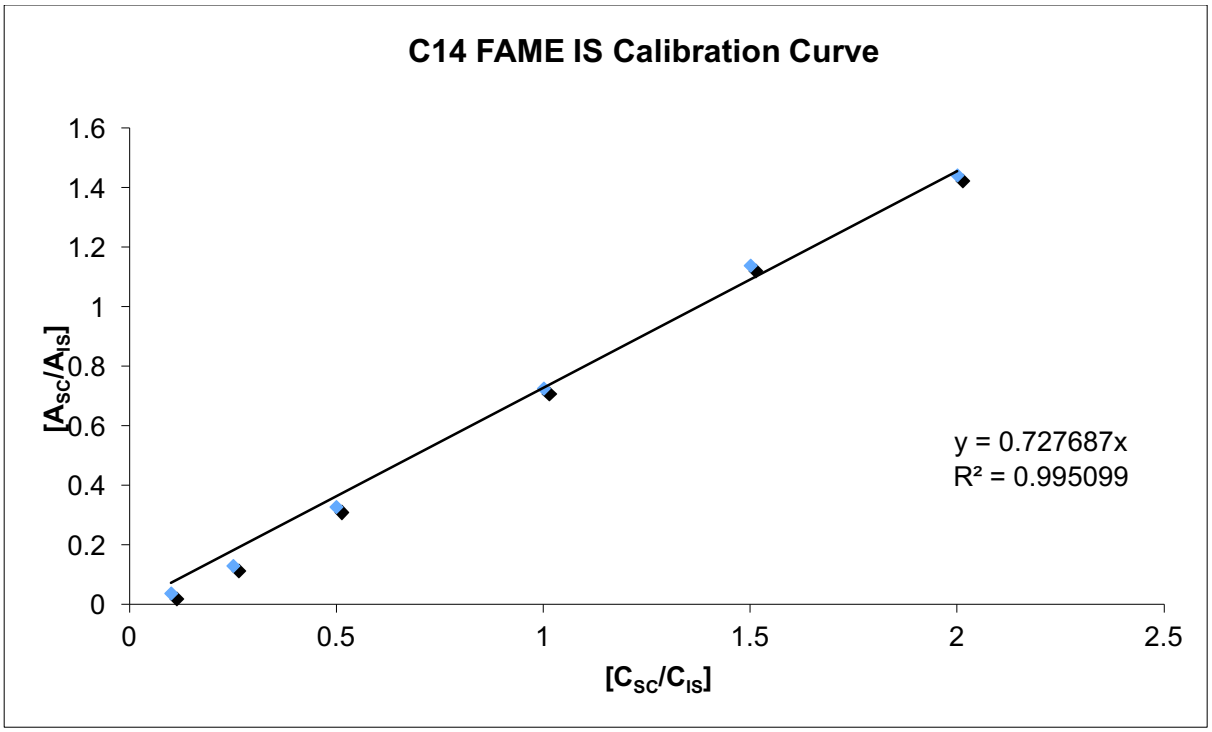

Figure A4. C14 FAME calibration curve.

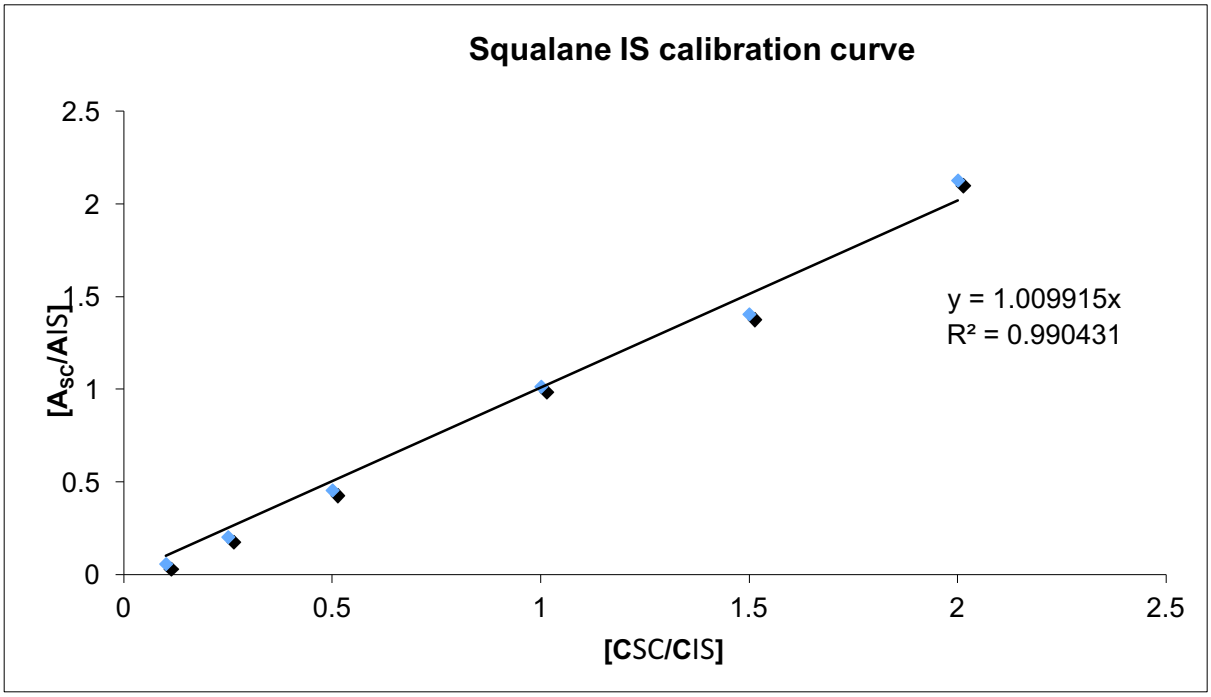

Figure A5. Squalane calibration curve.

Appendix B. GC-IRMS standard calibration curve

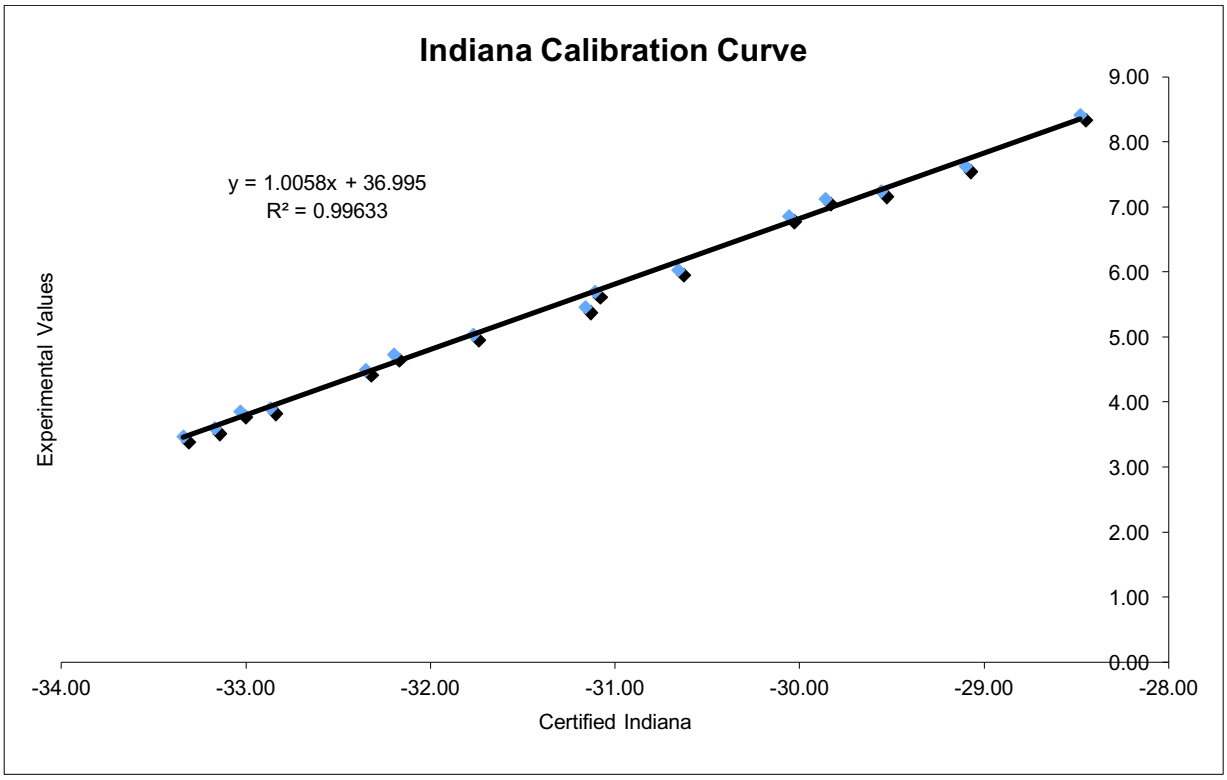

Figure A6. Indiana calibration curve

Appendix C. Gas and porewater analyses calibration curves

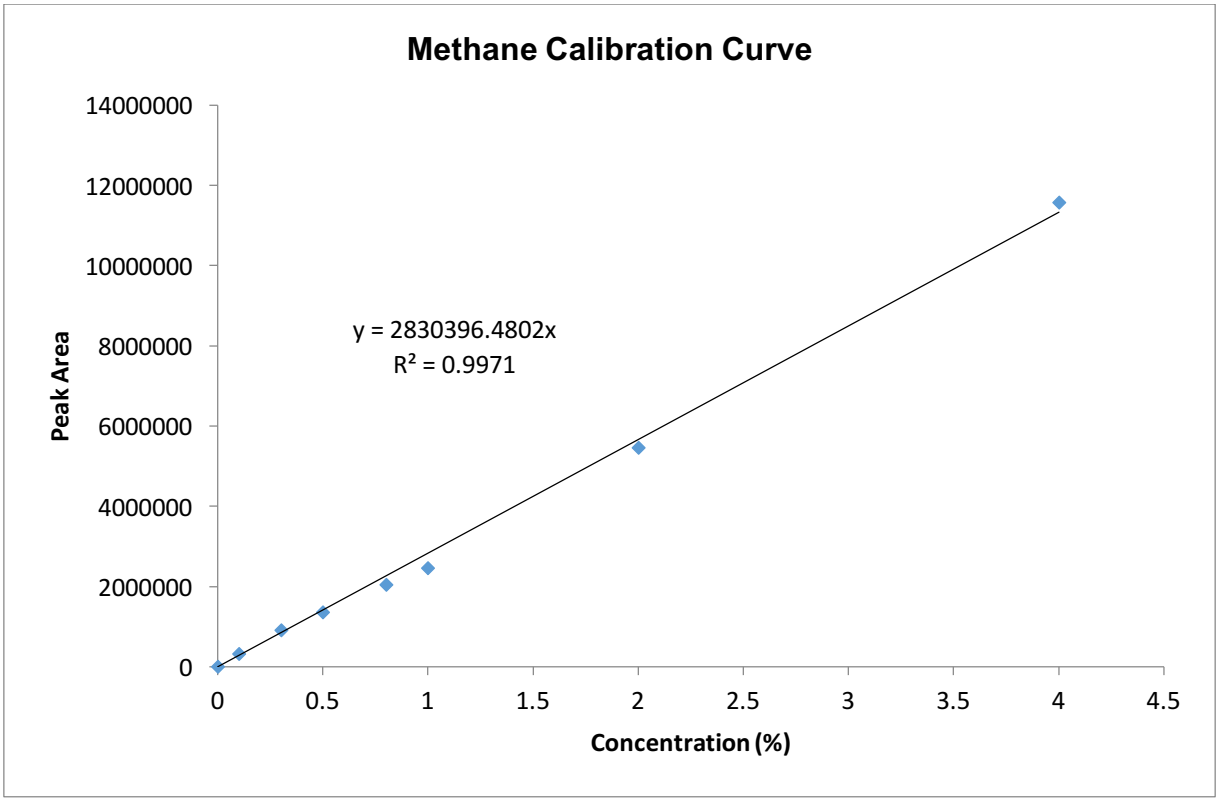

Figure A7. Methane calibration curve.

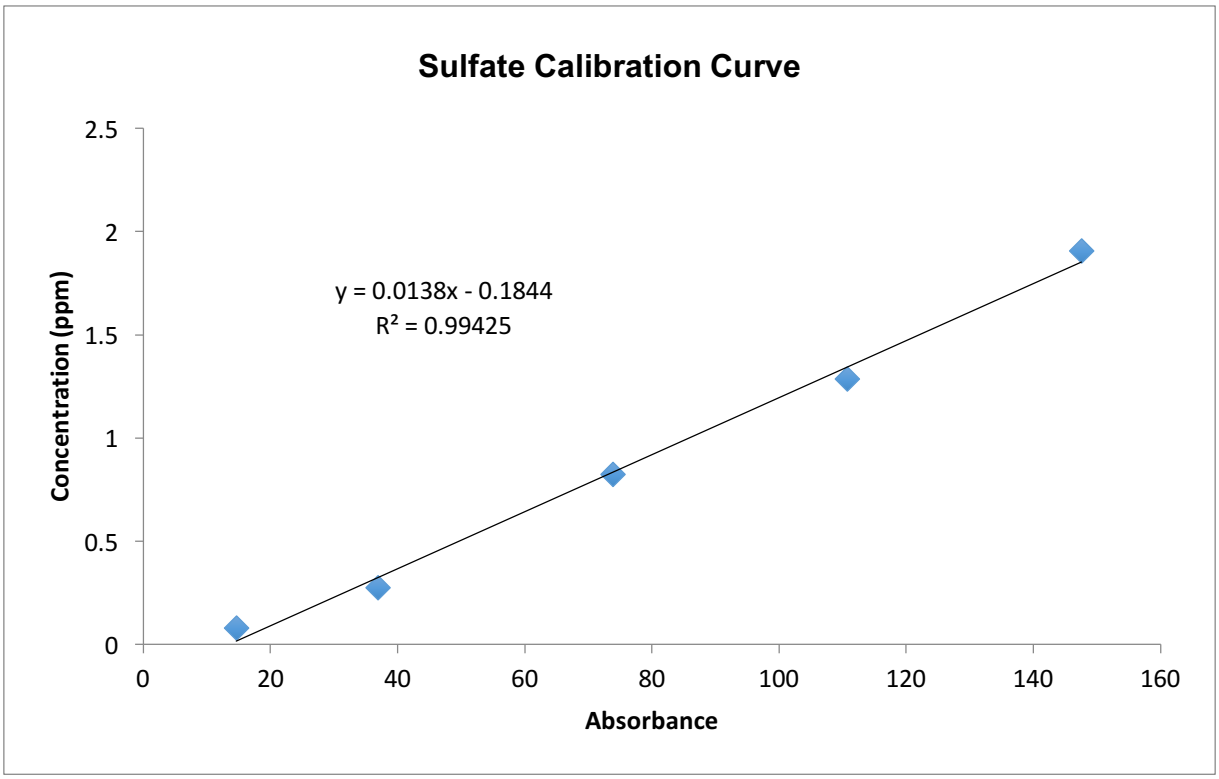

Figure A8. Sulfate calibration curve.

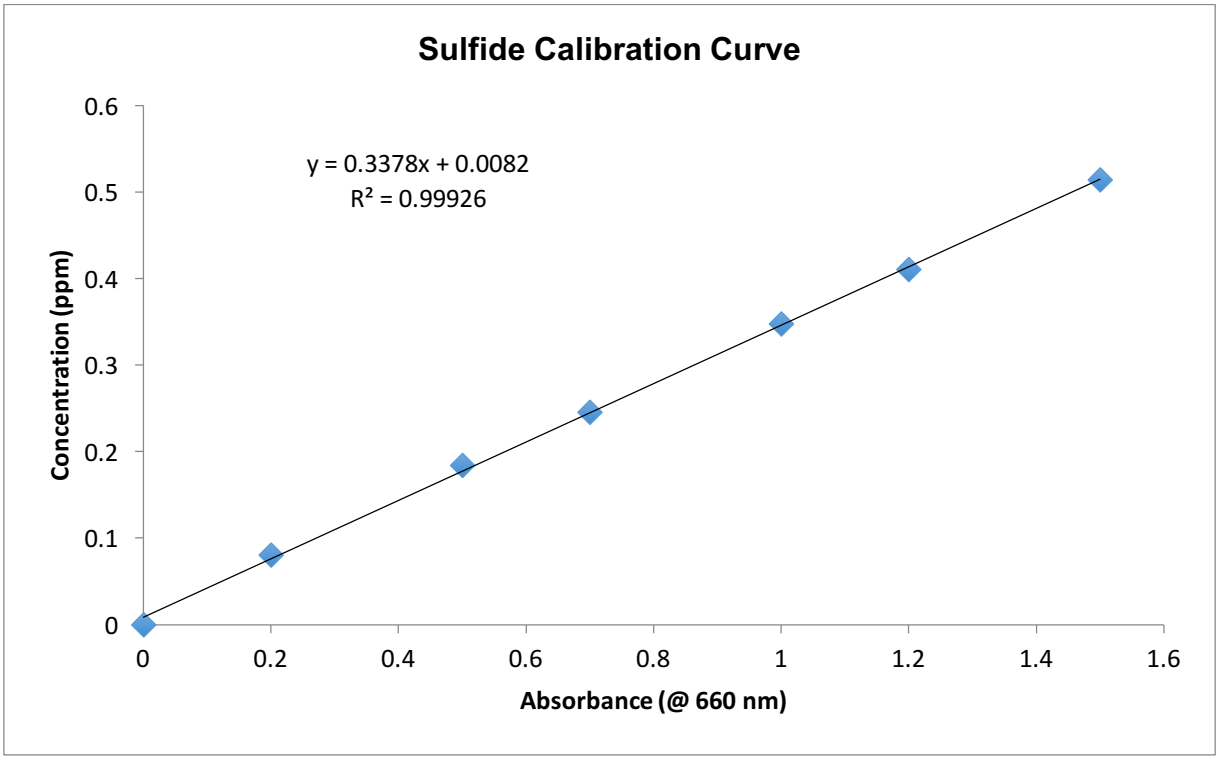

Figure A9. Sulfide calibration curve.

Appendix D. Statistical analyses

Table A1. Pearson correlation table containing all relevant elemental, lipid biomarker, and stable isotope data.

	TOC (%)	C/N	TS (%)	C23/C29 *a*	C23/C31 *a*	Paq	Pwax	13C C29 *a*	13C C31 *a*	13C C27 *b*	ACL *a*	ACL *c*	alc/alc+alk	Cholestanol	Ergostanol	24-Ethyl coprostanol	Campesterol	Campestanol	Stigmasterol	Beta-sitosterol	Stigmastanol	Taraxerone
TOC (%)		0.93	0.02	0.25	0.62	0.68	0.67	0.94	0.61	0.94	0.96	0.99	0.44	0.30	0.88	0.54	0.34	0.23	0.18	0.36	0.24	0.67
C/N	0.03		0.88	0.05	0.53	0.44	0.42	0.51	0.27	0.27	0.45	0.33	0.88	0.34	0.00	0.37	0.88	0.97	0.30	0.84	0.91	0.57
TS (%)	0.66	-0.05		0.48	0.91	0.90	0.79	0.84	0.39	0.70	0.82	0.05	0.49	0.49	0.59	0.90	0.80	0.53	0.44	0.99	0.68	0.36
C23/C29 *a*	-0.36	0.59	-0.23		0.01	0.00	0.00	0.62	0.67	0.86	0.32	0.94	0.91	0.51	0.02	0.29	0.76	0.86	0.53	0.66	0.84	0.15
C23/C31 *a*	-0.16	0.20	-0.03	0.74		0.00	0.00	0.17	0.50	0.04	0.00	0.93	0.36	0.71	0.48	0.47	0.70	0.25	0.57	0.91	0.50	0.24
Paq	-0.13	0.25	-0.04	0.82	0.95		0.00	0.51	0.88	0.07	0.00	0.85	0.60	0.93	0.30	0.45	0.83	0.37	0.72	0.89	0.71	0.18
Pwax	0.14	-0.26	0.08	-0.81	-0.96	-0.99		0.35	0.95	0.07	0.00	0.82	0.53	0.90	0.26	0.49	0.78	0.34	0.70	0.96	0.64	0.30
13C C29 *a*	0.02	-0.21	-0.06	-0.16	-0.43	-0.21	-0.30		0.87	0.01	0.06	0.75	0.12	0.53	0.46	0.39	0.67	0.39	0.42	0.39	0.41	0.17
13C C31 *a*	0.18	-0.37	-0.29	-0.15	-0.23	-0.05	-0.02	-0.06		0.94	0.62	0.32	0.65	0.40	0.86	0.67	0.36	0.47	0.27	0.27	0.43	0.21
13C C27 *b*	0.03	-0.35	-0.12	-0.06	-0.59	-0.53	-0.54	-0.70	-0.02		0.00	0.69	0.27	0.94	0.39	0.27	0.75	0.70	0.62	0.62	0.97	0.94
ACL *a*	0.01	0.24	-0.07	0.32	0.81	0.76	0.75	0.56	0.17	0.84		0.50	0.55	0.71	0.45	0.75	0.92	0.48	0.47	0.71	0.78	0.41
ACL c	0.00	0.31	0.57	0.03	-0.03	-0.06	0.08	-0.10	-0.33	-0.13	0.22		0.01	0.83	0.99	0.73	0.71	0.76	0.99	0.74	0.85	0.90
alc/alc+alk	0.24	-0.05	0.22	0.04	0.29	0.17	0.20	0.48	0.15	0.35	0.19	-0.74		0.77	0.56	0.77	0.67	0.61	0.81	0.60	0.74	0.42
Cholestanol	-0.32	0.30	-0.22	0.21	0.12	0.03	0.04	0.20	0.28	0.02	0.12	-0.07	0.10		0.25	0.01	0.00	0.00	0.00	0.00	0.00	0.90

Ergostanol	0.05	0.86	-0.17	0.65	0.22	0.32	-0.36	-0.24	-0.06	-0.27	0.24	0.00	0.19	0.36		0.46	0.60	0.85	0.26	0.96	0.76	0.58
24-Ethyl coprostanol	-0.20	-0.29	-0.04	-0.34	-0.23	-0.24	-0.22	-0.27	-0.15	-0.34	-0.10	-0.11	-0.09	-0.69	-0.24		0.00	0.00	0.02	0.02	0.00	0.14
Campesterol	-0.30	-0.05	-0.08	-0.10	-0.12	-0.07	-0.09	-0.14	-0.31	-0.10	-0.03	-0.12	-0.14	-0.93	-0.17	-0.77		0.00	0.00	0.00	0.00	0.96
Campestanol	-0.38	-0.01	-0.20	-0.06	-0.36	-0.29	-0.30	-0.27	-0.24	-0.13	-0.23	-0.10	-0.16	-0.92	-0.06	-0.79	-0.93		0.00	0.00	0.00	0.65
Stigmasterol	-0.42	-0.32	-0.25	-0.20	-0.18	-0.12	-0.13	-0.26	-0.36	-0.16	-0.23	-0.01	-0.08	-0.98	-0.35	-0.65	-0.91	-0.94		0.00	0.00	0.87
Beta-sitosterol	-0.29	-0.07	0.00	-0.14	-0.04	-0.04	-0.02	-0.28	-0.36	-0.16	-0.12	-0.11	-0.17	-0.84	-0.02	-0.65	-0.92	-0.86	-0.81		0.00	0.34
Stigmastanol	-0.37	-0.04	-0.13	-0.06	-0.21	-0.12	-0.15	-0.26	-0.27	-0.01	-0.09	-0.06	-0.11	-0.95	-0.10	-0.78	-0.96	-0.98	-0.94	-0.92		0.93
Taraxerone	0.14	0.18	0.29	0.44	0.37	0.42	-0.33	-0.42	-0.41	-0.02	-0.26	-0.04	-0.25	-0.04	-0.18	-0.45	-0.02	-0.15	-0.05	-0.30	-0.03	
C27-one/ C31-ane	-0.28	-0.07	-0.13	-0.64	-0.84	-0.81	-0.77	-0.23	-0.27	-0.57	-0.66	-0.27	-0.47	-0.17	-0.04	-0.29	-0.11	-0.35	-0.21	-0.06	-0.18	0.54

a – *n*-alkane(s)
b – *n*-alkan-2-one(s)
c – *n*-alkanols